INSULIN AND LEPTIN ACTION: ROLES IN DIABETES AND OBESITY.

A thesis submitted to the University of London

for the degree of Doctor of Philosophy

by

David Charles Bedford.

Department of Medicine
University College London
Rayne Institute
5 University Street
London, WC1E 6JJ.

November 2004.

ProQuest LLC
789 East Eisenhower Parkway
P.O. Box 1346
Ann Arbor, MI 48106-1346

ABSTRACT.

Obesity is a major risk factor for insulin resistance and therefore type 2 diabetes. However, the precise mechanisms whereby obesity causes insulin resistance are complex and not completely understood. The adipocyte derived hormone leptin and the pancreatic derived hormone insulin act as satiety factors to the central nervous system, regulating long-term energy homeostasis. In addition both hormones have been shown to act in the central nervous system (CNS) to acutely regulate peripheral glucose homeostasis. Leptin and insulin have also been shown to regulate pancreatic islet function.

A growing amount of evidence suggests there is considerable overlap in the pathways by which these hormones act to mediate their physiological effects. The insulin receptor substrate-2 (IRS-2) protein is a critical mediator of cellular responses to insulin, especially those associated with somatic growth and carbohydrate metabolism. It has been suggested that IRS-2 signalling pathways act as a potential point of convergence for insulin and leptin signalling.

Much of our current understanding of both the cellular and molecular effects of leptin and insulin has been derived from studies of murine models of obesity and diabetes. In this thesis I have exploited three such models to generate mice with defective 1) IRS-2 function (*IRS-2 KO*) and leptin production (*ob/ob*) and 2) IRS-2 function and leptin receptor (*db/db*) function. I have also produced mice which lack IRS-2 and STAT-3 specifically in their β-cells and hypothalamus. As insulin resistance and leptin resistance coexist in obese subjects, it was hoped that such murine models would give some insights into the contribution of these processes to the obesity phenotype and its associated insulin resistance and type 2 diabetes. In particular it was hoped to address the hypothesis that a linear relationship exists between IRS-2 and STAT-3 in mediating the effects of insulin and leptin action, with IRS-2 being upstream of the events that lead to the phosphorylation of STAT-3.

Considering either systemic or tissue-specific approaches, it was evident that insults to leptin signalling in combination with *Irs-2* deletion results in additive effects upon growth, adiposity, glucose homeostasis and islet function. These additive effects would indicate that IRS-2 and STAT-3 mediate these effects by acting in separate signalling pathways, as opposed to converging upon a linear pathway. However cross-talk between these parallel pathways is likely to be critical for the maintenance of insulin and leptin sensitivity in target tissues.

ACKNOWLEDGEMENTS:

I would like to thank Professor Dominic Withers for his expert guidance throughout the duration of this research and for providing me with the opportunity to work in his laboratory. In addition I would also like to express my gratitude to DiabetesUK for sponsoring this research.

I would like to thank all the members of the Withers lab (past and present) for their help over the years. In particular, Marcus and Helen for their company during the many hours spent in the BSU at Hammersmith.

I am grateful to Dr Marika Charalambous, Dr Gavin McCall, Dr Colin Selman and Dr Julie Wilsher for their assistance in the proofreading of this thesis.

I wish to thank Asha for her support and encouragement other the last year.

I thank Julie, Darren and Elizabeth for allowing me to stay in their home this year. Indeed I am indebted to my sister Julie, as she has been very influential in my decision to pursue a career in research.

Finally I would like to say a very special thank you for the patience and understanding of my parents over the last three years. Their love and encouragement has always been there for me and for this reason, I dedicate this work to them.

CONTENTS

LIST OF FIGURES

LIST OF TABLES

CHAPTER 1

INTRODUCTION.

1.1 Obesity and type 2 diabetes: a worldwide epidemic

Obesity and its associated pathologies are major causes of ill health and death worldwide (1). The incidence of obesity is increasing in both developed and developing countries. For example in the UK currently over two thirds of men and half of women are overweight or obese (2). Obesity increases the risk of insulin resistance, type II diabetes mellitus, cardiovascular disease, osteoarthritis and some types of cancers, resulting in increased mortality at any given age. Indeed, the increasing prevalence of type 2 diabetes associated with obesity in UK teenagers further highlights this as a major cause of morbidity with significant implications for future health-care provision (3, 4). However, despite significant progress in our understanding of the mechanisms by which energy homeostasis is regulated, the precise pathophysiological relationships between obesity, insulin resistance and type 2 diabetes are not completely understood.

1.2 Overview of insulin resistance, type 2 diabetes and obesity

Type 2 diabetes is a complex metabolic disorder characterised by a triad of 1) resistance to insulin action on glucose uptake in peripheral tissues, especially skeletal muscle and adipocytes, 2) impaired insulin action to inhibit hepatic glucose production and 3) dysregulated insulin secretion. Insulin resistance is one of the earliest abnormalities in the clinical history of type 2 diabetes, and is also seen in non-diabetic relatives of diabetic subjects (5). However, initially, insulin resistance does not cause overt hyperglycaemia because normally β-cells are capable of secreting sufficient amounts of insulin to offset the defects in insulin action. This β-cell compensation in the face of insulin resistance occurs due to both an increase in the production of insulin by individual β-cells but also an overall increase in β-cell mass (6, 7). However, once

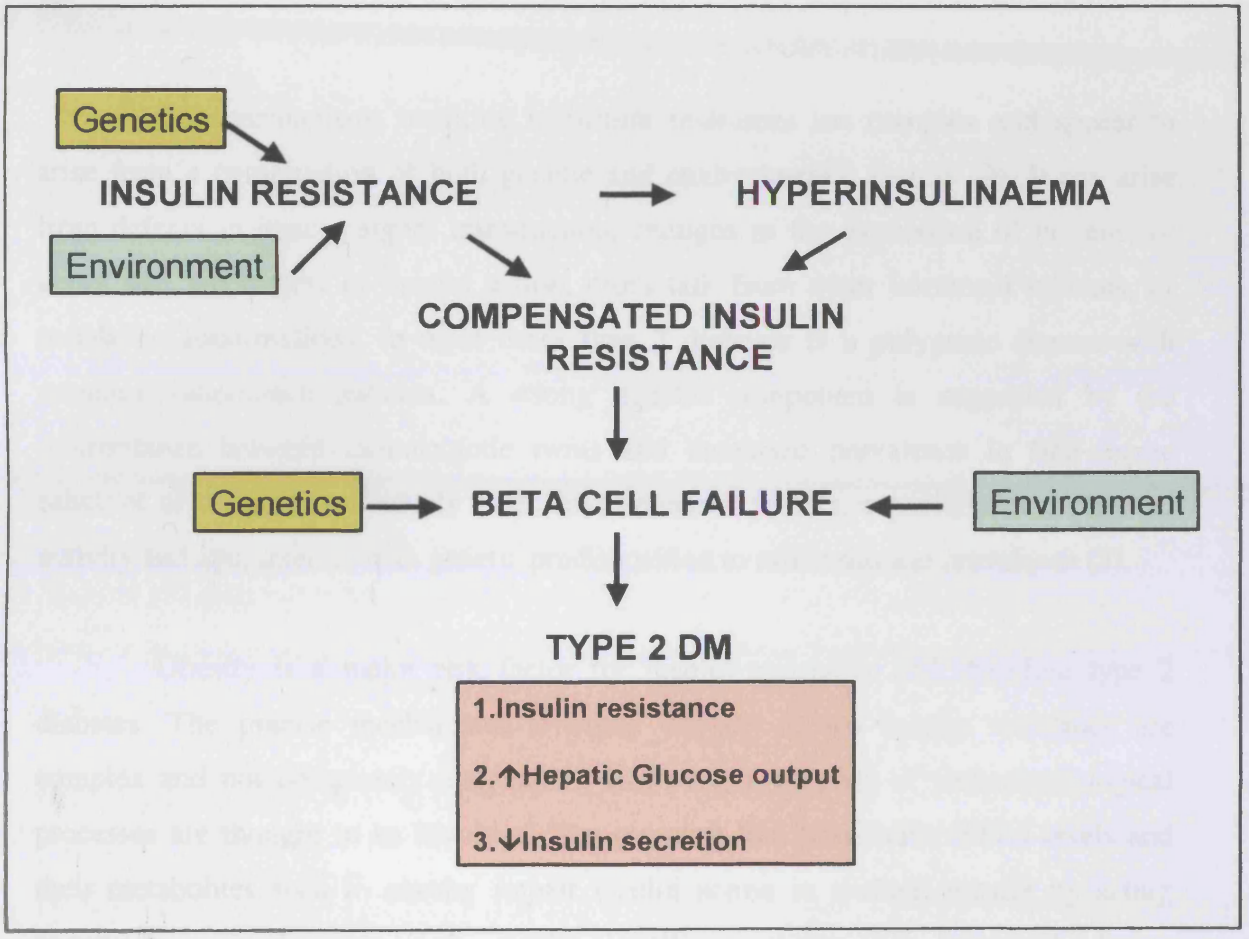

Figure 1.1 Pathogenesis of type 2 diabetes

The presence of insulin resistance places an increased demand upon the pancreatic β-cell to compensate by secreting more insulin. Both genetic and environmental factors may limit compensation leading to relative β-cell failure and type 2 diabetes mellitus.

this compensation fails, glucose intolerance supervenes. Hence the development of overt type 2 diabetes requires the presence of two defects; insulin resistance and β-cell failure (Fig 1.1). Insulin resistance is thus a fundamental factor in the aetiology of type 2 diabetes and is linked to a wide array of other pathophysiological conditions including hypertension, hyperlipidemia, atherosclerosis, and polycystic ovarian disease (8).

The mechanisms resulting in insulin resistance are complex and appear to arise from a combination of both genetic and environmental factors (9). It can arise from defects in insulin signal transduction, changes in the expression of proteins or genes that are targets of insulin action, cross talk from other hormonal systems, or metabolic abnormalities. In most cases type 2 diabetes is a polygenic disease with complex inheritance patterns. A strong genetic component is suggested by the concordance between monozygotic twins and increased prevalence in first-degree relatives of affected individuals (10). Environmental factors, especially diet, physical activity and age, interact with genetic predisposition to affect disease prevalence (5).

Obesity is a major risk factor for insulin resistance and therefore type 2 diabetes. The precise mechanisms whereby obesity causes insulin resistance are complex and not completely understood. However, a number of pathophysiological processes are thought to be involved. The elevated free fatty acids (FFA) levels and their metabolites seen in obesity impair insulin action in skeletal muscle by acting negatively upon elements of the insulin-signalling pathway (11). Increased adipose tissue production of cytokines, such as tumour necrosis factor-α, inhibits insulin signalling. Similarly reduced expression of the adipocyte hormones adiponectin and leptin (see below) are associated with insulin resistance. It is apparent that the excess FFAs seen in obesity may also impair pancreatic islet function and thus contribute to the α-cell defect seen in type 2 diabetes (12, 13).

It is therefore clear that an understanding of the mechanisms that regulate glucose homeostasis, insulin sensitivity and whole body energy storage will have an important role in our understanding of the pathophysiology of type 2 diabetes.

1.3 Acute regulation of peripheral glucose homeostasis by insulin

1.3.1 Pancreatic islet function and glucose uptake

The brain and central nervous system require glucose as the sole or primary source of energy. While hypoglycaemia may produce cellular death, chronic hyperglycaemia also can result in organ damage. Therefore, plasma glucose levels are tightly regulated between 4 and 7 mM in normal individuals (5). This narrow range, is governed by, a balance between glucose absorption from the gut, production by the liver and uptake by peripheral tissues and organs. The balance between the utilization and production of glucose is maintained at equilibrium by the opposing actions of insulin and glucagon (Fig 1.2). In response to a meal, blood glucose levels increase and insulin is released from the β-cells within the islets of Langerhans, stimulating glucose transport into muscle and fat via GLUT4 glucose transporter mechanisms, whilst inhibiting hepatic glucose production (8). Similarly, when glucose levels fall, glucagon, released from the α-cells, promotes the release of stored and newly synthesised glucose into the bloodstream. Insulin and glucagon therefore act in concert to ensure that glucose homeostasis is maintained throughout a wide variety of physiological states.

1.3.2 Insulin and gene expression

In addition to these acute effects upon glucose uptake, insulin also regulates metabolism at the level of gene transcription and translation, regulating such processes as gluconeogenesis and lipogenesis. For example, at the transcriptional level, acute insulin treatment decreases the messenger RNAs encoding gluconeogenic enzymes, such as phosphoenolpyruvate carboxykinase and increases the mRNAs encoding lipogenic enzymes via the action of the transcription factor, sterol regulatory element binding protein (SREBP-1c) (14). Central administration of insulinomimetics and insulin receptor anti-sense has also indicated that insulin can act centrally to regulate gene expression in peripheral tissues (15).

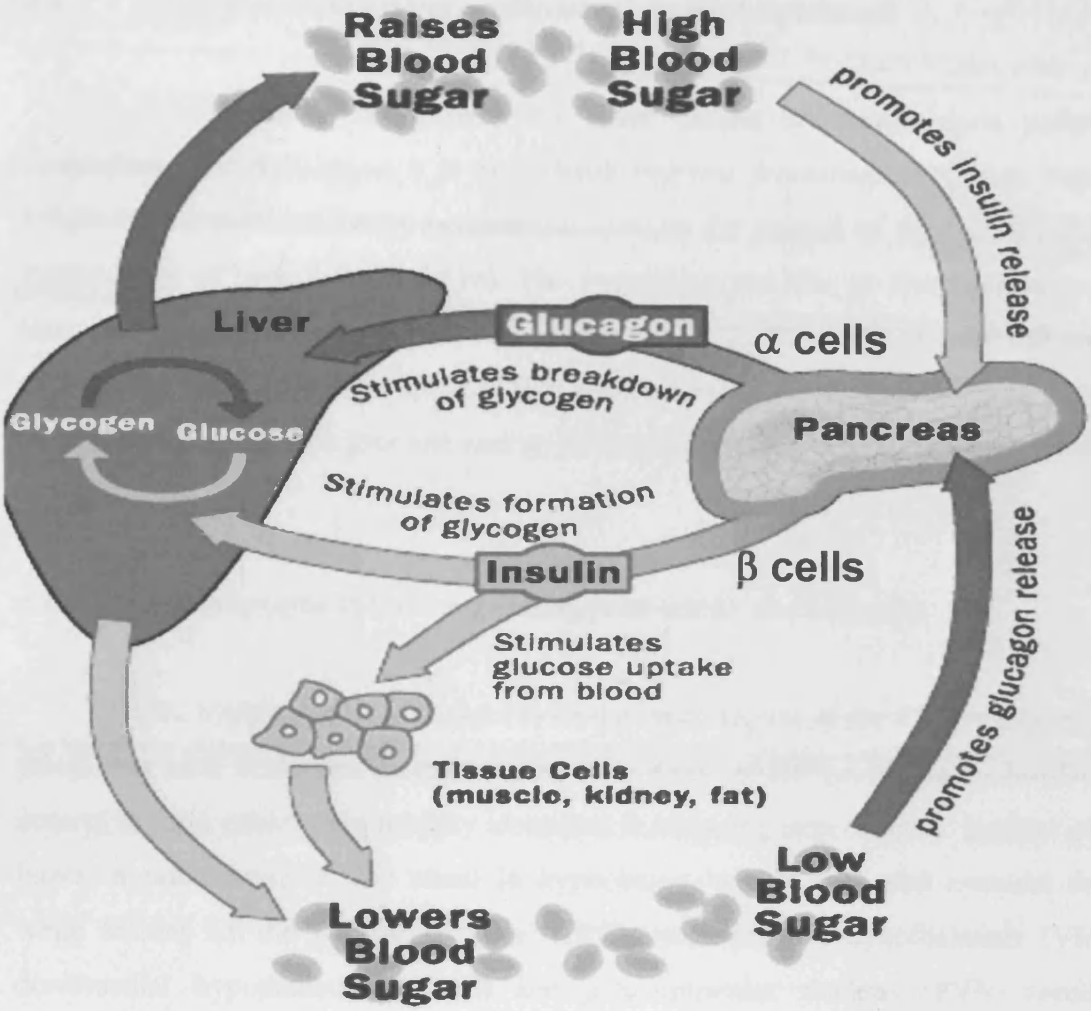

Figure 1.2 Regulation of plasma blood glucose by opposing actions of insulin and glucagon

Blood glucose levels are maintained between 4 and 7mM in normal individuals by the opposing actions of insulin and glucagon. When blood glucose levels increase, insulin is secreted from β-cells in the pancreas, promoting the uptake of blood glucose into peripheral metabolic tissues such as muscle and fat, whilst inhibiting hepatic glucose output. Similarly, when blood glucose levels are low, glucagon is released from α-cells in the pancreas and stimulates the secretion of newly synthesized glucose from the liver into the bloodstream.

1.4 Central nervous system regulation of energy homeostasis

In contrast to these relatively acute effects of insulin upon peripheral metabolism described above it is well-established that physiological systems regulate longer-term aspects of energy homeostasis such as the control of food intake and the maintenance of body fat stores (16). The impressive stability of body adiposity over long periods of time, despite often marked variation in daily food intake and energy expenditure, led Kennedy to propose that a signal generated in proportion to body fat stores acts in the brain to promote energy homeostasis (17).

1.4.1 Hypothalamic circuits regulating food intake and adiposity

The hypothalamus is thought to be the major region of the CNS regulating and integrating food intake and energy homeostasis. Areas of the hypothalamus involved in control of food intake were initially identified in lesioning experiments. Lesions of the lateral hypothalamus (LHA) result in hypophagia, weight loss and eventual death, while lesions of the arcuate nucleus (ARC), ventromedial hypothalamus (VMH), dorsomedial hypothalamus (DMH) and paraventricular nucleus (PVN) result in hyperphagia and weight gain (18). Subsequent work has identified various neuropeptides present in these hypothalamic nuclei, along with their sites of synthesis, release and their receptor fields. It has now become apparent that the hypothalamic nuclei form a complex neural network involved in the regulation of food intake and energy expenditure. It has also become clear that there is a complex interplay between these circuits and peripheral signals (16).

1.4.2 Arcuate nucleus (ARC)

The arcuate nucleus is located at the base of the hypothalamus on either side of the third ventricle. The ARC effectively lies outside the blood brain barrier and thus, ARC neurones are accessible to circulating hormones and nutrients. Two adjacent groups of neurons in the ARC, the agouti-related protein (AgRP)/neuropeptide Y (NPY) neurones (orexigenic) and the proopiomelanocortin (POMC)/ cocaine-

amphetamine-regulated transcript (CART) neurones (anorectic), act as the primary site in the brain for receiving the humoral signals that reflect body energy status (Fig 1.3). Projections between ARC AgRP/NPY and POMC/CART allow cross talk and hence a co-ordinated response. These neurons are often referred to as "first order neurons" because of their direct contact with peripheral signals. From the ARC, neurons project to "second order neurons" in the PVN, VMH, DMH, and LHA (19). Second order neurons project to the nucleus of the solitary tract (NTS) in the brainstem and the dorso-motor nucleus of the vagus (DMV). The communication between hypothalamic pathways and the caudal brainstem, in response to peripheral satiety signals, is essential for the long-term regulation of energy homeostasis.

1.5 Peripheral signals of long-term energy balance

The neuronal and molecular hypothalamic circuits described in brief above are now known to represent a major component of the brain centres that Kennedy proposed as responding to humoral adiposity signals. However, in contrast to the complexity and significant numbers of factors involved in hypothalamic function, the search for peripherally produced adiposity signals has to date revealed only a few key molecules. The pancreatic hormone insulin, which enters the brain from the circulation and acts there to reduce energy intake was the first hormonal signal implicated in the control of body weight by the CNS (20). However, it was the subsequent identification of the adipocyte hormone leptin (21) and the delineation of its role in the CNS regulation of energy homeostasis that provided the impetus for many of the recent advances in our understanding of these pathways and mechanisms. The interactions between the peripheral and central mechanisms regulating energy homeostasis are summarised in Figure 1.3.

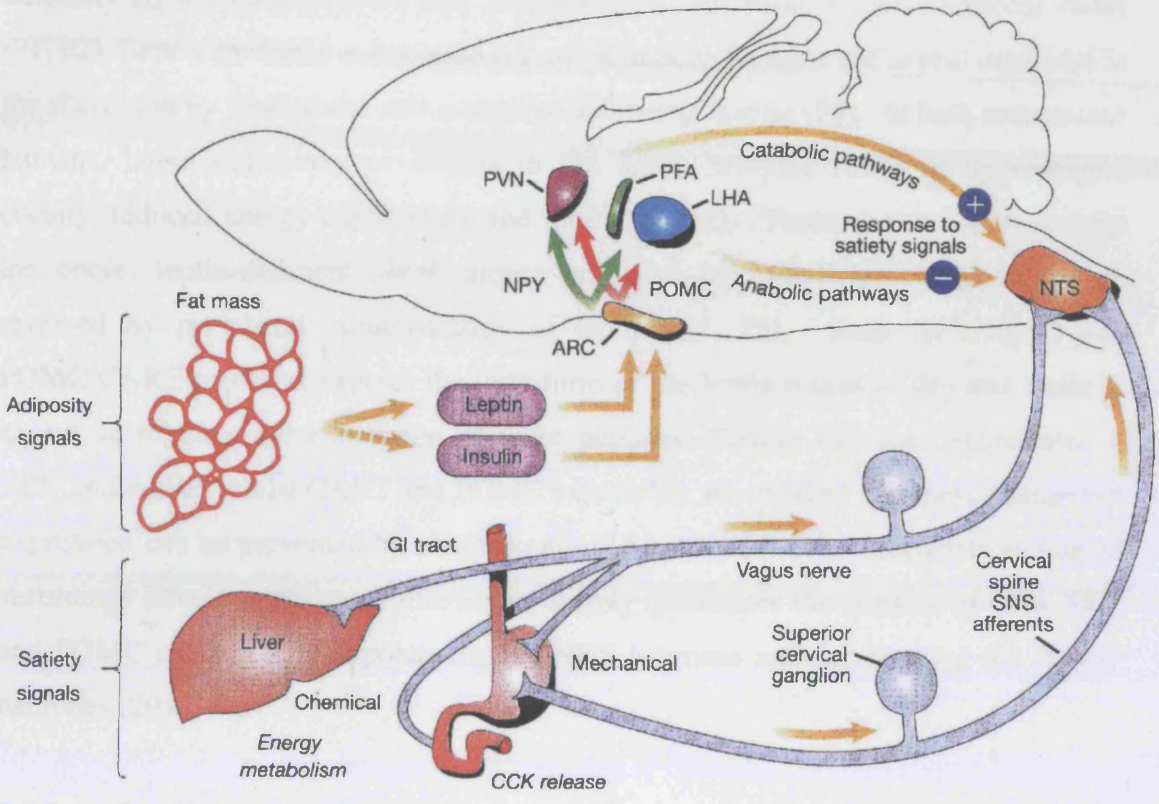

Figure 1.3 Representation of how insulin and leptin act as adiposity signals to the CNS and regulate energy homeostasis

Both insulin and leptin act upon the first order neurons, stimulating the anorectic Proopiomelanocortin (POMC)/Cocaine-amphetamine-regulated transcript (CART) neurones and inhibiting the orexigenic Agouti-related protein (AgRP)/ Neuropeptide Y (NPY) neurones. Projections between ARC AgRP/NPY and POMC/CART allow cross talk and hence a co-ordinated response that signals to second order neurones, which then relay signals to the caudal brainstem. It is also known that hormones, such as cholecystokinin (CCK), are released from the gut in response to food intake and act in the CNS to rely satiety. Both adiposity and satiety signals act within the CNS to regulate whole body energy homeostasis. Figure adapted with permission from (19).

1.5.1 Leptin: an adiposity signal acting in the CNS

The adipocyte-derived hormone leptin is the best-characterised peripheral adiposity signal. Its expression and circulating concentration reflect nutritional status (21, 22). Leptin synthesis and release is proportional to fat mass but is also regulated in the short term by food intake and is reduced following fasting (23). In both rodents and humans, leptin deficiency or defects in the leptin receptor result in hyperphagia, obesity, reduced energy expenditure and infertility (21). These abnormalities seen in the obese, leptin-deficient *ob/ob* mouse and also leptin-deficient humans can be reversed by peripheral administration of leptin (24, 25). Both NPY/AgRP and POMC/CART neurones express the long-form of the leptin receptor (26) and leptin is known to regulate the expression of these peptides. Fasting increases expression of NPY and AgRP, whilst CART and POMC expression are reduced and these changes in expression can be prevented by administration of leptin (27, 28). Electrophysiological recordings have demonstrated that leptin acutely modulates the activity of both NPY and POMC neurones, hyperpolarizing the NPY neurones and depolarising the POMC neurones (29).

1.5.2 Insulin: actions in the CNS

Insulin is another important adiposity signal to the brain but in contrast to leptin its role in the central regulation of energy homeostasis has been less intensively studied (19). Insulin receptors are expressed in the hypothalamus particularly in the ARC and PVN (30). Early studies demonstrated a role for intracerebroventricularly administered insulin in the control of food intake and body weight (20). Recently, deletion of the insulin receptor in the murine brain has been shown to cause mild hyperphagia and adiposity in female mice and diet-sensitive obesity in both sexes (31). Central administration of insulinomimetics and insulin receptor anti-sense also support a role for CNS insulin signalling in the regulation of energy homeostasis (15, 32). In addition to suppressing food intake and reducing body weight, hypothalamic administration of insulin has been shown to regulate NPY and AgRP expression (19). It has therefore been suggested that insulin and leptin target the same neurones in the hypothalamus, ie NPY/AgRP and POMC/CART neurones.

In addition to its role as a peripheral signal, acting in the hypothalamus to regulate long-term energy homeostasis, there is evidence that leptin may act in the CNS to acutely regulate peripheral glucose homeostasis. For example intracerebroventricular administration of leptin has been shown to modulate hepatic glucose fluxes (33). Central administration of leptin has also been shown to regulate fatty acid oxidation in skeletal muscle acting via AMP-activated protein kinase (AMPK) (34). AMPK is activated following an increase in the AMP:ATP ratio within the cell that occurs following a decrease in ATP levels (35). Minokoshi et al demonstrated that leptin directly stimulates phosphorylation and activation of the α2 catalytic subunit of AMPK (α2 AMPK) in skeletal muscle. It was also noted that early activation of AMPK occurs by leptin acting directly on muscle, whereas later activation requires leptin to function through the hypothalamic-sympathetic nervous system axis (34).

1.6 Insulin and leptin signal transduction pathways

Our understanding of the underlying cellular and molecular mechanisms by which insulin and leptin mediate their physiological effects have increased significantly in recent years. In particular, studies have delineated much of the signalling pathways that are stimulated by these hormones and have started to demonstrate similarities and differences between the signalling mechanisms involved.

1.6.1 Insulin receptor signalling cascade

Insulin action on glucose uptake in muscle and fat results from a cascade of signalling events emanating from the insulin receptor and culminating in translocation of the major insulin responsive glucose transporter, GLUT-4, from intracellular vesicles to the plasma membrane (36, 37), (summarised in Fig 1.4). Insulin binds to its cell surface transmembrane receptor stimulating receptor autophosphorylation and activation of the intrinsic kinase activity. Resulting in tyrosine phosphorylation of several cytosolic docking proteins called insulin receptor substrate (IRS) proteins. There are at least four closely related insulin receptor substrate proteins. Findings from transgenic mouse models have revealed distinct physiological roles for the four major

IRS proteins (38). Mice lacking IRS1 display profound growth retardation and insulin resistance, but do not develop diabetes due to β cell compensation (39). IRS-3 and IRS-4 null mice have minimal metabolic, endocrine and growth phenotypes (reviewed in (38)). In contrast, mice lacking IRS2 have mild growth defects but develop diabetes due to β cell failure in the face of peripheral insulin resistance. Once phosphorylated IRS proteins bind to various effector molecules including the regulatory subunit (P85α) of phosphoinositide 3-kinase (PI3K), via Src homology 2 (SH2) domains.

The primary function of the PI3K enzyme in insulin signalling appears to be the transduction of tyrosine phosphorylation into a signal leading to activation of serine/threonine kinases. P85α dimerizes the p110 catalytic subunit of the PI3K enzyme. Deletion of P85α in mice resulted in increased insulin sensitivity and hypoglycaemia due to increased glucose transport in skeletal muscle and adipocytes (40). The lipid products of PI3K and in particular PIP_3, are thought to be involved in recruitment and perhaps activation of enzymes and proteins containing pleckstrin-homology (PH) domains which are able to bind phospholipids. The 3-Phosphoinositide-dependent kinase-1 (PDK-1) is one such kinase and activates a family of serine/threonine kinases grouped under the acronym of AGC kinases (41), these include $p70^{s6k}$, Akt, and SgK isoforms. It has been shown that autophosphorylation of PDK-1 on Ser-241 residue is required for full kinase activity (42). Interestingly the global deletion of PDK-1 in mice results in embryonic lethality, while hypomorphic alleles are associated with decreased cell size (43).

The Akt kinase (also known as PKB) was initially thought to play a major role in insulin signalling because of its rapid insulin-dependent activation (44) and ability to mimic many of insulin's actions when overexpressed (45). It is now accepted that Akt activates a number of downstream targets to mediate insulin effects upon cell growth and metabolism. Activation of Akt requires phosphorylation of Thr-308 in the activation loop and Ser-473 in the C- terminal hydrophobic motif.

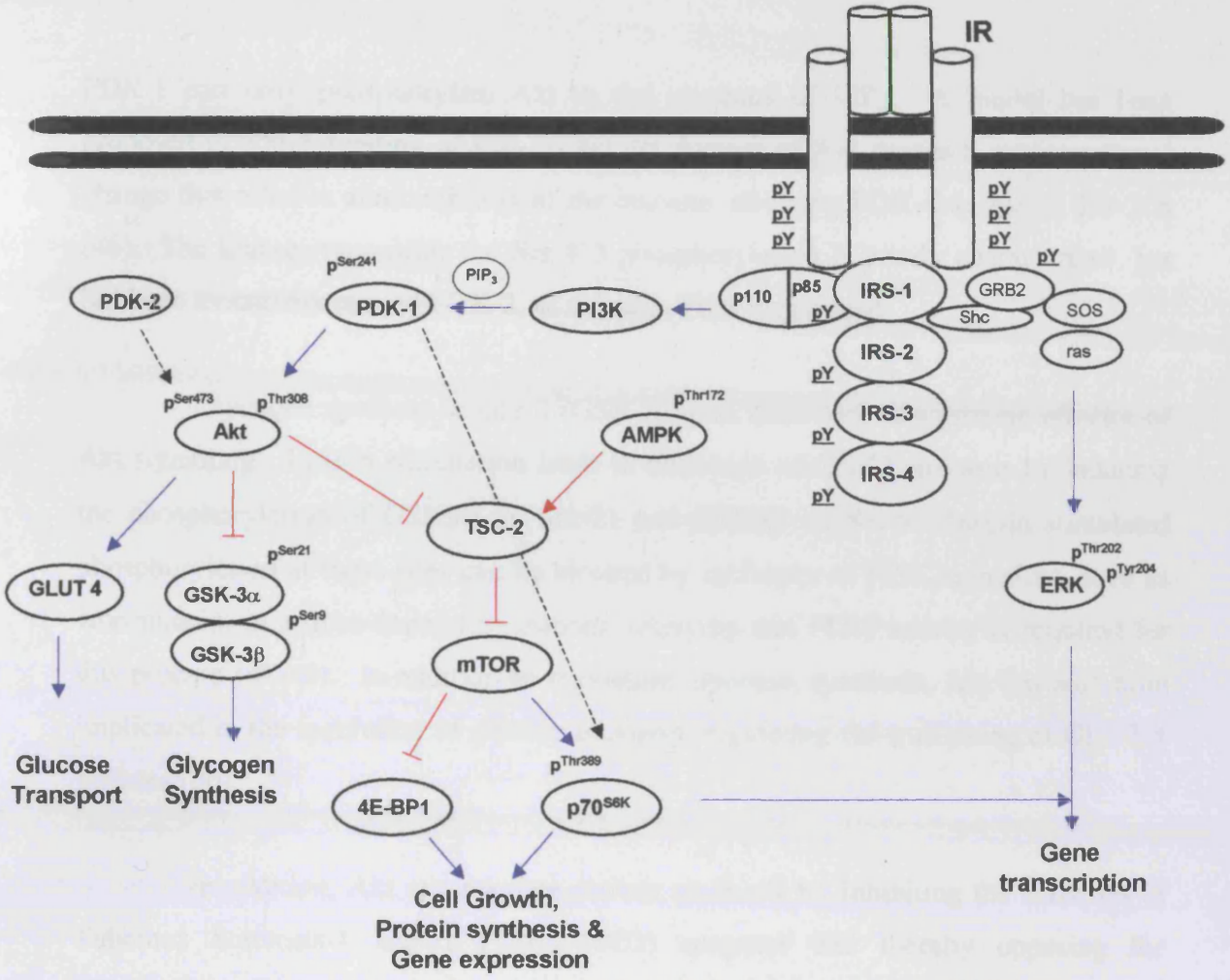

Figure 1.4 Simplified insulin signalling cascade

Insulin binds to its transmembrane receptor, stimulating receptor autophosphorylation and activation of the intrinsic kinase activity, resulting in tyrosine phosphorylation of several cytosolic docking proteins called insulin receptor substrate (IRS) proteins. Cellular responses to insulin, especially those that are associated with somatic growth and carbohydrate metabolism, are largely mediated through IRS-1 and IRS-2. Once phosphorylated IRS proteins bind to various effector molecules including the regulatory subunit of phosphoinositide 3-kinase (PI3K) via Src homology 2 (SH2) domains. The lipid products of the PI3K enzyme, particularly PIP_3 recruit and activate enzymes containing Pleckstrin-homology (PH) domains. These include Akt (also known as PKB), which requires phosphorylation at Ser473 to become fully active. Akt is capable of regulating glucose transport, glycogen synthesis by inhibiting the activity of the Glycogen Synthase Kinase enzyme by phosphorylating residues Ser-9 (GSK-3β) and Ser-21 (GSK-3α). In addition, Akt can regulate protein synthesis by inhibiting the activities of Tuberous Sclerosis-1 and 2 (TSC1-TSC2) enzymes and thereby opposing the stimulatory actions of AMP-activated Protein Kinase (AMPK). It is also known that the mitogenic effects of insulin are mediated by the MAP-kinase signalling pathway. Indeed, it is likely that there is much crosstalk between the metabolic and mitogenic limbs of insulin signalling.

PDK-1 can only phosphorylate Akt in the presence of PIP_3. A model has been proposed in which binding of PIP_3 to the PH domain of Akt causes a conformational change that relieves autoinhibition of the enzyme, allowing PDK-1 access to Thr-308 (46). The kinase responsible for Ser-473 phosphorylation is poorly characterised, but has been tentatively termed PDK-2, as it is also PI3K-dependent.

Glycogen synthase kinase 3 (GSK-3) is an important downstream effector of Akt signalling. Insulin stimulation leads to inhibition of GSK3 isoforms by inducing the phosphorylation of GSK3α on Ser-21 and GSK3β on Ser-9. Insulin stimulated phosphorylation at these sites can be blocked by inhibitors of PI3K signalling, such as wortmannin, in a dose-dependent manner, implying that PI3K activity is required for this process (47-49). In addition to regulating glycogen synthesis, Akt has also been implicated in the regulation of glucose transport, regulating the trafficking of GLUT 4 vesicles (50).

In addition, Akt can regulate protein synthesis by inhibiting the activities of Tuberous Sclerosis-1 and 2 (TSC1-TSC2) enzymes and thereby opposing the stimulatory actions of AMP-activated Protein Kinase (AMPK) (51). TSC-1 and TSC-2 have an inhibitory role on the mammalian Target of Rapamycin (mTOR), which mediates protein synthesis by its stimulatory effects upon elongation factor-4E binding protein (4E-BP1) and the p70 ribosomal s6 protein kinase ($p70^{s6k}$) (51). The $p70^{s6k}$ protein is responsible for phosphorylation of the 40 S ribosomal protein S6 and thereby regulates the translation of several hundred mRNAs. These mRNAs largely encode proteins necessary for the assembly of the translational machinery, including ribosomes and elongation factors (52). Insulin-stimulated activation of the PDK/Akt signalling pathway has been implicated in the activation of the p70 ribosomal s6 protein kinase ($p70^{s6k}$). However, the initial step in $p70^{s6k}$ activation appears to involve a phosphorylation-induced conformational change in the C-terminus of the kinase domain, revealing additional phosphorylation sites. The activation of MAP-kinase has been implicated in this initial phosphorylation event (53).

Other effector molecules that bind to IRS proteins include the Grb2/SOS complex, which bind p21ras to activate the Mitogen Activated Protein Kinase (MAPK) cascade (Erk1/Erk2). Activation of the MAPK cascade leads to phosphorylation and

activation of various transcription factors (ie. elk1, c-*fos*) which then mediate the mitogenic effects of insulin.

1.6.2 Leptin receptor signalling cascade

The leptin receptor was first isolated from the mouse choroid plexus using an expression cloning strategy (54). It does not have homology to the insulin receptor but belongs to the cytokine receptor family and consists of a single membrane spanning domain. Alternative splicing of the LepR gene results in the expression of at least six leptin receptor isoforms, Ob-Ra, OB-Rb, Ob-Rc, Ob-Rd, Ob-Re and Ob-Rf (Fig 1.5). These isoforms are expressed in a tissue-specific manner, having an identical extracellular ligand-binding domain at the amino terminus but differ from one another at the carboxy terminus. Five isoforms, Ob-Ra, Ob-Rb, Ob-Rc, Ob-Rd, and Ob-Rf have transmembrane domains; with the Ob-Rb (the long receptor isoform) believed to be the primary receptor that mediates leptin-induced signal transduction (55). However, several studies have reported that short isoforms of the receptor are capable of mediating signal transduction (56-58) (see below). Upon leptin binding the receptor recruits and activates a member of the janus kinase (Jak) family, primarily Jak2 (59). Once activated, Jak molecules phosphorylate the intracellular domain of the leptin receptor, creating a binding site for the signal transducers and activators of transcription (STAT) molecules. In response to leptin stimulation, activated STAT-3 translocates to the nucleus where it functions as a transcription factor (59). Intracellular negative feedback to this signalling system is provided by a family of suppressor of cytokine signalling (SOCS) molecules that are synthesized in response to STAT-3 activation following leptin stimulation. Leptin receptor activation is also known to activate ERK-regulated pathways (59) (Fig 1.5).

The fact that STAT-3 can also be activated by a number of cytokines, suggests that it may not play a primary role in leptin function. However, the importance of STAT-3 signalling in relation to leptin's effects upon energy balance *in vivo,* in mice was demonstrated by the ablation of tyrosine phosphorylation at Tyr^{1138}, by the replacement of the Tyr^{1138} residue with a serine residue on the leptin receptor (Y1138S mutant mice).

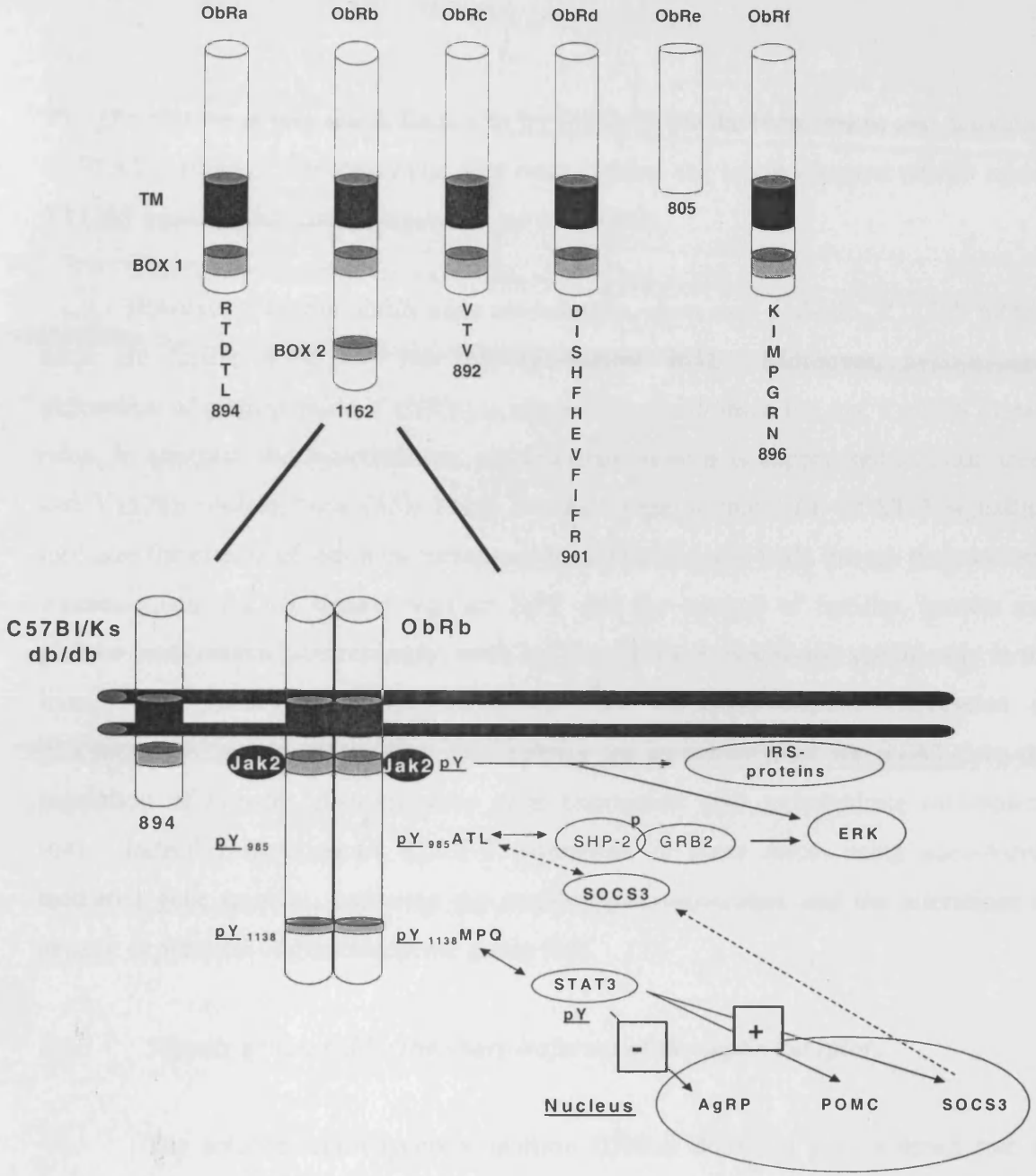

Figure 1.5 Leptin signalling cascade

There are at least six leptin receptor isoforms, Ob-Ra, OB-Rb, Ob-Rc, Ob-Rd, Ob-Re and Ob-Rf. The long form the Ob-Rb receptor contains intracellular motifs required for activation of signal transducer and activator of transcription 3 (STAT-3) molecules. Upon leptin binding the receptor recruits and activates a member of the janus kinase (Jak) family, primarily Jak-2 (59) Activated, Jak molecules phosphorylate the intracellular domain of the leptin receptor, at Tyrosine residues 985 and 1138. Phosphorylation at Tyr985 leads to activation of ERK signalling pathway via recruitment of SH2-containing tyrosine phosphatase (SHP-2), whilst phosphorylation at Tyr1138 leads to recruitment and activation of STAT-3 molecules. In response to leptin stimulation, activated STAT-3 translocates to the nucleus where it acts as a transcription factor, activating leptin-dependent gene transcription (59). Negative feedback to leptin signalling is achieved by the Suppressor of Cytokine Signalling 3 (SOCS3) molecules binding to phosphorylated Tyr985 residues on the leptin receptor.

Phosphorylation at this site is known to be essential for the recruitment and activation of STAT-3 (60-62). Interestingly, like mice lacking the leptin receptor (*db/db* mice), Y1138S mutant mice are hyperphagic and obese (63).

However whereas *db/db* mice are infertile, short and diabetic, Y1138S mutant mice are fertile, long and less hyperglycaemic (63). Moreover, hypothalamic expression of neuropeptide Y (NPY) is elevated in *db/db* mice but not Y1138S mutant mice. In contrast, the hypothalamic melanocortin system is suppressed in both *db/db* and Y1138S mutant mice (63). These findings suggest that LRb-STAT-3 signalling mediates the effects of leptin on melanocortin production and body energy homeostasis, whereas distinct LRb signals regulate NPY and the control of fertility, growth and glucose homeostasis. Interestingly, mice lacking STAT-3 expression specifically in the liver, show insulin resistance associated with increased hepatic expression of gluconeogenic genes (64). Thus highlighting an important role for STAT-3 in the regulation of hepatic gluconeogenic gene expression and carbohydrate metabolism (64). Indeed restoration of STAT-3 expression in these mice, using adenovirus-mediated gene transfer, corrected the metabolic abnormalities and the alterations in hepatic expression of gluconeogenic genes (64).

1.6.3 Signals generated by the short-isoforms of the leptin receptor:

The soluble leptin receptor isoform (ObRe) does not play a direct role in leptin signalling but is likely to be important in determining the amount of circulating free leptin (65). Indeed, the proportion of leptin circulating in the free and protein-bound form may be an important physiological determinant of leptin action (66). Considering the other leptin receptor isoforms, whereas the ObRb long-isoform contains an intracellular domain of approximately 306 amino acids, the short-isoforms contain an intracellular domain ranging between 32-40 amino acids. However common between these receptor isoforms is an identical 29 amino acid sequence, containing a "Box 1" Janus-family tyrosine kinase (JAK) binding domain in the juxtamembrane region (as shown in Fig 1.5). In addition to this "Box 1" JAK-binding domain, the ObRb isoform also contains a "Box 2" motif. As described above this region has been

shown to be essential for leptin to recruit and activate the STAT-3 transcription factor (59).

Interestingly, expression of ObRb is highest in the hypothalamus (67), yet, it is also found in many peripheral tissues at lower levels (68, 69). In contrast, the ObRa isoform is expressed fairly ubiquitously and represents the major isoform of many peripheral tissues (67, 70). However, it should be noted that examination of ObR isoform expression by RT-PCR has often been inconsistent (71).

Although the ObRb long-isoform receptor has been proposed as the "signalling isoform", there is clear evidence that the short receptor isoforms are capable of initiating signal transduction, even showing divergent signalling capacities (57, 58, 72). Indeed the mechanism underlying the stimulation of PI3K by leptin often involves phosphorylation of the IRS proteins. In some cells (57, 72-74), but not all (75) leptin can induce phosphorylation of IRS proteins, often via the activation of JAK proteins. For example, tyrosine phosphorylation of IRS-1 was increased by leptin in HEK293 cells coexpressing the long or short form of leptin receptor, with JAK2 and IRS-1 (57). It has also been demonstrated that leptin increased PI3K activity in C_2C_{12} cells via a JAK2- and IRS-2-dependent mechanism (72). Indeed, the activation of PI3K by either long or short form leptin receptor mechanisms may be an important potential point of crosstalk between the insulin and leptin signalling pathways (see below).

1.7 Murine models of obesity and type 2 diabetes: insights into leptin and insulin signalling

Much of our current understanding of both the cellular and molecular activities of leptin and insulin has been derived from studies of murine models of obesity and diabetes. These models include spontaneously occurring mutants as well as a variety of models generated either by transgenic or gene-targeting approaches. The use of such models has been reviewed extensively elsewhere (38, 76) and for the purposes of this thesis, only models utilised in the current studies will be described in detail.

1.7.1 Ob and db mice: spontaneous mouse mutants of leptin action

Recessive mutations in the mouse obese (*ob*) and diabetes (*db*) genes result in obesity and later develop diabetes in a syndrome that resembles morbid human obesity (77, 78). *ob/ob* mice maintained on the C57Bl/6J genetic background arise due to a non-sense mutation in the leptin gene, which results in a truncated protein that is degraded in the adipocyte (21). Similarly, a spontaneous G to T point mutation in the genomic ObRb sequence in *db/db* mice, results in the generation of a donor splice site that converts a 106 nucleotide region to a novel exon retained in the ObRb transcript (79). This splice variant creates a premature stop codon resulting in a truncated protein resembling the ObRa receptor isoform and hence loss of Jak-STAT box binding motifs.

Both *ob/ob* and *db/db* mice have similar phenotypes, each weighing up to three times more than normal mice (even when fed the same diet) and both exhibit a five-fold increase in body fat content. The *ob/ob* mice show many of the abnormalities seen in starved animals, including decreased body temperature, hyperphagia, decreased energy expenditure (including activity), decreased immune function, and infertility (77). Administration of leptin to *ob/ob* mice corrects all of these abnormalities, implying that *ob/ob* mice exist in a state of "perceived starvation" and that the resulting biological response in the presence of food leads to obesity. *db/db* are resistant to the effects of leptin implicating the long-form of the receptor in mediating the physiological actions of this hormone.

Initial findings in *ob/ob* mice implicated leptin as a satiety factor that potentially could act as an anti-obesity drug. However the fact that most cases of obesity are associated with high circulating leptin levels indicated that leptin resistance contributes significantly to the obese phenotype. Indeed the role of leptin is now considered to be far more complex, acting as a messenger between the CNS and periphery to report whole-body energy status. More recently leptin receptors have been deleted specifically in POMC neurons in mice. These mice were mildly obese, hyperleptinemic, and had altered expression of hypothalamic neuropeptides (80). This finding highlights the importance of leptin receptors in POMC neurons. However the

milder obesity suggests that leptin action in other neuronal populations is essential for complete regulation of body weight homeostasis.

1.7.2 β-HypSTAT3KO mice

The importance of leptin signalling in the regulation of energy homeostasis has been further demonstrated by the deletion of STAT-3 specifically in the β-cell of mice (β-HypSTAT3KO) (81, 82). Deletion was achieved by using a transgene expressing Cre-recombinase driven by the rat insulin promoter. These mice were glucose intolerant as early as five weeks of age as a result of a deficiency in early-phase insulin secretion. In addition β-HypSTAT-3KO mice also displayed impaired islet morphology, with α-cells frequently appearing in central regions of the islets (81, 82). Unexpectedly, these mice also exhibited partial leptin resistance, becoming hyperphagic and obese at eight weeks of age or older. This impairment to appetite control is believed to result from the expression of the rat insulin II promoter (RIP)-cre transgene in the hypothalamus, leading to deletion of STAT-3 in hypothalamic regions implicated in the control of food intake (81, 82).

1.7.3 Insulin receptor substrate (IRS) 2 knockout mice

Another murine model that results in the development of an insulin resistant metabolic phenotype is the insulin receptor substrate 2 knockout mouse (83). These mice were generated by standard murine gene targeting strategies and lack expression of *Irs-2* in all tissues. *Irs-2* null mice exhibit mild peripheral insulin resistance and β-cell deficiency at birth but have adequate compensatory insulin secretion for several weeks. However, subsequent relative β-cell failure in the face of continued peripheral insulin resistance causes overt fasting hyperglycaemia without ketoacidosis, the common characteristic of human type 2 diabetes (5). As well as developing a diabetic phenotype, global deletion of *Irs-2* also results in an increase in food intake, this being particularly evident in female mice. Deletion of *Irs-2* also causes an increase in fat stores despite elevated plasma leptin levels. These findings not only suggest the

presence of CNS leptin resistance but also suggest that insulin action in the CNS or that components of the insulin signalling pathways are also necessary for intact neuronal responsiveness to leptin. Indeed, STAT-3 phosphorylation in response to leptin is defective in *Irs-2* null mice suggesting some signalling convergence between leptin and insulin (84). Such findings support the notion that *Irs-2* may act as a convergence point for insulin and leptin signalling in the CNS. The demonstration of a role for insulin signalling pathways in the central regulation of energy homeostasis has also been supported by deletion of the insulin receptor in the brain of mice (31), which also resulted in mice with pathological expansion of fat stores despite elevated leptin levels. Furthermore, both *Irs-2* null mice and brain-specific insulin receptor null mice have defects in reproductive function (84). Infertility is a significant feature of the phenotype of *ob/ob* and *db/db* mice as described above. Taken together, these findings have therefore added increased evidence for convergence in the physiological roles of insulin and leptin upon the central regulation of energy homeostasis.

1.7.4 β-HypIRS2KO mice

Recently, our laboratory and others have attempted to address the importance of β-cell autonomous IRS-2 dependent signalling by generating mice lacking IRS-2 specifically in β-cells. Firstly, mice were generated in which both alleles of the *Irs-2* gene were floxed (flanked by LoxP DNA recombination sites). Once generated these mice were bred with the rat insulin II promoter (RIP)-cre transgenic mice (as described above for β-HypSTAT3 KO mice). This transgenic mouse had previously been used to delete a number of floxed alleles in the pancreatic β-cell (85, 86). However early analysis of these mice revealed that they had an obvious hypothalamic phenotype. Further examination of the distribution Cre-recombinase was determined using ZEG fluorescent indicator mice and showed that in addition to the β-cell, Cre was also expressed in a population of neurons within the hypothalamus (87-89). It was noted that β-HypIRS2KO mice progressively developed glucose intolerance and pancreatic morphometric analysis showed that by 12 weeks of age they had a 40% reduction in islet mass and number compared to controls mice (87). In contrast to *Irs-2* null mice, β-

HypIRS2KO mice did not develop marked fasting blood glucose levels, β-cell failure and a progressive diabetic phenotype.

These findings demonstrate that intrinsic β-cell IRS-2 signalling pathways are important for islet function and in particular the development and maintenance of β-cell mass. Although β-cell-specific deletion of IR or IGF-1R in mice did not result in such a profound defect in β-cell mass, their combined β-cell-specific deletion has not been reported. It follows that IRS-2 could either mediate the combined effects of these receptors upon islet function or the actions of other, as yet uncharacterised receptors upon β-cell mass (87). Moreover the resulting obesity phenotype in these mice implicates IRS-2 signalling pathways as being important in hypothalamic function.

1.8 Peripheral metabolic actions of leptin and insulin

It is evident from such physiological studies that insulin and leptin have complex and often convergent physiological roles in the regulation of whole body energy homeostasis (19). For example, both leptin and insulin have been implicated in regulating β-cell function. Leptin has been shown to modulate insulin secretion reducing its release (90, 91). Insulin signalling mechanisms have been shown to regulate insulin production and secretion and regulate β-cell development and growth (85, 92). Cross talk between insulin and leptin is complex with their relative sensitivity in one metabolic tissue having dramatic effects upon their sensitivity in other tissues. More recently it has been suggested that insulin and leptin utilise common signal transduction processes to mediate their physiological effects (16, 19).

I will now review the evidence for insulin and leptin interaction in each of the major peripheral metabolic tissues. I will then describe some of signalling intermediates that have been shown to mediate insulin and leptin action, highlighting, the potential for direct interaction between insulin and leptin signalling.

1.8.1 Skeletal muscle

The accumulation of lipid deposits in non-adipose tissues, termed "lipotoxicity", is suggested to be a major cause of insulin resistance and other complications associated with obesity. Leptin has a protective effect against lipotoxicity in non-adipose tissues (93, 94). Leptin may regulate lipid metabolism by promoting the oxidation of fatty acids, rather than their storage (94).

Both *in vitro* and *in vivo* studies have highlighted the importance of leptin in promoting muscle fatty acid (FA) oxidation (93, 95). In contrast, exposure to insulin had the opposite effect upon muscle FA metabolism, reducing FA oxidation and promoting Triacylglyceride (TAG) synthesis. Interestingly, when both hormones were added together, leptin could attenuate insulin's antioxidative and lipogenic effects upon lipid utilization (95, 96). How leptin exerts its effects upon lipid metabolism is still not fully understood. As described above the AMP-activated protein kinase (AMPK) has been identified as a principle mediator of leptin's effects on fatty-acid metabolism in muscle. However the activation of AMPK can occur through both direct and indirect actions of leptin upon skeletal muscle, suggesting a complex role for AMPK in mediating the effects of leptin on fatty-acid metabolism.

In humans, skeletal muscle is the primary site of insulin-dependent glucose disposal (97). Resistance of skeletal muscle to insulin-dependent glucose uptake and phosphorylation is an early step in the development of type 2 diabetes (98). Surprisingly, conditional deletion of the insulin receptor in the muscle of mice (Muscle Insulin Receptor Knockout (MIRKO)) led to impaired insulin signalling and decreased insulin-dependent glucose transport but did not result in systemic insulin resistance (99). Two alternative pathways of glucose uptake that compensate for the decreased insulin receptor signalling are thought to prevent the development of systemic insulin resistance. These are Igf1r (100) and contraction-activated signalling (101), the latter acting again through AMPK.

1.8.2 Adipose tissue

Adipose tissue had traditionally been considered to function as an energy store, for times of energy depletion (ie. during times of starvation). However, the identification that a number of hormonal substances (including leptin) were synthesised and secreted mainly from adipocytes, suggested that adipose tissue represented an important endocrine organ, being capable of regulating a number of physiological and pathophysiological conditions, such as satiety, energy expenditure, insulin sensitivity, glucose homeostasis (102).

As described above it is clear that leptin deficiency in the *ob/ob* mouse, which results in massive obesity, is associated with insulin resistance. However, it has also been shown that in two distinct lipodystrophic murine models, leptin deficiency resulting from a lack of white adipose tissue can also lead to severe insulin resistance (103, 104).

The insulin-regulated transcription factor Sterol regulatory element binding protein-1c (SREBP-1c), is known to activate the transcription of multiple genes, including those encoding enzymes responsible for the synthesis of cholesterol and fatty acids in cells (105). In *aP2-SREBP-1c* (1-436) mice, a transgene expresses a truncated dominant-positive fragment of SREBP-1c (amino acids 1-436) under control of the fat-specific aP2 promoter. Unexpectedly, this truncated form of the SREBP-1c interferes with adipose tissue differentiation, creating a syndrome similar to that of congenital lipodystrophy in humans. The lack of white adipose tissue in these animals leads to a marked reduction in circulating leptin levels, leading to hyperphagia, hyperglycaemia and insulin resistance (14). Moreover, these lipodystrophic mice contained fatty livers, similar to those seen in *ob/ob* mice. Interestingly, such abnormalities in the liver and plasma of these lipodystrophic mice, like those of the *ob/ob* mice, can be reversed by the peripheral administration of recombinant leptin (106). Indeed, restoration of physiologic leptin levels over a 12-day period led to a decline in plasma insulin and glucose levels to normal, and the excess hepatic fat largely disappeared (106). Similar findings have been found in human subjects with lipodystrophy.

The adipose hormone adiponectin has recently been implicated in the regulation of insulin sensitivity. Indeed both the mRNA expression of adiponectin and its plasma levels are significantly reduced in obese/diabetic mice and humans (107, 108). It has also been demonstrated that these reduced expression levels of adiponectin coincide with insulin resistance in murine models of altered insulin sensitivity. Furthermore, treatment with physiological doses of adiponectin improved insulin resistance in mouse models of lipoatrophy and obesity (109). Such observations suggest that leptin or other adipose tissues products such as adiponectin or the hormone resistin may play roles in the regulation of insulin sensitivity, potentially acting in peripheral tissues or the CNS.

Despite adipose tissue accounting for only ~10% of glucose uptake (110, 111), it is a major site of insulin action. Insulin is known to act upon adipocytes to promote adipogenesis, stimulate glucose uptake and lipid synthesis, and inhibit lipolysis (112). In particular it is believed that insulin can act upon adipose tissue to regulate both the production and secretion of leptin (113).

Specific deletion of the insulin receptor in both white and brown fat (Fat Insulin Receptor Knockout (FIRKO)) in mice, resulted in a ~50% reduction in fat pad mass and a ~30% decrease in whole body triglyceride content, with normal circulating lipids, free fatty acids and glycerol levels. Moreover, FIRKO mice are resistant to gaining weight during aging or following induction of a hypothalamic lesion leading to hyperphagia. Consequently these mice display normal glucose tolerance and fail to develop impaired glucose tolerance despite hyperphagia (114). A further observation of FIRKO mice is that they exhibit inappropriately high leptin levels for their reduced fat mass.

The importance of insulin signalling in adipose tissue was further demonstrated by the generation of mice with combined global deletions for IRS-1 and IRS-3. These mice developed early-onset severe lipoatrophy associated with marked hyperglycaemia, hyperinsulinaemia and insulin resistance (115). These findings indicate that IRS-1 and IRS-3 have important complementary roles in adipogenesis. Interestingly, adenovirus-mediated expression of leptin in the livers of these mice

reversed the hyperglycaemia and hyperinsulinaemia, highlighting the complex interplay between leptin and insulin sensitivity.

1.8.3 Liver

The liver plays a central role in the control of glucose homeostasis and is subject to complex regulation by insulin and leptin (116-118). Insulin acts upon the liver to suppress glucose output by inhibiting glycolysis and gluconeogenesis. Insulin resistance in the liver and, in particular, the loss of the ability to suppress hepatic glucose output are closely linked to fasting hyperglycaemia in type 2 diabetes. Liver-specific deletion of the insulin receptor in mice (LIRKO mice) results in severe insulin resistance and overt glucose intolerance as early as two months of age (118). The ability of insulin to inhibit gluconeogenesis could be due to a direct effect of insulin on the liver, or could arise due to secondary effects of insulin action on muscle and fat, leading to a reduction in the supply of gluconeogenic precursors. The observation that LIRKO mice are resistant to the actions of exogenous insulin to suppress hepatic glucose production, whilst presumably suppressing lipolysis and the release of gluconeogenic precursors from muscle and fat, indicates that the direct effects of insulin on the liver are important in regulating gluconeogenesis in wild-type animals.

Assessment of insulin signalling in the livers of *ob/ob* mice demonstrated a significant reduction in the expression of both IRS-1 (29%) and IRS-2 (72%). Moreover this reduction led to a differential decrease in hepatic IRS-1 and IRS-2 phosphorylation, binding of the p85α regulatory subunit of PI3-Kinase, and the activation of PI3-Kinase in the livers of *ob/ob* mice (119).

As described above, mice with too little fat (lipodystrophy) or too much fat (*ob/ob*), display insulin resistance. In both these disorders, the liver overproduces glucose as a result of resistance to the actions of insulin to inhibit hepatic gluconeogenesis. Shimomura et al, utilised aP2-SREBP-1c and *ob/ob* mice to examine hepatic gene expression and explore how hepatic insulin signalling is effected by these insulin resistant states. The livers of both aP2-SREBP-1c and *ob/ob* mice exhibit both decreased IRS-2 mRNA expression and insulin stimulated Akt activity. Despite the decrease in IRS-2 expression and decreased levels of phosphorylation of Akt, insulin

continues to increase the mRNA for SREBP-1c in the liver, suggesting that insulin activates SREBP-1c by an IRS-2 independent pathway. Furthermore, this alternative pathway allows insulin to continue to stimulate SREBP-1c activity and lipogenesis in the livers of insulin-resistant animals. Increased lipogenesis, in addition to the inappropriate gluconeogenesis caused by insulin resistance creates a vicious cycle that increases insulin secretion and hence aggravates insulin resistance. More recently, it has been reported that SREBP molecules are actually capable of directly repressing the transcription of IRS-2 and inhibiting glycogen synthesis (120). Interestingly, the livers of *Irs-2* null mice are reported to exhibit increased hepatic SREBP-1 gene expression (121). Moreover, increased expression was also noted in genes downstream of SREBP-1, many of which are involved in fatty acid synthesis (121). These findings provide a molecular mechanism for the physiological switching from glycogen synthesis to lipogenesis and hepatic insulin resistance that is associated with hepatosteatosis.

The above findings implicate liver as an important site of interaction between insulin and leptin action. Dysregulation of insulin or leptin signalling endogenous to the liver can lead to dramatic alteration in peripheral insulin sensitivity.

1.8.4 Pancreatic β-cells

Both *ob/ob* and *db/db* mice exhibit hyperinsulinaemia even prior to development of their obese and diabetic phenotypes (122-124) suggesting that functional leptin signalling is important in the regulation of insulin sensitivity. The observation that mRNA of the long isoform (ObRb) of the leptin receptor was expressed in high abundance in the pancreatic islets of rodents (125), indicated that leptin might actually contribute to islet function. Interestingly functional leptin receptor expression (including ObRb) has also been demonstrated in β-cells derived from human pancreatic islets (126).

More recently both *in vitro* and *in vivo* assays of β-cell function have suggested that leptin may regulate insulin release, acting to suppress insulin secretion (90, 91, 127). However the exact effects of leptin upon insulin secretion are unclear at present, as most studies have yielded conflicting results (113). The inhibitory actions

of leptin upon insulin secretion appear to be determined by body fat stores. As previously mentioned, insulin can stimulate both leptin biosynthesis and secretion from white adipose tissue. This effect creates an endocrine adipo-insular feedback loop between the β-cell and fat tissue (Fig 1.6).

The adipo-insular axis is thought to play an important role during the development of type 2 diabetes in obese patients. During the development of this disease, hyperinsulinaemia is thought to represent a compensatory response of the pancreatic β-cells to peripheral insulin resistance (128, 129), and hyperglycaemia a consequence of pancreatic β–cell failure.

However, it has also been demonstrated that hyperinsulinaemia often precedes the development of insulin resistance, suggesting that obesity-induced insulin resistance might not fully explain the development of type 2 diabetes. For example, in obese subjects, resistance to the actions of leptin on the pancreatic β-cell could result in dysregulation of the adipo-insular axis, leading to increased insulin production and eventually a state of hyperinsulinaemia. Hyperinsulinaemia could then further promote insulin resistance, whilst increasing leptin production and secretion from adipose tissue. Increased circulating levels of leptin would then be likely to enhance leptin resistance of the β-cells, creating a vicious cycle that encourages the manifestation of type 2 diabetes.

It is now clear that insulin also acts on the pancreatic β-cell, with insulin receptor signalling being implicated in the regulation of insulin synthesis and secretion by the β-cell (85). The studies described above on *Irs-2* null mice have shown that *Irs-2* is required for the β-cell compensatory response to insulin resistance and may mediate the effects of insulin-like growth factor 1 upon islet function (92). Furthermore, it has been demonstrated that mice with β-cell specific deletion of the insulin receptor have defects in insulin secretion and develop glucose intolerance (85).

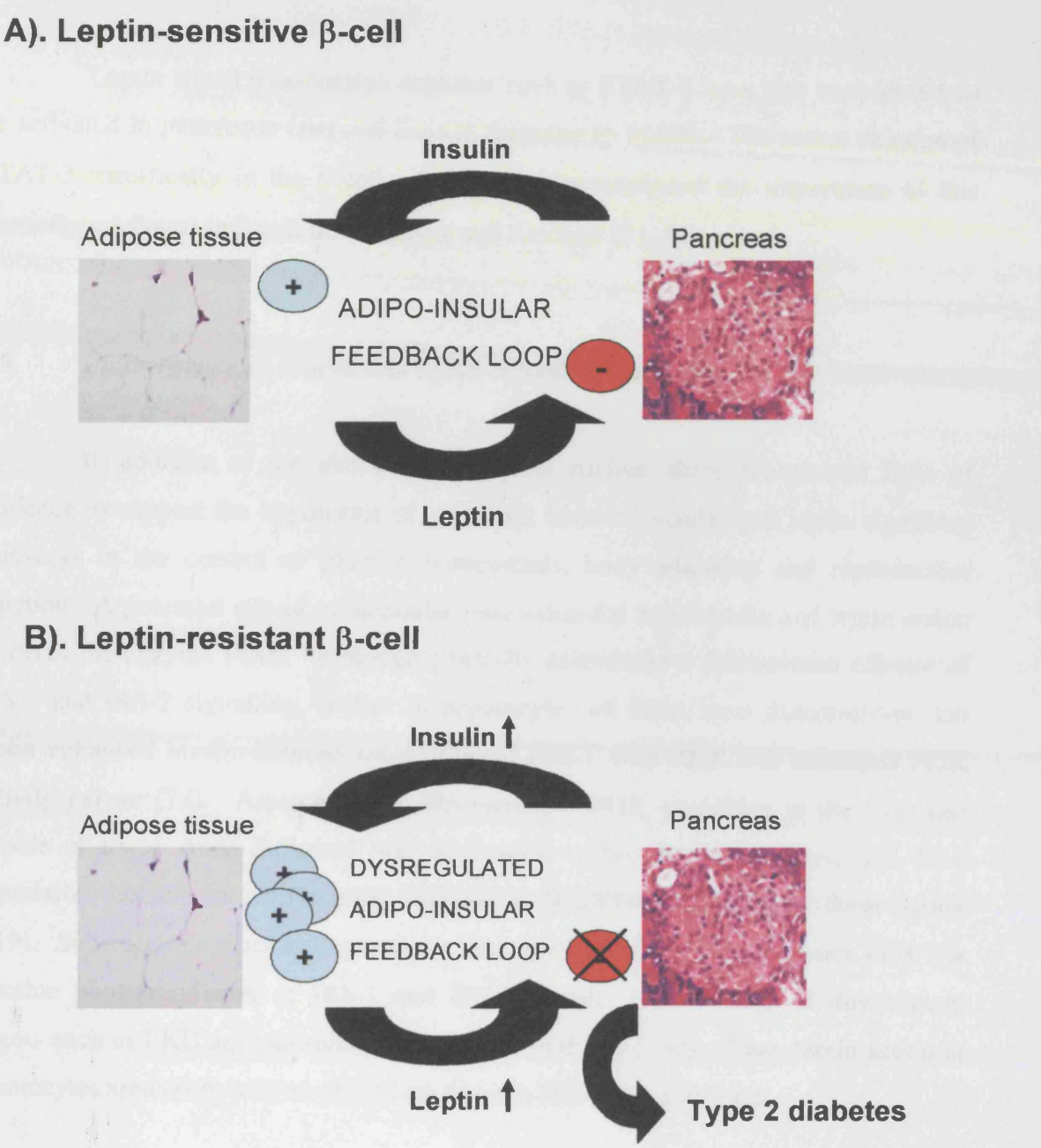

Figure 1.6 Dysregulation of the adipo-insular axis and pathogenesis of type 2 diabetes

A). In leptin-sensitive individuals, leptin is secreted from adipocytes and acts upon the pancreatic β-cells to suppress insulin secretion, regulating glucose homeostasis in accordance with body fat stores. B) In leptin-resistant obese individuals, diminished leptin signalling in pancreatic β-cells leads to hyperinsulinaemia. Elevated insulin levels promote both insulin resistance and increased leptin biosynthesis and secretion from adipose tissue, which may further desensitize leptin signalling in the endocrine pancreas and increase leptin resistance. Hypersecretion of insulin could eventually result in β-cell failure and the manifestation of type 2 diabetes.

Leptin signal transduction elements such as STAT-3 have also been shown to be activated in pancreatic islet cell lines in response to insulin. The recent deletion of STAT-3 specifically in the β-cell of mice has demonstrated the importance of this transcription factor in β-cell development and function (81, 82).

1.9 Convergence of insulin and leptin signalling pathways

In addition to the above physiological studies, there are several lines of evidence to support the hypothesis of cross-talk between insulin and leptin signalling pathways in the control of glucose homeostasis, body adiposity and reproductive function. A potential site of intracellular interaction for both insulin and leptin action involves the enzyme PI3K. Although generally considered a downstream effector of IRS-1 and IRS-2 signalling, studies in hepatocyte cell lines, have demonstrated that leptin enhanced insulin-induced association of IRS-1 with PI3K and increased PI3K activity *per se* (73). Assessment of IRS-mediated PI3K signalling in the liver and muscle of *ob/ob* mice indicated that these mice exhibited reduced *Irs-1* and *Irs-2* expression, leading to a differential decrease in IRS/PI3K signalling in these tissues (119). Subsequent studies in hepatocytes, demonstrated that leptin activates PI3K via tyrosine phosphorylation of IRS-1 and IRS-2 leading to activation of downstream targets such as PKB and phosphodiesterase 3B (PDE3B) (130). Thus, leptin action in hepatocytes appears to involve signalling through IRS-PI3K pathways.

The central actions of leptin may also be mediated through PI3K signalling. Electrophysiological experiments investigating the effects of leptin on hypothalamic neurons in rat brain slice cultures, showed that leptin caused a population of hypothalamic neurons in the arcuate and ventromedial nuclei to hyperpolarize through the activation of ATP-sensitive K+ channels (131). The same population of neurons were also hyperpolarized by insulin, indicating that the acute cellular effects of insulin and leptin might converge. Hence, an intracellular signalling pathway might exist in which activation of PI3K is the target not only of insulin signalling, but also of leptin signalling (Fig 1.7). In support of this model, the ability of insulin to regulate the firing of certain arcuate nucleus neurons is blocked by inhibitors of PI3K (132). Blocking of neuronal PI3K signalling, *in vivo,* using a specific PI3K inhibitor, resulted in complete

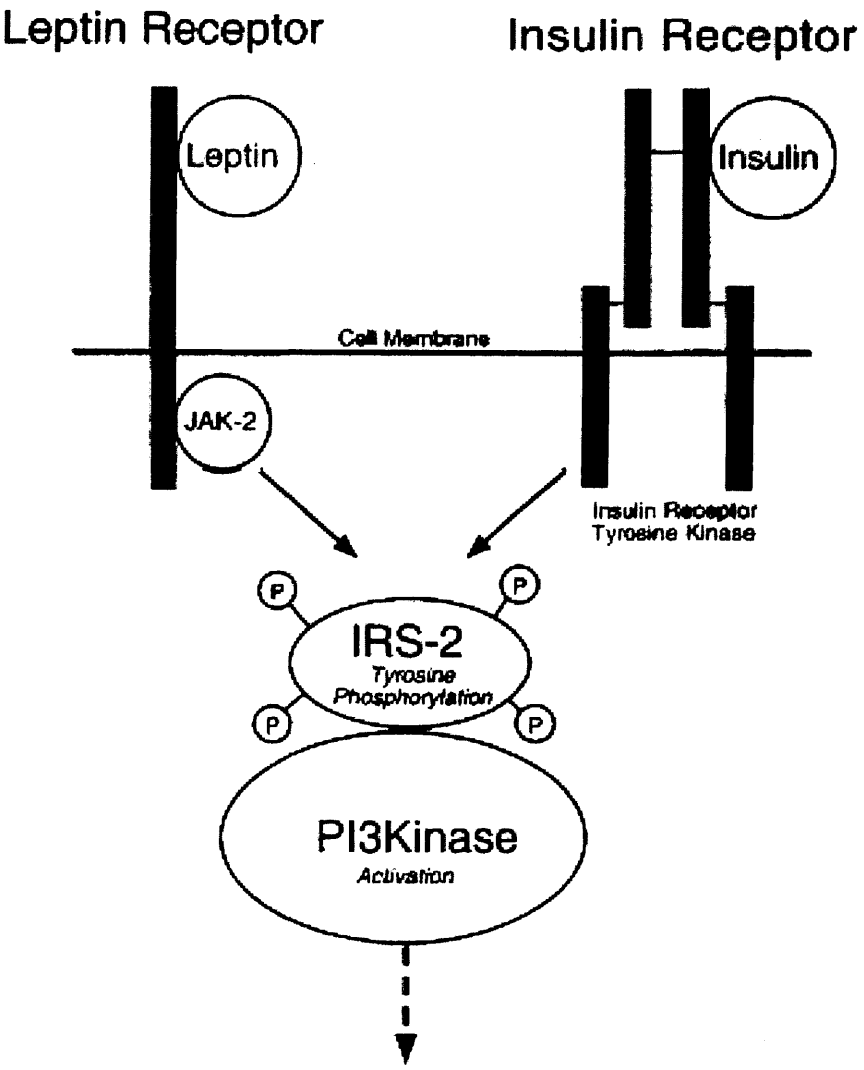

Regulation of energy homeostasis.

Figure 1.7 Potential cross-talk between insulin and leptin intracellular signalling via the enzyme, phosphoinositide 3-kinase (PI3Kinase)

The insulin receptor tyrosine kinase catalyzes the tyrosine phosphorylation of the insulin receptor substrate-2 (IRS-2) protein, which associates with PI3Kinase, resulting in activation of PI3Kinase enzyme activity and downstream signal transduction. It is hypothesized that JAK-2 can act through a similar, IRS-dependent mechanism to activate PI3Kinase. Both the leptin and insulin receptors interact with numerous other signal transduction pathways that are not shown but could be involved in the regulation of energy homeostasis (Adapted from (16)).

prevention of leptin-induced anorexia, as compared with control animals given a vehicle injection (132). It is evident that reduced PI3K signalling is a key factor that underlies insulin resistance in the periphery. Similar mechanisms could be mirrored in the brain, where resistance to both leptin and insulin at the level of PI3K might contribute to the onset of both obesity and diabetes.

A further potential site of convergence of leptin and insulin action in the regulation of glucose and energy homeostasis is the AMP-activated protein kinase (AMPK). This family of heterotrimeric enzymes are activated by cellular 5' AMP levels and the LKB1 tumour-suppressor protein. Physiological stimuli that activate AMPK include skeletal muscle contraction and the peptide hormones leptin (see above) and adiponectin (34, 133). The findings that the system is activated by exercise, and by adipocytokines involved in the control of appetite, body weight and insulin sensitivity point to its potential importance in energy homeostasis and as a point of convergence of insulin and leptin action.

Numerous *in vitro* studies have demonstrated the suppressor of signalling 3 (Socs3) is a negative regulator of leptin signalling (134, 135). Peripheral leptin administration to mice rapidly induces Socs3 mRNA in hypothalamic regions (135). It has been proposed that Socs3 binds to the activated leptin receptor via its Src homology-2 (SH2) domain and inhibits Jak tyrosine kinase activity through its N-terminal kinase inhibitory region, which functions as a pseudo-substrate (135-137). Evidence from *in vitro* studies has suggested that Socs3 achieves feedback inhibition by binding to Tyr^{985} of the leptin receptor. Moreover, deletion of Socs3 expression in the brains of mice, results in elevated leptin sensitivity and resistance to diet-induced obesity (138). This finding demonstrates the ability of Socs3 to negatively regulate leptin signalling *in vivo* and indicates that suppression of Socs3 in the brain could be of therapeutic value for leptin resistance in obesity. Interestingly, Socs3 has also been implicated as a physiological regulator of insulin signalling in adipocytes. Findings from 3T3-L1 adipocytes deficient for Socs3 showed these adipocytes had an increased IRS-associated PI3K activity (139). In addition lack of Socs3 substantially limited the inhibitory effects of tumour necrosis factor-α to suppress IRS-1 and IRS-2 tyrosine phosphorylation, PI3K activity, and glucose uptake in adipocytes (139). Such observations would suggest that endogenous Socs3 expression is a determinant of basal

insulin signalling in adipocytes and therefore may play an important role in mediating cytokine-induced insulin resistance in the adipocyte. Taken together these findings both *in vitro* and *in vivo* highlight the importance of Socs3 and implicated it as a potential mediator of both insulin and leptin signalling.

1.10 Summary

Insulin and leptin have complex and convergent physiological roles in the regulation of whole body energy homeostasis (19). Leptin is thought to predominantly work in the central nervous system to regulate adiposity through the control of food intake and energy expenditure. Insulin is primarily considered to act in insulin-sensitive peripheral tissues such as skeletal muscle, adipose tissue and liver, regulating glucose and lipid metabolism.

In addition to these roles both hormones have been implicated in regulating additional physiological processes. For example, insulin also serves as an adiposity signal acting upon the same CNS mechanisms as leptin (16). Both leptin and insulin have been implicated in regulating β-cell function. Leptin has been shown to modulate insulin secretion reducing its release (90, 91). Insulin signalling mechanisms have been shown to regulate insulin production and secretion and regulate β-cell development and growth (85, 92).

The interactions of insulin and leptin are often complex and involve a number of different physiological systems in different tissues. The murine models described above have given some insights into the overlapping roles of these two hormone-signalling pathways. Cross-talk between insulin and leptin can occur at an organ to organ level, for example, it is known that the livers of *ob/ob* mice exhibit reduced *Irs-2* gene expression (119). Similar to *ob/ob* mice, *Irs-2* null mice are infertile, hyperphagic and develop obesity associated with hyperleptinemia and leptin resistance. No such phenotype has been noted in animals null for any of the other IRS proteins (39).

Moreover it has been suggested that insulin and leptin utilise common signal transduction processes to mediate their physiological effects. For example, in mice with targeted disruption of *Irs2*, leptin-stimulated STAT-3 phosphorylation is impaired (84). Similarly, blockade of PI3K activity abrogrates leptin-mediated hyperpolarization and inhibition of LRb/NPY/AgRP hypothalamic neurons (74, 131). Furthermore, leptin stimulates IRS-2-associated PI3K activity in the hypothalamus and pharmacological blockade of PI3K activity in the hypothalamus blocks the anorectic effect of leptin *in vivo* (132). Importantly, inhibition of PI3K does not alter the anorectic effect of melanocortin agonists that operate downstream of LRb expressing neurons, suggesting that this effect of PI3K blockade is specific for LRb expressing neurons. More recently it has been demonstrated that PI3K activity is also required for leptin-regulated sympathetic nervous system function (140).

Moreover, as *in vivo* (132), it has recently been observed that LRb stimulation mediates the tyrosine phosphorylation of IRS proteins and activation of the PI3K pathway in cultured cells. This signal is mediated by Jak2 independently of tyrosine phosphorylation sites on LRb (141).

The recruitment of IRS proteins/PI3K by Jak2 is less robust than by the insulin receptor, however. Indeed, animals with decreased expression of neuronal insulin receptors (Neuronal Insulin Receptor Knockout (NIRKO) mice) display a modest obesity phenotype, similar to that seen in *Irs-2* null mice (31). Also, insulin activates the IRS-2/PI3K pathway in the hypothalamus and PI3K activity is also required for the anorectic activity of insulin in the brain (132).

Furthermore, as described above the deletion of either IRS-2 or STAT-3 function specifically in the β-cell and hypothalamus has demonstrated the importance of these intrinsic pathways to regulate the development and maintenance of β-cell mass, whilst highlighting the importance of insulin and leptin sensitivity in β-cell function (81, 82, 88, 89).

Therefore it has been suggested that IRS2/STAT-3 signalling pathways potentially act as one site of convergence for insulin and leptin action. Studies have suggested that a linear relationship exists between IRS-2 and STAT-3, with IRS-2 being upstream of the events that lead to the phosphorylation of STAT-3. This would lead to the model outlined in figure 1.8.

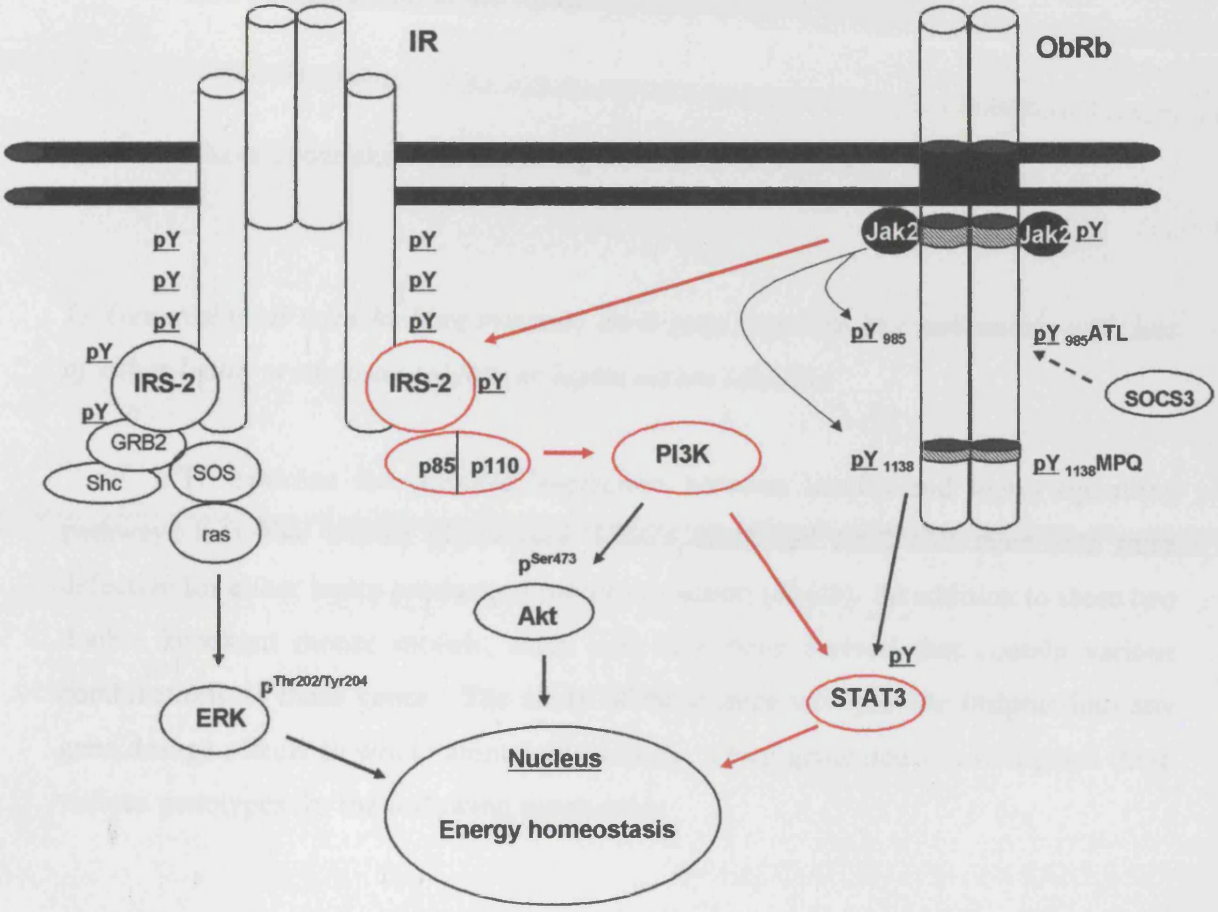

Figure 1.8: Insulin receptor substrate-2 may act as a potential site of convergence for insulin and leptin signalling pathways

IRS-2/PI3K signals may regulate the activation of STAT-3, thereby mediating the effects of insulin and leptin upon energy homeostasis

To address the interaction between insulin and leptin signalling and in particular to;

1). Examine the physiological interplay at the whole organism level.

2). The interaction at the signalling level in specific tissues.

I have undertaken the following lines of investigation.

1). Generation of mice lacking systemic Irs-2 gene function in combination with loss of either leptin production (ob/ob) or leptin action (db/db):

To examine the possible interaction between insulin and leptin signalling pathways in whole animal physiology, I have combined *Irs-2* null mice with mice defective for either leptin production (*ob/ob*) or action (*db/db*). In addition to these two double knockout mouse models, mice will have been derived that contain various combinations of these genes. The study of these mice will provide insights into any gene dosage effects to whole animal physiology. Once generated I have studied these various genotypes for the following parameters;

- Body and tissue weights.
- Glucose metabolism.
- Pancreatic β-cell function.
- Assessment of insulin signalling pathways in peripheral metabolic tissues.

2). Generation of mice lacking Irs-2 and Stat-3 gene function specifically in the β-cell and hypothalamus of mice:

To address the roles of IRS-2 and STAT-3 in the β-cell and hypothalamus, I have generated mice with a combined deletion for IRS-2 and STAT-3 in only their β-cells and hypothalamus (β-HypIRS2+STAT3KO mice). Assessment of the above parameters in β-HypIRS2+STAT3KO mice would provide insight into the relationship between these proteins within insulin and leptin signalling specifically in the β-cell and hypothalamus. This would potentially investigate directly the intrinsic role of these molecules in these specific tissues.

Insulin resistance and leptin resistance coexist in obese subjects. Studies on such murine models may give insights into the contribution of these processes to the obese phenotype and its association with insulin resistance and type 2 diabetes.

CHAPTER 2

METHODS & MATERIALS

2.1 Animals

All animal procedures were approved by the British Home Office Animals Scientific Procedures Act 1986 (Project Licence no. 70/5179, personal licence no.70/17202). Animals were maintained under a controlled environment (temperature 21-23 °C, 12 hour light-dark cycle, lights on at 07:00) with *ad libitum* access to food (RM1 diet SDS UK Ltd) and water.

The *Irs-2*$^{+/-}$ mice had previously generated using standard gene targeting strategies (83). The *ob/ob* mice and *db/db* mice were purchased from Harlan UK. The *ob/ob* mouse on the C57Bl/6J background has a non-sense mutation in the leptin gene, which results in a truncated protein that is degraded in the adipocye (21). *db/db* mice on a C57Bl/KS background have a premature stop codon in the ObRb long form of the receptor resulting in a truncated protein resembling the ObRa receptor isoform, with loss of Jak STAT box binding motifs. Unfortunately, genetic background is known to influence the course of disease in *db/db* mice. However, maintainance upon the C57BL/KS background allows a number of features to be observed, particularly those associated with glucose metabolism. To backcross the *db/db* mice on to a pure C57Bl/6J genetic background was deemed to be an inefficient use of funding and time.

Both RIP-CreIRS2lox+/+ and RIP-CreSTAT-3lox+/+ mice were generated in the laboratory of Professor D.Withers and maintained upon a C57BL/6J genetic background. The rat insulin II promoter (RIP-cre) mice were obtained from the Jackson laboratories (http://www.jax.org/) (86). The STAT-3lox+/+ mice were obtained from Professor V.Poli from the Univeristy of Dundee (now University of Turin). The IRS-2lox+/+ mice were generated within the laboratory of Professor D.Withers.

2.2 *Generation of mice with impaired insulin and leptin function*

2.2.1 *Generation of Irs-2$^{+/-}$ ob$^{+/-}$ mice*

Irs-2 and *ob/ob* mouse lines were both maintained on a C57Bl/6J genetic background to facilitate a comparative analysis. To obtain mice that were compound heterozygotes for alleles of Irs-2 and ob (*Irs-2$^{+/-}$ ob$^{+/-}$*), Irs-2$^{+/-}$ and ob$^{+/-}$ animals were intercrossed. *Irs-2$^{+/-}$ob$^{+/-}$* animals were viable and obtained with expected mendelian frequency (12.5 %). *Irs-2$^{+/-}$ob$^{+/-}$* mice were fertile and intercrossed to obtain progeny of all combinations of deletion of *Irs-2* and *ob*.

2.2.2 *Generation of Irs-2$^{+/-}$db$^{+/-}$ mice*

The *db/db* mice were maintained on a C57BL/KS background. To obtain *Irs-2$^{+/-}$ db$^{+/-}$* mice, *Irs-2$^{+/-}$* and *db$^{+/-}$* mice were intercrossed. *Irs-2$^{+/-}$db$^{+/-}$* mice were viable and obtained at the expected mendelian frequency (12.5%). *Irs-2$^{+/-}$db$^{+/-}$* mice were fertile and intercrossed to obtain progeny of all combinations of deletion of *Irs-2* and *db*. The *Irs-2* null and *db/db* phenotypes were indistinguishable on the mixed C57BL/KS/ C57Bl/6 background compared to mice on their respective pure genetic background.

2.2.3 *Generation of β-HypIRS2+STAT3KO mice*

In order to obtain β-HypIRS2+STAT3KO mice, β-HypIRS2KO and β-HypSTAT3KO mice were inter-crossed. This produced β-HypIRS2$^{lox/+}$+STAT3 $^{lox/+}$KO mice, these mice were floxed for one allele at both the *Irs-2* and *stat-3* gene loci and carried the RIP-Cre transgene. These mice were then intercrossed with each other to obtain β-HypIRS2+STAT3KO mice.

2.3 *Genotyping Strategies*

Mice were tail tipped upon weaning (18-21 days of age) using ethyl chloride spray as local anaesthesia. Polymerase chain reaction (PCR) genotyping was then carried out upon DNA extracted from the tail tip in order to determine the genotype of the mouse.

2.3.1 *DNA extraction*

Each tail tip was placed in a 1.5 ml eppendorf tube and 100 µl of digestion buffer added (6.7 mM Tris-HCl, pH 8.8, 1.66 mM $(NH_4)_2SO_4$, 0.67 mM $MgCl_2$, 0.5 % Triton X-100, autoclaved H_2O and 1 % β-mercaptoethanol) and heated to 95 °C for 10 minutes in a heating block. Proteinase K was then added at a final concentration of 1 mg/ml (5 µl of 20 mg/ml stock) and the tails incubated overnight at 55 °C. Each sample was then heated to 95 °C for a further 10 minutes to heat inactivate the proteinase K. Samples were then centrifuged for 5 minutes at 12, 000 rpm and the supernatant used for subsequent PCR genotyping.

2.3.2 *PCR genotyping strategies*

PCR was used to confirm the genotypes of mice. The details of various PCR strategies for detecting the genotypic status are outlined below. Detection of PCR products was by TAE buffered electrophoresis, resolving on 2% agarose TAE gels. A complete list of primer sequences needed for these genotyping strategies are provided in appendix II.

<u>50 x Tris-Acetate-EDTA (TAE) buffer (per litre):</u>

Tris-base	242 g
Glacial acetic acid	57.1 ml
0.5M EDTA pH8.0	100 ml

2% agarose TAE gel:

2 g of routine agarose in 100 ml 1 x TAE buffer.

Irs-2 Genotyping Strategy:

The *Irs-2* genotyping was carried out using a set of three primers and the PCR reaction conditions detailed below. In the case of wild-type samples, the successful annealing of primers *Irs-2* upper and *Irs-2* lower to both alleles of the *Irs-2* gene resulted in a single 530 base-pair product. The *Irs-2* gene targeting strategy results in removal of the coding sequence and thus the internal binding site for the *Irs-2* lower primer and the introduction of a neomycin cassette, which binds the *Irs* neo primer, resulting in the production of a larger 660 base-pair PCR product (Fig 2.1a) Hence, if deletion of the *Irs-2* gene was homozygous (occurring on both alleles) then only a 660 base-pair product would be visualized on a 2% TAE gel. In contrast if the *Irs-2* gene was heterozygous (deleted on one allele) then both the 530 and 660 base-pair products would be present.

PCR REACTION MIX:	
DNA	1.0µl
RedTaq Polymerase (250 units)	0.5µl
IRS-2 upper (10µM)	0.5µl
IRS-2 lower (10µM)	0.5µl
IRS-2 neo (10µM)	1.0µl
RedTaq buffer (10x)	2.5µl
dNTPs mix (5mM)	1.0µl
H_2O	18.0µl
	25.0µl

PCR PROFILE:

94°C for 1 min

Then 30 cycles of;

94°C for 30 secs

65°C for 30 secs

72°C for 1min, 30 secs.

Followed by;

72°C for 10 mins

stored at 4 °C.

ob genotyping strategy:

Determination of the genotypic status of the *ob* gene locus required the use of a set of four primers and optimised reaction conditions detailed below. The *ob/ob* mice arise as a result of a nonsense mutation that leads to the expression of a truncated *leptin* gene product. The PCR strategy used makes use of this nonsense mutation by use of two primers OB-WT and OB-MUT. These primers only differ in their outmost 3' bases, which are complimentary to position 369 in *Lep*-cDNA and when annealed form a 155 base-pair product with the OB-F primer. In wild-type alleles this base is a "C" but is a "T" in the *ob/ob* allele. Hence two PCR reactions are run in parallel one containing the OB-WT primer the other the OB-MUT primer. The presence of the APC-F and APC-R primers acts as an internal control, always resulting in a 223 base-pair product. If wild-type then both the 223 and 155 base-pair products will be produced by the PCR mix containing the OB-WT primer but only the 223 base-pair product will be produced by the PCR reaction containing the OB-MUT primer. The opposite applies given a homozygous sample and heterozygous samples result in the production of both size products in both PCR reactions (Fig 2.1b).

PCR REACTION MIX No.1:

DNA	1.0µl
RedTaq Polymerase (250 units)	0.5µl
APC-Fow (10µM)	1.0µl
APC-Rev (10µM)	1.0µl
OB-Fow (10µM)	1.0µl
OB-WT (10µM)	1.0µl
RedTaq buffer (10x)	2.5µl
dNTPs mix (5mM)	1.0µl
H_2O	16.0µl
	25.0µl

PCR REACTION MIX No.2:

As for reaction mix No.1 but exchange 1.0µl of Primer – OB-WT for OB-MUT.

PCR PROFILE:

94°C for 1 min

Then 30 cycles of

1). 94°C for 30 secs

2). 67°C for 30 secs

3). 72°C for 1min and 30 secs.

Followed by;

72°C for 10 mins

stored at 4 °C.

db genotyping strategy:

The PCR protocol was designed to take advantage of the unique restriction cut site found in the *db/db* mutation site. This region of mutant DNA was amplified using the primers db-F and db-R and reaction conditions as below and restricted using the *Rsa I* restriction enzyme. Determination of *db* genotype was confirmed by running digested samples on a 3% TAE gel under TAE buffer. The PCR yields a 109 base-pair product, once digested the presence of a single 85 base-pair product denotes a wild-type, whereas homozygous mutated alleles are denoted by the presence of a single 58 base-pair product. When both of these digest fragments are present the sample is heterozygous for the db mutation (summarised in Fig 2.1c).

PCR MIX (per 25µl reaction):	
DNA	1.0µl
RedTaq Polymerase (250 units)	0.5µl
db - Fow (10µM)	0.5µl
db - Rev (10µM)	0.5µl
RedTaq buffer (10x)	2.5µl
dNTPs mix (5mM)	1.0µl
H_2O	19.0µl
	25.0µl

PCR PROFILE:

95°C for 3 mins

Then 35 cycles of;

95°C for 1 min

58°C for 1 min

72°C for 1 min.

Followed by;

72°C for 10 mins

stored at 4 °C.

Each PCR product was then digested using the following reaction mix, incubating at 37 °C for 2 hrs.

Rsa I restriction enzyme (Reaction mix):

PCR Product	10 µl
Rsa I enzyme	0.3 µl
NEB Buffer #1 (10x)	2.0 µl
Sterile-filtered H_2O	7.7 µl
	20µl.

β-HypIRS2+STAT-3KO genotyping strategy:

Genotyping of β-HypIRS2+STAT3KO mice required three additional PCR protocols, which are outlined below.

1). IRS-2lox PCR:

This was carried out to determine the status of loxP sites at the *Irs-2* locus (ie. were both alleles of *Irs-2* flanked by loxP sites).

PCR MIX (per 25µl reaction):		PCR PROFILE:
DNA	1.0µl	95°C for 5 mins
RedTaq Polymerase (250 units)	0.5µl	Then 35 cycles of;
LoxP - Fow (10µM)	0.5µl	95°C for 30 secs
LoxP - Rev (10µM)	0.5µl	60°C for 30 secs
RedTaq buffer (10x)	2.5µl	72°C for 1 min.
dNTPs mix (5mM)	1.0µl	Followed by;
H_2O	19.0µl	72°C for 10 mins
	25.0µl	stored at 4 °C.

a). *Irs-2 genotyping analysis:*

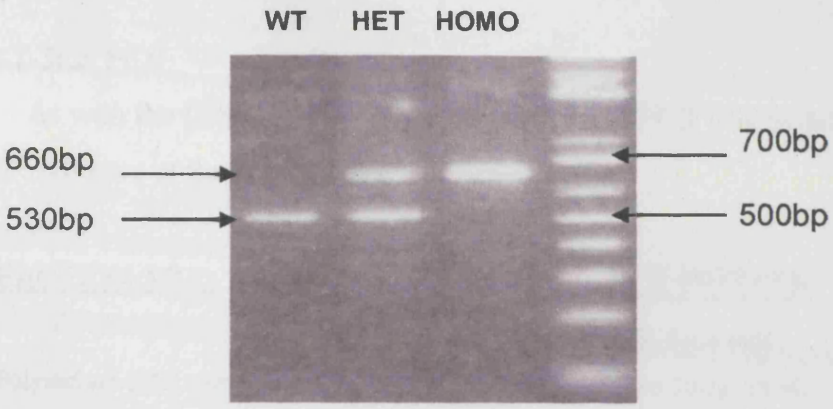

b). *ob genotyping analysis:*

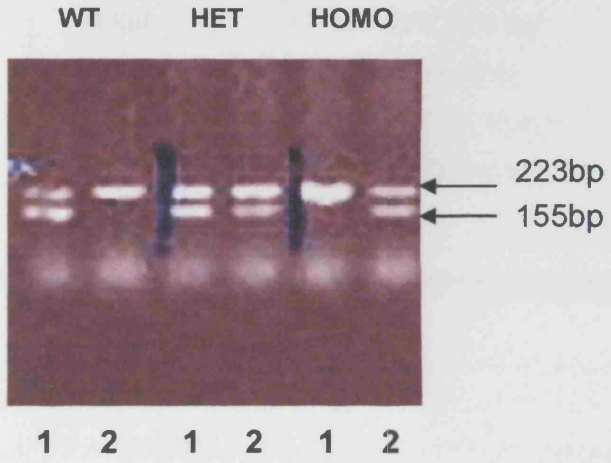

1=OB-WT primer reaction.

2=OB-MUT primer reaction.

c). *db genotyping analysis:*

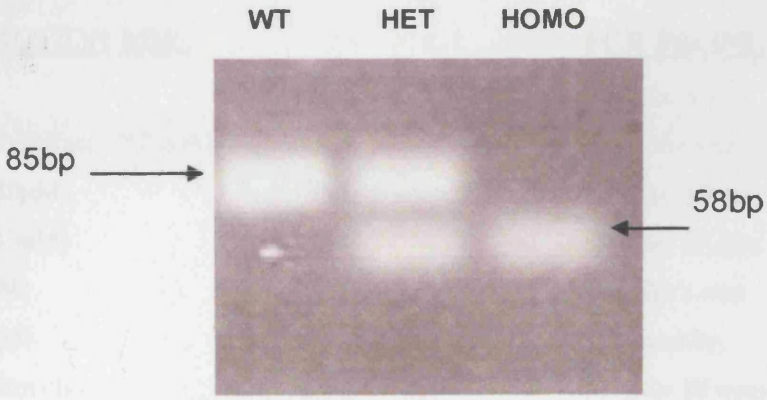

***Figure 2.1 A*nalysis of PCR products obtained from the genotyping of *Irs-2, ob/ob* and *db/db* mice.**

2). STAT-3lox PCR:

As with the IRS-2lox PCR, the purpose of this PCR was to determine the status of loxP sites at the stat-3 locus.

PCR REACTION MIX:		PCR PROFILE:
DNA	1.0µl	94°C for 4 min
RedTaq Polymerase (250 units)	0.5µl	Then 30 cycles of;
APRF-11 UP (10µM)	1.0µl	94°C for 1 min
APRF-11 DOWN (10µM)	1.0µl	60°C for 2 min
APRF-14 DOWN (10µM)	1.0µl	72°C for 3 min
RedTaq buffer (10x)	2.5µl	Followed by;
dNTPs mix (5mM)	1.0µl	72°C for 10 mins
H_2O	17.0µl	stored at 4 °C.
	25.0µl	

3). RIP-Cre PCR:

The following PCR reaction was carried out to determine the presence of the RIP-Cre transgene.

PCR REACTION MIX:		PCR PROFILE:
DNA	1.0µl	94°C for 3 min
RedTaq Polymerase (250 units)	0.5µl	Then 30 cycles of;
Cre 1084 (10µM)	1.0µl	94°C for 30 secs
Cre 1085 (10µM)	1.0µl	60°C for 30 secs
IL2 F (10µM)	1.0µl	72°C for 1 min
IL2 R (10µM)	1.0µl	Followed by;
RedTaq buffer (10x)	2.5µl	72°C for 10 mins
dNTPs mix (5mM)	1.0µl	stored at 4 °C.
H_2O	17.0µl	
	25.0µl	

2.4 *Investigation of serial body weights of progeny from Irs-2$^{+/-}$ob$^{+/-}$and Irs-2$^{+/-}$ db$^{+/-}$ intercross*

All body weights were recorded during the early light phase between 10:00am and 12:00pm using a Sartorius Master Pro LA balance (Sartoruis, Goettingen, Germany) recording to the nearest 0.01 g. Mice were weighed daily from day 10 until day 21 to enable tracking of each individual pup within a litter. Following weaning and ear-marking at day 21, mice resulting from the *Irs-2$^{+/-}$ob$^{+/-}$* intercross were weighed weekly until 12 weeks of age. In contrast, offspring resulting from the *Irs-2$^{+/-}$db$^{+/-}$* intercross were weighed weekly until 8 weeks of age.

2.5 Metabolic studies

2.5.1 *Determination of fasting blood glucose levels*

Mice were fasted for 15 hours overnight and blood glucose levels were determined during the early light phase (8:00 – 10:00) via tail vein bleeds after local anaesthesia using a Glucometer Elite glucometer (Bayer).

2.5.2 *Determination of glucose homeostasis using intra-peritoneal glucose-tolerance tests*

Mice were fasted for 15 hours and blood glucose levels determined as described in section 3.2.2. Mice were then injected with 2 g kg^{-1}of D-glucose intraperitoneally (i.p) and blood glucose measured at 15, 30, 60 and 120 minutes post-injection.

2.5.3 *Determination of fasting insulin and leptin levels*

Mice were fasted overnight for 15 hr and then terminally anaesthetized (25 % Midazolam, 25 % Hypnorm, 50 % water for injection) and cardiac puncture performed. Blood samples were centrifuged at 13,000 rpm for 20 minutes at 4 °C, serum was then immediately removed and frozen at -80 °C until assayed. Fasting insulin levels were

measured using a commercially available ultra sensitive Rat insulin ELISA kit (Crystal Chem Inc, cat# 90060) including mouse insulin standards (Crystal Chem Inc, cat# 90090). Fasting leptin levels were also determined using a commercially available mouse leptin ELISA kit (Crystal Chem Inc, cat# 90030). All samples were assayed in duplicate. The mouse insulin standard (lyophilised) was reconstituted in 100µl of distilled water. This stock solution was 12.8 ng/ml and was serially diluted 1:1 with the sample diluent (provided in the rat insulin ELISA kit) to produce mouse insulin standards at the following concentrations; 0, 0.1, 0.2, 0.4, 0.8, 1.6, 3.2 and 6.4ng/ml.

2.6 Investigation of Pancreatic Islet morphology

2.6.1 Haematoxylin and eosin staining

Four week old, fasted mice were terminally anaesthetised as described in section 2.5.3. The pancreas was then removed, cleared of fat and fixed in Bouin's fixative solution (see below) for 2 hours. Following fixation samples were stored in 75 % ethanol prior to being processed and paraffin embedded (using automatic embedder).

Bouin's Fixative solution:

375 ml saturated picric acid
125 ml stock formaldehyde (37% w/w)
25 ml glacial acetic acid
500ml

For haematoxylin and eosin staining 5 µm sections were then cut onto glass slides, which were then deparaffinised and rehydrated by carrying out the following series of washes;

2 x 5 minutes	Xylene
1 x 5 minutes	100 % Ethanol
1 x 5 minutes	95 % Ethanol
1 x 5 minutes	80 % Ethanol
1 x 5 minutes	deionised H_2O

Deparaffinised slides were blotted of excess water and then stained for 5 minutes with haematoxylin stain. Stained slides were then rinsed with and submerged in tap water for 5 minutes, to allow staining to develop. Slides were then destained by agitation in acid ethanol, rinsed with tap water (2 x 1 minutes), and finally in deionised water (1 x 2 minute). Slides were then stained with eosin (1 x 30 seconds) and washed 2 x 3 minutes in 95 % ethanol, 2 x 3 minutes 100 % ethanol. Slides were blotted of excess ethanol before submerging in xylene (1 x 5 minutes). Slides were then allowed to air-dry before mounting coverslips, using DPX medium. Stained sections were then viewed using light microscopy.

2.6.2 Immunofluorescence staining for insulin

For insulin staining 5 μm sections were cut onto poly-lysine coated slides. Slides were deparaffinised by successive 5 minute washes in 100 % xylene, 100 % ethanol, 70 % ethanol, 50 % ethanol respectively, followed by 2 x 2 minute washes in 1 x phosphate buffer saline (PBS). Prior to staining slides were placed into a beaker of pre-boiled 0.01 M sodium citrate pH 6.0 and heated for 8 mins at the lowest microwave setting. Slides were allowed to cool before being blocked for 30 mins in 1ml of 1 x PBS + 2% chicken serum inside a moisture chamber. Slides were then washed three times with 1 x PBS + 0.05% Tween-20. Following washing slides were further blocked by incubating for 30 mins in 100 μl of 2 % chicken serum dissolved in 1 x PBS + 2 % BSA. This helps to reduce non-specific binding of the secondary antibody, which is raised in chicken against mouse IgG. Slides were then incubated for 2 hours, at room temperature, in 200 μl of insulin monoclonal antibody (1:500) (sigma I-2018) dissolved in 1 x PBS + 2 % BSA + 2 % chicken serum. After incubation in primary antibody slides had excess fluid removed by gentle tapping onto tissue paper, before being washed three times in 1 x PBS + 0.05 % Tween-20 for 2 mins. Slides were then placed back into the moisture chamber and incubated in secondary antibody (Alexa-Fluor

594δ, Molecular probes A-21200) at 5 μg/ml in 1 x PBS + 0.05 % Tween-20, for 2 hours at room temperature. Slides were then washed once with 1 x PBS + 0.05 % Tween-20, before mounting.

2.6.3 Quantification of relative islet density and relative islet area

Relative islet density and relative islet area was determined by morphometric analysis of four whole pancreatic sections (5 μM) immunostained for insulin, from four animals per genotype.

2.7 Insulin treatment of Irs-2$^{-/-}$ob$^{-/-}$ double-knockout mice

Double-knockout mice were administered daily injections of insulin (Lantus – Glargine 100iu/ml cartridges, Aventis) just prior to the start of their 12 hr dark-cycle (17:00 – 18:00) over a period of 6 weeks. Injections were administered subcutaneous using an insulin pen (Aventis), carrying a 6mm needle (Disetronic medical systems Ltd). The amount of insulin given was determined by measurements of body weight and urine glucose and ketone content, taken once in the early light phase (08:00 – 09:00) and again just prior to time of injection. In addition cages were supplemented with wet chow-diet for the first two weeks of injections to encourage the double-knockouts to feed and hence reducing the risk of hypoinsulinemia.

2.8 Generation of recombinant GST-fusion proteins for the production of IRS-1 and IRS-2 polyclonal antibodies

Constructs had previously been designed in the laboratory for the expression of Glutathione-S-transferase (GST)-fusion proteins containing either the residues 735-900 of murine IRS-1 or residues 619-746 of murine IRS-2, subcloning into the pGEX6p1 GST-expression vector system (Amersham Biosciences cat# 27-4597-01).

2.8.1 Optimisation of induction conditions for IRS-1 and IRS-2 GST-fusion proteins

Plasmid constructs were transformed into BL-21 bacterial cells and incubated upon L-agar plates containing 50 μg/ml ampicillin. In addition the pGEX vector alone was also transformed to use as a positive control during the purification strategy.

L-agar plates (per litre = 40 plates):

Tryptone	10g
Yeast Extract	5g
NaCl	10g
Agar	15g

Make up to 1 litre with distilled water and sterilise by autoclaving. Plates should be stored at 4 °C. Plates were briefly incubated at 37 °C prior to use to allow surface moisture to dry.

Transformants were then selected and grown in 10 ml L-broth overnight at 37 °C with agitation. Three 50 ml induction cultures were set-up by adding 500□l of overnight culture into each 50 ml L-broth culture. These 50 ml cultures were grown until mid log-phase (ie. OD_{600} = 0.6), when a 1 ml pre-induction control sample was taken and clarified by centrifugation (13,000 rpm for 1 min at 4 °C). The cultures were then induced by the addition of either; 0.1 mM, 0.5 mM or 1.0 mM isopropyl b-D-thiogalactoside (IPTG). IPTG induces expression of the GST-fusion proteins by relieving repression of the *lacZ* promoter. Cultures were incubated at 37 °C for three hours with agitation, taking a 2 ml sample pellet at each hour time point. Sample pellets were reconstituted in 100 μl of 1 x PBS, of which 5μl was denatured in 5 μl SDS-sample buffer by boiling at 95 °C for 5 mins. Samples were then resolved by 12% SDS-polyacrylamide gel electrophoresis and protein content was assessed by Coomassie staining.

Coomassie Blue Stain (1 litre):

Coomassie Blue R-250 (0.025%)	0.25g
Methanol (40%)	400ml
Acetic acid (7%)	70ml

Destain (1 litre):

Methanol (5%)	50ml
Acetic acid (7%)	70ml

2.8.2 Large-scale purification of GST-IRS1 and GST-IRS2 fusion proteins

2.8.2.1 Lysis of BL-21 bacterial cells for GST-fusion protein purification

Using these optimal induction conditions of 1.0 mM IPTG at 37°C for 2 hours, 1 litre cultures of BL-21 bacterial cells containing either GST-IRS1 or GST-IRS2 fusion protein constructs were induced. The resulting bacterial pellets were sonicated in 20 ml of ice-cold 1 x GST lysis buffer (recipe below). Lysates were clarified by centrifugation at 3,500 rpm for 10 mins at 4°C and then further cleared by passing through a glass-wool mesh.

1 X GST lysis Buffer:

1 x PBS
1mM EDTA pH8.0
1mM Dithiothreitol (DTT)
1mM Sodium Fluoride
1mM Sodium Orthovanadate
Nonidet P-40
Protease inhibitor tablets (Roche)

2.8.2.2 *Purification of GST-IRS1 and GST-IRS2*

Purification of both the induced GST-IRS1 and GST-IRS2 fusion proteins was achieved by applying the ~15mls of lysate that was retained from lysis to Redipack GST-purification columns (2 ml columns with 20 mg protein capacity, Amersham cat# 27-4570-02).

The Redipack columns were equilibrated by washing with 5 x column volumes of 20% ethanol, followed by 5 x column volumes of 1 x PBS. The ~15mls of induced lysate (either GST-IRS1 or GST-IRS2) was then applied to the Redipack columns, collecting the flow-through for subsequent analysis. Redipack columns were then washed with 10 x column volumes of 1 x PBS, again collecting the flow-through for subsequent analysis. The GST-fusion proteins were then eluted by addition of 10mM glutathione to the columns. Eluted protein was collected in 500 µl fractions, of which a 50 µl fraction was taken for further analysis.

2.8.2.3 *Analysis of large-scale GST-IRS1 and GST-IRS2 purifications*

In order to determine the concentration of eluted fractions and generally assess the efficiency of purification a Bio-Rad protein assay (BioRad cat#500-0006) was carried out.

The Bio-Rad assay is a colorimetric assay for the measurement of total protein concentration, adapted from the method of Bradford (142). The Bio-Rad assay is based on the colour change of coomassie brilliant blue G-250 dye, in response to various concentrations of protein. The dye binds primarily basic, (especially arginine) and aromatic amino acid residues.

2.8.3 *Desalting of GST-IRS1 and GST-IRS2 purified fusion proteins*

HiTrap desalting columns (Amersham, Cat# 17-1408-01) were used following the manufacturers recommended protocol. GST-fusion proteins were eluted using 1 x PBS + 20 % glycerol, in preparation for injections into sheep.

2.8.4 *Evaluation of anti-IRS-1 (S918A) and anti-IRS-2 (S919A) antisera*

The anti-IRS-1 (S918A) and anti-IRS-2 (S919A) sheep polyclonal antisera were evaluated by testing their ability to immunoprecipitate native IRS-1 and IRS-2 proteins in brain lysates (Fig 2.2). Tissue lysates were prepared and immuoprecipitated with either anti-IRS-1 (S918A) or anti-IRS-2 (S919A) antisera were carried out as described in below.

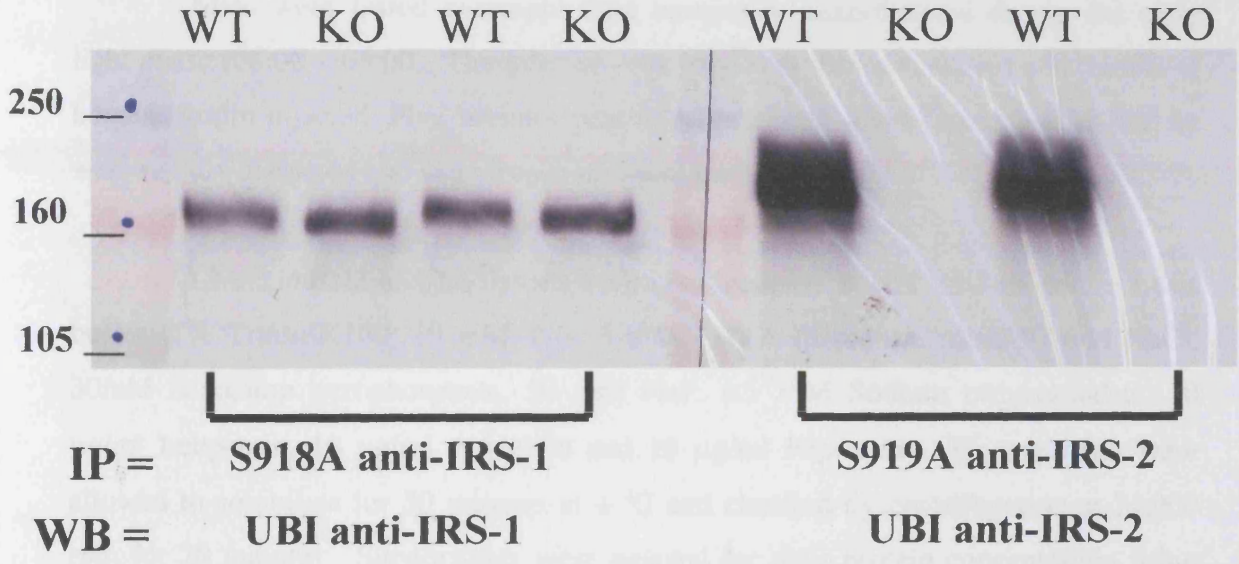

Figure 2.2: Western blot analysis of immunoprecipitations for IRS-1 and IRS-2 in brain lysates, using S918A anti-IRS-1 and S919A anti-IRS-2 sheep polyclonal antibodies.

Brain lysates were obtained from 2 x wild-type and 2 x Irs-2$^{-/-}$ mice. Brain lysates (2mg in total) were then immunoprecipitated with 10μl of either S918A or S919A antisera. Immunoprecipitates were resolved by 6% SDS-PAGE, transferred and blotted for IRS-2 using the UBI anti-IRS-2 (Upstate, cat# 06-508 (1:1,000) also see Table 2.1).

2.9 *Signalling analysis of peripheral tissues*

2.9.1 *Harvesting of tissues in the fasted state*

Mice were fasted overnight for 15 h and then terminally anaesthetized (25 % Midazolam, 25 % Hypnorm, 50 % water for injection) samples of liver, quadriceps muscles, fat were then rapidly dissected and snap frozen in liquid nitrogen for subsequent signalling analysis.

2.9.2 *Insulin-stimulated signalling analysis*

Mice were fasted overnight then terminally anaesthetised during the early light phase (08:00 – 09:00). The inferior vena cava was then cannulated and 5 units of human insulin injected. Five minutes post-injection, liver, quadriceps muscles and fat were rapidly dissected and snap frozen in liquid nitrogen.

Liver, muscle and fat tissues were homogenized at 4 °C in 3 ml of 1 x Lysis buffer (1% Triton-X100, 10 mM Tris, 5 mM EDTA (disodium salt), 50 mM NaCl, 30mM Disodium pyrophosphate, 50 mM NaF, 0.1 mM Sodium orthovanodate, 10 µg/ml Leupeptin, 10 µg/ml Aprotinin and 10 µg/ml Pepstatin). Homogenates were allowed to solubilize for 30 minutes at 4 °C and clarified by centrifugation at 14,000 rpm for 20 minutes. Supernatants were assayed for their protein concentration using the Bradford reaction assay (BioRad). Lysates were used in either immunoprecipitations or western blotting to analyse a number of signalling proteins.

2.9.3 *Immunoprecipitation of IRS1 and IRS2*

For the immunoprecipitation of IRS-1, 10 µl of anti-IRS1 (S918A) sheep polyclonal antibody was incubated with 2 mg of lysate at 4 °C on a rotary mixer overnight. Similarly for IRS-2 immunoprecipitations the same conditions were used but using 10 µl of the anti-IRS-2 (S919A) sheep polyclonal antibody. Following overnight incubation with antibody, samples had 20 µl total bead volume of pre-washed protein-G agarose (Roche; Cat#1243233) added to them and were incubated for a further hour

at 4 °C, again with agitation. Immunoprecipitations were then clarified by gentle centrifugation and washed twice with 750 µl of 1 x lysis buffer. Samples were then denatured in 20 µl of 2x SDS-sample buffer at 100 °C for 5 mins. Samples were then clarified by centrifugation and analysed by western blotting.

2.9.4 Western blotting

Lysates were resolved on 10% SDS-PAGE, loading 100 µg of total lysate per lane. Gels were usually run at 120 volts for 90 minutes before transferring onto PVDF membrane at 100 volts for 2 hours. The blots were then blocked for 45 mins in 1 x PBS + 0.1% Tween + 5 % milk and then incubated overnight at 4 °C with primary antibody (1:1,000) diluted in 1 x PBS + 0.1% Tween + 5 % milk. All antibodies used are detailed in table 2.1). The primary antibodies used for detection of proteins involved in insulin signalling are detailed below. The Blots were washed for 3 x 5 min in 1 x PBS + 0.1% Tween and then incubated with HRP-conjugated Goat anti-Rabbit secondary antibody (1:10,000) (Dako Ltd). Blots were given a final set of 3 x 5 min washes with 1 x PBS + 0.1% Tween, before detection using Enhanced Chemiluminesence (ECL kit, Amersham Pharmacia cat# RPN 2106).

2.10 Data handling and statistics

All data was expressed as an average ± s.e.m for all data points, unless otherwise indicated. Results are representative of at least four animals per genotype, except where indicated. Statistical analyses were carried out using two-tailed student's unpaired t test, with significance being rejected at $p \geq 0.05$. Standard error of the mean was determined using Prism Version 4.0.

ANTIBODY	Supplier	Species	Catalogue #	Species Cross-Reactivity	Antigen	Detection on western blot (1 x band unless stated)
Anti-IRS2	University of Dundee	Sheep polyclonal	S919A	H,M,R	GST-fusion protein	Used for immuno-precipitation
Anti-IRS2	Upstate cell signaling solutions	Rabbit polyclonal	#06-506	H,M,R	GST-fusion protein	160-180 KDa
Anti-PI3 Kinase, p85	Upstate cell signaling solutions	Rabbit polyclonal	#06-195	H,M,R,Mo	GST-fusion protein	85 KDa
Anti-phospho-PDK1^{Ser241}	New England Biolabs	Rabbit polyclonal	#3061S	H,M,R	Phospho-peptide	58 to 68 KDa
Anti-total PDK1	New England Biolabs	Rabbit polyclonal	#3062	H,M,R	Peptide	58 to 68 KDa
Anti-phospho-Akt^{Ser473}	New England Biolabs	Rabbit polyclonal	#9271S	H,M,R,C,Hm	Phospho-peptide	60 KDa
Anti-total Akt	New England Biolabs	Rabbit polyclonal	#9272	H,M,R,C,Dr,Hm	Peptide	60 KDa
Anti-phospho-MAPK$^{Thr202/Tyr204}$	New England Biolabs	Rabbit polyclonal	#9101S	H,M,R,C,Hm,Z	Phospho-peptide	2 x bands at 42 and 44 KDa
Anti-total MAPK	New England Biolabs	Rabbit polyclonal	#9102	H,M,R,Hm,Z	Peptide	2 x bands at 42 and 44 KDa
Ant-phospho-p70^{s6kThr389}	New England Biolabs	Rabbit polyclonal	#9205S	H,M,R	Phospho-peptide	75-80 KDa
Anti-total-p70^{s6k} (C-18)	Santa cruz biotechnology inc	Rabbit polyclonal	SC-230	M,R,H,C,X	Peptide	70 KDa
Anti-phospho GSK-3α/β$^{Ser9/21}$	New England Biolabs	Rabbit polyclonal	#9331S	H,M,R,Z	Phospho-peptide	46 KDa GSK-3β and 51 Kda GSK-3
Anti-total GSK-3β	New England Biolabs	Rabbit polyclonal	#9332	H,M,R,X,Z	Peptide	46 KDa
Anti-Cyclin D1 (DCS6)*	BD Biosciences (Clonetech)	Mouse monoclonal	556470	H,M,R	Peptide	36 KDa
Anti-Cyclin D2 (DCS 3.1)*	BD Biosciences (Clonetech)	Mouse monoclonal	554200	H,M,R	Peptide	35 KDa
Anti-Cyclin D3 (DCS 22)*	BD Biosciences (Clonetech)	Mouse monoclonal	554195	H,M,R	Peptide	30 - 35 KDa
Species codes: C = Chicken; Dr = Drosophila; H = Human; Hm = Hamster; M = Mouse; Mo = Monkey; R = Rat; X = Xenopus; Z = Zebra fish * These antibodies were a research gift from Dr Michelle Garrett but newer clones my be purchased from BD Biosciences.						

Table 2.1: Summary of primary antibodies used for insulin signalling analysis in peripheral tissues of wild-type, Irs-2$^{-/-}$, ob/ob and double knockout mice (see chapter 6). It should be noted that the anti-phospho-PDK1^{Ser241} recognises three bands running between 58-68 KDa.

CHAPTER 3

Analysis of body weight and anatomy in offspring derived from *Irs-2*$^{+/-}$*ob*$^{+/-}$ and *Irs-2*$^{+/-}$*db*$^{+/-}$ intercrosses.

3.1 Generation and genotypic frequencies of Irs-2$^{+/-}$*ob*$^{+/-}$ *offspring*

Irs-2 and *ob/ob* mice were maintained on the same C57Bl/6J genetic background to facilitate analysis. To obtain all genetic combinations of the *Irs2* and *ob* genes, double heterozygote male and female mice were intercrossed. However, since *ob/ob* mice and female *Irs-2*$^{-/-}$ mice are infertile, initially single heterozygote males and females were mated to produce double heterozygote animals. Double heterozygote mice were fertile and produced litters of comparable size to wild-type matings (data not shown). There also appeared to be no difficulties in maternal care for litters.

The intercross of *Irs-2*$^{+/-}$*ob*$^{+/-}$ mice produced 1221 offspring representing all 9 possible genotypes. PCR genotyping conducted at 3 weeks of age indicated that the frequency of these genotypes was generally in accordance with the expected Mendelian ratios (Table 3.1).

3.2 Growth characteristics of progeny of Irs-2$^{+/-}$*ob*$^{+/-}$ *intercross*

Growth curves were generated based on daily weights from ten days after birth to twenty-one days and weekly weights thereafter until twelve weeks of age, for both male and female offspring resulting from the intercross of *Irs-2*$^{+/-}$*ob*$^{+/-}$ mice (Fig 3.1).

The growth of the *Irs-2*$^{-/-}$, *ob/ob* and wild-type mice was consistent with previous reports (83, 143). Compound heterozygote mice (*Irs-2*$^{+/-}$*ob*$^{+/-}$) had similar growth profiles to wild-type mice but usually weighed 1-2 grams more and this weight difference was significant by eight weeks of age (Fig 3.2c-d). Mice lacking single alleles of either *Irs-2* (*Irs-2*$^{+/-}$*ob*$^{+/+}$) or *ob* (*Irs-2*$^{+/+}$*ob*$^{+/-}$) had no obvious change in growth pattern over the 12-week period and mirrored the wild-type weight profile (data not shown).

GENOTYPES	NUMBERS			% OFFSPRING	
	FEMALE	MALE	TOTAL	ACTUAL	EXPECTED
WILD-TYPE	50	54	**104**	8.52	**6.25**
IRS-2+/+OB+/-	87	83	**170**	13.92	**12.50**
IRS-2+/-OB+/+	97	97	**194**	15.89	**12.50**
IRS-2+/-OB+/-	137	172	**309**	25.31	**25.00**
ob/ob	30	37	**67**	5.49	**6.25**
IRS-2 KO	26	36	**62**	5.08	**6.25**
IRS-2+/-OB-/-	70	86	**156**	12.78	**12.50**
IRS-2-/-OB+/-	53	51	**104**	8.52	**12.50**
DOUBLE-KNOCKOUT	29	26	**55**	4.5	**6.25**
		TOTAL	**1221**	**100**	**100**

Table 3.1 Genetic frequencies of all 9 possible genotypes resulting from the intercross of Irs-2$^{+/-}$ob$^{+/-}$ mice. Animals were PCR genotyped at three weeks of age.

Irs-2$^{+/-}$*ob*$^{-/-}$ mice were obese like the *ob/ob* mice, also weighing over double that of the wild-type mice by eight weeks of age. In contrast, mice lacking both *Irs*-2 and *ob* genes (*Irs-2*$^{-/-}$*ob*$^{-/-}$, termed; double knockouts) were markedly growth retarded (Fig 3.2) only growing to a mean peak body weight of 11 grams by six weeks of age (Fig 3.1). Therefore double knockout mice displayed a 50% reduction in body weight compared to wild-type mice of the same age. After six to eight weeks these double knockout mice gradually lost weight and became increasingly frail. In contrast, this striking impairment of growth was not seen in the *Irs-2*$^{-/-}$*ob*$^{+/-}$mice. These mice were of comparable weight to the *Irs-2*$^{-/-}$ up to twelve weeks of age although there was a non-significant reduction in body weight from approximately six weeks of age. This finding suggested that the presence of a single allele of the *ob* gene was sufficient to rescue the phenotype seen in the double knockout mice.

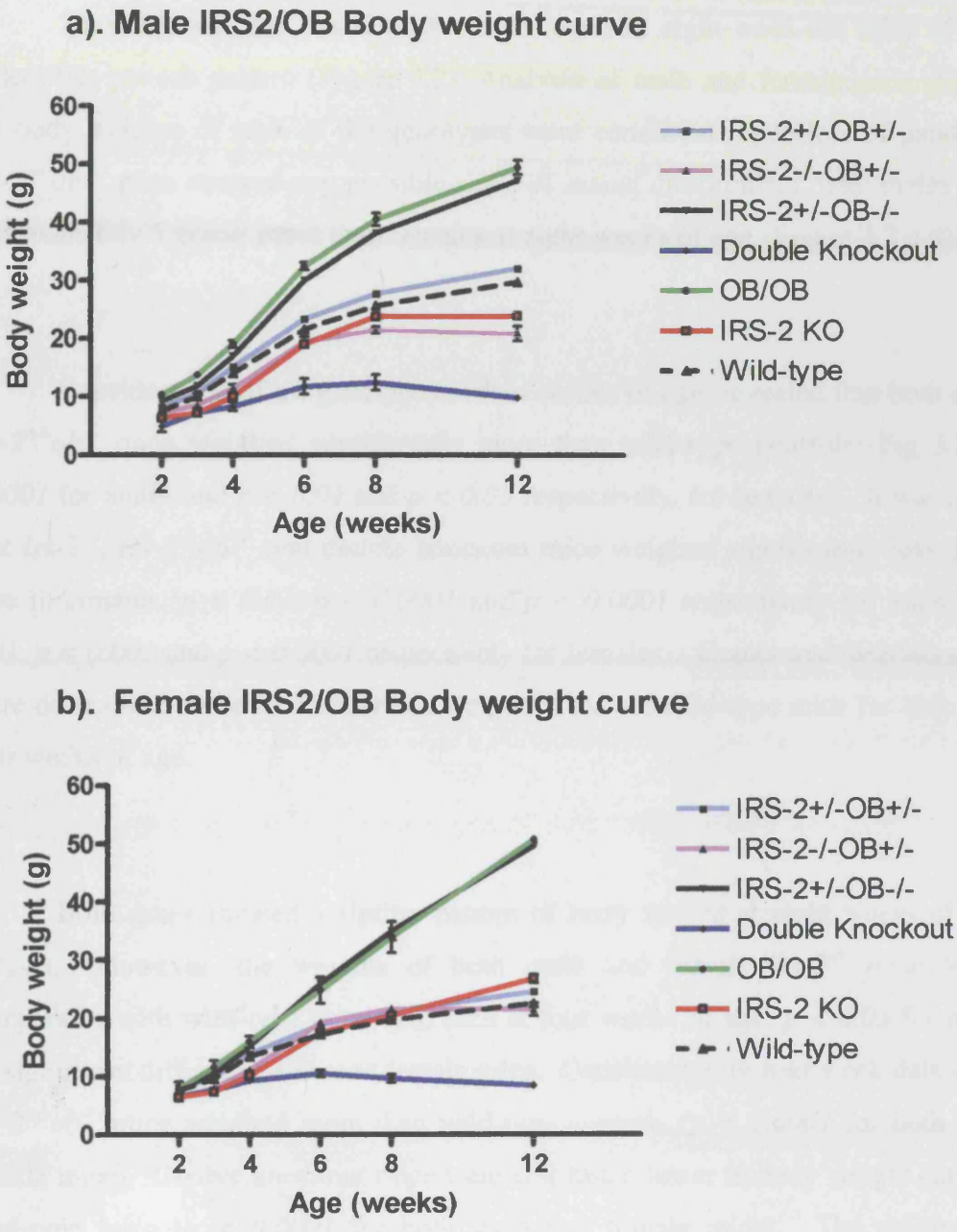

Figure 3.1 Growth curves showing mean weights±s.e.m of a). male and b). female offspring resulting from the Irs-2$^{+/-}$ob$^{+/-}$ intercross at the indicated ages (weeks). *Results are representative of at least 8 animals per genotype.*

The body weights measured for both four and eight-week-old mice of each sex reflect this growth pattern (Figure 3.2). Analysis of male and female mice showed that the body weights of each of the genotypes were consistent regardless of gender. Only *Irs-2*$^{+/-}$*ob*$^{+/-}$ mice showed any possible signs of sexual dimorphism, with males weighing approximately 5 grams more than females at eight weeks of age (Figure 3.2 c-d).

Consideration of all genotypes at four weeks of age, revealed that both *ob/ob* and *Irs-2*$^{+/-}$*ob*$^{-/-}$ mice weighed significantly more than wild-type controls (Fig 3.2a-b $p < 0.0001$ for males and $p < 0.01$ and $p < 0.05$ respectively, for females). It was also noted that *Irs-2*$^{-/-}$, *Irs-2*$^{-/-}$*ob*$^{+/-}$ and double knockout mice weighed significantly less than wild-type littermates ($p < 0.01$, $p < 0.0001$ and $p < 0.0001$ respectively for males and $p < 0.01$, $p < 0.001$ and $p < 0.0001$ respectively for females). Compound heterozygous mice were determined to be of comparable weight to that of wild-type mice for both sexes, at four weeks of age.

Both sexes showed a similar pattern of body weight at eight weeks of age (Fig 3.2c-d). However, the weights of both male and female *Irs-2*$^{-/-}$ mice was more comparable with wild-type mice than seen at four weeks of age, $p < 0.05$ for males and no significant difference between female mice. Consistent with four week data *ob/ob* and *Irs-2*$^{+/-}$*ob*$^{-/-}$ mice weighed more than wild-type controls ($p < 0.0001$ for both male and female mice). Double knockout mice were still much lower in body weight compared to wild-type mice ($p < 0.0001$ for both male and female mice). The striking growth retardation seen in the double knockout mice is demonstrated in figure 3.3. The mice depicted are eight weeks of age and were weaned from the same litter.

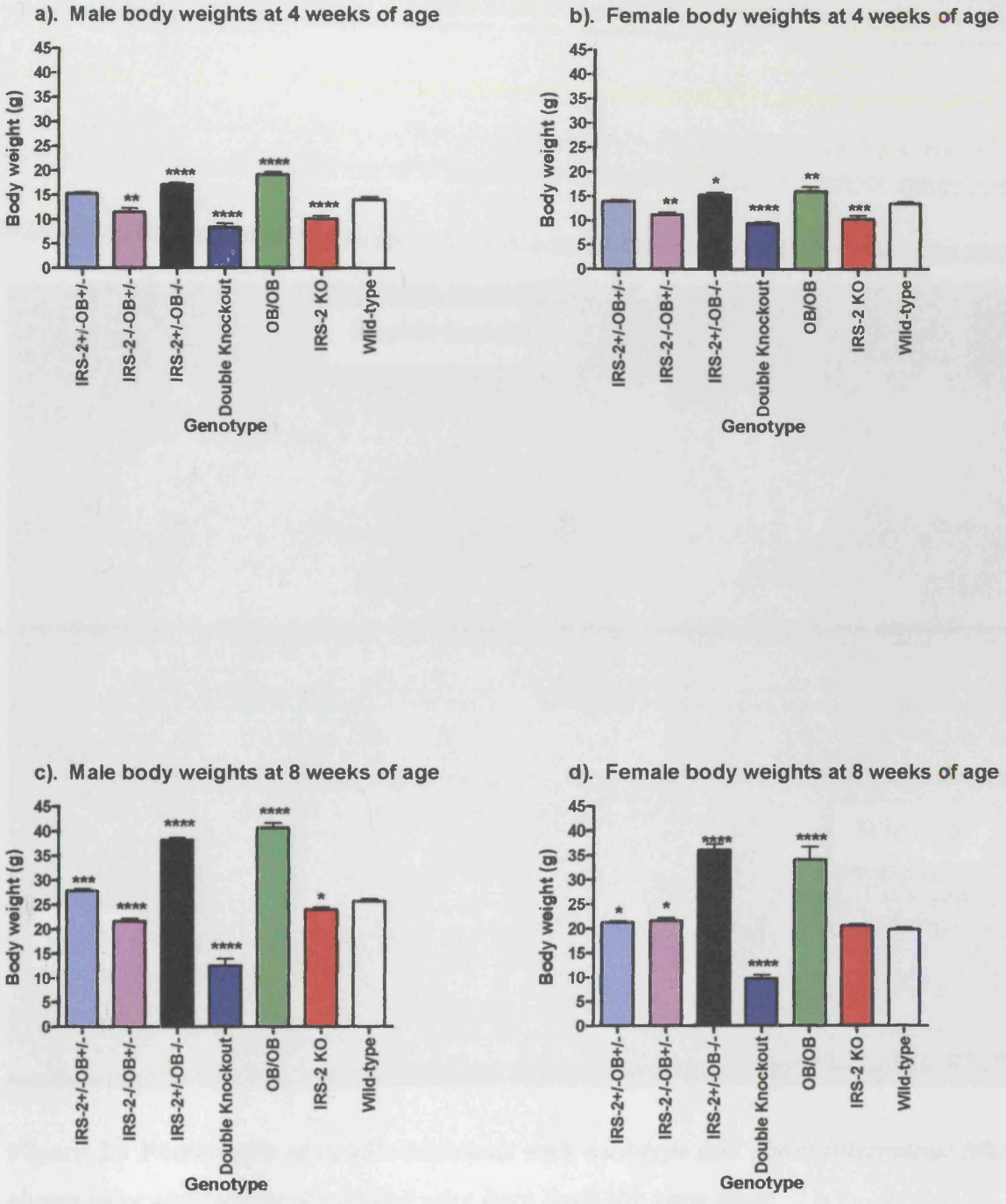

Figure 3.2 Analysis of body weights of male and female offspring from the Irs-2$^{+/-}$ob$^{+/-}$ intercross at a-b). 4 weeks and c-d). 8 weeks of age.

*Results are representative as mean weights ± s.e.m of at least 8 animals per genotype. Statistical analysis was carried out by means of t-tests comparing all genotypes to their wild-type controls; *, $p < 0.05$, **, $p < 0.01$, ***, $p < 0.001$, ****, $p < 0.0001$.*

Figure 3.3 Photograph of double-knockout with wild-type and ob/ob littermates: Mice shown were eight weeks of age and were born from the same litter.

3.3 *Generation and genotypic frequencies of Irs-2$^{+/-}$db$^{+/-}$ offspring*

In contrast to the *Irs-2*$^{-/-}$ and *ob/ob* mice, *db/db* mice were maintained on the C57Bl/KS genetic background. As with the *Irs-2*$^{+/-}$*ob*$^{+/-}$ intercross single heterozygote male and female (*Irs-2*$^{+/-}$*x db*$^{+/-}$) mice were mated to produce double heterozygote animals (*Irs-2*$^{+/-}$*db*$^{+/-}$). These double heterozygotes were then intercrossed to obtain all genetic combinations of the *Irs2* and *db* genes. Double heterozygote mice were fertile and produced litters of comparable size to wild-type matings (data not shown). There also appeared to be no difficulties in maternal care for litters.

The intercross of *Irs-2*$^{+/-}$*db*$^{+/-}$ mice produced 286 offspring representing all 9 possible genotypes. PCR genotyping conducted at three weeks of age indicated that the frequency of these genotypes was generally in accordance with the expected Mendelian ratios (Table 3.2). However, it was observed that male *Irs-2*$^{-/-}$ mice were obtained at a very low frequency (3 in total, Table 3.2). As male *Irs-2*$^{-/-}$*db*$^{+/-}$ mice were obtained from the intercross of *Irs-2*$^{+/-}$*db*$^{+/-}$ mice (14 in total, Table 3.2) the low numbers of male *Irs-2*$^{-/-}$ mice obtained is very surprising. Unfortunately there is no explanation for this finding at present.

GENOTYPES	NUMBERS			% OFFSPRING	
	FEMALE	MALE	TOTAL	ACTUAL	EXPECTED
WILD-TYPE	14	13	27	9.44	6.25
IRS-2+/+db+/-	21	16	37	12.94	12.50
IRS-2+/-db+/+	20	26	46	16.08	12.50
IRS-2+/-db+/-	26	41	67	23.43	25.00
db/db	6	14	20	6.99	6.25
IRS-2 KO	10	3	13	4.55	6.25
IRS-2+/-db -/-	13	16	29	10.14	12.50
IRS-2-/-db+/-	15	14	29	10.14	12.50
DOUBLE-KNOCKOUT	7	11	18	6.29	6.25
		TOTAL	286	100	100

Table 3.2 Genetic frequencies of all 9 possible genotypes resulting from the intercross of Irs-2$^{+/-}$db$^{+/-}$ mice. Animals were PCR genotyped at three weeks of age.

3.4 *Body weight analysis of offspring from Irs-2$^{+/-}$db$^{+/-}$intercross*

Body weight analysis of offspring resulting from the *Irs-2*$^{+/-}$*db*$^{+/-}$intercross showed a similar pattern to that seen in the *Irs-2*$^{+/-}$*ob*$^{+/-}$ intercross (Fig 3.4). Again the *Irs-2*$^{-/-}$*db*$^{-/-}$ double knockouts resulting from this cross were growth retarded, weighing 40% of that of wild-type littermates at four weeks of age (Fig 3.5 a-b). Compound heterozygous mice, *Irs-2*$^{+/-}$*db*$^{+/-}$ mice exhibited a similar growth profile to that of wild-type littermates but weighed significantly more at eight weeks of age ($p < 0.01$), weighing on average 5 grams more. Mice containing a single allele of either the *Irs-2* or *db* genes (*Irs-2*$^{+/-}$ and *db*$^{+/-}$ mice) were similar to that of wild-type littermates (data not shown). Similar to *Irs-2*$^{-/-}$*ob*$^{+/-}$ mice, *Irs-2*$^{-/-}$*db*$^{+/-}$mice weighed more than their double knockout littermates, again being comparable to *Irs-2*$^{-/-}$ mice at eight weeks of age.

The body weights of *Irs-2*$^{-/-}$ and *db/db* mice resembled that of their equivalents from the *Irs-2*$^{+/-}$*ob*$^{+/-}$ intercross (Fig 3.4). In contrast, *Irs-2*$^{+/-}$*db*$^{-/-}$ mice did not appear to gain as much weight over the eight week period as *db/db* mice and were significantly smaller than their equivalents from the *Irs-2*$^{+/-}$*ob*$^{+/-}$ intercross (Fig 3.6). The difference between the body weights of *Irs-2*$^{+/-}$*db*$^{-/-}$ mice and *Irs-2*$^{+/-}$*ob*$^{-/-}$ mice at 8 weeks of age was significant (Fig 3.6, $p < 0.0001$). This difference in body weight between *Irs-2*$^{+/-}$*db*$^{-/-}$ and *Irs-2*$^{+/-}$*ob*$^{-/-}$ mice is an interesting observation but could be a consequence of the *db/db* mice being derived from a different genetic background. However the similarity of growth profiles for the other equivalent genotypes from these two intercrosses, would suggest that there is a true difference in the level of weight gain observed in *Irs-2*$^{+/-}$*db*$^{-/-}$ compared to *Irs-2*$^{+/-}$*ob*$^{-/-}$.

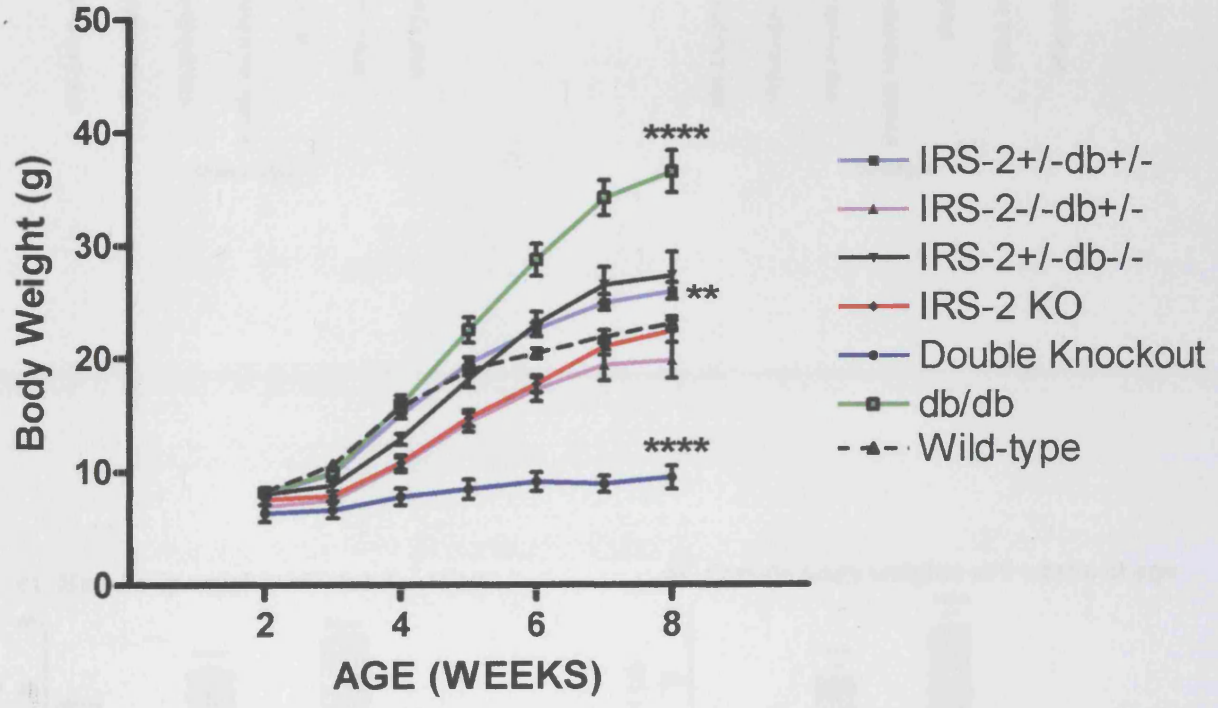

Figure 3.4 Growth curves showing mean weights ± s.e.m of offspring resulting from the Irs-2$^{+/-}$db$^{+/-}$ intercross at the indicated ages (weeks).

*Results are representative of at least 8 animals per genotype; **, $p < 0.01$, ****, $p < 0.0001$.*

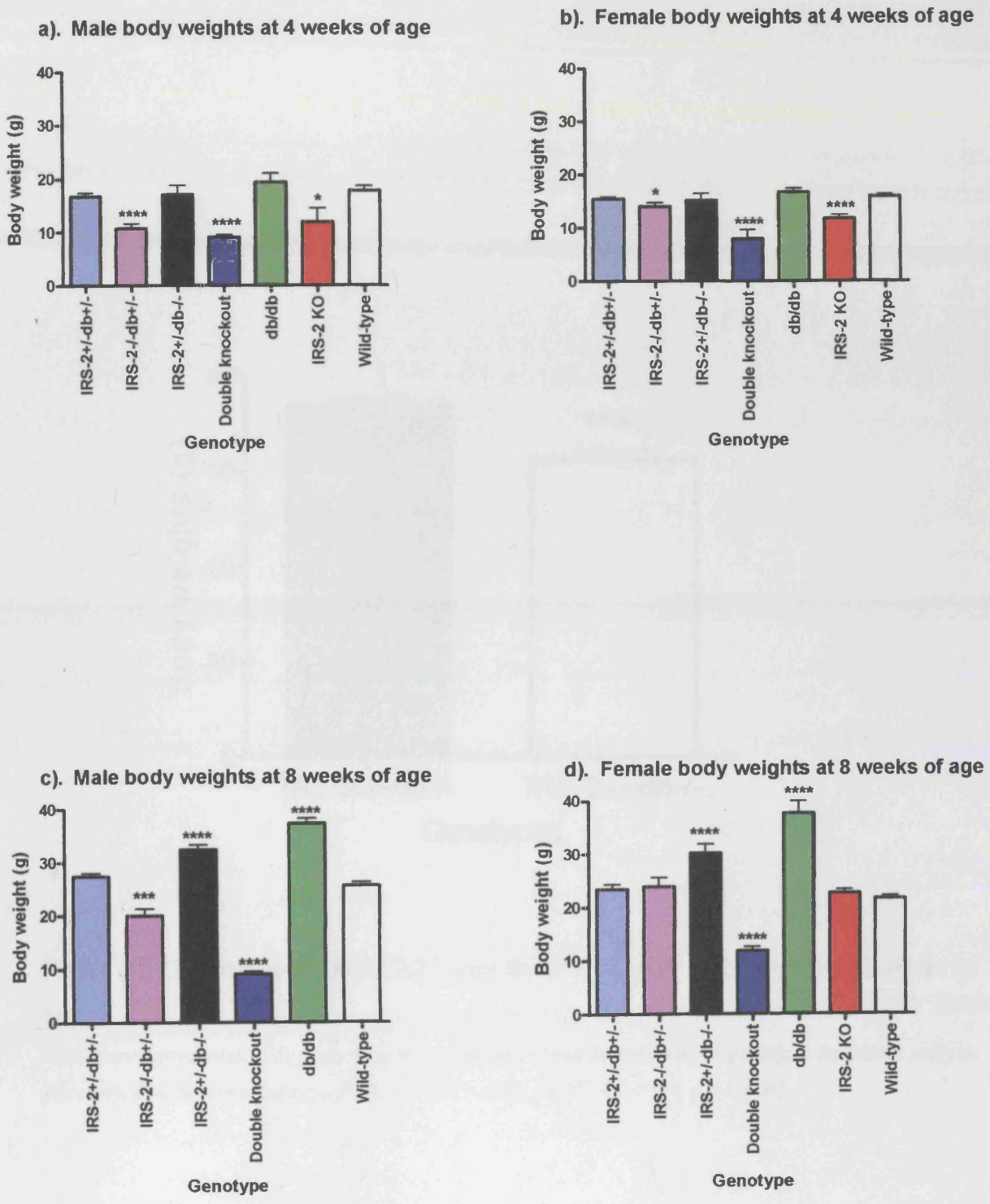

Figure 3.5 Analysis of body weights of male and female offspring from the Irs-2$^{+/-}$db$^{+/-}$ intercross at a-b). 4 weeks and c-d). 8 weeks of age.

*Results are representative as mean weights ± s.e.m of at least 4 animals per genotype. Statistical analysis was carried out by means of t-tests; *, $p < 0.05$, ***, $p < 0.001$, ****, $p < 0.0001$, of all genotypes versus wild-types.*

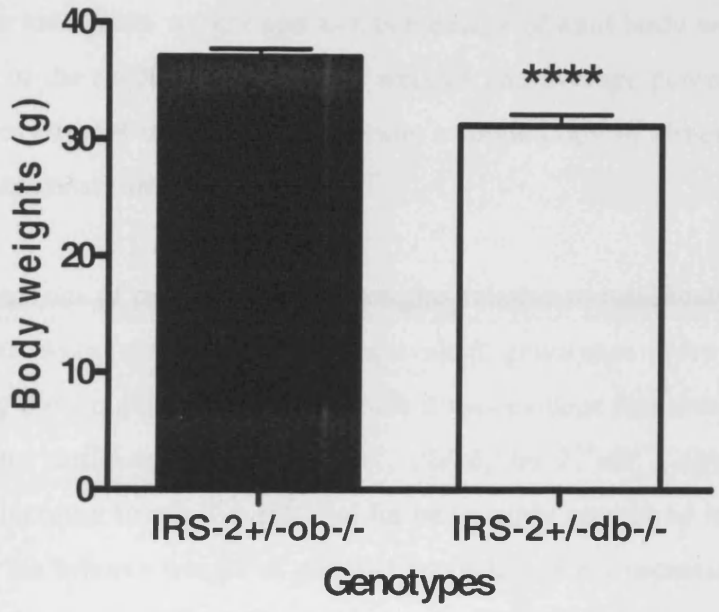

Figure 3.6 Comparison of Irs-2$^{+/-}$db$^{-/-}$ and Irs-2$^{+/-}$ob$^{-/-}$ mice body weights at 8 weeks of age.

*Results are representative as mean weights ± s.e.m of at least 26 animals per genotype. Statistical analysis was carried out by means of t-test for Irs-2$^{+/-}$db$^{-/-}$ versus Irs-2$^{+/-}$ob$^{-/-}$ ****, $p < 0.0001$.*

3.5 Tissue weight analysis of offspring resulting from both the Irs-2$^{+/-}$ob$^{+/-}$ and Irs-2$^{+/-}$db$^{+/-}$ intercrosses

The various offspring resulting from the two intercrosses were dissected at four weeks of age, brain and peripheral tissue weights were assessed. The weights of gonadal fat pads, muscle groups (gastronemius soleus and quadricep muscles pooled), liver and spleen taken from the various genotypes are presented as a percentage of total body weight in figures 3.7, 3.8, 3.9 and 3.10 respectively. Similarly, brain weight is presented as total brain weight and as a percentage of total body weight in figure 3.11. In the interest of the reader, average body weights and average percentage tissue weights of all genotypes (except those mice containing a single copy of either gene) are presented in for both intercrosses in Table 3.3.

Analysis of peripheral tissue weights relative to total body weight, demonstrated that weights were similar between equivalent genotypes from the two intercrosses. Considering the weight of gonadal fat pads it was evident that either leptin or leptin long-form receptor deficiency, in *Irs-2$^{+/-}$ob$^{-/-}$, ob/ob, Irs-2$^{+/-}$db$^{-/-}$, db/db* mice, resulted in a significant increase in relative gonadal fat pad weight compared to wild-type littermates. In contrast, the relative weight of gonadal fat pads was not increased to such levels in the double knockout mice (Fig 3.7). Indeed upon dissection it was noted that many double knockout mice were almost deplete of any white adipose tissue. Catabolism and development can both effect adipogenesis, the contribution of these parameters to the lack of white adipose tissue observed in double knockout mice will be discussed in chapter five. Interestingly, both *Irs-2$^{-/-}$ob$^{-/-}$* and *Irs-2$^{-/-}$db$^{-/-}$* double knockouts displayed marked sexual dimorphism with regards to gonadal fat pad weight, with male fat pads tending to weigh more than females (Fig 3.7). This sexual dimorphism was also evident in the *Irs-2$^{+/-}$ob$^{-/-}$* genotype, where the weight of male fat pads as a percentage of total body weight, were significantly increased compared to females ($^{**}p < 0.01$). Although this trend appeared to be the same in their equivalent genotype (*Irs-2$^{+/-}$db$^{-/-}$*), the increase seen in males was not determined to be significant.

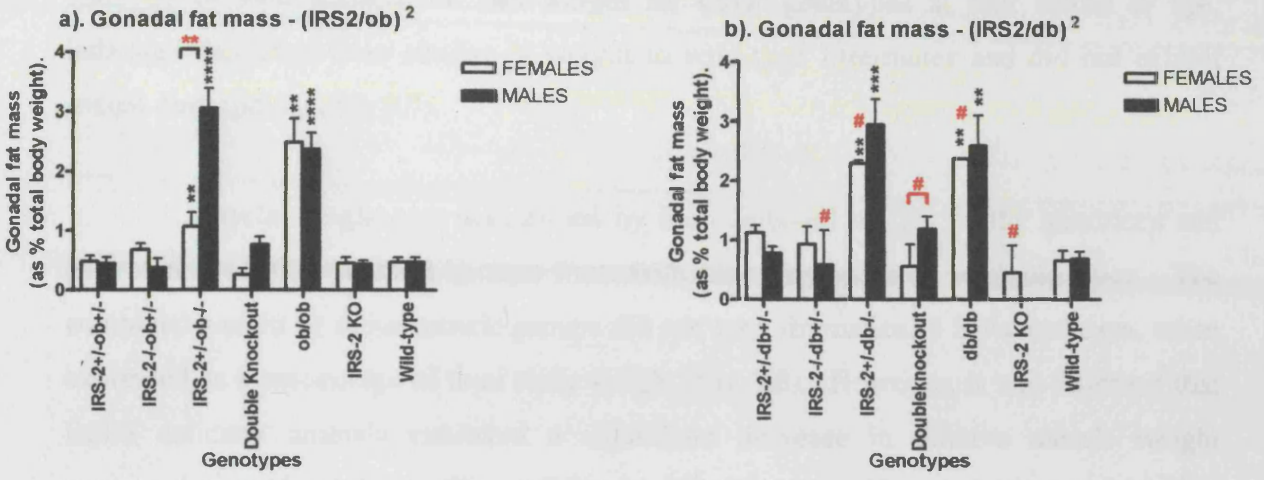

Figure 3.7 Gonadal fat mass of offspring from both Irs-2$^{+/-}$ob$^{+/-}$ and Irs-2$^{+/-}$db$^{+/-}$ intercrosses at 4 weeks of age.

*Gonadal fat weights were expressed as means of percentage total body weight ± s.e.m of at least 4 animals per genotype, except where indicated # n=3, **, $p < 0.01$, ***, $p < 0.001$, ****, $p < 0.0001$. Unfortunately, as only three male Irs-2 null mice were obtained from the Irs-2$^{+/-}$db$^{+/-}$ intercross, no fat weights were obtained for this particular group.*

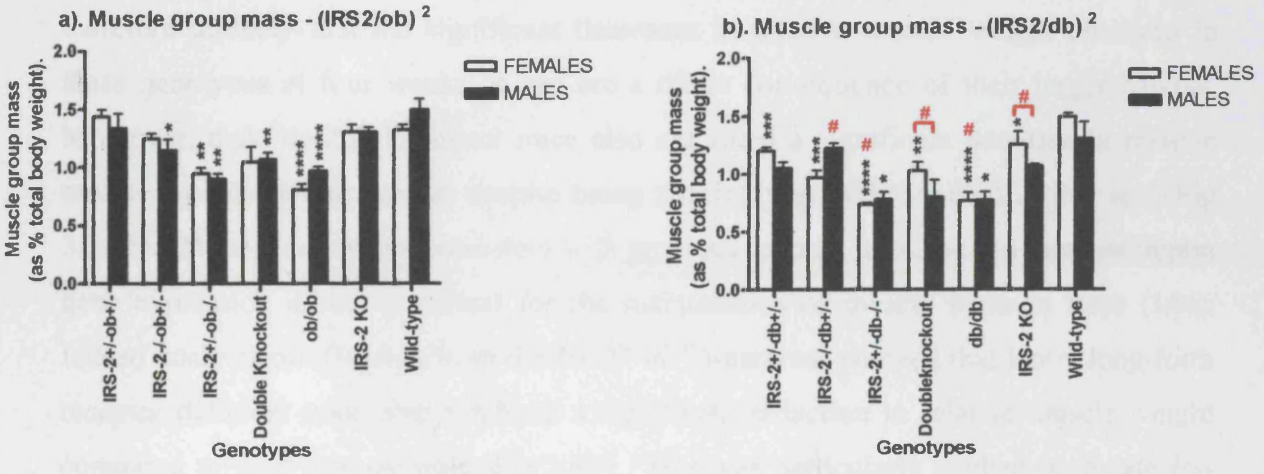

Figure 3.8 Muscle group mass of offspring from both Irs-2$^{+/-}$ob$^{+/-}$ and Irs-2$^{+/-}$db$^{+/-}$ intercrosses at 4 weeks of age.

*Gastronemius soleus and quadriceps muscle weights were pooled and expressed as means of percentage total body weight ± s.e.m of at least 4 animals per genotype, except where indicated, # n=3, *, $p < 0.05$, **, $p < 0.01$, ***, $p < 0.001$, ****, $p < 0.0001$.*

Analysis of total gonadal fat pad weight for other genotypes at four weeks of age, indicated that they were similar in weight to wild-type littermates and did not exhibit sexual dimorphism (Fig 3.7).

Muscle weight was determined by the combined weight of the quadricep and gastronemius soleus muscle groups from both hind legs of four-week-old mice. The combined weight of these muscle groups did not vary dramatically between sexes, when expressed as a percentage of total body weight (Fig 3.8). However, it was observed that leptin deficient animals exhibited a significant decrease in relative muscle weight compared to wild-type mice (Figure 3.8a; *Irs-2*$^{+/-}$*ob*$^{-/-}$, $p < 0.01$ *and ob/ob,* $p < 0.0001$ *vs wild-type controls*). A significant decrease in relative muscle weight was also noted in male *Irs-2*$^{-/-}$*ob*$^{-/-}$ double knockout mice ($p < 0.01$). Double knockout female mice tended to have a decreased relative muscle weight compared to wild-type controls but this was not proven to be significant. Interestingly, *Irs-2*$^{+/-}$*ob*$^{+/-}$, *Irs-2*$^{-/-}$*ob*$^{+/-}$ and *Irs-2*$^{-/-}$ mice had relative muscle weights comparable to wild-type controls, with only male *Irs-2*$^{-/-}$*ob*$^{+/-}$ mice showing a significant decrease relative to male wild-type littermates (Fig 3.8a; $p < 0.05$). The body weights of *Irs-2*$^{+/-}$*ob*$^{-/-}$ and *ob/ob* mice, although significant at four weeks of age, are not dramatically greater than wild-type littermates (Fig 3.2a-b). It is therefore unlikely that the significant decreases in relative muscle weight observed in these genotypes at four weeks of age are a direct consequence of their larger habitus. Moreover, male double knockout mice also exhibited a significant decrease in relative muscle weight at four weeks, despite being strikingly growth retarded at this age (Fig 3.2a-b). These findings are consistent with previous reports, implicating functional leptin gene expression as being critical for the maintenance of muscle mass in mice (144). Indeed analysis of offspring from the *Irs-2*$^{+/-}$*db*$^{+/-}$intercross showed that leptin long-form receptor deficient mice also exhibited a significant reduction in relative muscle weight compared to wild-type controls (Fig 3.8b). This was particularly evident in female *Irs-2*$^{+/-}$*db*$^{-/-}$ and *db/db* mice ($p < 0.0001$ versus wild-type controls). Double knockout female mice from this intercross also displayed a significant decrease in relative muscle weight (Fig 3.8b; $p < 0.01$). Similarly, male double knockouts tended to have reduced relative muscle weight but this was not shown to be significant. Interestingly, female *Irs-2*$^{+/-}$*db*$^{+/-}$, *Irs-2*$^{-/-}$*db*$^{+/-}$ and *Irs-2*$^{-/-}$ mice also exhibited significant decreases in relative muscle weight (Fig 3.8b). Considering male offspring from the *Irs-2*$^{+/-}$*db*$^{+/-}$intercross, only male *Irs-2*$^{+/-}$ *db*$^{-/-}$ and

db/db mice exhibited a decrease in relative muscle weight (Fig 3.8b; $p < 0.05$). This finding provides further evidence that functional leptin action is important for the maintenance of muscle mass in mice.

Consistent with previous reports both *ob/ob* and *db/db* mice had enlarged livers, demonstrating a significant increase in relative liver weight at four weeks of age (Fig 3.9a-b). It was observed that this increase was more significant in female mice ($p < 0.001$ compared to $p < 0.05$ for males). Enlarged livers were also observed in *Irs-2*$^{+/-}$*ob*$^{-/-}$ and *Irs-2*$^{+/-}$*db*$^{-/-}$ mice (Fig 3.9a-b; $p < 0.001$ for females and $p < 0.05$ for males versus sex matched wild-type controls). Considering other genotypes it was noted that female *Irs-2*$^{-/-}$*ob*$^{+/-}$and *Irs-2*$^{-/-}$ mice also displayed significant increases in relative liver weight, compared to wild-type controls (Fig 3.9a; $p < 0.0001$ and $p < 0.05$ respectively). In comparison all other genotypes resulting from the two intercrosses had relative liver weights comparable to wild-type controls.

Interestingly when spleen weights were expressed as a percentage of total body weight, it was observed that *Irs-2*$^{+/-}$*ob*$^{-/-}$, *ob/ob, Irs-2*$^{+/-}$*db*$^{-/-}$ and *db/db* mice showed significant reductions in relative spleen weights compared to wild-type controls (Fig 3.10). In comparison the relative weights of spleen in all other genotypes was comparable to wild-type mice.

Analysis of total brain weights indicated that mice homozygous for *Irs-2* generally had a significantly reduced total brain weight compared to wild-type littermates (Fig 3.11 c-d). Only female *Irs-2*$^{-/-}$ mice resulting from the intercross of *Irs-2*$^{+/-}$*db*$^{+/-}$mice showed a non-significant reduction in total brain weight, with all other *Irs-2* homozygous mice demonstrating an extremely significant reduction in total brain weight (Fig 3.11 c-d, $p < 0.0001$), this was consistent with previous reports (145).

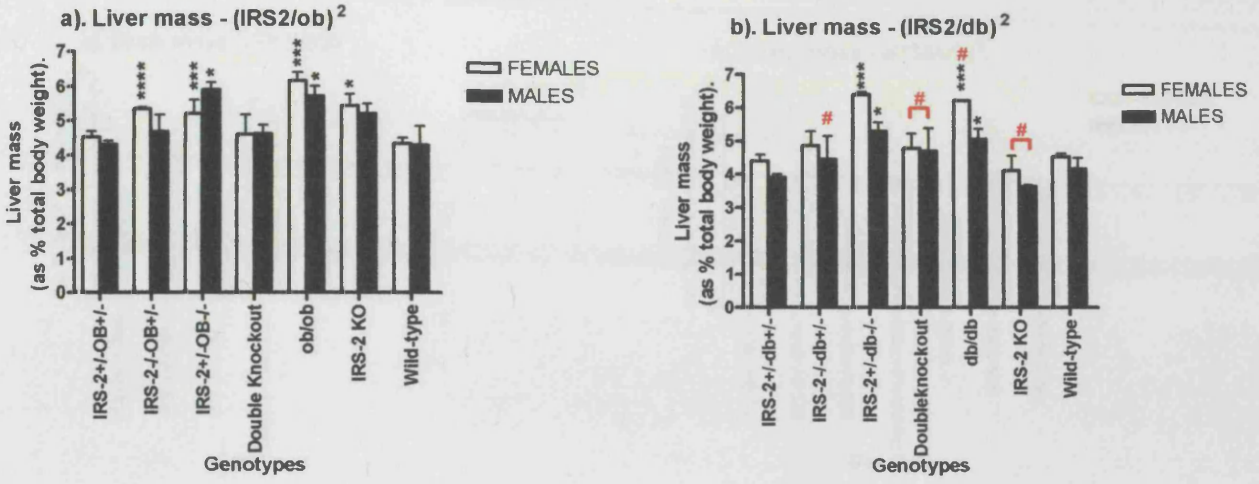

Figure 3.9 Liver mass of offspring from both Irs-2$^{+/-}$ob$^{+/-}$ and Irs-2$^{+/-}$db$^{+/-}$ intercrosses at 4 weeks of age.

*Results are representative as means of percentage total body weight ± s.e.m of at least 4 animals per genotype, except where indicated, # n=3, *, $p < 0.05$, ***, $p < 0.001$, ****, $p < 0.0001$.*

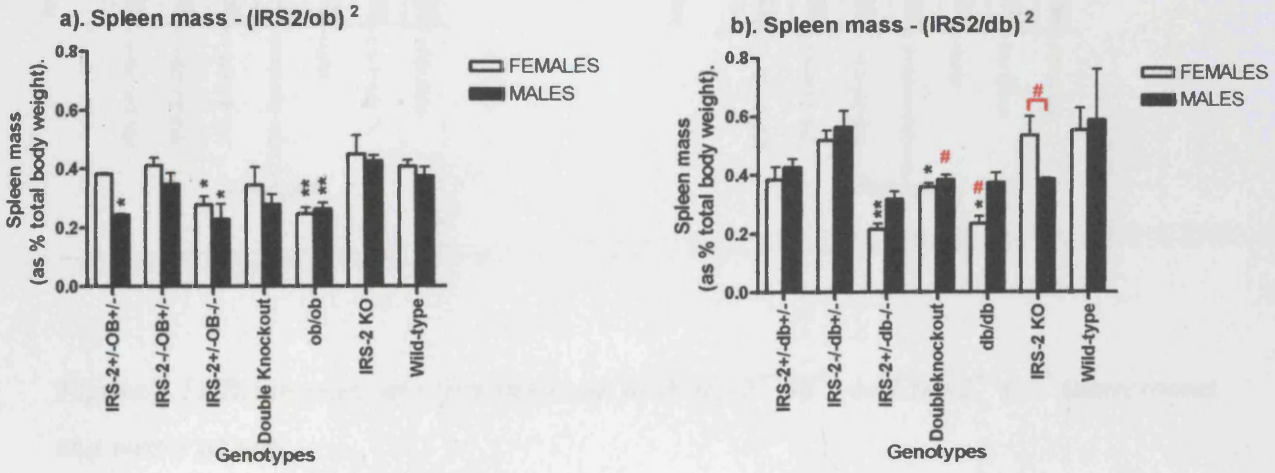

Figure 3.10 Spleen mass of offspring from both Irs-2$^{+/-}$ob$^{+/-}$ and Irs-2$^{+/-}$db$^{+/-}$ intercrosses at 4 weeks of age.

*Results are representative as means of percentage total body weight ± s.e.m of at least 4 animals per genotype, except where indicated. # n=3, *, $p < 0.05$, **, $p < 0.01$.*

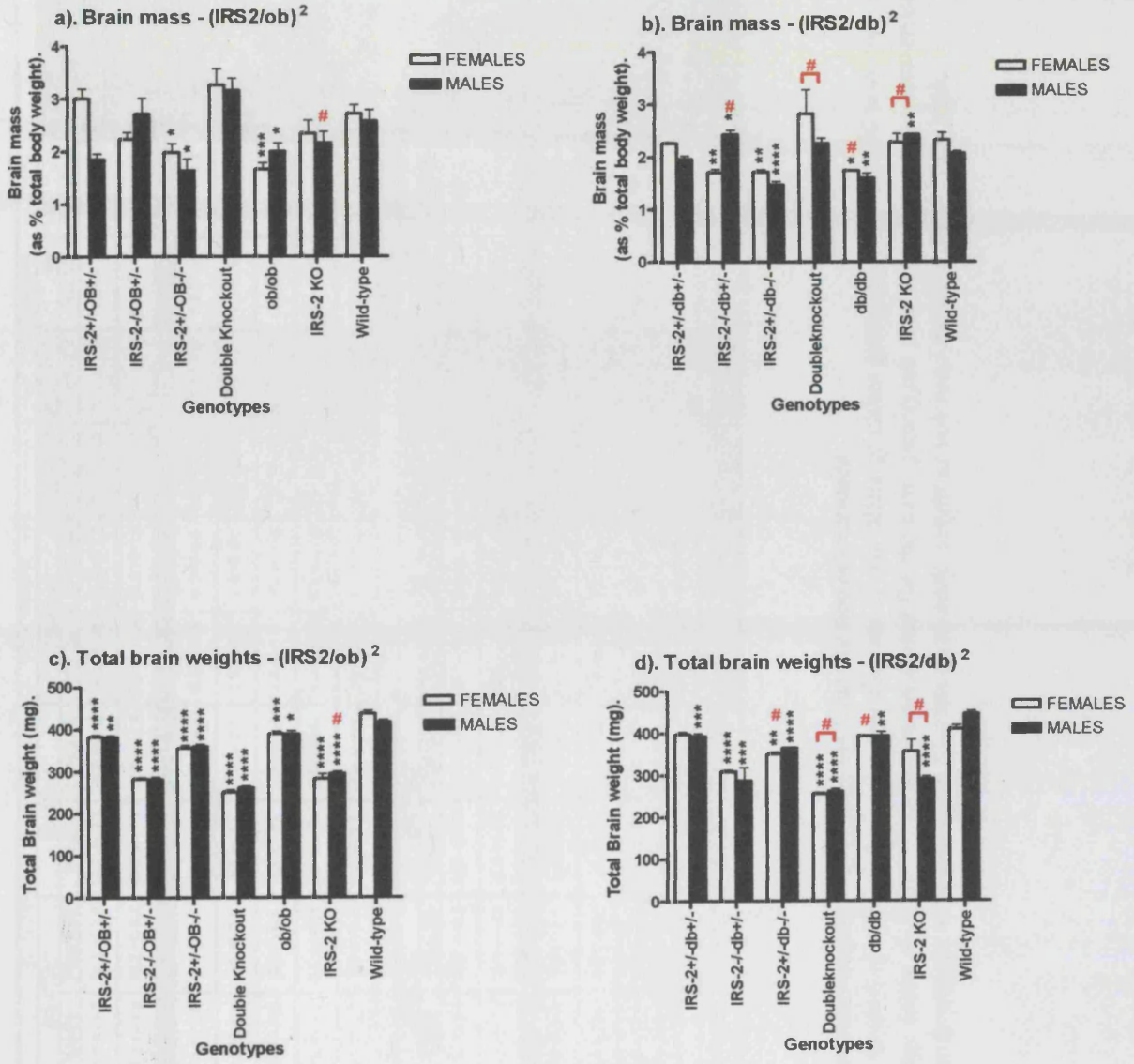

Figure 3.11 Brain mass of offspring from both Irs-2$^{+/-}$ob$^{+/-}$ and Irs-2$^{+/-}$db$^{+/-}$ intercrosses at 4 weeks of age.

*Results are represented as (a-b) means of percentage total body weight ± s.e.m and (c-d) means of total brain weights ± s.e.m. of at least 8 animals per genotype for the Irs-2$^{+/-}$ob$^{+/-}$ intercross and at least 4 animals per genotype for the Irs-2$^{+/-}$db$^{+/-}$ intercross, except where indicated, # n=3, *, $p < 0.05$, **, $p < 0.01$, ***, $p < 0.001$, ****, $p < 0.0001$.*

$IRS\text{-}2^{+/-}ob^{+/-}$ X $IRS\text{-}2^{+/-}ob^{+/-}$	INCREASING ← BODY WEIGHT → DECREASING													
	ob/ob		$IRS\text{-}2^{+/-}ob^{-/-}$		$IRS\text{-}2^{+/-}ob^{+/-}$		Wild-type		IRS-2 KO		$IRS\text{-}2^{-/-}ob^{+/-}$		Double knockout	
Mean body weight (grams):	MALES	FEMALES	MALES	FEMALES	MALES	FEMALES	MALES	FEMALES	MALES	FEMALES	MALES	FEMALES	MALES	FEMALES
4 weeks of age	19.1 +/- 1.7	16.0 +/- 2.6	17.0 +/- 1.3	15.2 +/- 2.5	15.2 +/- 2.3	13.9 +/- 1.6	14.0 +/- 2.1	13.4 +/- 1.5	10.0 +/- 2.1	10.2 +/- 2.0	11.5 +/- 2.3	11.2 +/- 2.2	8.4 +/- 2.0	9.3 +/- 1.2
8 weeks of age	40.6 +/- 2.9	34.0 +/- 5.1	38.2 +/- 1.9	15.2 +/- 2.5	27.8 +/- 1.7	21.2 +/- 1.6	26.7 +/- 1.4	13.4 +/- 1.5	23.9 +/- 1.5	10.2 +/- 2.0	21.5 +/- 1.6	21.6 +/- 1.6	12.5 +/- 2.4	9.3 +/- 1.2
Tissue weights (as % total body weight)														
Gonadal Fat mass	2.4 +/- 0.7	2.5 +/- 1.0	3.1 +/- 0.6	1.1 +/- 0.4	0.5 +/- 0.1	0.5 +/- 0.2	0.5 +/- 0.2	0.5 +/- 0.1	0.4 +/- 0.1	0.5 +/- 0.2	0.4 +/- 0.4	0.7 +/- 0.2	0.8 +/- 0.3	0.3 +/- 0.2
Muscle mass	1.0 +/- 0.1	0.8 +/- 0.1	0.9 +/- 0.1	1.0 +/- 0.1	1.3 +/- 0.1	1.4 +/- 0.1	1.5 +/- 0.2	1.3 +/- 0.1	1.3 +/- 0.1	1.3 +/- 0.1	1.2 +/- 0.2	1.3 +/- 0.1	1.1 +/- 0.1	1.1 +/- 0.2
Liver mass	5.7 +/- 0.8	6.2 +/- 0.6	5.9 +/- 0.3	5.2 +/- 0.5	4.3 +/- 0.1	4.5 +/- 0.4	4.3 +/- 1.1	4.3 +/- 0.3	5.2 +/- 0.6	5.4 +/- 0.5	4.7 +/- 1.0	5.3 +/- 0.1	4.6 +/- 0.5	4.6 +/- 0.9
Spleen mass	0.3 +/- 0.1	0.3 +/- 0.1	0.2 +/- 0.1	0.3 +/- 0.01	0.2 +/- 0.01	0.4 +/- 0.01	0.4 +/- 0.1	0.4 +/- 0.03	0.4 +/- 0.04	0.5 +/- 0.1	0.4 +/- 0.1	0.4 +/- 0.1	0.3 +/- 0.1	0.4 +/- 0.1
Brain mass	2.0 +/- 0.4	1.7 +/- 0.3	1.6 +/- 0.3	2.0 +/- 0.3	1.9 +/- 0.1	3.0 +/- 0.4	2.6 +/- 0.6	2.7 +/- 0.3	2.2 +/- 0.4	2.3 +/- 0.3	2.7 +/- 0.6	2.2 +/- 0.2	3.2 +/- 0.5	3.3 +/- 0.6
$IRS\text{-}2^{+/-}db^{+/-}$ X $IRS\text{-}2^{+/-}db^{+/-}$	INCREASING ← BODY WEIGHT → DECREASING													
	db/db		$IRS\text{-}2^{+/-}db^{-/-}$		$IRS\text{-}2^{+/-}db^{+/-}$		Wild-type		IRS-2 KO		$IRS\text{-}2^{-/-}db^{+/-}$		Double knockout	
Mean body weight (grams):	MALES	FEMALES	MALES	FEMALES	MALES	FEMALES	MALES	FEMALES	MALES	FEMALES	MALES	FEMALES	MALES	FEMALES
4 weeks of age	19.4 +/- 5.0	16.7 +/- 2.4	17.1 +/- 5.2	15.2 +/- 3.3	16.8 +/- 2.7	15.5 +/- 1.5	17.8 +/- 2.7	15.9 +/- 1.5	11.9 +/- 3.5	11.8 +/- 1.9	10.7 +/- 2.5	14.0 +/- 2.3	9.1 +/- 1.1	8.0 +/- 2.7
8 weeks of age	37.2 +/- 2.6	37.7 +/- 4.2	32.4 +/- 2.3	30.2 +/- 4.9	27.5 +/- 2.4	23.5 +/- 3.1	25.5 +/- 1.9	21.6 +/- 1.5	NO DATA	22.6 +/- 1.9	20.1 +/- 4.0	24.0 +/- 3.8	9.1 +/- 0.9	11.9 +/- 1.1
Tissue weights (as % total body weight)														
Gonadal Fat mass	2.6 +/- 0.8	2.4 +/- 0.01	3.0 +/- 0.8	2.3 +/- 0.1	0.8 +/- 0.2	1.1 +/- 0.2	0.7 +/- 0.2	0.7 +/- 0.3	NO FAT	0.3 +/- 0.4	0.4 +/- 0.5	0.9 +/- 0.5	1.2 +/- 0.2	0.6 +/- 0.5
Muscle mass	0.8 +/- 0.1	0.8 +/- 0.1	0.8 +/- 0.1	0.7 +/- 0.01	1.1 +/- 0.1	1.2 +/- 0.1	1.3 +/- 0.3	1.5 +/- 0.1	1.1 +/- 0.02	1.3 +/- 0.1	1.2 +/- 0.05	1.0 +/- 0.1	0.6 +/- 0.01	1.0 +/- 0.1
Liver mass	5.1 +/- 0.6	6.2 +/- 0.3	5.3 +/- 0.4	6.4 +/- 0.1	3.9 +/- 0.1	4.4 +/- 0.3	4.2 +/- 0.6	4.5 +/- 0.1	3.6 +/- 0.04	4.1 +/- 0.4	4.5 +/- 0.7	4.9 +/- 0.7	4.7 +/- 0.7	4.8 +/- 0.6
Spleen mass	0.4 +/- 0.1	0.2 +/- 0.03	0.3 +/- 0.05	0.2 +/- 0.03	0.4 +/- 0.1	0.4 +/- 0.1	0.8 +/- 0.3	0.6 +/- 0.1	0.4 +/- 0.01	0.5 +/- 0.1	0.6 +/- 0.1	0.5 +/- 0.1	0.4 +/- 0.02	0.4 +/- 0.02
Brain mass	1.6 +/- 0.1	1.7 +/- 0.02	1.5 +/- 0.1	1.7 +/- 0.1	2.0 +/- 0.1	2.3 +/- 0.05	2.1 +/- 0.1	2.3 +/- 0.2	2.4 +/- 0.01	2.3 +/- 0.2	2.4 +/- 10.1	1.7 +/- 0.1	2.3 +/- 0.1	2.8 +/- 0.6

Table 3.3: Summary of Body and tissue weights for various genotypes resulting from the two intercrosses

The mean body weights +/- s.e.m of all genotypes (excluding those mice containing the loss of one allele of either gene) are presented at both four and eight weeks of age. In addition the mean percentage tissue weights +/- s.e.m are presented for the same genotypes resulting from the two intercrosses. Genotypes are presented in the table according to body weight, with genotypes decreasing in body weight as you read the table from left to right.

3.6. Summary and discussion:

Both *Irs-2*$^{-/-}$ and *ob/ob* mice are hyperphagic, leading to obesity and eventually the development of insulin resistance and type 2 diabetes. It was hypothesised that the combined deletion of these genes in mice was likely to produce an exaggerated adiposity phenotype prior to the development of diabetes, particularly in female mice in which the diabetic *Irs-2*$^{-/-}$ phenotype is mild and obesity predominates. In contrast, *Irs-2*$^{-/-}$*ob*$^{-/-}$ mice were dramatically growth retarded. Similarly *Irs-2*$^{-/-}$*db*$^{-/-}$ double knockout mice also displayed severe growth retardation. In addition to growth retardation, both double knockout mice failed to thrive. As *Irs-2*$^{-/-}$, *ob/ob* and *db/db* mice are insulin resistant and develop type 2 diabetes, it was considered that double knockout mice might be suffering from a more severe metabolic phenotype at an earlier age.

Growth retardation was not observed in either *Irs-2*$^{-/-}$*ob*$^{+/-}$ or *Irs-2*$^{-/-}$*db*$^{+/-}$ mice, where it appeared a single allele of either the *ob* or *db* gene was sufficient to restore the body weight of these animals to that of *Irs-2*$^{-/-}$ mice. Consistent with previous reports, *Irs-2*$^{-/-}$ mice resulting from the intercross of *Irs-2*$^{+/-}$*ob*$^{+/-}$ mice displayed sexual dimorphism with regard to body weight. Between eight and twelve weeks of age male *Irs-2*$^{-/-}$ mice become more catabolic and start to lose weight. In contrast female *Irs-2*$^{-/-}$ mice are known to have a relatively normal glucose metabolism between eight and twelve weeks and this is reflected in their comparable body weights to wild-type animals at this age. Due to the surprisingly low numbers of male *Irs-2*$^{-/-}$ mice derived, this sexual dimorphism was hard to assess in the *Irs-2*$^{+/-}$*db*$^{+/-}$ intercross. The low number of male *Irs-2*$^{-/-}$ mice derived from this intercross was surprising given the reasonable numbers of male *Irs-2*$^{-/-}$*db*$^{+/-}$ mice obtained. It would have been interesting to see if more male *Irs-2*$^{-/-}$ mice would have been gained from further breeding of this intercross. However, at present there is no explanation for the low numbers of male *Irs-2*$^{-/-}$ obtained from this intercross.

Mice homozygous for either leptin or the leptin long-form receptor were obese as previously described (77, 78). It was also evident that *Irs-2*$^{+/-}$*ob*$^{-/-}$ and *Irs-2*$^{+/-}$*db*$^{-/-}$ mice exhibited an obese phenotype. However it was clear that *Irs-2*$^{+/-}$*db*$^{-/-}$ mice weighed significantly less than *Irs-2*$^{+/-}$*ob*$^{-/-}$ mice at eight weeks of age. As *db*$^{+/-}$ mice were derived from a slightly different genetic background, this may influence our observations. Subtle

variations in phenotypic traits of mice have been documented when mice have been bred upon different genetic backgrounds. However, although *ob/ob* and *db/db* mice have strikingly similar phenotypes, it should be noted that they are not exactly identical. Indeed, as *db/db* mice do not express the long-form of the leptin receptor, they are highly leptin resistant, resulting in an increase in circulating leptin levels. Although the leptin long-form receptor is believed to be the main mediator of leptin action, the shorter isoforms may not be completely redundant (56-58). If this were true, short-isoform receptor expression in *db/db* mice could facilitate some of leptin's actions in target tissues. In contrast, leptin signalling is completely absent in *ob/ob* mice, as these mice do not express leptin (the ligand). Therefore it is reasonable to assume that there may be subtle differences between *Irs-2*$^{+/-}$*ob*$^{-/-}$ and *Irs-2*$^{+/-}$*db*$^{-/-}$ mice.

Interestingly, dissections carried out upon four-week-old double knockout mice revealed that they contained significantly reduced gonadal fat-pad mass (white adipose tissue). As it is well documented that the insulin receptor substrate proteins have pivotal roles in adipogenesis (146), it was considered that the double knockout mice might be suffering with a form of lipodystrophy. As both development and catabolism can affect adipogenesis it would be essential to determine if and to what extent, the double knockout mice were catabolic. However the fact that small traces of white adipose tissue could be found around the gonadal region of some double knockout mice, indicated that this relative lipodystrophy was probably a result of catabolism. This issue is addressed in more detail in chapter five.

As expected, *ob/ob* and *db/db* mice both exhibited significant increases in relative gonadal fat pad mass compared to wild-type mice. This was also observed in *Irs-2*$^{+/-}$*ob*$^{-/-}$ and *Irs-2*$^{+/-}$*db*$^{-/-}$ mice. Considering all other genotypes there was no significant change in gonadal fat mass relative to wild-type controls.

Muscle mass was significantly reduced in leptin and leptin-receptor deficient genotypes (including male *Irs-2*$^{-/-}$*ob*$^{-/-}$ and female *Irs-2*$^{-/-}$*db*$^{-/-}$ double knockout mice) compared to wild-type controls. It is known that *ob/ob* mice exhibit muscle hypoplasia, this being particularly evident in the quadriceps (144). Moreover, leptin administration in *ob/ob* mice over a four week period had no effect on the morphology or function of skeletal muscle despite a reduction in body mass (147).

Increases in liver size (hepatomegaly) can occur due to an increase hepatocyte proliferation (hepatocarcinogenesis) (148). However obesity is often accompanied by the manifestation of a fatty liver phenotype. Both leptin and leptin long-form receptor deficient rodents exhibit fatty livers, which are known to be increased for triacylglycerides and free-fatty acids (106, 149).

The observation that *ob/ob*, *Irs-2*$^{+/-}$*ob*$^{-/-}$, *db/db* and *Irs-2*$^{+/-}$*db*$^{-/-}$ mice exhibited an significant increase in liver weight was consistent with such reports (150). Similarly female *Irs-2*$^{-/-}$and *Irs-2*$^{-/-}$*ob*$^{+/-}$ mice also displayed a significant increase in liver size but this was not evident in male mice. This finding is consistent with the sexual dimorphism seen in the *Irs-2*$^{-/-}$ genotype and was thought to be indicative of the less severe disorder of glucose homeostasis and more pronounced obesity, exhibited by female *Irs-2*$^{-/-}$ mice compared to males. Interestingly the livers of female double knockout mice were comparable in weight to that of wild-type controls. It would be interesting to assess if liver triacylglyceride and free-fatty acid content were increased in double knockout mice, similar to previous reports in *ob/ob* and *db/db* mice.

The main function of the spleen is to monitor blood for potentially harmful foreign molecules. The blood vessels of the spleen are surrounded by nests of B lymphocytes. As blood passes through the spleen, it is monitored by T-cells for the presence of foreign bodies. Once detected T-cells present the foreign molecule to B lymphocytes and division of the appropriate memory B cell leads to the production of antibodies directed against the invading antigen.

Immune responses are intrinsically energy expensive and come at a cost to the responding organism (151). Leptin plays an important role in the generation and maintenance of immune responses (152, 153). Similar to previous reports, the spleens of leptin and leptin long-form receptor deficient animals were significantly smaller compared with those of age-matched wild-type mice (154, 155). In contrast spleens of *Irs-2*$^{-/-}$, *Irs-2*$^{-/-}$*ob*$^{+/-}$ *and Irs-2*$^{-/-}$*db*$^{+/-}$ were comparable in size to those of wild-type controls. Similarly IRS-2 has been implicated in immune function but these abnormalities are relatively mild compared to the disorders found in *ob/ob* and *db/db* mice (156).

In summary the finding that double knockout mice were growth retarded and did not exhibit an obese phenotype was unexpected. Previous studies on *Irs-2*$^{-/-}$ mice revealed that disorder to glucose homeostasis is less profound in females. Therefore the observation that female double knockout mice were also severely growth retarded is particularly surprising and would indicate that deletion of *Irs-2* in combination with leptin or leptin receptor function has an additive effect upon peripheral glucose metabolism. To understand why this genotype develops such a profound phenotype that is surprisingly not obese, several metabolic studies were carried out to assess glucose homeostasis in double knockout mice. These are presented in the next two chapters (chapters 4 and 5).

CHAPTER 4

Metabolic studies of offspring resulting from *Irs-2*$^{+/-}$*ob*$^{+/-}$ and *Irs-2*$^{+/-}$*db*$^{+/-}$ intercrosses.

Irs-2$^{-/-}$, *ob/ob* and *db/db* mice all develop obesity, insulin resistance and eventually overt type 2 diabetes. The growth retardation and failure to thrive seen in the double knockout mice suggested that these mice might be developing a more severe metabolic phenotype at an earlier age. In order to determine the extent that these animals had lost control of glucose homeostasis, a number of metabolic studies were carried out immediately post-weaning and at later ages.

4.1 Fasting blood glucose levels of offspring from the Irs-2$^{+/-}$*ob*$^{+/-}$ *intercross at 4 and 8 weeks of age*

At four weeks of age, double knockout mice had fasting blood glucose levels in excess of 12-17mmol/L and thus were markedly diabetic (Fig 4.1a). In comparison, all other genotypes had normal fasting blood glucose levels below 5mmol/L at four weeks of age (Fig 4.1a). These included the *Irs-2*$^{-/-}$ mice, in which overt diabetes does not usually manifest itself until approximately eight to ten weeks of age. There were no differences at this age between fasting glucose levels in male and female animals of all the other genotypes.

Fasting blood glucose levels taken at eight weeks of age showed the double knockout mice to now have fasting blood glucose exceeding 20mmol/L (Fig 4.1b). In addition, *Irs-2*$^{-/-}$*ob*$^{+/-}$, *Irs-2*$^{+/-}$*ob*$^{-/-}$, *Irs-2*$^{-/-}$, and *ob/ob* mice now had high fasting blood glucose levels when compared to wild-type animals. These mice had fasting blood glucose in the range of 7-15mmol/L suggesting the presence of glucose intolerance. It was also observed that the hyperglycemia seen in these genotypes was more pronounced in males than females. This finding is consistent with previous reports on the *Irs-2*$^{-/-}$ mice, with males developing glucose intolerance earlier than females (83, 84).

a).

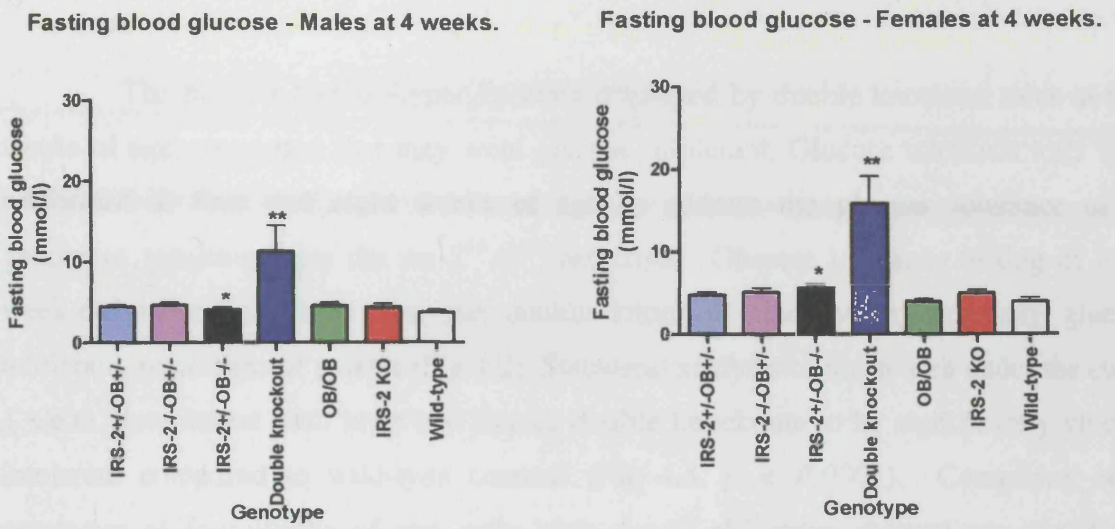

b).

Figure 4.1 Fasting blood glucose of offspring from Irs-2$^{+/-}$ob$^{+/-}$ intercross at a) 4 weeks and b) 8 weeks of age.

Results are expressed as mean fasting blood glucose ± s.e.m and are representative of 8 animals per sex per genotype.

4.2. *Glucose tolerance tests of offspring from the Irs-2$^{+/-}$ob$^{+/-}$ intercross at 4 and 8 weeks of age*

The marked fasting hyperglycemia displayed by double knockout mice at four weeks of age, suggested that they were glucose intolerant. Glucose tolerance tests were performed at four and eight weeks of age to address the glucose tolerance of all genotypes resulting from the *Irs-2*$^{+/-}$*ob*$^{+/-}$intercross. Glucose tolerance testing of four-week-old mice confirmed that the double knockout mice were extremely glucose intolerant, regardless of gender (Fig 4.2). Statistical analysis of mean area under the curve ± s.e.m, determined both male and female double knockouts to be significantly glucose intolerant compared to wild-type controls (Fig 4.4, $p < 0.0001$). Comparing other genotypes at four weeks of age, only male *Irs-2*$^{+/-}$*ob*$^{-/-}$ mice showed any significant glucose intolerance relative to wild-type controls (Fig 4.4, $p < 0.01$). *Irs-2*$^{-/-}$*ob*$^{+/-}$, *Irs-2*$^{+/-}$*ob*$^{+/-}$, *Irs-2*$^{-/-}$ and *ob/ob* mice displayed normal glucose tolerance at four weeks of age (Fig 4.2). Normal glucose tolerance was also seen in the *Irs-2*$^{+/-}$and *ob*$^{+/-}$, mice (data not shown).

Further glucose tolerance tests carried out at eight weeks of age showed that double knockout mice were now severely glucose intolerant with blood glucose levels often failing to return within the range of the glucometer (Fig 4.4, $p < 0.0001$). Moreover, *Irs-2*$^{-/-}$*ob*$^{+/-}$, *Irs-2*$^{+/-}$*ob*$^{-/-}$, and *ob/ob* mice all now displayed marked glucose intolerance, regardless of gender (Fig 4.3). Analysis of area under the curve showed the glucose intolerance in these animals to be significant compared to wild-type controls (Fig 4.4). Glucose tolerance tests carried out at eight weeks highlighted the sexual dimorphism seen in *Irs-2*$^{-/-}$ mice, with males displaying severe glucose intolerance, while females were still relatively sensitive to a glucose load (Fig 4.3). Analysis of area under the curve for *Irs-2*$^{-/-}$ mice showed male *Irs-2*$^{-/-}$ mice to be significantly more glucose intolerant than wild-type controls (Fig 4.4, $p < 0.001$), whereas female *Irs-2*$^{-/-}$ mice were shown to be not significantly different to sex matched wild-type controls (Fig 4.4). Interestingly *Irs-2*$^{+/-}$*ob*$^{+/-}$ mice remained glucose tolerant, with an area under the curve comparable to that of wild-type controls for both sexes. Similarly, *Irs-2*$^{+/-}$ and *ob*$^{+/-}$ mice displayed, normal glucose tolerance at eight weeks of age (data not shown).

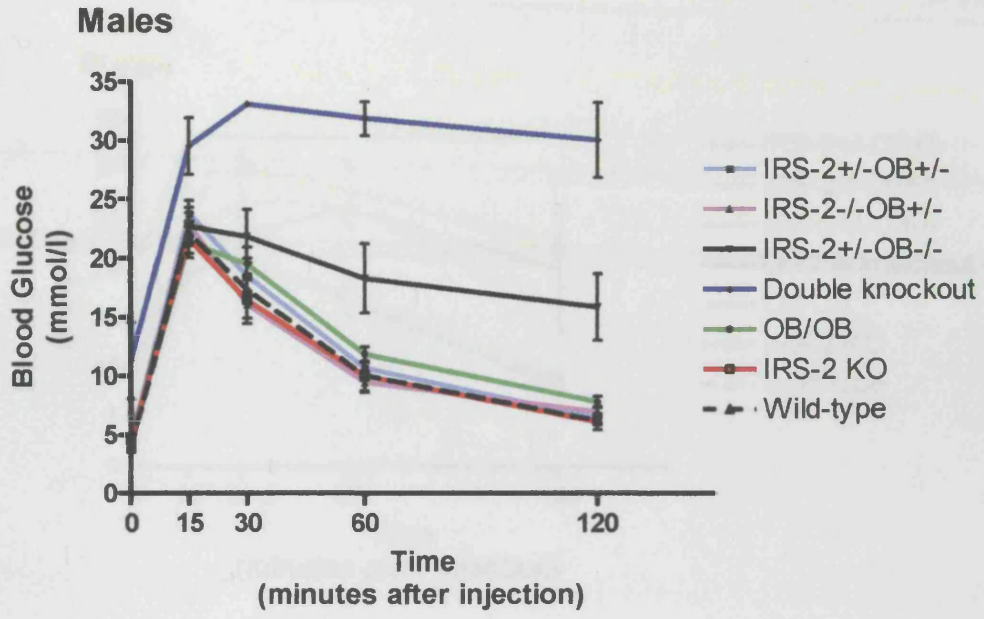

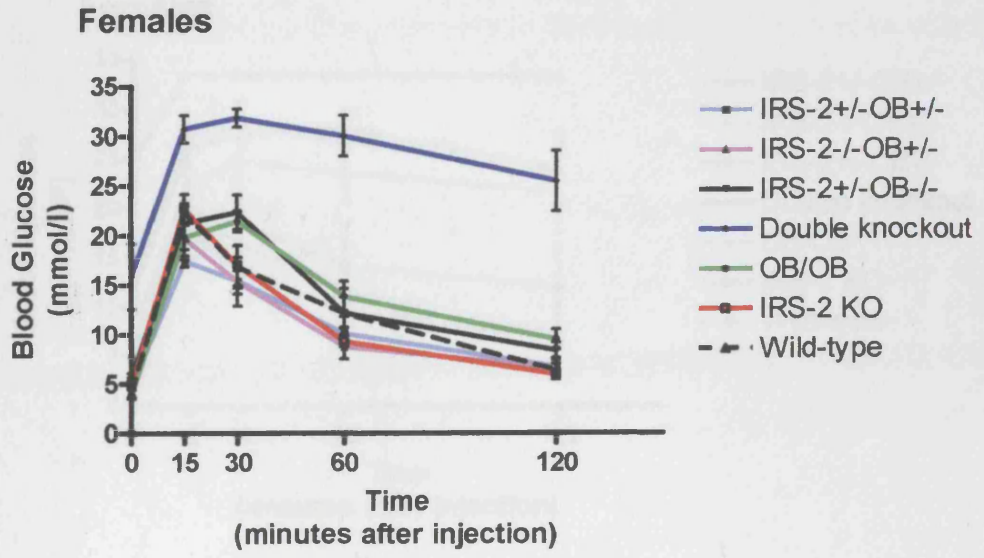

Figure 4.2 Glucose tolerance tests of offspring from the Irs-2$^{+/-}$ob$^{+/-}$ intercross at 4 weeks of age.

Results are expressed as mean blood glucose ± s.e.m and are representative of 8 animals per sex per genotype.

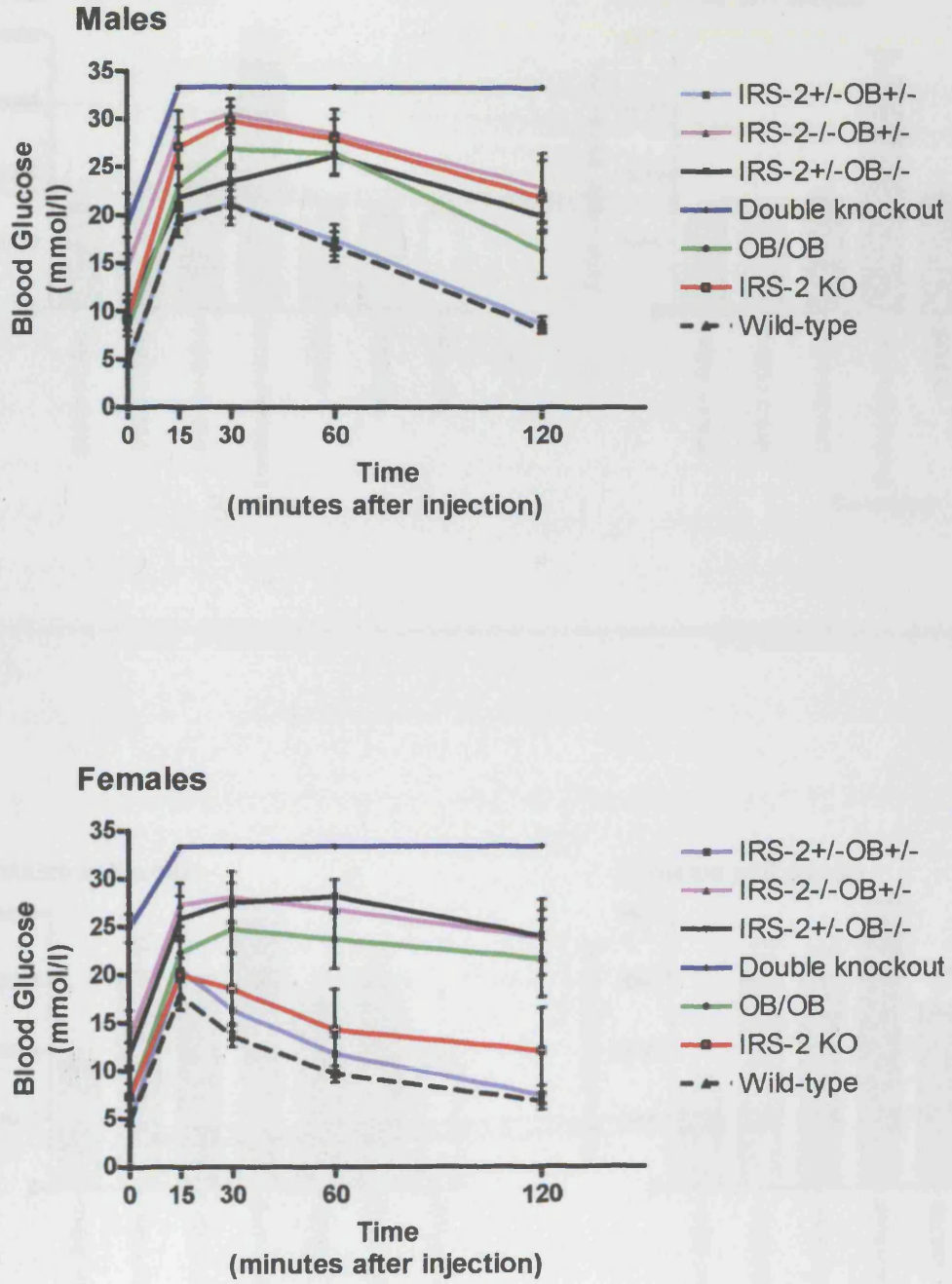

Figure 4.3 Glucose tolerance tests of offspring from the Irs-2$^{+/-}$ob$^{+/-}$ intercross at 8 weeks of age.

Results are expressed as mean blood glucose ± s.e.m and are representative of 8 animals per sex per genotype.

a).

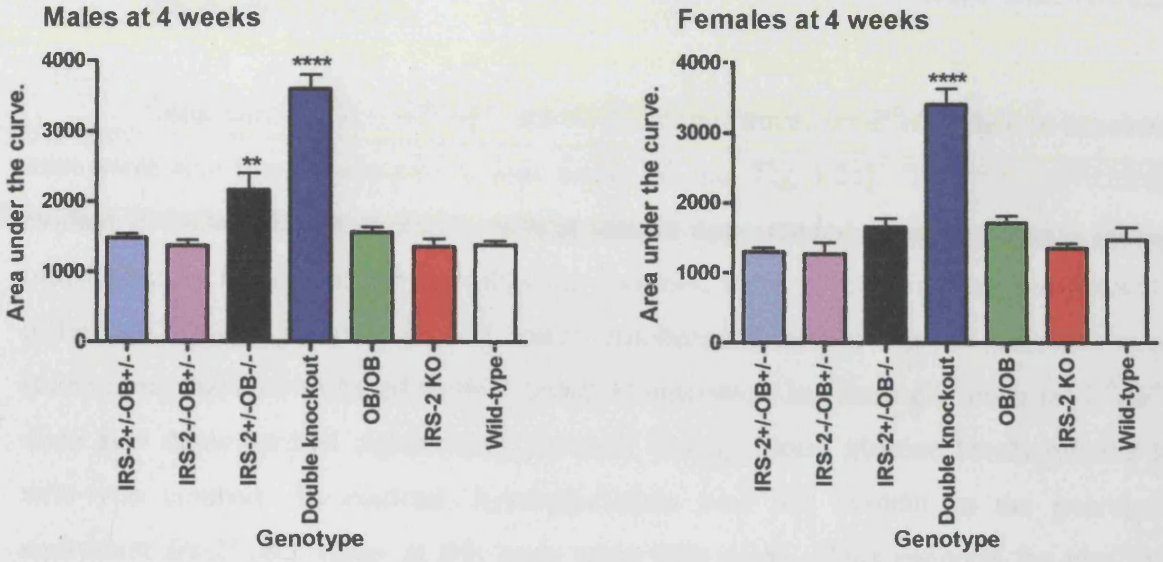

b).

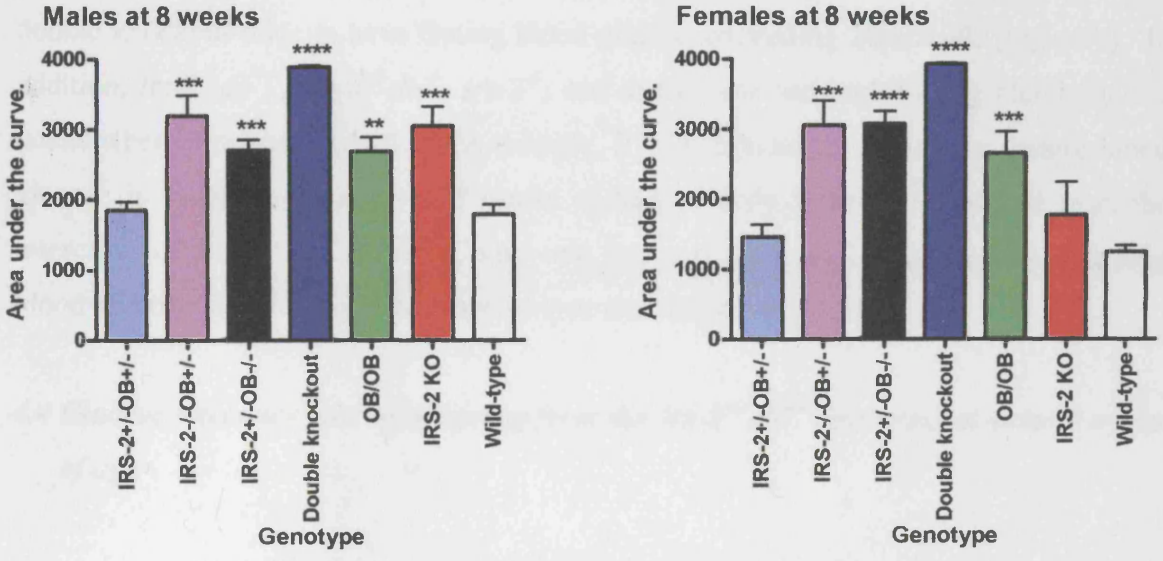

Figure 4.4 Statistical analysis of glucose tolerance tests carried out at 4 and 8 weeks of age on offspring from the Irs-2$^{+/-}$ob$^{+/-}$ intercross.

*Results are expressed as mean area under the curve ± s.e.m from glucose tolerance test curves presented in Figures 4.2 and 4.3, being representative of 8 animals per sex per genotype. t-tests were performed comparing all genotypes to their wild-type controls; **, $p < 0.01$, ***, $p < 0.001$, ****, $p < 0.0001$.*

4.3 *Fasting blood glucose levels of offspring from the Irs-2$^{+/-}$db$^{+/-}$ intercross at 4 and 8 weeks of age*

Consistent wiith *Irs-2$^{-/-}$ob$^{-/-}$* double knockout mice, *Irs-2$^{-/-}$db$^{-/-}$* double knockout mice were also hyperglycaemic at four weeks of age (Fig 4.5a). This was particularly evident in male mice ($p < 0.05$). Whilst female mice tended to have elevated fasting blood glucose levels relative to wild-type controls, these levels were not significantly different (Fig 4.5a). However, the lower numbers of female double knockout mice studied may have contributed to this statistical outcome. Interestingly, male *Irs-2$^{-/-}$db$^{+/-}$* mice also demonstrated significantly elevated fasting blood glucose levels relative to wild-type controls. In contrast, hyperglycaemia was not evident in the genotypic equivalent *Irs-2$^{-/-}$ob$^{+/-}$* mice, at this early stage (Fig 4.1a). This supports the idea that there are differences in the effects of reducing receptor expression as opposed to reducing leptin expression. In comparison, all other genotypes resulting from the intercross of *Irs-2$^{+/-}$db$^{+/-}$* mice had normal fasting blood glucose levels below 5mmol/L at four weeks of age (Fig 4.5a).

Analysis of fasting blood glucose levels taken at eight weeks of age showed the double knockout mice to have fasting blood glucose exceeding 20mmol/L (Fig 4.5b). In addition, *Irs-2$^{-/-}$db$^{+/-}$*, *Irs-2$^{+/-}$db$^{-/-}$*, *Irs-2$^{-/-}$*, and *db/db* now had high fasting blood glucose levels when compared to wild-type animals. It was difficult to assess the fasting blood glucose in male *Irs-2$^{-/-}$* mice at 8 weeks of age, as only three were weaned from the intercross of *Irs-2$^{+/-}$db$^{+/-}$*mice. Compound heterozygous *Irs-2$^{+/-}$db$^{+/-}$*mice had fasting blood glucose levels comparable to wild-type littermates (Fig 4.5b).

4.4 *Glucose tolerance tests of offspring from the Irs-2$^{+/-}$db$^{+/-}$ intercross at 4 and 8 weeks of age*

The elevated fasting blood glucose levels demonstrated by double knockout mice at 4 weeks of age suggested these mice were also glucose intolerant. Glucose tolerance tests were therefore performed to address the glucose tolerance of all genotypes resulting from the *Irs-2$^{+/-}$db$^{+/-}$*intercross.

a).

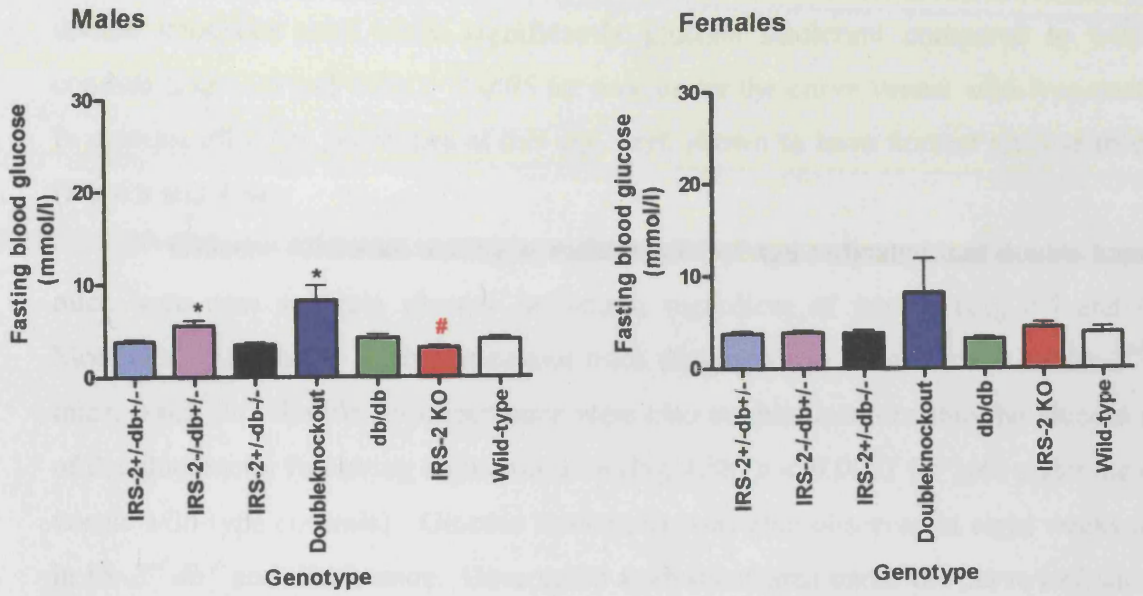

b).

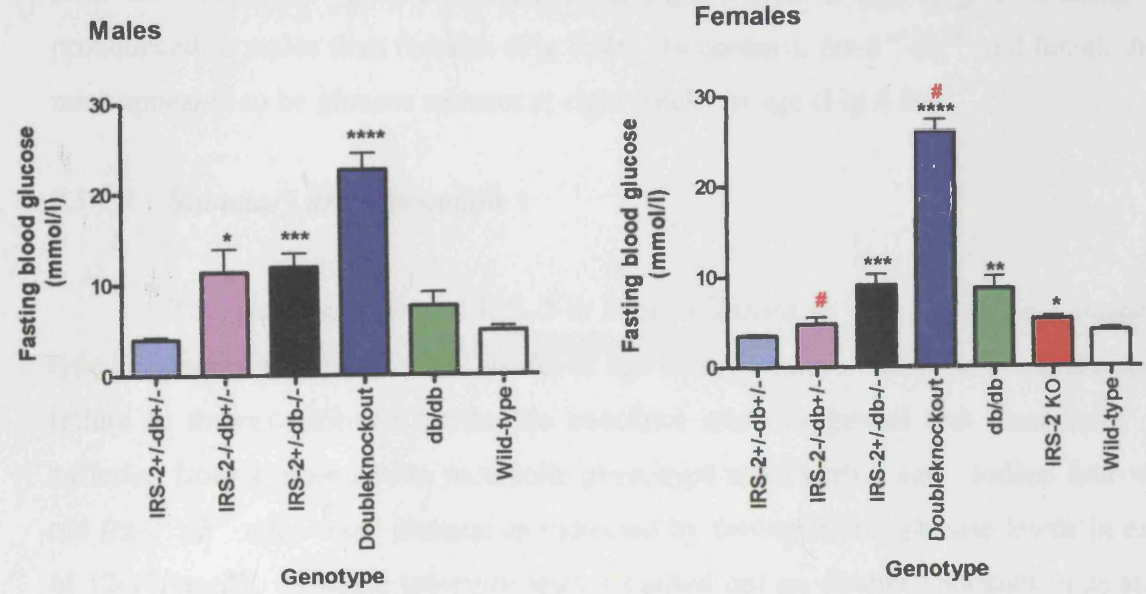

Figure 4.5 Fasting blood glucose of offspring from Irs-2$^{+/-}$db$^{+/-}$ intercross at a) 4weeks and b) 8 weeks of age.

*Results are expressed as mean fasting blood glucose ± s.e.m and are representative of at least 4 animals per sex per genotype (except where indicated, # n=3 *, $p < 0.05$, **, $p < 0.01$, ***, $p < 0.001$, ****, $p < 0.0001$.*

Glucose tolerance testing of four-week-old mice confirmed that male *Irs-2*$^{-/-}$*db*$^{-/-}$ double knockout mice were significantly glucose intolerant compared to wild-type controls (Figs 4.6 and 4.8a, $p < 0.05$ for area under the curve versus wild-type controls). In contrast all other genotypes at this age were shown to have normal glucose tolerance (Fig 4.6 and 4.8a).

Glucose tolerance testing at eight weeks of age indicated that double knockout mice were now severely glucose intolerant, regardless of gender (Fig 4.7 and 4.8b). Moreover, as with the double knockout mice derived from the intercross of *Irs-2*$^{+/-}$*ob*$^{+/-}$ mice, *Irs-2*$^{-/-}$*db*$^{-/-}$ double knockout mice were also unable to return into the glucose range of the glucometer following a glucose dose (Fig 4.8b, $p < 0.0001$ for area under the curve versus wild-type controls). Glucose intolerance was also observed at eight weeks of age in *Irs-2*$^{+/-}$*db*$^{-/-}$ and *db/db* mice. Once again analysis of area under the curve indicated that female *Irs-2*$^{+/-}$*db*$^{-/-}$ and *db/db* mice were more significantly glucose intolerant relative to sex matched wild-type controls, than were male mice of the same genotype (Fig 4.8b, $p < 0.0001$ for female *Irs-2*$^{+/-}$*db*$^{-/-}$ and *db/db* mice versus wild-types, compared to $p < 0.001$ for male *Irs-2*$^{+/-}$*db*$^{-/-}$ and $p < 0.05$ for male *db/db* mice versus wild-types). *Irs-2*$^{-/-}$*db*$^{+/-}$ mice also displayed glucose intolerance at eight weeks of age (Fig 4.7), being more pronounced in males than females (Fig 4.8b). In contrast, *Irs-2*$^{+/-}$*db*$^{+/-}$ and female *Irs-2*$^{-/-}$ mice appeared to be glucose tolerant at eight weeks of age (Fig 4.8b).

4.5 Summary and discussion

The global deletion of IRS-2 in mice is known to lead to the manifestation of type-2 diabetes as early as eight weeks of age in male mice. The growth retardation and failure to thrive exhibited by double knockout mice suggested that these mice were suffering from a more severe metabolic phenotype at an earlier age. Indeed four-week-old *Irs-2*$^{-/-}$*ob*$^{-/-}$ mice were diabetic as indicated by fasting blood glucose levels in excess of 12-17mmol/l. Glucose tolerance testing carried out on double knockout mice at four and eight weeks, highlighted their severe glucose intolerance. It was evident that despite having similar fasting blood glucose levels to *Irs-2*$^{-/-}$*ob*$^{-/-}$ mice at four weeks of age (Fig 4.4a AUC = ~4000), *Irs-2*$^{-/-}$*db*$^{-/-}$ mice (Fig 4.8a AUC ~ 2000) exhibited only mild glucose intolerance.

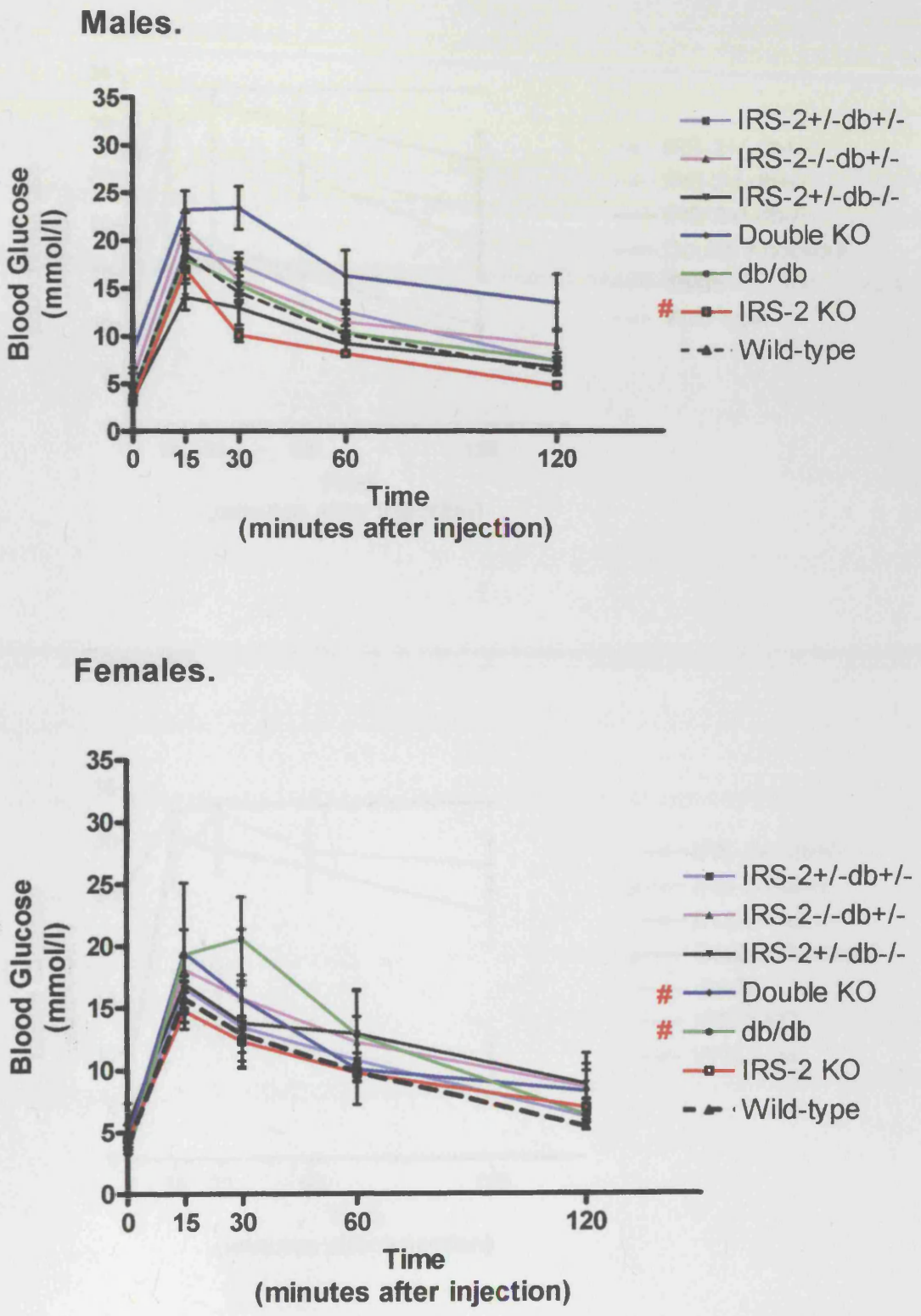

Figure 4.6 Glucose tolerance tests of offspring from the Irs-2$^{+/-}$db$^{+/-}$ intercross at 4 weeks of age.

Results are expressed as mean blood glucose ± s.e.m and are representative of at least 8 animals per sex per genotype (except where indicated, #n= at least 3).

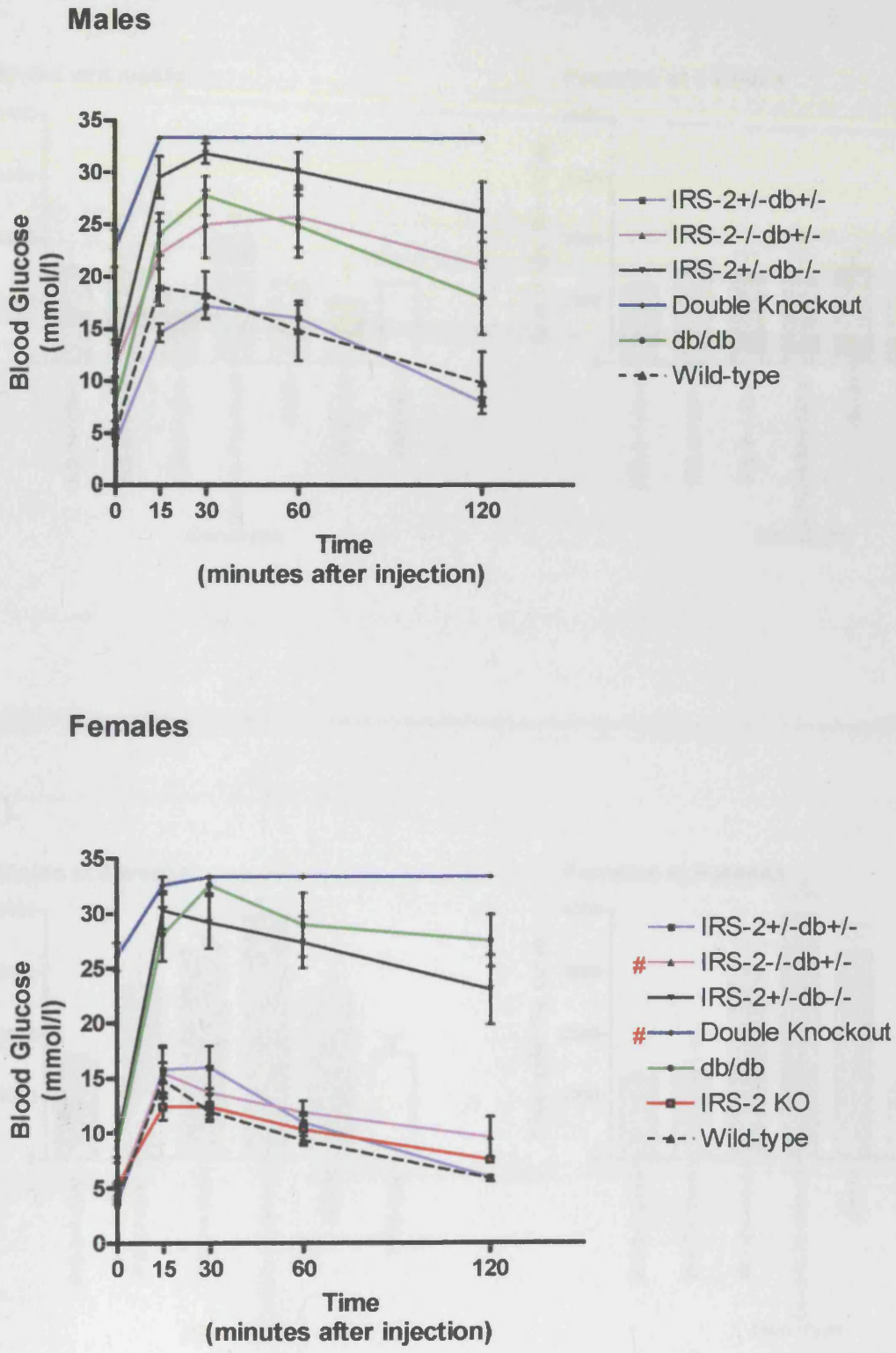

Figure 4.7 Glucose tolerance tests of offspring from the Irs-2$^{+/-}$db$^{+/-}$ intercross at 8 weeks of age.

Results are expressed as mean blood glucose ± s.e.m and are representative of at least 4 animals per sex per genotype (excepted where indicated, #n=3).

a).

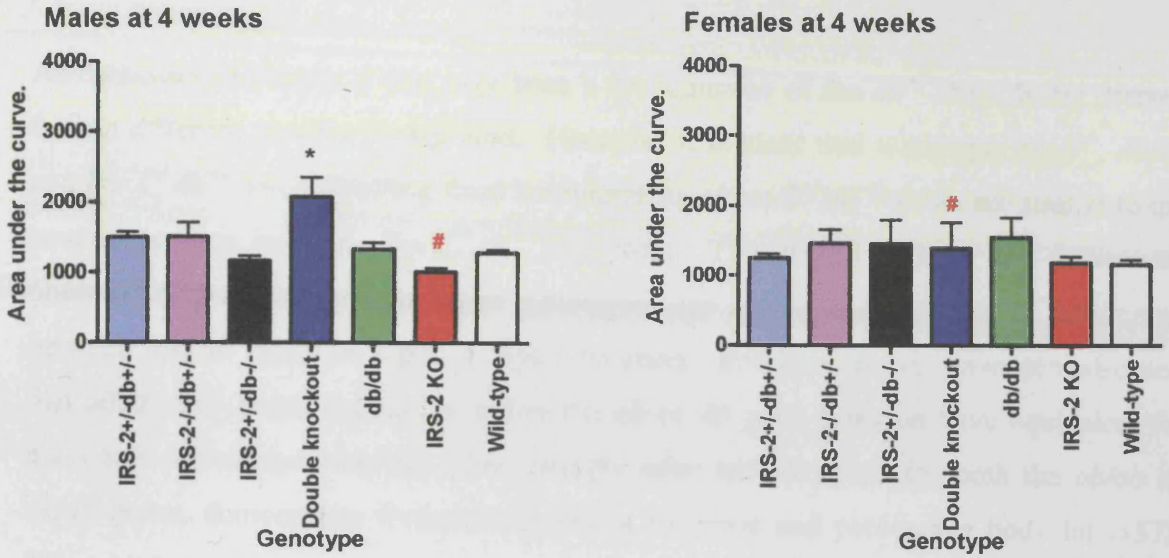

b).

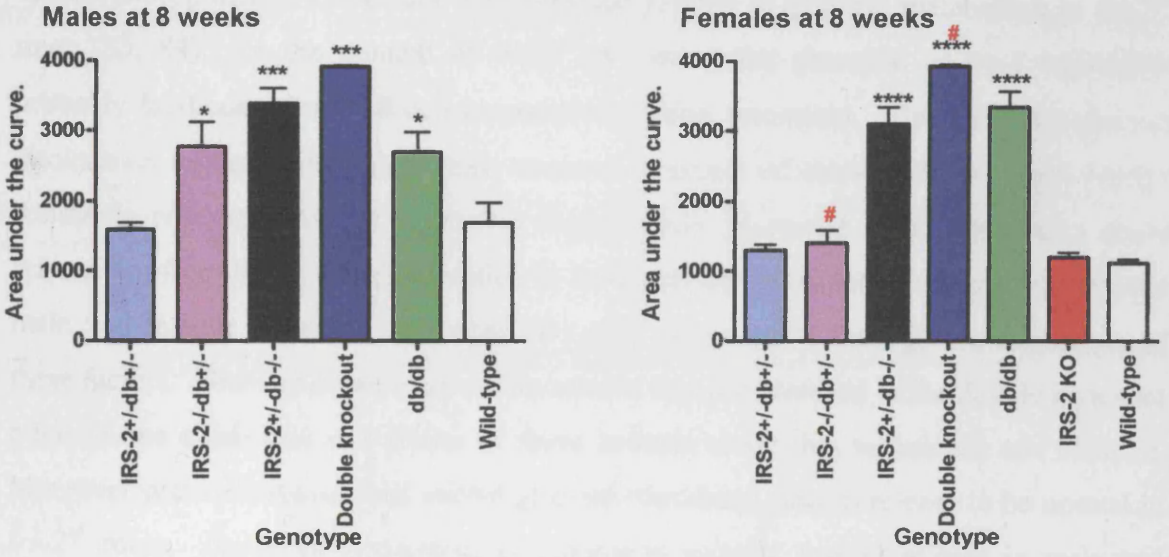

Figure 4.8 Statistical anaylsis of glucose tolerance tests carried out at a) 4 and b) 8 weeks of age on offspring from the Irs-2$^{+/-}$ob$^{+/-}$ intercross.

*Results are expressed as mean area under the curve ± s.e.m from glucose tolerance test curves presented in Figures 4.6 and 4.7, being representative of at least 4 animals per sex per genotype (except where indicated, #n=3). t-tests were performed comparing all genotypes to their wild-type controls; *, $p < 0.05$, **, $p < 0.01$, ***, $p < 0.001$, ****, $p < 0.0001$.*

As discussed in chapter 3 this may been a consequence of the $db^{+/-}$ mice being derived from a different genetic background. However it is clear that wild-type, *Irs-2*$^{-/-}$, *db/db* and *Irs-2*$^{+/-}$*db*$^{+/-}$ mice resulting from the intercross of *Irs-2*$^{+/-}$*db*$^{+/-}$ mice, are similar to the equivalent mice from the *Irs-2*$^{+/-}$*ob*$^{+/-}$ intercross. This would indicate that differences observed between other equivalent genotypes, are a true consequence of differences between loss of leptin or leptin receptor function. Previous reports have demonstrated that adult mice heterozygous for either the *ob* or *db* gene function have equivalent fat mass and percentage body fat. Interestingly mice heterozygous for both the *ob/ob* or *db/db* genes, demonstrate further increases in fat mass and percentage body fat (157). This additive effect would support the idea that there are subtle differences in the effects of deleting either leptin or leptin long-form receptor function.

Considering all other genotypes at four weeks of age, only male and female *Irs-2*$^{+/-}$*ob*$^{-/-}$ mice exhibited significantly elevated fasting blood glucose levels relative to wild-type controls, with only males proving to be mildly glucose intolerant. This finding of sexual dimorphism is consistent with previous reports of glucose metabolism in *Irs-2*$^{-/-}$ mice (83, 84). In the context of *Irs-2*$^{+/-}$*ob*$^{-/-}$ mice, the presence of *Irs-2* expression probably facilitates a mild β-cell response to insulin resistance. The increased glucose intolerance reported in males, may occur as a result of increased peripheral insulin resistance compared to that present in female mice. Increased insulin resistance could arise either from the systemic reduction in *Irs-2* expression or due to differences between male and female mice lacking leptin (*ob*) gene function, or through a combination of these factors. Glucose-stimulated insulin release was not assessed in the double knockout mice, as the small size and frailty of these animals made this technically too difficult. Moreover previous studies had shown glucose-stimulated insulin release to be normal in *Irs-2*$^{-/-}$ mice. However assessment of glucose-stimulated insulin release in male and female *Irs-2*$^{+/-}$*ob*$^{-/-}$ mice may provide further insight into the metabolic differences described for this genotype. Interestingly, both female and male *Irs-2*$^{+/-}$*db*$^{-/-}$ mice, were glucose tolerant at four weeks of age.

The observation that *Irs-2*$^{-/-}$*ob*$^{+/-}$ mice exhibit normal glucose tolerance at four weeks of age, illustrates that a single allele of leptin is sufficient to avoid the onset of the dramatic metabolic phenotype seen in double knockout mice. The presence of a single allele of leptin upon an *Irs-2*$^{-/-}$ background was also sufficient in preventing the growth retardation seen in double knockout mice. Taken together these findings emphasize the importance of leptin sensitivity and in particular how leptin action is essential for the maintenance of insulin sensitivity. The observation that eight-week-old *Irs-2*$^{-/-}$*ob*$^{+/-}$ female mice were more glucose intolerant than *Irs-2*$^{-/-}$ female mice but less so than female double knockout mice, further illustrates the importance of leptin sensitivity in regulating peripheral glucose metabolim.

Considering *Irs-2*$^{-/-}$*db*$^{+/-}$ mice, only males were glucose intolerant at eight weeks, with female mice remaining relatively glucose tolerant. This finding supports the idea that subtle differences exist between the loss of leptin and leptin long-form receptor function, when on an *Irs-2*$^{-/-}$ background. In this context it would appear that, the loss of leptin (*ob*) gene expression induces a slightly more severe metabolic phenotype than observed when leptin long-form receptor (*db*) gene expression is lost. Indeed if leptin signalling does converge at IRS-2, these observations could be explained by shorter-isoforms of the leptin receptor mediating some leptin action upon IRS-2 in *db/db* mice. In contrast *ob/ob* mice are unable to mediate any leptin action as they lack leptin expression.

Elevated fasting blood glucose levels present in *Irs-2*$^{-/-}$*ob*$^{+/-}$, *Irs-2*$^{+/-}$*ob*$^{-/-}$, *ob/ob* and *Irs-2*$^{-/-}$ mice at eight weeks of age, indicated that they were now also glucose intolerant. As described above *Irs-2*$^{-/-}$ mice displayed sexual dimorphism, with males being more glucose intolerant than females. Glucose tolerance testing of eight-week-old *Irs-2*$^{+/-}$*ob*$^{-/-}$ mice, showed female mice were now as glucose intolerant as males. Similarly, *Irs-2*$^{+/-}$*db*$^{-/-}$ and *db/db* mice resulting from the *Irs-2*$^{+/-}$*db*$^{+/-}$ intercross were also glucose intolerant at eight weeks of age. Interestingly both compound heterozygous mice (*Irs-2*$^{+/-}$*ob*$^{+/-}$ and *Irs-2*$^{+/-}$*db*$^{+/-}$mice) showed normal glucose tolerance at eight weeks of age.

In summary assessment of glucose metabolism in offspring resulting from the intercross of either *Irs-2*$^{+/-}$*ob*$^{+/-}$ or *Irs-2*$^{+/-}$*db*$^{+/-}$mice, has demonstrated that both double knockout mice are extremely diabetic, characterised by, elevated fasting blood glucose levels and glucose intolerance at four weeks of age. However glucose tolerance was more impaired in *Irs-2*$^{-/-}$*ob*$^{-/-}$ mice compared to *Irs-2*$^{-/-}$*db*$^{-/-}$ mice. Similar differences were also evident in other equivalent genotypes resulting from the two intercrosses. Such findings suggest that in combination with *Irs-2* deficiency, insults to leptin gene expression are more detrimental to glucose homeostasis, than insults to leptin receptor gene expression. The fact that female *Irs-2*$^{-/-}$*ob*$^{+/-}$ mice are glucose intolerant at eight weeks of age but female *Irs-2*$^{-/-}$*db*$^{+/-}$ mice are glucose tolerant at this age, further highlights this point. Possibly of more importance is that either a single allele of leptin or leptin receptor gene expression was sufficient to delay the marked glucose intolerance exhibited by double knockout mice. Taken together these findings exemplify the importance of leptin sensitivity to regulate whole-body glucose homeostasis. The wide range of glucose tolerance presented by the various genotypes, would suggest differences in peripheral insulin sensitivity. Leptin has also been shown to influence β-cell function directly (90, 91, 127). Therefore assessment of pancreatic islet function will provide useful insights into the peripheral insulin sensitivity of these animals.

CHAPTER 5

Pancreatic β-cell function in offspring from *Irs-2*$^{+/-}$*ob*$^{+/-}$ and *Irs-2*$^{+/-}$*db*$^{+/-}$ intercrosses.

Pancreatic β-cell function

In view of the impaired glucose tolerance seen in the double knockout mice at four weeks of age and the markedly diabetic phenotype seen in these animals by eight weeks of age, pancreatic β-cell function was assessed. Initially fasting serum insulin levels were assayed at four and eight weeks of age. This measurement gives indication of insulin resistance as hyperinsulinaemia suggests the presence of insulin resistance. The markedly impaired glucose intolerance seen in the double knockout mice at eight weeks of age in male and female animals also suggests that by this age the mice have an inadequate insulin production and could therefore be relatively insulinopaenic.

In addition, pancreatic morphology was assessed. In rodent models, the β-cell compensatory response to insulin resistance includes both an increase in insulin production and also an increase in β-cell mass. Assessment of islet size was therefore performed by histological examination, staining of islets for insulin and morphometric analysis.

5.1 Fasting insulin levels of offspring from the Irs-2$^{+/-}$*ob*$^{+/-}$ *intercross*

Fasting insulin levels were measured in male and female animals at four and eight weeks of age. At four weeks of age, both male and female double knockout mice display elevated fasting insulin levels compared to wild-type mice suggesting the presence of insulin resistance (Fig 5.1a, $p < 0.01$ for both males and females). Similarly *ob/ob*, *Irs-2*$^{-/-}$, *Irs-2*$^{-/-}$*ob*$^{+/-}$ and *Irs-2*$^{+/-}$*ob*$^{-/-}$ mice also displayed elevated fasting insulin levels compared to wild-type littermates (Fig 5.1a). Consistent with previous reports (83), *Irs-2*$^{-/-}$ mice exhibit sexual dimorphism, with males having significantly higher fasting insulin levels compared to wild-types ($p < 0.01$) and females showing a non-significant increase in fasting insulin levels.

a). 4 weeks of age

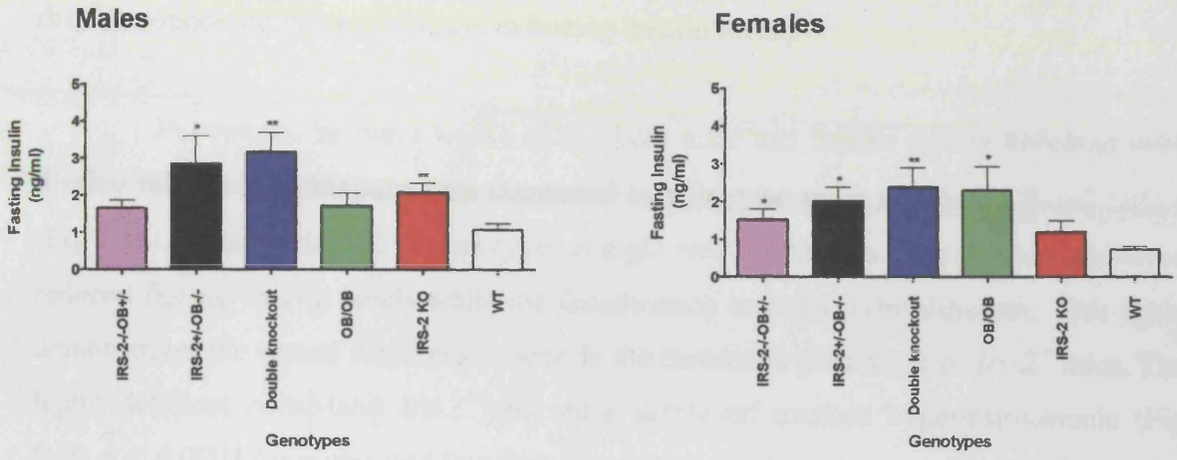

b). 8 weeks of age

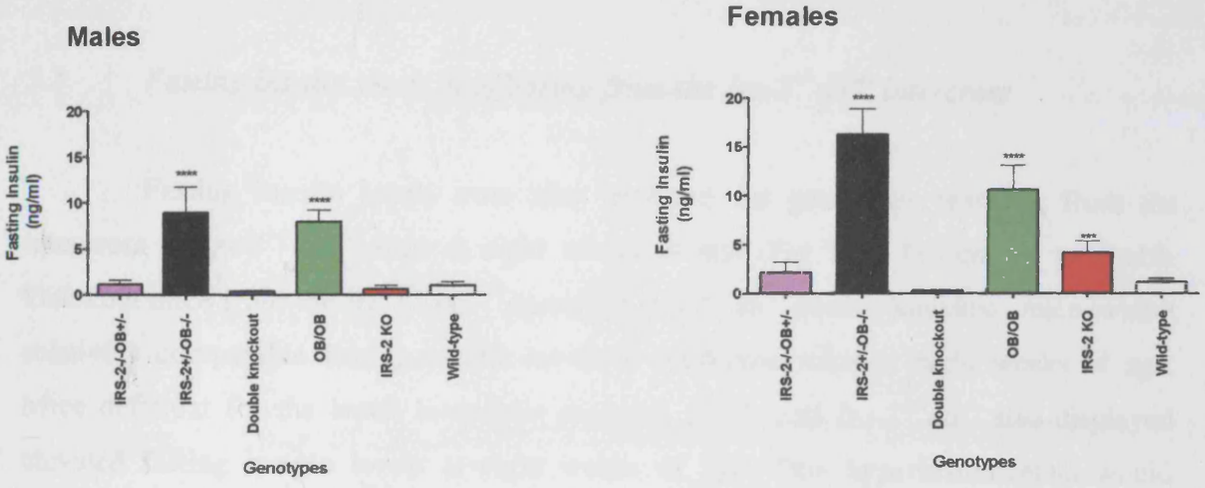

Figure 5.1 Fasting insulin levels of offspring from the Irs-2$^{+/-}$ob$^{+/-}$ intercross at a) four and b) eight weeks of age.

Cardiac puncture was performed on terminally anaesthetized, 15 hr fasted mice. Blood samples were clarified by centrifugation (13,000rpm for 20 mins at 4°C) and the resulting serum was quantified for insulin concentration by a commercially available rat insulin ELISA assay (using a mouse insulin standard). All assays were assayed in duplicate and results are presented as average plasma insulin ± s.e.m, being representative of 5 animals per sex per genotype.

It is well documented that male *Irs-2*$^{-/-}$ mice are more insulin resistant at this age compared to female *Irs-2*$^{-/-}$ mice. Hence the it follows that male *Irs-2*$^{-/-}$ mice would display a more significant increase in fasting insulin levels.

In contrast, by eight weeks of age both male and female double knockout mice display relative hypoinsulinaemia compared to wild-type mice suggesting β-cell failure (Fig 5.1b). Considering other genotypes at eight weeks, male *Irs-2*$^{-/-}$ mice now displayed reduced fasting insulin levels while the female mice were hyperinsulinaemic. This again demonstrates the sexual dimorphism seen in the metabolic phenotype of *Irs-2*$^{-/-}$ mice. The leptin deficient *ob/ob* and *Irs-2*$^{+/-}$*ob*$^{-/-}$ mice displayed marked hyperinsulinaemia (Fig 5.1b, $p < 0.0001$ *for males and females*), suggesting insulin resistance. Interestingly, mice with a single allele of *ob* in an *Irs-2*$^{-/-}$ background appeared to have fasting insulin levels that were comparable or higher than wild-type mice suggesting that a single allele of *ob* may ameliorate the β-cell defect or insulin resistance seen in the double knockout mouse.

5.2 *Fasting insulin levels of offspring from the Irs-2*$^{+/-}$*db*$^{+/-}$ *intercross*

Fasting insulin levels were also analysed for genotypes resulting from the intercross of *Irs-2*$^{+/-}$*db*$^{+/-}$ mice at eight weeks of age (Fig 5.2). In contrast to double knockout mice from the *Irs-2*$^{+/-}$*ob*$^{+/-}$ intercross, *Irs-2*$^{-/-}$*db*$^{-/-}$ double knockout mice exhibit relatively comparable fasting insulin levels to wild-type mice at eight weeks of age. Mice deficient for the leptin long-form receptor, *db/db* and *Irs-2*$^{+/-}$*db*$^{-/-}$ also displayed elevated fasting insulin levels at eight weeks of age. This hyperinsulinaemia would suggest that these mice were also insulin resistant. Unfortunately due to the low numbers of male *Irs-2*$^{-/-}$ mice derived from the intercross of *Irs-2*$^{+/-}$*db*$^{+/-}$mice, none were analysed for fasting insulin levels. However, female *Irs-2*$^{-/-}$mice were shown to have significantly elevated fasting insulin levels (Fig 5.2, $p < 0.01$). This was consistent with age matched female *Irs-2*$^{-/-}$ mice from the *Irs-2*$^{+/-}$*ob*$^{+/-}$ intercross. Consistency between the two intercrosses was further highlighted by the finding that *Irs-2*$^{-/-}$*db*$^{+/-}$mice of both sexes had comparable fasting insulin levels to wild-type controls at eight weeks of age (Fig 5.2).

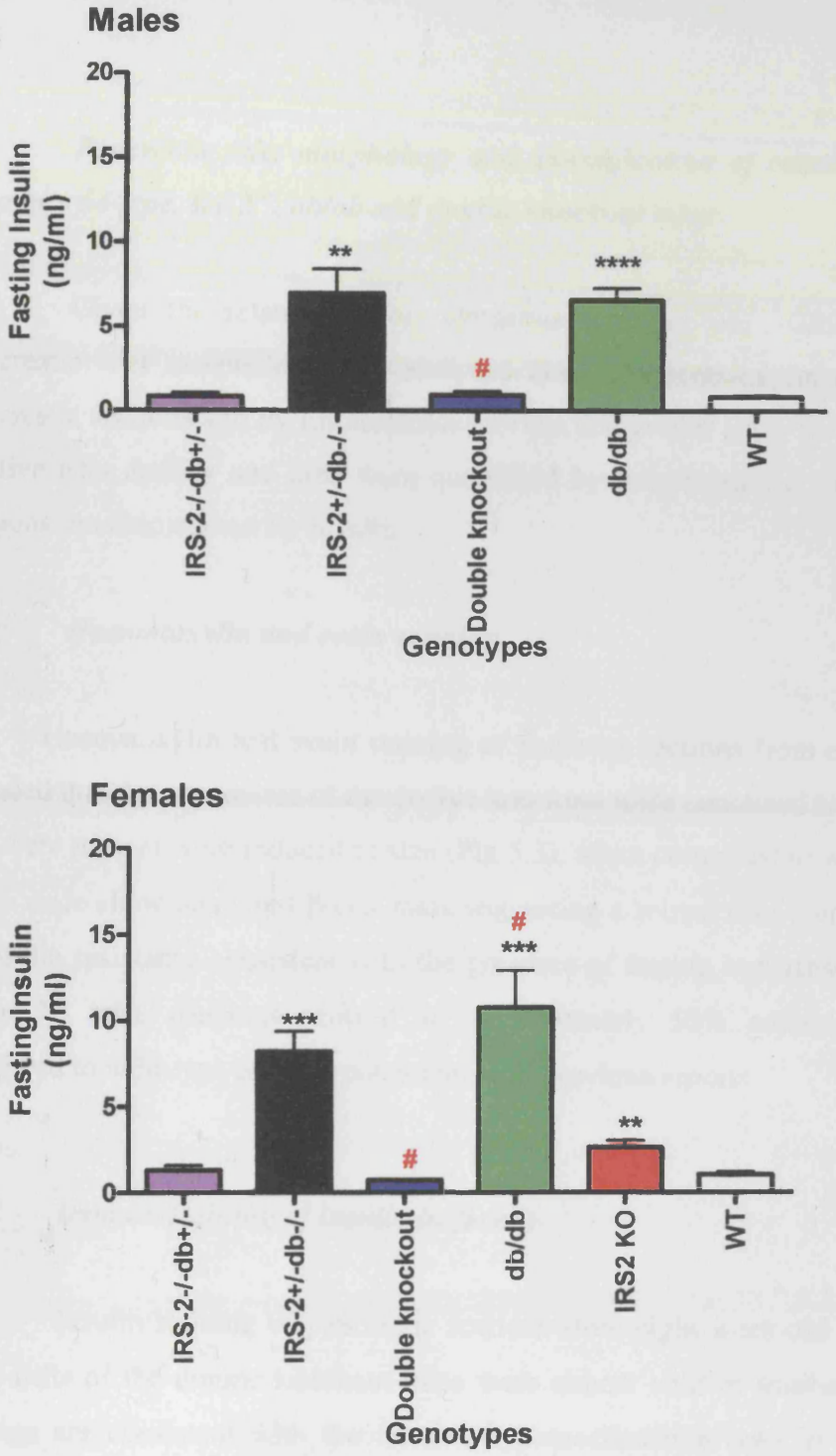

Figure 5.2 Fasting insulin levels of offspring from the Irs-2$^{+/-}$db$^{+/-}$ intercross at eight weeks of age.

Cardiac puncture was performed on terminally anaesthetized, 15 hr fasted mice. Bloods were clarified by centrifugation (13,000rpm for 20 mins at 4°C) and the resulting serum was quantified for insulin concentration by a commercially available mouse insulin ELISA assay. All assays were assayed in duplicate and results are presented as average plasma insulin ± s.e.m, being representative of at least 5 animals per sex per genotype (except where indicated, #n=3).

5.3 *Pancreatic islet morphology and quantification of relative islet density and area in wild-type, Irs-2$^{-/-}$, ob/ob and double knockout mice*

Given the relative hypoinsulinaemia of *Irs-2$^{-/-}$ob$^{-/-}$*, double knockout mice, pancreatic islet morphology was analysed both by haematoxylin & eosin staining of pancreatic sections and by immunofluorescence analysis of islets for insulin. In addition relative islet density and area were quantified by morphometric analysis of pancreatic sections immunostained for insulin.

5.3.1 *Haematoxylin and eosin staining*

Haematoxylin and eosin staining of pancreas sections from eight-week-old mice revealed that the pancreases of the double knockout mice contained fewer islets and those that were present were reduced in size (Fig 5.3), when compared to wild-type mice. The *ob/ob* mice show increased β-cell mass suggesting a robust islet compensatory response to insulin resistance consistent with the presence of fasting hyperinsulinaemia. Analysis of *Irs-2$^{-/-}$* mice pancreas showed an approximately 50% reduction in β-cell mass compared to wild-type animals consistent with previous reports.

5.3.2 *Immunostaining of insulin in β-cells*

Insulin staining of pancreatic sections from eight-week-old mice revealed that the β-cells of the double knockout mice were almost void of insulin (Fig 5.4). These findings are consistent with the relative hypoinsulinaemia seen in these animals and would explain provisionally their rapid development of diabetes. In the case of the *Irs-2$^{-/-}$* mice, their islets although generally smaller than wild-type were still able to produce insulin (Fig 5.4). This is likely to be why diabetes does not ensue so rapidly in these animals, as it does in the double knockout mice.

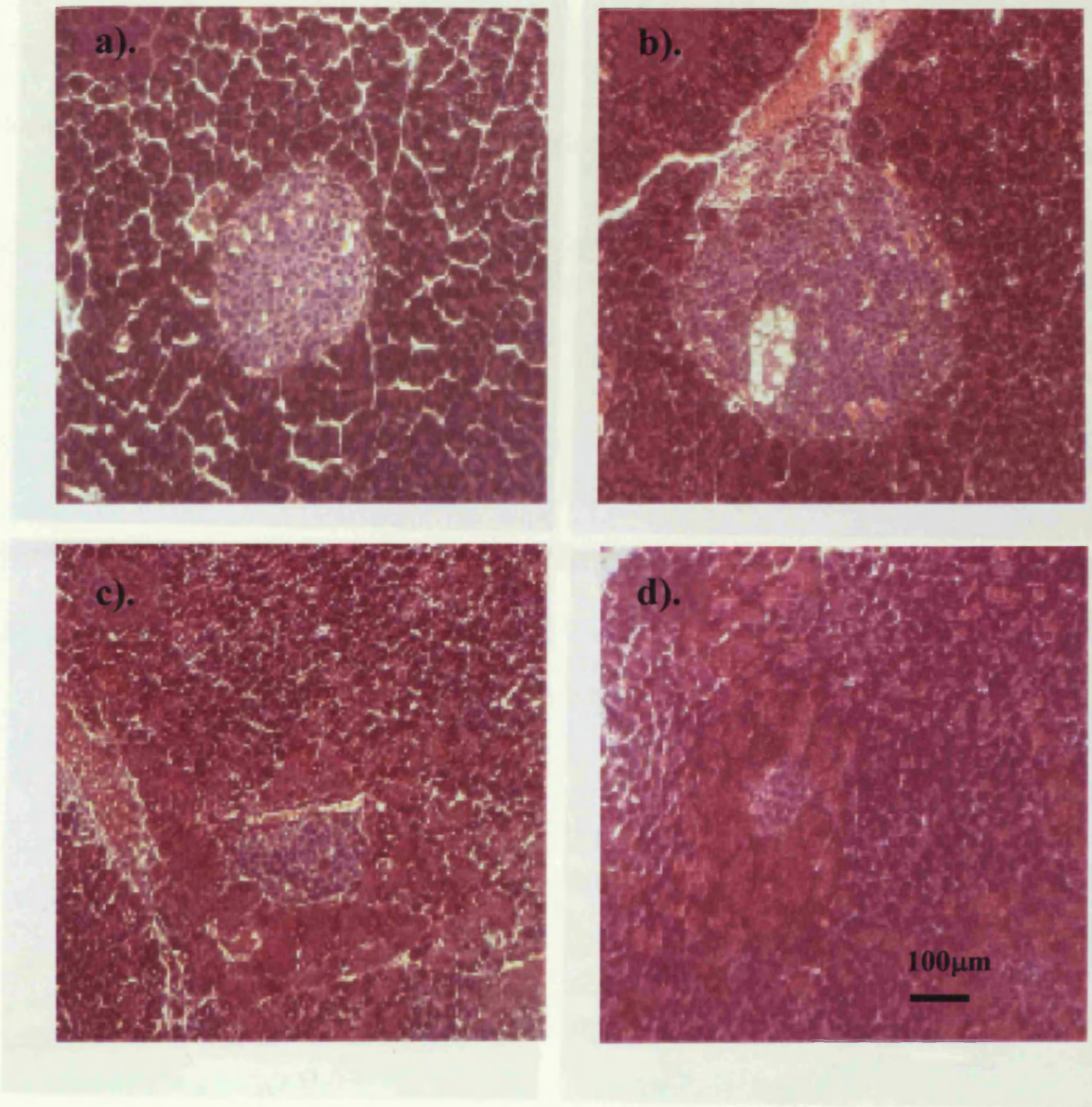

Figure 5.3 Islet morphology of double knockout (d) compared to wild-type (a), ob/ob (b) and Irs-2$^{-/-}$ (c) mice at eight weeks of age.

Pancreas sections (5µm) were stained with haematoxylin and eosin to analyse islet morphology. Images were captured at 200 x magnification. Representative islets are pictured and are typical of three independent experiments.

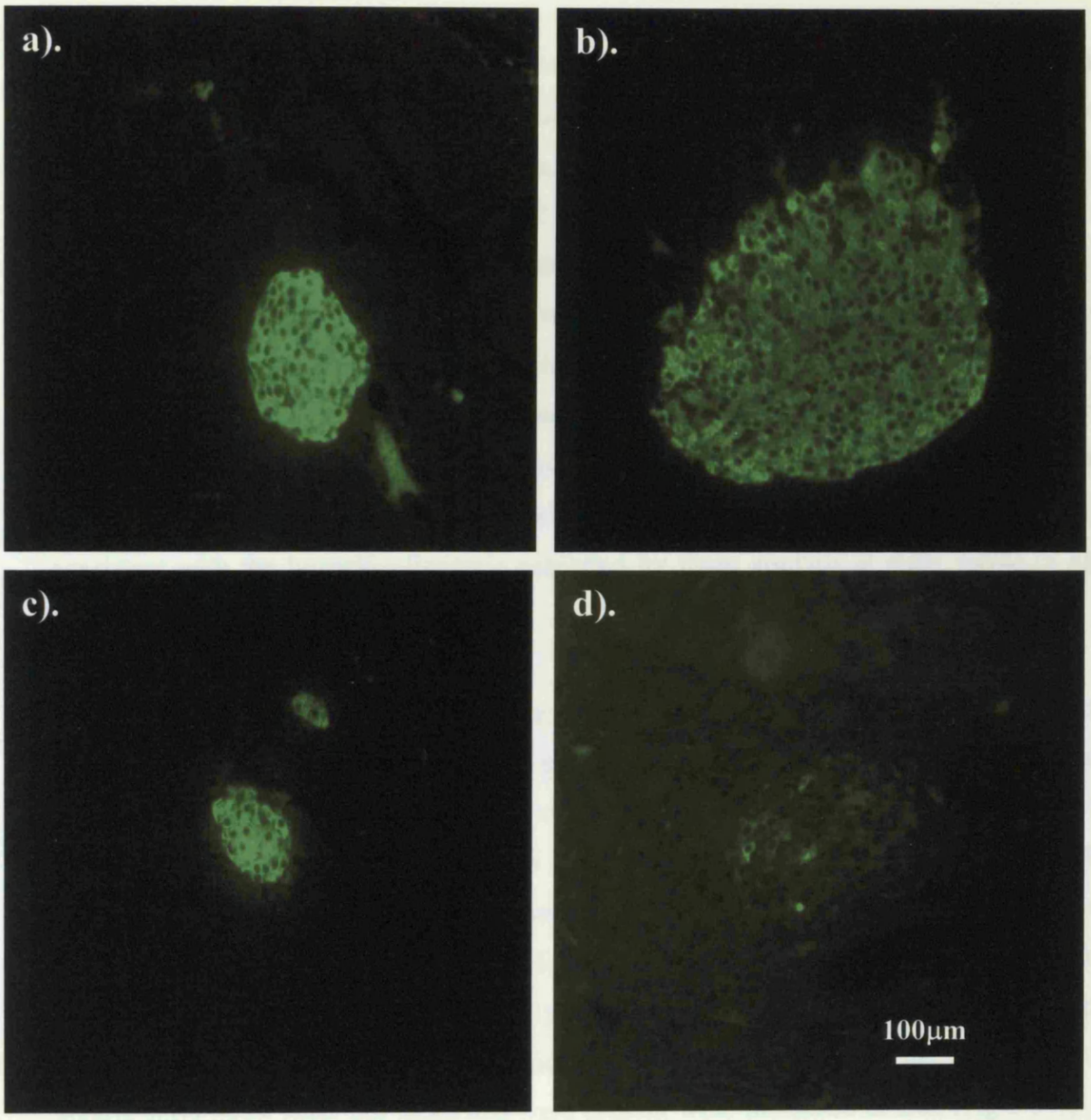

Figure 5.4 Immunostaining of insulin in β-cells of Pancreas sections from eight week old; wild-type (a), ob/ob (b), Irs-2$^{-/-}$ (c) and double knockout (d) mice.

Pancreas sections (5μm) were mounted onto poly-lysine coated slides, deparaffinised and probed with an anti-insulin monoclonal antibody (1:1,000) (sigma I-2018) with Subsequent detection by Alexa-Fluor 594 α secondary antibody (molecular probes). Fluorescent images were captured at 200 x magnification. Representative islets are pictured and are typical of three independent experiments.

5.3.3 *Quantification of relative islet density and relative islet area in wild-type, ob/ob, Irs-2$^{-/-}$, Irs-2$^{-/-}$ob$^{+/-}$, double knockout mice*

Relative islet density and relative islet area of four and eight-week-old; wild-type, *ob/ob*, *Irs-2*$^{-/-}$, *Irs-2*$^{-/-}$*ob*$^{+/-}$, and double knockout mice was determined by quantative analysis of four whole pancreatic sections, from four animals, immunostained for insulin. At four weeks of age, *ob/ob*, *Irs-2*$^{-/-}$, *Irs-2*$^{-/-}$*ob*$^{+/-}$, and double knockout mice all showed a non-significant increase in relative islet density compared to wild-type mice (Fig 5.5a). Analysis of relative islet density at eight weeks of age indicated that both, *Irs-2*$^{-/-}$and *Irs-2*$^{-/-}$*ob*$^{+/-}$mice generally contained fewer islets than wild-type mice (Fig 5.5b). In contrast the relative density of islets in double knockout mice was determined to be equal to or greater than that observed in wild-type mice. The relative islet density of *ob/ob* mice was significantly increased compared to wild-type controls ($p < 0.01$). This finding was consistent with the hyperinsulinaemia exhibited by these animals at eight weeks of age (Fig 5.1b).

The ~50% reduction in relative islet area observed in *Irs-2*$^{-/-}$mice at four and eight weeks of age, was consistent with previous reports (83) (Fig 5.6 a-b). In contrast, *Irs-2*$^{-/-}$*ob*$^{+/-}$ and double knockout mice both contained relative islet areas comparable to that of wild-types at four weeks of age (Fig 5.6a). Indeed although not proven to be significant, it was noticed that double knockout mice tended to have an increased relative islet area compared to wild-type mice. However the relative islet area of *Irs-2*$^{-/-}$*ob*$^{+/-}$ and double knockout mice was dramatically reduced by eight weeks of age (Fig 5.6b). Analysis of eight-week-old *ob/ob* mice showed that not only did they contain significantly more islets but those that were present were increased in area (Fig 5.6b, $p < 0.05$). These findings are summarised in Table 5.1 as a percentage increase or decrease in mean relative islet density and area compared to that observed in wild-type controls.

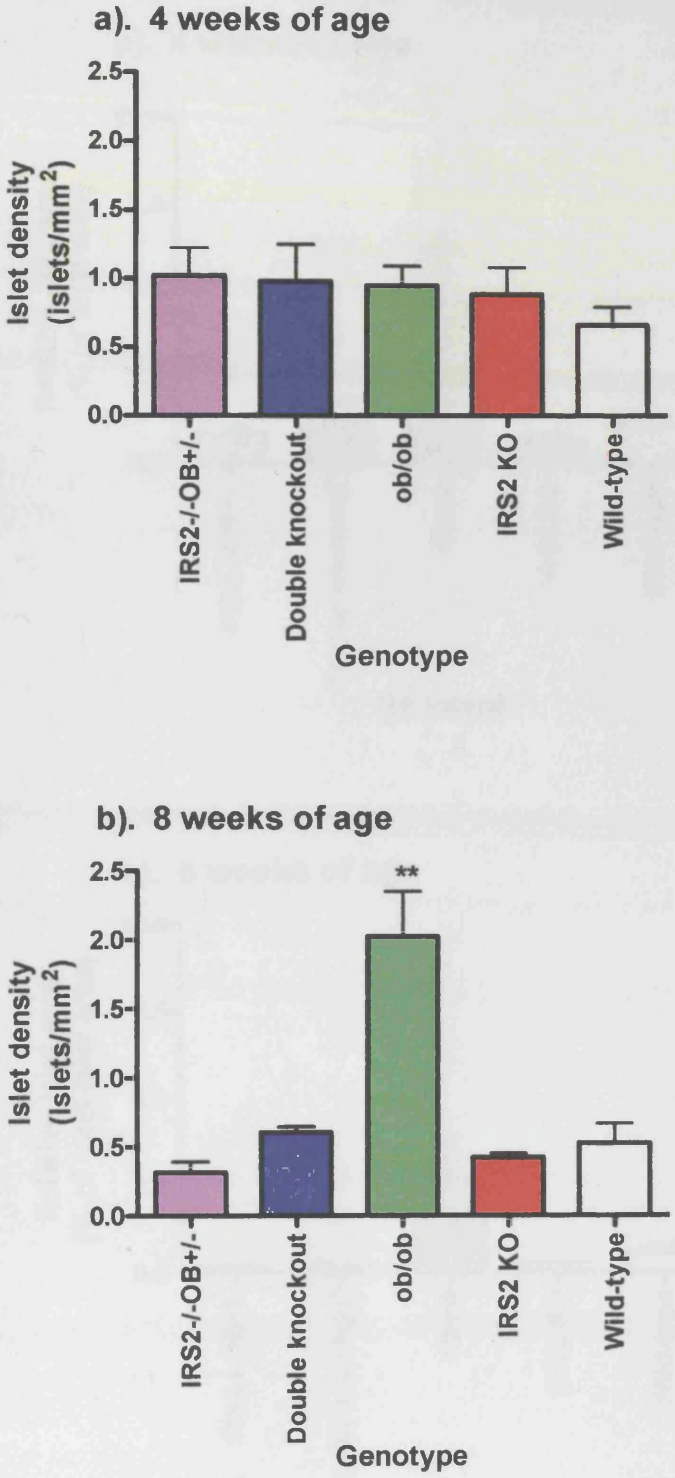

Figure 5.5 Quantification of relative islet density in Irs-2$^{-/-}$ob$^{+/-}$, double knockout, ob/ob, Irs-2$^{-/-}$ and wild-type mice, at a). four and b). eight weeks of age.

The total islet count for a pancreatic section was expressed as islets/mm2. Results are representative of four pancreatic sections of four animals per genotype.

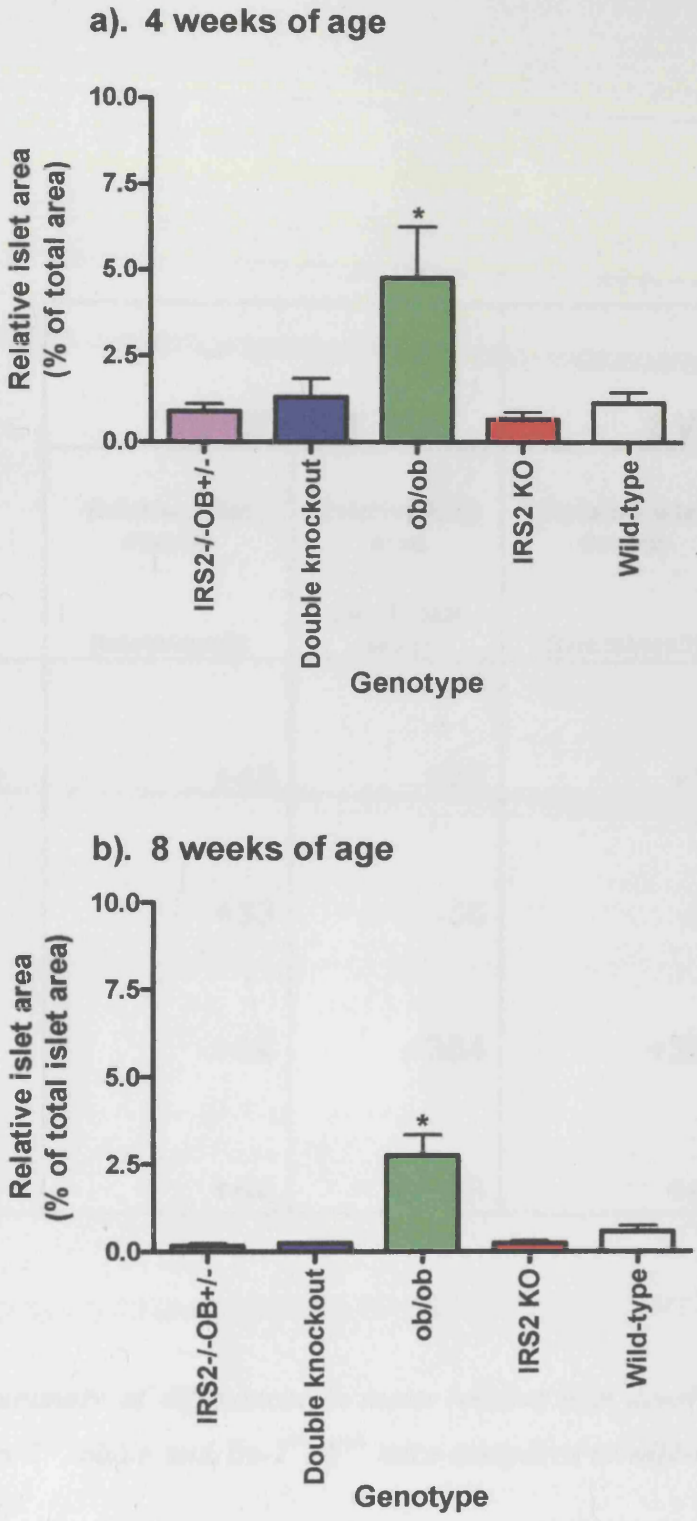

Figure 5.6 Quantification of relative islet area in Irs-2$^{-/-}$ob$^{+/-}$, double knockout, ob/ob, Irs-2$^{-/-}$ and wild-type mice, at a). four and b). eight weeks of age.

The total islet area for a pancreatic section was expressed as a percentage of total section area. Results are representative of four pancreatic sections of four animals per genotype.

	4 WEEKS		8 WEEKS	
	Relative islet density (islets/mm2)	Relative islet area (% of total area)	Relative islet density (islets/mm2)	Relative islet area (% of total area)
Double knockout	+48	+27	+15	-59
Irs-2 KO	+33	-35	-20	-58
ob/ob	+44	+364	+285	+375
Irs-2-/- ob+/-	+54	-13	+40	-71

Table 5.1 Summary of differences in mean relative islet density and area in double knockout, Irs-2$^{-/-}$, ob/ob and Irs-2$^{-/-}$ob$^{+/-}$ mice compared to wild-types at four and eight weeks of age.

Results are expressed as a percentage increase or decrease in mean relative islet density or area compared to that observed in wild-type controls.

5.4 *Assessment of fasting leptin levels in offspring from the Irs-2$^{+/-}$ob$^{+/-}$ and Irs-2$^{+/-}$db$^{+/-}$ intercrosses*

The adipocyte-hormone leptin is known to act upon the β-cell to suppress insulin secretion. Given the various levels of fasting insulin and adiposity displayed by offspring resulting from either *Irs-2*$^{+/-}$*ob*$^{+/-}$ or *Irs-2*$^{+/-}$*db*$^{+/-}$ intercrosses, fasting leptin levels were determined at eight weeks of age (Figs 5.7 and 5.8).

As would be expected fasting leptin was not detectable in animals, homozygous for the leptin gene (data not shown). Considering other genotypes from the *Irs-2*$^{+/-}$*ob*$^{+/-}$ intercross at eight weeks of age, both male and female *Irs-2*$^{+/-}$*ob*$^{+/-}$ and *Irs-2*$^{-/-}$*ob*$^{+/-}$ mice had fasting leptin levels comparable to wild-types (Fig 5.7). Similarly male *Irs-2*$^{-/-}$ mice had fasting leptin levels comparable to wild-type mice. In contrast, female *Irs-2*$^{-/-}$ mice displayed fasting leptin levels that were significantly elevated compared to wild-type controls (Fig 5.7b, $p < 0.05$). It is known that female *Irs-2*$^{-/-}$ mice do not become catabolic as quickly as male *Irs-2*$^{-/-}$ mice. The increased fasting leptin levels presented by female *Irs-2*$^{-/-}$ mice at eight weeks is presumably a consequence of the increased adiposity exhibited by female *Irs-2*$^{-/-}$ at this age.

Consistent with previous reports mice homozygous for the leptin long-form receptor (*db/db* and *Irs-2*$^{+/-}$*db*$^{-/-}$) were hyperleptinemic at eight weeks of age (Fig 5.8, $p < 0.001$). Such hyperleptinemia would indicate that these mice were leptin resistant. In contrast, *Irs-2*$^{-/-}$*db*$^{-/-}$ double knockout mice were not hyperleptinemic but had fasting leptin levels comparable to wild-type mice. The observation that loss of functional leptin receptor signalling upon an *Irs-2*$^{-/-}$ background did not result in hyperleptinemia, can be explained by the markedly reduced adiposity exhibited by these animals. As white adipose tissue (WAT) is responsible for the majority of leptin expression, the lack of adiposity (particularly WAT) in *Irs-2*$^{-/-}$*db*$^{-/-}$ mice would therefore limit leptin synthesis in response to peripheral leptin resistance. Due to the low numbers of male *Irs-2*$^{-/-}$ mice derived from this intercross, no fasting leptin levels were measured at eight weeks of age. However, female *Irs-2*$^{-/-}$ mice displayed a significant increase in fasting leptin levels relative to wild-type controls (Fig 5.8b, $p < 0.001$).

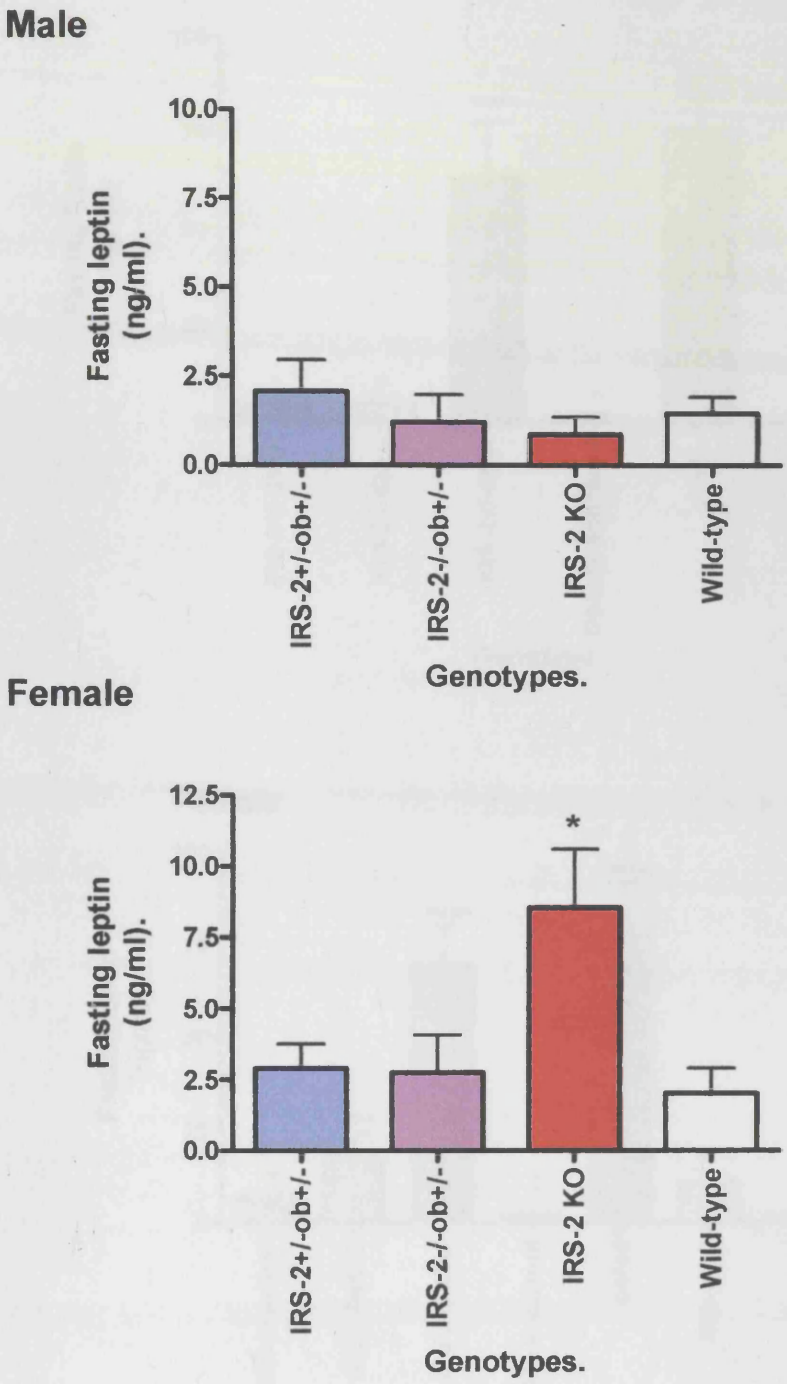

Figure 5.7 Fasting leptin levels of offspring from the Irs-2$^{+/-}$ob$^{+/-}$ intercross at eight weeks of age.

*Cardiac puncture was performed on terminally anaesthetized, 15 hr fasted mice. Bloods were clarified by centrifugation (13,000rpm for 20 mins at 4°C) and the resulting serum was quantified for leptin concentration by a commercially available mouse leptin ELISA assay. All assays were assayed in duplicate and results are presented as average plasma leptin ± s.e.m, being representative of at least 5 animals per sex per genotype. As expected leptin was undetectable in the leptin deficient; ob/ob, Irs-2$^{+/-}$ob$^{-/-}$ and double knockout mice. *P < 0.05.*

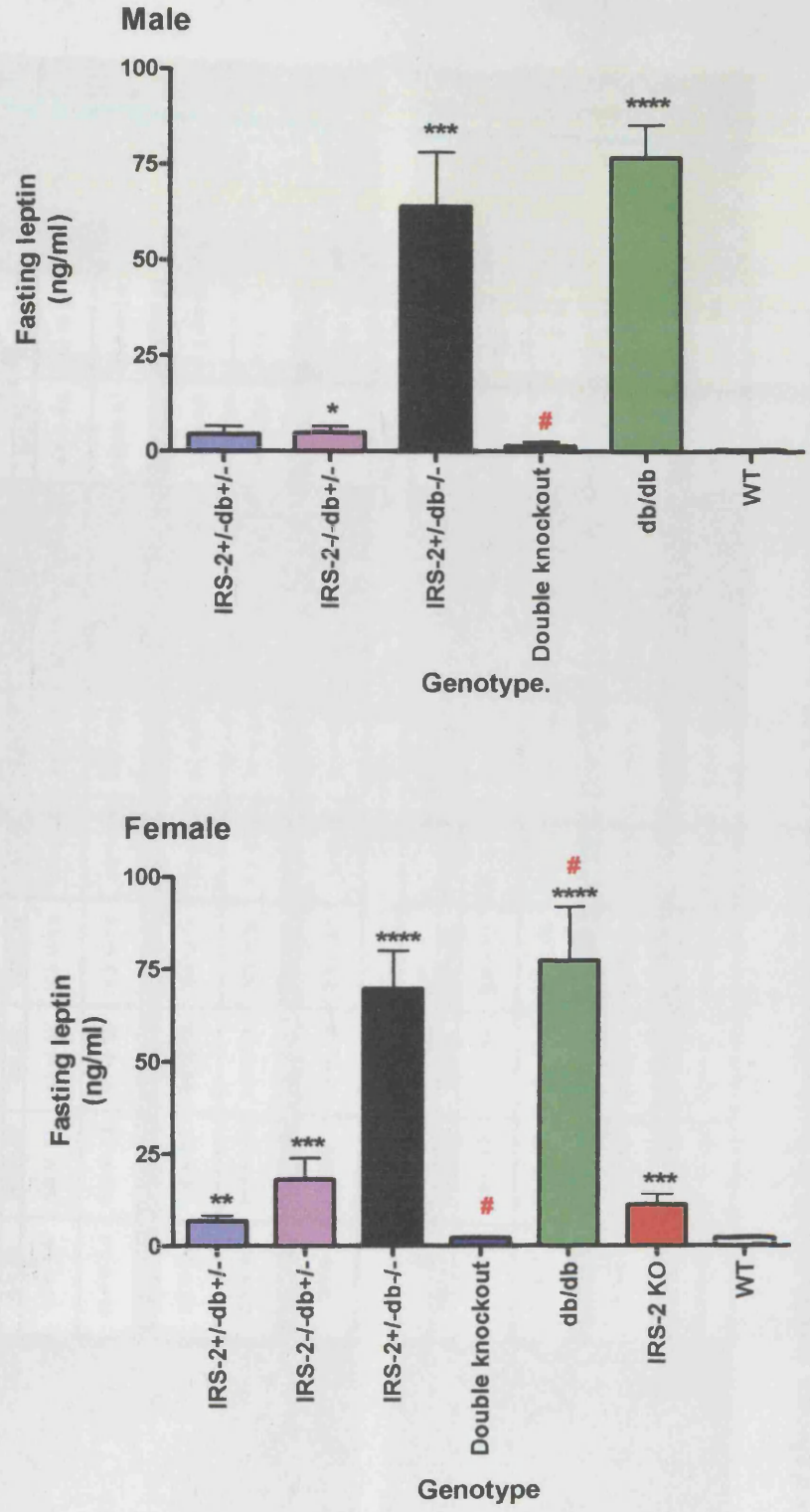

Figure 5.8 Fasting leptin levels of offspring from the Irs-2$^{+/-}$db$^{+/-}$ intercross at eight weeks of age.

Cardiac puncture was performed on terminally anaesthetized, 15 hr fasted mice. Bloods were clarified by centrifugation (13,000rpm for 20 mins at 4°C) and the resulting serum was quantified for leptin concentration by a commercially available mouse leptin ELISA assay. All assays were assayed in duplicate and results are presented as average plasma leptin ± s.e.m, being representative of at least 5 animals per sex per genotype (except where indicated, #n=3).

IRS-2$^{+/-}$ob$^{+/-}$ X IRS-2$^{+/-}$ob$^{+/-}$	INCREASING <---------- BODY WEIGHT ----------> DECREASING													
	ob/ob		IRS-2$^{+/-}$ob$^{-/-}$		IRS-2$^{+/-}$ob$^{+/-}$		Wild-type		IRS-2 KO		IRS-2$^{-/-}$ob$^{+/-}$		Double knockout	
Fasting blood Glucose (mmol/l):	MALES	FEMALES	MALES	FEMALES	MALES	FEMALES	MALES	FEMALES	MALES	FEMALES	MALES	FEMALES	MALES	FEMALES
4 weeks of age	4.6 +/- 0.7	4.0 +/- 0.7	4.1 +/- 0.9	5.6 +/- 1.1	4.5 +/- 0.5	5.0 +/- 1.0	3.8 +/- 0.7	4.0 +/- 1.1	4.4 +/- 1.0	5.0 +/- 0.8	4.7 +/- 0.8	5.1 +/- 1.3	11.6 +/- 6.6	15.9 +/- 9.2
8 weeks of age	8.4 +/- 0.9	7.3 +/- 3.1	10.0 +/- 2.6	11.7 +/- 2.9	4.7 +/- 0.5	4.9 +/- 0.8	4.6 +/- 0.9	4.6 +/- 0.5	9.3 +/- 4.0	7.3 +/- 4.8	14.8 +/- 8.1	13.4 +/- 7.4	19.2 +/- 4.4	24.9 +/- 2.5
Fasting insulin levels (ng/ml)														
4 weeks of age	1.7 +/- 0.8	2.3 +/- 1.2	2.8 +/- 1.2	2.0 +/- 0.7	NO DATA	NO DATA	1.1 +/- 0.4	0.7 +/- 0.1	2.1 +/- 0.4	1.2 +/- 0.4	1.7 +/- 0.5	1.5 +/- 0.5	3.2 +/- 1.0	2.4 +/- 0.8
8 weeks of age	7.9 +/- 1.3	10.6 +/- 2.4	9.0 +/- 2.7	16.2 +/- 2.6	NO DATA	NO DATA	1.0 +/- 0.4	1.2 +/- 0.4	0.6 +/- 0.4	4.1 +/- 1.2	1.1 +/- 0.4	2.1 +/- 1.0	0.4 +/- 0.1	0.3 +/- 0.1
Fasting leptin levels (ng/ml)														
8 weeks of age	NONE	NONE	NONE	NONE	2.1 +/- 1.4	2.9 +/- 2.2	1.5 +/- 0.8	2.0 +/- 1.2	0.9 +/- 0.8	8.5 +/- 3.3	1.2 +/- 1.3	2.7 +/- 2.8	NONE	NONE
IRS-2$^{+/-}$db$^{+/-}$ X IRS-2$^{+/-}$db$^{+/-}$	INCREASING <---------- BODY WEIGHT ----------> DECREASING													
	db/db		IRS-2$^{+/-}$db$^{-/-}$		IRS-2$^{+/-}$db$^{+/-}$		Wild-type		IRS-2 KO		IRS-2$^{-/-}$db$^{+/-}$		Double knockout	
Fasting blood Glucose (mmol/l):	MALES	FEMALES	MALES	FEMALES	MALES	FEMALES	MALES	FEMALES	MALES	FEMALES	MALES	FEMALES	MALES	FEMALES
4 weeks of age	4.2 +/- 0.9	3.2 +/- 0.4	3.4 +/- 0.6	3.8 +/- 0.9	3.8 +/- 0.6	3.8 +/- 0.5	4.1 +/- 0.5	3.8 +/- 1.1	3.1 +/- 0.3	4.4 +/- 0.9	5.5 +/- 1.4	3.8 +/- 0.7	8.3 +/- 4.1	8.2 +/- 5.5
8 weeks of age	7.7 +/- 2.8	8.6 +/- 2.2	11.9 +/- 3.1	9.1 +/- 2.4	4.0 +/- 0.5	3.5 +/- 0.3	4.9 +/- 0.9	4.0 +/- 0.9	NO DATA	5.3 +/- 0.6	11.4 +/- 6.3	4.7 +/- 1.0	22.7 +/- 2.8	26.1 +/- 1.7
Fasting insulin levels (ng/ml)														
8 weeks of age	6.6 +/- 1.3	10.8 +/- 3.0	7.0 +/- 2.6	8.2 +/- 2.7	NO DATA	NO DATA	0.8 +/- 0.2	1.1 +/- 0.2	NO DATA	2.6 +/- 0.7	0.8 +/- 0.4	1.3 +/- 0.5	0.9 +/- 0.3	0.7 +/- 0.1
Fasting leptin levels (ng/ml)														
8 weeks of age	77.0 +/- 13.3	77.2 +/- 18.8	64.2 +/- 29.7	69.7 +/- 18.4	4.4 +/- 4.1	6.8 +/- 2.5	0.5 +/- 0.3	2.2 +/- 1.4	NO DATA	11.2 +/- 6.0	4.9 +/- 3.7	18.0 +/- 8.8	1.5 +/- 1.1	2.2 +/- 0.0

Table 5.2: Summary of fasting blood glucose, insulin and leptin levels of genotypes resulting from both Irs-2+/-ob+/- and Irs-2+/-db+/-intercrosses. *Results are presented as mean values +/- s.e.m and are extracted from earlier figures describing fasting blood glucose levels (Chapter 4: Figures 4.1 and 4.5), insulin levels (Chapter 5: Figures 5.1 and 5.2) and leptin levels (Chapter 5: Figures 5.7 and 5.8) levels for each of the intercrosses. Hence, the data is representative of the n-numbers described in such figures.*

Similarly, significantly elevated fasting leptin levels were also observed in both male and female *Irs-2*$^{-/-}$*db*$^{+/-}$ mice (Fig 5.8, $p < 0.05$ for males and $p < 0.001$ for females). Interestingly *Irs-2*$^{+/-}$*db*$^{+/-}$ mice also displayed elevated fasting leptin levels, which was significant for female mice (Fig 5.8b, $p < 0.001$).

5.5 Insulin treatment of double knockout mice

The striking growth retardation and apparent absence of an obesity phenotype in the double knockout mice compared to either *Irs-2*$^{-/-}$ or *ob/ob* mice suggested that either the loss of both genes impaired adipogenesis or that the marked diabetic phenotype leading to a state of catabolism contributed to this lack of marked adiposity. The results suggested that the predominant effect of the loss of both alleles was upon β-cell function and the ability to compensate for insulin resistance. To attempt to determine whether the growth retardation was a secondary effect to the dramatic diabetes seen in these mice, three double knockout mice were treated with insulin over a 20 day period. In addition *Irs-2*$^{-/-}$ and *Irs-2*$^{-/-}$*ob*$^{+/-}$ mice were also treated with insulin.

Insulin treatment was successful at reducing the glucose and ketone levels in the urine of these three double knockout mice (data not shown) and this was paralleled with a rescuing of their growth retardation. Following 20 days of insulin treatment double knockout mice weighed almost double that of the average, untreated double knockout of the same age (Fig 5.9). Further treatment of double knockout mice over a period of 6 weeks indicated that the rescuing of growth in the double knockout mice was so dramatic that they now weighed more than their wild-type littermates and were similar in body habitus to *ob/ob* mice (Figure 5.10).

5.5 Summary and discussion

The dramatic impairment to glucose homeostasis described at four weeks of age in *Irs-2*$^{-/-}$*ob*$^{-/-}$ double knockout mice, suggested that these mice were insulin resistant. Fasting insulin levels determined at four weeks of age showed double knockout mice to be significantly hyperinsulinaemic relative to wild-type mice, indicating the presence of

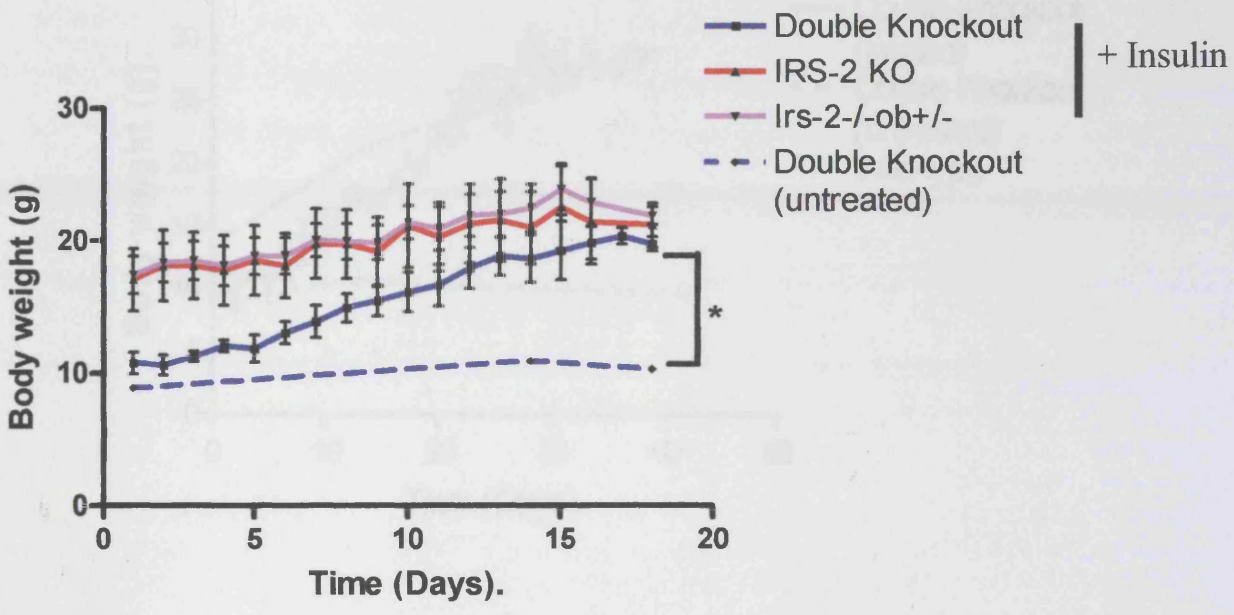

Figure 5.9 Insulin treatment of Irs-2$^{-/-}$, Irs-2$^{-/-}$ob$^{+/-}$ and double knockout mice.

Three four-week-old Irs-2$^{-/-}$, Irs-2$^{-/-}$ob$^{+/-}$ and double knockout mice were administered daily injections of Lantus (a long-acting insulin), in accordance with daily measurements of body weight and urine glucose and ketone content. Following 20 days of treatment double knockout mice weighed significantly more than age-matched untreatred double knockout mice ($p < 0.05$).*

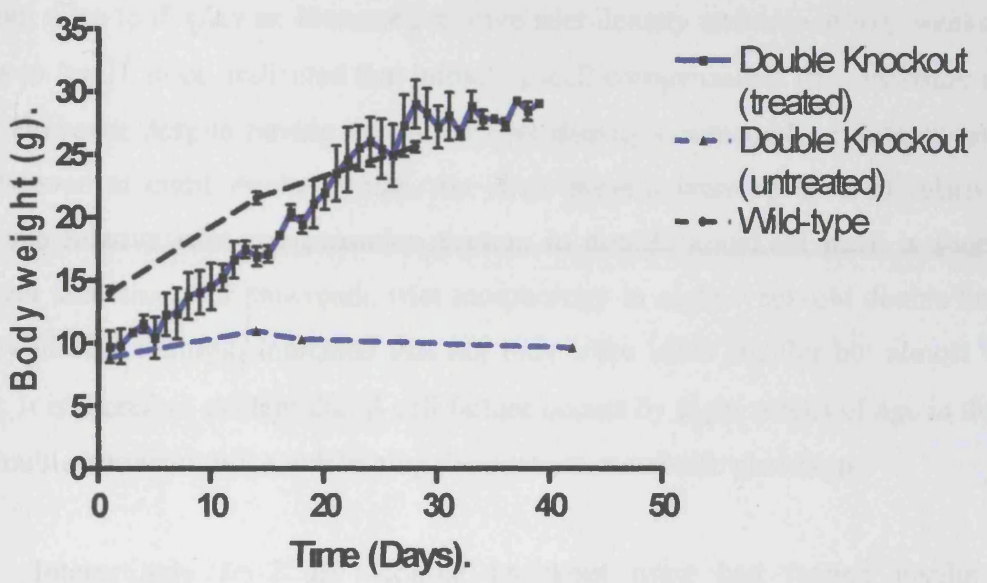

Figure 5.10 Insulin treatment of double knockout mice over a forty-day period.

Double knockout mice were administered daily injections of Lantus (a long-acting insulin), in accordance with daily measurements of body weight and urine glucose and ketone content. Following thirty days of treatment double knockout mice weighed more than age-matched wild-type mice. Indeed double knockout mice now had the habitus of ob/ob mice.

insulin resistance. Interestingly by eight weeks of age *Irs-2*$^{-/-}$*ob*$^{-/-}$mice were relatively hypoinsulinaemic, suggesting β-cell failure.

Quantification of relative islet density and area at four and eight weeks of age was consistent with this pattern of fasting insulin levels. Relative islet density and area in four-week-old double knockout mice was equal to (if not greater) than that of wild-type mice. Although the difference did not reach statistical significance, the trend for double knockout mice to display an increased relative islet density and area at four weeks of age relative to *Irs-2*$^{-/-}$ mice, indicated that initially β-cell compensation was occurring in these mice. However despite having a relative islet density comparable to that of wild-type controls even at eight weeks of age, the islets present were reduced in relative area. Hence the relative islet compensation present in double knockout mice is short-lived. Moreover assessment of pancreatic islet morphology in eight-week-old double knockout mice by insulin staining, indicated that not only were islets smaller but almost void of insulin. It is therefore evident that β-cell failure occurs by eight weeks of age in the *Irs-2*$^{-/-}$*ob*$^{-/-}$ double knockout mice, explaining their severe metabolic phenotype.

Interestingly *Irs-2*$^{-/-}$*db*$^{-/-}$ double knockout mice had fasting insulin levels comparable to wild-type controls at eight weeks of age. Although *Irs-2*$^{-/-}$*db*$^{-/-}$ double knockout mice also exhibit a severe early-onset diabetic phenotype, they appear to be less glucose intolerant than their *Irs-2*$^{-/-}$*ob*$^{-/-}$ equivalents. As discussed in chapter four, this was certainly evident when considering glucose tolerance testing of four-week-old mice (Figs 4.2 and 4.6). However, if *Irs-2*$^{-/-}$*db*$^{-/-}$ mice are more glucose tolerant and insulin sensitive than *Irs-2*$^{-/-}$*ob*$^{-/-}$ mice, it is plausible that *Irs-2*$^{-/-}$*db*$^{-/-}$ mice may still mount a mild β-cell response at eight weeks of age. The possibility that the shorter isoforms of the leptin receptor are capable of mediating some of leptin's actions in *db/db* mice, finds further support from these findings.

Similarly to double knockoukout mice, male *Irs-2*$^{-/-}$ mice exhibited elevated fasting insulin levels at four weeks, followed by relative hypoinsulinaemia at eight weeks of age. In contrast female *Irs-2*$^{-/-}$ mice had fasting insulin levels comparable to wild-type mice at four weeks of age but displayed hyperinsulinaemia by eight weeks of age. This highlighted the sexual dimorphism presented by this genotype and indicated that male *Irs-2*$^{-/-}$ mice suffer with increased insulin resistance.

Leptin deficient (*ob/ob* or *Irs-2*$^{+/-}$*ob*$^{-/-}$) or the leptin long-form receptor deficient (*db/db* or *Irs-2*$^{+/-}$*db*$^{-/-}$) mice were hyperinsulinaemic at eight weeks of age. Analysis of islet morphology in *ob/ob* mice demonstrated the presence of β-cell hyperplasia, consistent with such fasting hyperinsulinaemia. Moreover quantification of relative islet density and area in *ob/ob* mice showed them to have a significant increase in both relative density and area compared to wild-type controls (Table 5.1, >300% increased relative islet area, relative to that exhibited by wild-type controls). Although not addressed it is suspected that the dramatic hyperinsulinaemia reported in *Irs-2*$^{+/-}$*ob*$^{-/-}$, *db/db* and *Irs-2*$^{+/-}$ *db*$^{-/-}$mice was also the result of β-cell hyperplasia.

Taken together these findings highlight the importance of both insulin and leptin action in maintainance of the β-cell response to insulin resistance. In the absence of leptin or its receptor *Irs-2*$^{-/-}$ mice had an increased β-cell response compared to mice just lacking IRS-2. These findings suggest that leptin negatively regulates β-cell mass, acting either in the periphery or intrinsically to the β-cell. It is also possible that defects in the central actions of leptin result in the negative regulation of β-cell mass in response to insulin resistance.

Consistent with their improved glucose homeostasis, *Irs-2*$^{-/-}$*ob*$^{+/-}$ mice displayed fasting insulin levels comparable to *Irs-2*$^{-/-}$ mice at eight weeks of age. Interestingly *Irs-2*$^{-/-}$*ob*$^{+/-}$ mice had a reduced relative islet area compared to double knockout mice at eight weeks of age. However, immunostaining with insulin reveal that those islets present contained more insulin (data not shown). This could account for the increased fasting insulin levels seen in *Irs-2*$^{-/-}$*ob*$^{+/-}$ mice compared to double knockout mice at this age. Hence the expression of a single allele of leptin in *Irs-2*$^{-/-}$*ob*$^{+/-}$ mice was sufficient to permit increased β-cell compensation compared to that seen in double knockout mice.

Although not quantified it was presumed that the improved glucose homeostasis reported in *Irs-2*$^{-/-}$*db*$^{+/-}$ mice was also a result of improved insulin and leptin sensitivty.

It was evident that the various genotypes exhibit differences in both fat mass (as % total body weight – see chapter 3) and insulin sensitivity. Both obesity and relative lipodystrophy (lack of white adipose tissue) can lead to severe insulin resistance. It follows that adipokines, such as leptin act as regulators of insulin sensitivity. To assess the role of leptin in these various genotypes, fasting serum leptin levels were determined at eight weeks of age. The lack of leptin expression was confirmed in mice homozygous delete for the leptin gene (*ob/ob*, *Irs-2*$^{+/-}$*ob*$^{-/-}$ and *Irs-2*$^{-/-}$*ob*$^{-/-}$ mice). Considering other genotypes from the intercross of *Irs-2*$^{+/-}$*ob*$^{+/-}$ mice, only female *Irs-2*$^{-/-}$ mice had elevated fasting serum leptin levels. This finding suggested the presence of leptin resistance in female *Irs-2*$^{-/-}$ mice. In contrast male *Irs-2*$^{-/-}$ mice showed a non significant trend towards having reduced fasting serum leptin levels. It is known that female *Irs-2*$^{-/-}$ mice exhibit increased adiposity compared to male *Irs-2*$^{-/-}$ mice (84). This is exaggerated by the increased catabolic nature of male *Irs-2*$^{-/-}$ mice, which leads to a depletion of fat stores. Hence despite the presence of leptin resistance, reduced fat mass in eight-week-old male *Irs-2*$^{-/-}$ mice may lead to lower circulating leptin levels compared to females. This in turn may contribute to the progressive metabolic phenotype.

As discussed in chapter one, dysregulation of the adipo-insular axis is thought to be a major contributor to the onset of type 2 diabetes in obese subjects. Female *Irs-2*$^{-/-}$ mice are obese and eventually develop type 2 diabetes. The presence of both elevated fasting plasma insulin and leptin levels at eight weeks of age could imply these mice may have a dysregulated adipo-insular axis. Interestingly *Irs-2*$^{-/-}$*ob*$^{+/-}$ female mice did not display either elevated fasting insulin or leptin levels, indicating that expression of a single allele of leptin was sufficient to preserve insulin sensitivity.

Although fasting insulin and leptin levels were not assessed in male *Irs-2*$^{-/-}$ mice derived from the *Irs-2*$^{+/-}$*db*$^{+/-}$ intercross, female *Irs-2*$^{-/-}$ mice resulting from this cross displayed elevated fasting insulin and leptin levels. In contrast to female *Irs-2*$^{-/-}$*ob*$^{+/-}$ mice, whilst exhibiting normal fasting insulin levels female *Irs-2*$^{-/-}$*db*$^{+/-}$ mice had elevated fasting leptin levels compared to female *Irs-2*$^{-/-}$ mice. Studies assessing the responsiveness of isolated islets and adipocytes from female *Irs-2*$^{-/-}$*ob*$^{+/-}$, *Irs-2*$^{-/-}$*db*$^{+/-}$, *Irs-*

$2^{-/-}$ mice to leptin and insulin (or both) may provide useful insights into mechanisms responsible for dysregulation of the adipo-insular axis.

In *Irs-2*$^{+/-}$*db*$^{-/-}$ and *db/db* mice the complete loss of leptin receptor function resulted in significant hyperleptinaemia at eight weeks of age indicating that these mice were highly leptin resistant. In contrast, fasting leptin levels in *Irs-2*$^{-/-}$*db*$^{-/-}$ double knockout mice were comparable with that observed in wild-type animals. This was presumably due to the lack of white adipose tissue in these double knockout mice.

The accumulation of lipid deposits in non-adipose tissues, termed "lipotoxicity", is a major cause of insulin resistance (158). Leptin is thought to have a protective effect against lipotoxicity by promoting fatty acid oxidation, whilst inhibiting the production of triacylglycerides (158). Therefore assessment of serum free fatty acid (FFAs) levels would have provided useful insight into the fatty acid metabolism of these animals. Unfortunately, the growth retardation exhibited by double knockout mice made it impractical to obtain the blood volumes required for analysis of FFAs.

Finally, it is clear that the fat mass is critical for the maintenance of normal growth and also peripheral insulin sensitivity. Both *in vitro* and *in vivo* studies have demonstrated the importance of IRS-signalling in adipogenesis (115). The relative lipodystrophy and growth retardation observed in *Irs-2*$^{-/-}$*ob*$^{-/-}$ double knockout animals could have been a consequence of impaired adipogenesis or may simply have been a secondary effect of their marked diabetes. Hence four-week-old double knockout mice were administered daily injections of insulin. Treatment successfully reduced urine glucose and ketone levels in double knockout mice and this was paralleled with a rescue of their fat mass and growth retardation. Moreover double knockout mice treated over a six week period weighed more than their wild-type littermates and resembled *ob/ob* mice in habitus. This demonstrates that the marked diabetes present in double knockout mice promotes a state of catabolism that contributes to the lack of white adipose tissue.

CHAPTER 6

Analysis of insulin and leptin signal transduction in peripheral tissues of double knockout mice.

The marked insulin resistance present in the double knockout mice at four weeks of age suggested that there were potentially defects in insulin signalling mechanisms in insulin-sensitive tissues. Previously, it has been demonstrated that in *Irs2*$^{-/-}$ mice, insulin-stimulated activation of PI3K (one of the major signalling mediators of the metabolic effects of insulin) is dysregulated in both liver and skeletal muscle (83). Likewise in *ob/ob* mice, PI3K activation in liver and muscle, in response to insulin was shown to been reduced (119). In contrast, activation of the mitogenic limb of the insulin-signalling pathway including MAPK kinase often appears to be unaffected in insulin resistant states characterised by defects in glucose homeostasis. However the effects of deletion of *Irs-2* upon this limb of the cascade have not been reported.

The serine/threonine kinase Akt, and in particular the isoforms Akt-1 and Akt-2, are activated by insulin in metabolic tissues in a PI3K-dependent manner and mediate many of the metabolic effects of insulin. Global deletion of Akt-2 results in insulin resistance and a diabetes-mellitus like syndrome in mice (159). Indeed Akt-2 has also been identified as an insulin resistance gene in humans (160).

Therefore both the PI3K/Akt and mitogenic MAP-kinase limbs of the insulin signalling cascade were compared in the liver and skeletal muscle of wild-type, *Irs-2*$^{-/-}$, *ob/ob* and double knockout mice at four weeks of age. To assess the insulin signalling in these peripheral tissues, anaethetised mice were stimulated with either saline or insulin (5IU) for five minutes. Muscle and liver samples were then harvested for subsequent protein extraction. Initially, to assess the effect of deleting both *ob* and *Irs-2* genes upon insulin signalling, PDK-1 and Akt kinase activation in response to insulin stimulation was assessed in liver homogenates by western blot analysis, using phospho-specific antibodies to these kinase proteins (Fig 6.2).

6.1 Insulin-stimulated activation of IRS/PI3K signalling in the liver and skeletal muscle of wild-type, double knockout, Irs-2$^{-/-}$ and ob/ob mice

Activation of Akt requires phosphorylation of Thr-308 in the activation loop and Ser-473 in the C-terminal hydrophobic motif. PDK-1 can only phosphorylate Akt in the presence of PIP_3 and therefore a model has been proposed in which binding of PIP_3 to the PH domain of Akt causes a conformational change that relieves autoinhibition of the enzyme, allowing PDK-1 access to Thr-308. The kinase responsible for Ser-473 phosphorylation is poorly characterised, but has been tentatively termed PDK-2 as it is also PI3K-dependent. Phosphorylation at Thr-308 is thought to facilitate in the subsequent phosphorylation of Ser-473. Hence phosphorylation at Ser-473 is considered a good indicator of Akt activity.

Assessment of the expression and phosphorylation of these PI3K-dependent proteins was carried out in liver and skeletal muscle lysates obtained from wild-type, *Irs-2*$^{-/-}$, *ob/ob* and double knockout mice.

Initially it was planned to assess both IRS-1 and IRS-2 expression in all tissue. To achieve this I generated and purified GST-fusion proteins for both IRS-1 and IRS-2 which were subsequently used for the production of polyclonal antibodies in sheep. Analysis of the immunised sheep serum indicated that both anti-IRS-1 and anti-IRS-2 polyclonal antibodies could be used for immunoprecipitation of their respective proteins (see chapter 2, for details of antibody generation and function). Indeed the resulting anti-IRS-2 polyclonal was used to confirm deletion of IRS-2 in the skeletal muscle of both double knockout and *Irs-2*$^{-/-}$ mice (Fig 6.1).

p85 expression in the liver appeared to be comparable between all genotypes (Fig 6.2). Insulin-stimulated activation of PDK-1 was evident in wild-type and *ob/ob* livers. However *ob/ob* mice demonstrated a slightly higher level of PDK-1 phosphorylation at Ser-241 in the basal state (Fig 6.2). Interestingly insulin-stimulated phosphorylation of PDK-1 at Ser-241 appeared to be significantly reduced in livers from both *Irs-2*$^{-/-}$ and double knockout animals with the effect being more pronounced in the double knockout animals (Fig 6.2). Moreover it appeared that whereas *Irs-2*$^{-/-}$mice displayed basal PDK-1 phosphorylation at Ser-241 comparable to that seen in wild-type mice, basal phosphorylation of PDK-1 at this residue was reduced in the livers of double knockout mice (Fig 6.2).

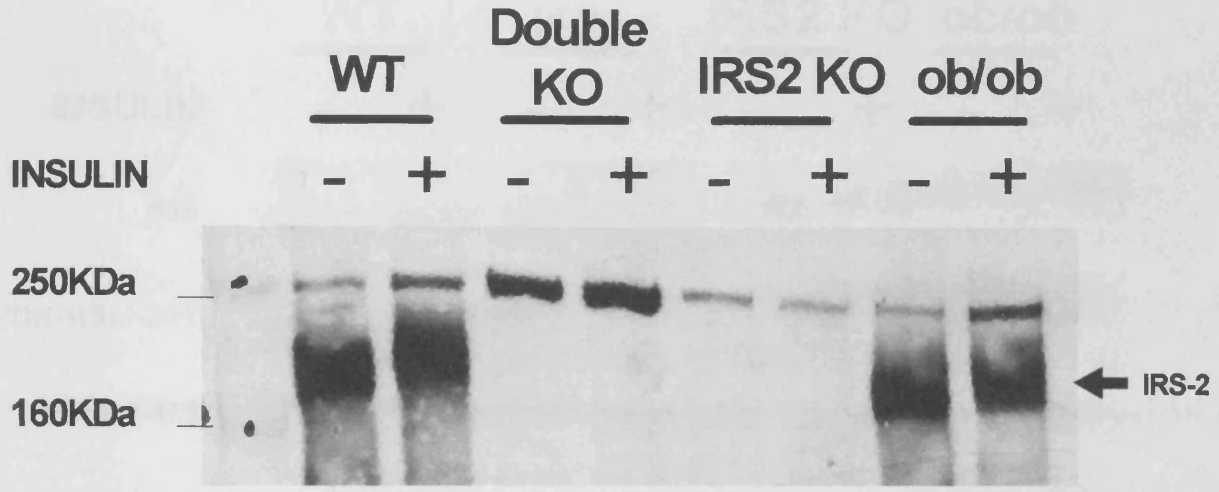

Figure 6.1 Insulin receptor substrate-2 expression in the skeletal muscle of wild-type, double knockout, Irs-2$^{-/-}$ and ob/ob mice.

Muscle lysates were obtained from wild-type, double knockout, Irs-2$^{-/-}$ and ob/ob mice that had been stimulated with either saline or insulin (5 i.u. via inferior vena cava injections) for 5 minutes. Muscle lysates (2 mg in total) were then immunoprecipitated with 10 μl of anti-IRS-2(S919A) serum. Immunoprecipitates were resolved by 6% SDS-PAGE, transferred and blotted for IRS-2 using anti-IRS-2 antibody (Upstate, cat# 06-508 (1:1,000)).

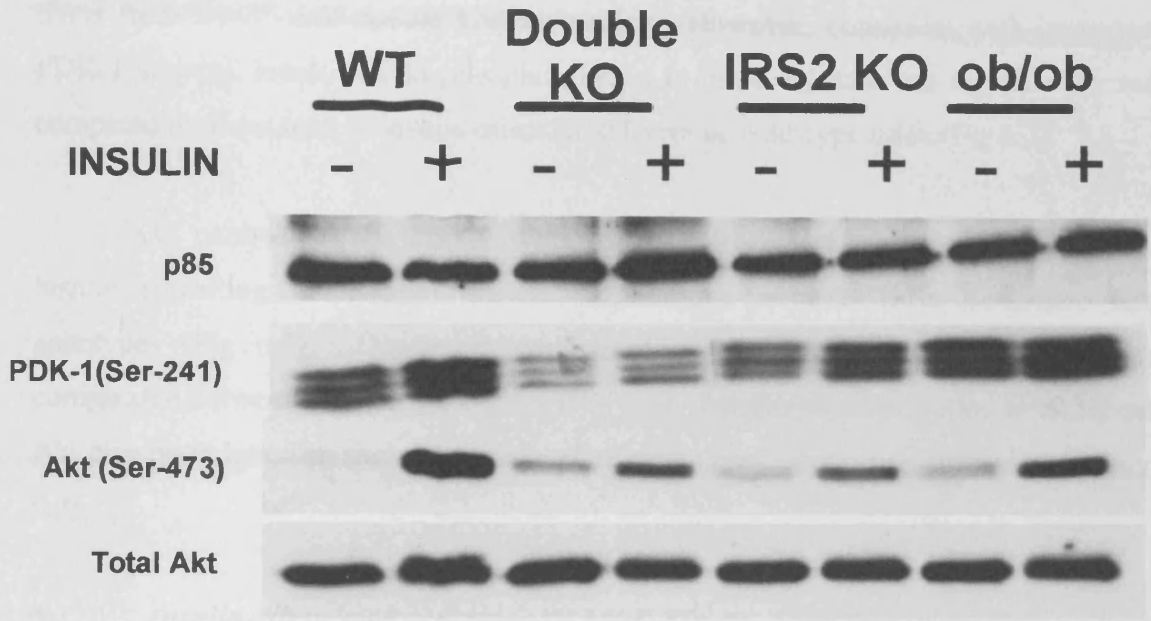

Figure 6.2 Insulin signalling analysis of the livers of wild-type, Irs-2$^{-/-}$, ob/ob and double-knockout mice.

Insulin stimulated liver was compared with basal liver for the activation of downstream markers of the IRS/PI3K limb of the insulin signalling cascade; p85, PDK-1 and Akt in wild-type, Irs-2$^{-/-}$, ob/ob and double knockout mice by western blotting with phospho-specific and total antibodies to these proteins. Results are representative of three independent experiments.

The increased phosphorylation of PDK-1 in insulin-stimulated livers of wild-type and *ob/ob* mice resulted in activation of Akt as evidenced by an increased phosphorylation at Ser-473 (Fig 6.2). Increased Akt phosphorylation was also noted in insulin-stimulated livers from *Irs-2*$^{-/-}$ and double knockout mice. However, consistent with impairment to PDK-1 activity, levels of Akt phosphorylation in these animals was significantly reduced compared to those seen in insulin-stimulated livers of wild-type mice (Fig 6.2).

In contrast to the observations made in liver assessment of the PI3K limb of insulin signalling in skeletal muscle surprisingly revealed little difference between genotypes (Fig 6.3). Consistent with liver p85 expression in skeletal muscle was comparable between all four genotypes (Fig 6.3). Insulin-stimulation led to an increase in Akt phosphorylation in skeletal muscle of all genotypes, suggesting increased activity (Fig 6.3).

6.2 Insulin-stimulated activation of MAP-Kinase signalling in the liver and skeletal muscle of wild-type, double knockout, Irs-2$^{-/-}$ *and ob/ob mice*

The mitogenic limb of insulin signalling was also assessed in the liver and skeletal muscle of wild-type, double knockout, *Irs-2*$^{-/-}$ and *ob/ob* mice. The expression of MAP-kinase was comparable between basal and insulin-stimulated states and similar levels were seen for all genotypes (Fig 6.4). Insulin-stimulated activation of MAP-kinase was assessed by comparing basal and insulin-stimulated phosphorylation at Thr202/Tyr204 residues. Phosphorylation at these residues was almost undetectable in the liver lysates obtained from wild-type, double knockout and *ob/ob* mice during the basal state. In contrast basal phosphorylation of MAP-kinase was dramatically increased in the livers of *Irs-2*$^{-/-}$ mice (Fig 6.4), this finding has not been reported previously and was reproducible. A dramatic increase in phosphorylation at Thr202/Tyr204 was seen in the livers of insulin-stimulated wild-type mice, suggesting an increased MAP-kinase activity. This increased phosphorylation in response to insulin was not evident in the livers of double knockout or *ob/ob* mice (Fig 6.4).

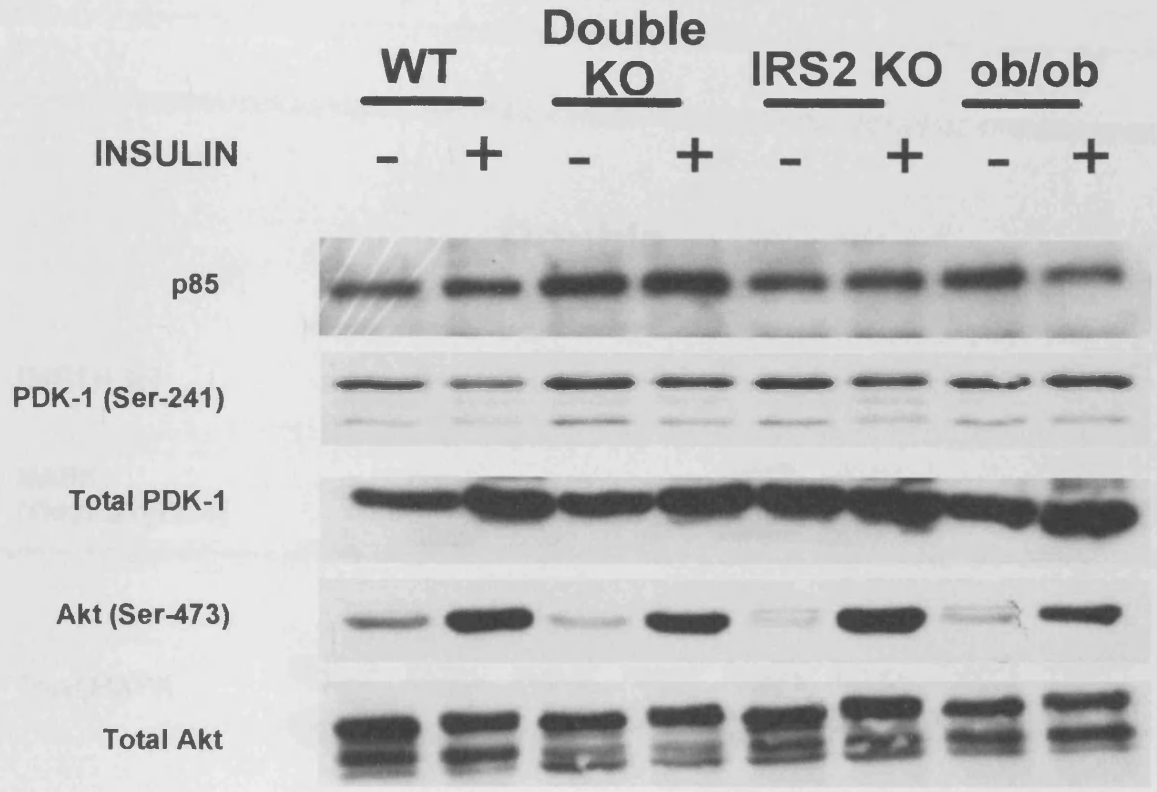

Figure 6.3 Insulin signalling analysis in skeletal muscle of wild-type, Irs-2$^{-/-}$, ob/ob and double-knockout mice.

Insulin stimulated skeletal muscle was compared with basal skeletal muscle for the activation of downstream markers of the IRS/PI3K limb of the insulin signalling cascade; p85, PDK-1, Akt and in wild-type, Irs-2$^{-/-}$, ob/ob and double knockout mice by western blotting with phopho-specific and total antibodies to these proteins. Results are representative of three independent experiments.

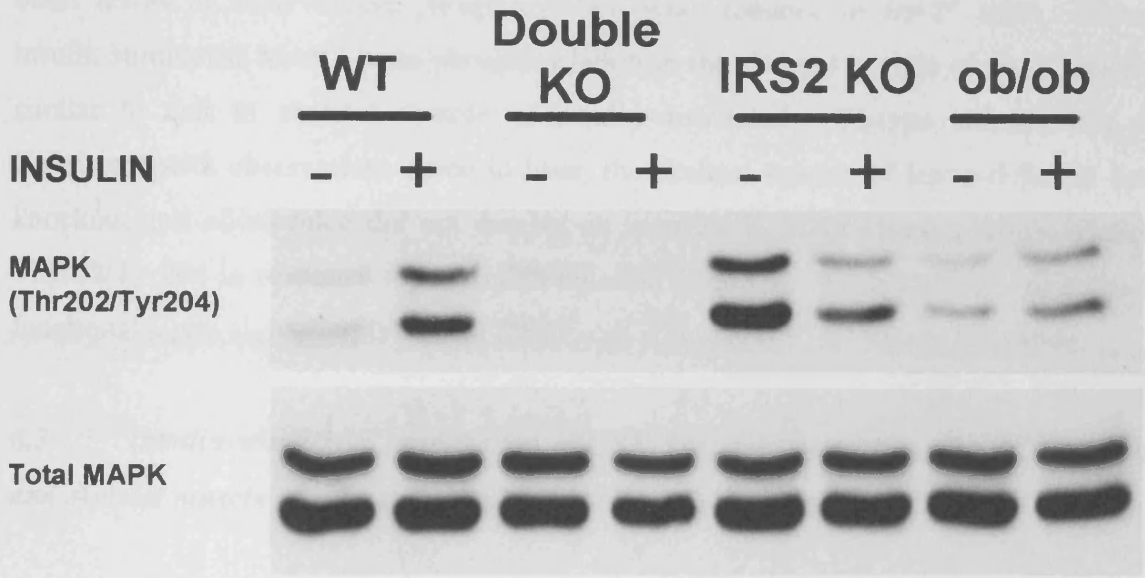

Figure 6.4 Insulin signalling analysis of livers of wild-type, Irs-2$^{-/-}$, ob/ob and double-knockout mice.

MAP Kinase phosphorylation in response to insulin stimulation was assessed in the livers of wild-type, Irs-2$^{-/-}$, ob/ob and double knockout mice at 4 weeks of age. Results are representative of three independent experiments.

Interestingly, levels of MAP-kinase phosphorylation were similar in the livers of insulin-stimulated wild-type and *Irs-2*$^{-/-}$ animals. However in *Irs-2*$^{-/-}$ mice insulin-stimulated MAP-kinase phosphorylation was surprisingly reduced compared to basal levels of phosphorylation in *Irs-2*$^{-/-}$ livers (Fig 6.4).

Basal MAP-kinase expression was comparable in the skeletal muscle of all genotypes and was not affected by insulin-stimulation (Fig 6.5). In comparison to liver, basal levels of MAP-kinase phosphorylation were reduced in *Irs-2*$^{-/-}$ mice. However insulin-stimulated MAP-kinase phosphorylation in the skeletal muscle of *Irs-2*$^{-/-}$ mice was similar to that in skeletal muscle of insulin-stimulated wild-type animals (Fig 6.5). Consistent with observations made in liver, the skeletal muscle of leptin-deficient double knockout and *ob/ob* mice did not display an increase in MAP-kinase phosphorylation at Thr202/Tyr204 in response to insulin stimulation (Fig 6.5). Such findings suggested that functional leptin signalling is critical for insulin-stimulated MAP-kinase activation.

6.3 Insulin-stimulated inactivation of GSK-3α/β and activation of p70^{s6k} in the liver and skeletal muscle of wild-type, double knockout, Irs-2$^{-/-}$ and ob/ob mice

Given the impaired phosphorylation of Akt in the livers of *Irs-2* deficient animals, GSK-3α/β and p70^{s6k} phosphorylation was assessed in the livers and skeletal muscle of mice. These are two key downstream mediators of insulin signalling.

Glycogen synthase kinase-3 (GSK-3α/β) inhibits the conversion of glucose into glycogen by phosphorylating the glycogen synthase enzyme. Therefore its activity in cells is reduced by insulin stimulation. Inhibition is achieved by insulin inducing phosphorylation of GSK-3α on Ser-21 and GSK-3β on Ser-9 (46).

p70 ribosomal s6 protein kinase (p70^{s6k}) controls the translation of several hundred mRNAs required for the assembly of the translational machinery (53). Its deletion in mice results in growth retardation and the development of a metabolic phenotype similar to that displayed by *Irs-2*$^{-/-}$ mice (161).

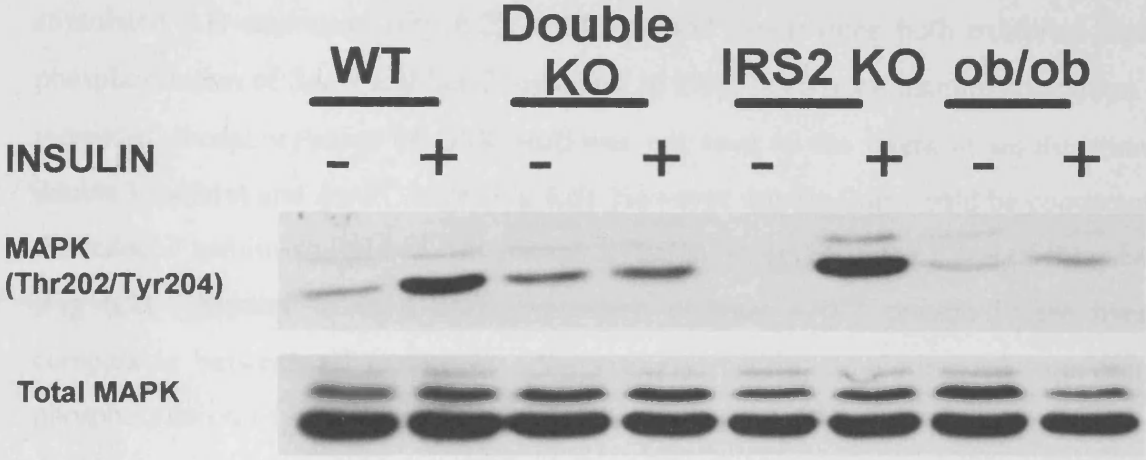

Figure 6.5 Insulin signalling analysis of skeletal muscle of wild-type, Irs-2$^{-/-}$, ob/ob and double-knockout mice.

MAP Kinase phosphorylation in response to insulin stimulation was assessed in the skeletal muscle of wild-type, Irs-2$^{-/-}$, ob/ob and double knockout mice at 4 weeks of age. Results are representative of three independent experiments.

The more recent finding that $p70^{s6k-/-}$ mice are resistant to age- and diet-induced obesity but have enhanced insulin sensitivity (162), suggests that p70s6k may act as an important mediator of insulin and leptin action.

Total GSK-3α/β expression in liver was determined to be comparable between wild-type, double knockout and *ob/ob* mice. However expression appeared to be reduced in the livers of *Irs-2*$^{-/-}$ mice compared to other genotypes (Fig 6.6). Consistent with insulin-stimulated Akt-activation (Fig 6.2), wild-type and *ob/ob* mice both exhibited increased phosphorylation of Ser-9 and Ser-21 residues of GSK-3α/β upon insulin-stimulation. This increased phosphorylation of GSK-3α/β was not seen in the livers of insulin-stimulated double knockout and *Irs-2*$^{-/-}$ mice (Fig 6.6). However this finding would be consistent with the reduced insulin-stimulated Akt-phosphorylation observed in the livers of these animals (Fig 6.2). Similar to GSK-3α/β, expression of total $p70^{s6k}$ protein in the liver was comparable between all genotypes. Surprisingly insulin-stimulation led to a decreased phosphorylation of $p70^{s6k}$ on Thr-389 in all genotypes. This was particularly evident in double knockout and *ob/ob* mice (Fig 6.6). Interestingly, basal phosphorylation of $p70^{s6k}$ was reduced in the livers of *ob/ob* mice relative to that seen in the other genotypes (Fig 6.6).

The expression of both GSK-3α/β and $p70^{s6k}$ in skeletal muscle was comparable for all genotypes (Fig 6.7). Insulin-stimulated phosphorylation of GSK-3α/β at Ser-9 and Ser-21 was evident in the skeletal muscle of all genotypes. This finding was expected, as activation of both the PI3K and MAP-kinase limbs of insulin signalling appeared to be comparable in the skeletal muscle of *Irs-2*$^{-/-}$ and wild-type mice (Figs 6.3 and 6.5). Insulin-stimulation in skeletal muscle resulted in an increase in phosphorylation of $p70^{s6k}$ in wild-type, double knockout, *Irs-2*$^{-/-}$ and *ob/ob* mice (Fig 6.7).

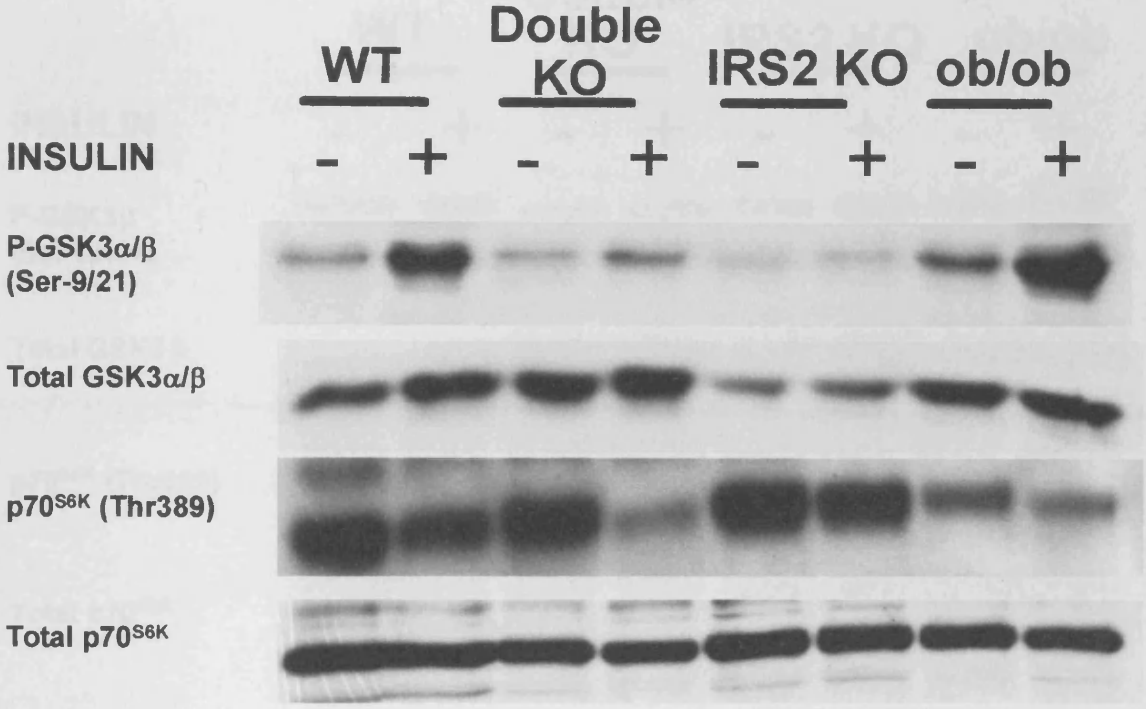

Figure 6.6 Insulin signalling analysis of the livers of wild-type, Irs-2$^{-/-}$, ob/ob and double-knockout mice.

Insulin stimulated liver was compared with basal liver for the activation of downstream markers of the Akt signalling; GSK-3α/β and p70^{S6K} in wild-type, Irs-2$^{-/-}$, ob/ob and double knockout mice by western blotting with phopho-specific and total antibodies to these proteins. Results are representative of three independent experiments.

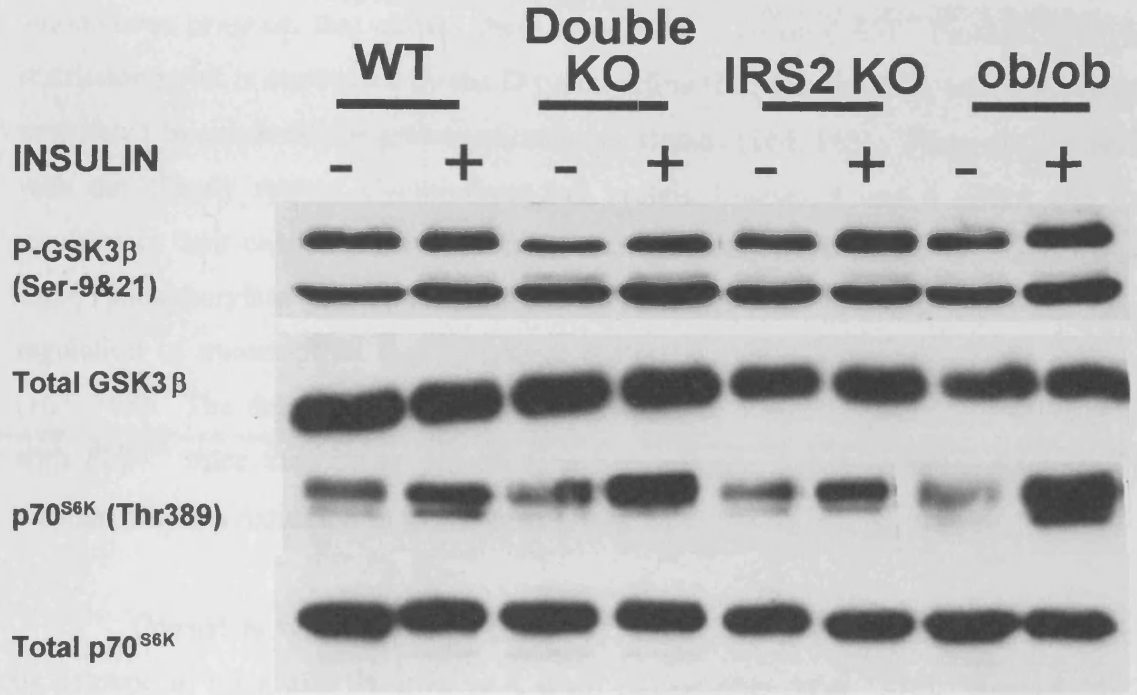

Figure 6.7 Insulin signalling analysis in skeletal muscle of wild-type, Irs-2$^{-/-}$, ob/ob and double-knockout mice.

Insulin stimulated muscle was compared with basal muscle for the activation of downstream markers of the Akt signalling cascade; GSK-3α/β and p70^{S6K} in wild-type, Irs-2$^{-/-}$, ob/ob and double knockout mice by western blotting with phopho-specific and total antibodies to these proteins. Results are representative of three independent experiments.

6.4 Assessment of D-type cyclin expression in the liver and skeletal muscle of wild-type, double knockout, Irs-2$^{-/-}$ and ob/ob mice

The decision for cells to divide occurs at a restriction point late in G1, after which they become refractory to extracellular growth regulatory signals and are commited to an autonomous program that carries them through to division (163). Passage through this restriction point is controlled by the D-type cyclins (D1, D2 and D3), whose expression is modulated by extracellular growth-stimulatory signals (164, 165). These cyclins associate with the closely related Cyclin-dependent protein kinases 4 and 6 (Cdk4 and Cdk6), resulting in their catalytic activation and substrate recognition (166). Activated Cdk4 and Cdk6 phosphorylate the retinoblastoma (Rb) family of proteins, relieving negative regulation of transcription factors critical for G1/S transition and cell cycle progression (167, 168). The deletion of Cdk4 in mice results in a similar phenotype to *Irs-2*$^{-/-}$mice, with *Cdk4*$^{-/-}$ mice also being growth retarded, infertile and developing insulin-deficient diabetes due to a reduction in β-cell mass (169).

Consistent with the notion that p70^{s6k} controls cell size, growth and proliferation, its deletion in mice also resulted in a small mouse phenotype (170). Remarkably later studies revealed that like both *Irs-2*$^{-/-}$and *Cdk4*$^{-/-}$ mice, p70$^{s6k-/-}$ mice were also hypoinsulinaemic, glucose intolerant and had a reduced β-cell mass (161).

In view of these strikingly similar phenotypes and the surprising insulin-stimulated decrease in p70^{s6k} phosphorylation, observed in the livers of wild-type, double knockout, *Irs-2*$^{-/-}$ and *ob/ob* mice, the basal expression levels of D-type cyclins (D1, D2 and D3), was assessed in the livers and skeletal muscle of these four genotypes.

The expression of cyclin D1 appeared to be similar in the livers of wild-type, *Irs-2*$^{-/-}$ and *ob/ob* mice. However cyclin D1 expression was reduced in the livers of double knockout animals (Fig 6.8). In contrast the expression of cyclins D2 and D3 was comparable in the livers of all genotypes (Fig 6.8).

Assessment of cyclin expression in skeletal muscle indicated that there was no obvious change in basal expression of any of the D-type cyclins between the different genotypes (Fig 6.9).

6.5 *Summary and discussion*

Assessment of the PI3K limb of the insulin signalling cascade in the liver and skeletal muscle of wild-type, double knockout, *Irs-2*$^{-/-}$ and *ob/ob* mice, indicated that insulin resistance was more prevalent in the livers of these animals. In particular, insulin-stimulated phosphorylation of Akt was reduced in the livers of double knockout, *Irs-2*$^{-/-}$ and *ob/ob* mice. This reduced Akt phosphorylation implied a reduction in the activity of this critical intermediate of insulin action. Indeed consistent with a reduced Akt activity, livers from *Irs-2* deficient animals also displayed decreased GSK-3α/β phosphorylation, in response to insulin. As GSK-3α/β is a downstream effector of Akt signalling this finding would also suggest a reduction in Akt activity.

In physiological terms it is likely that *Irs-2* deficient animals have impaired glycogen metabolism with their livers being unable to convert glucose into glycogen. Insulin resistance in the livers of these mice would be a contributor to the elevated fasting blood glucose levels observed in these animals. It was also evident that the livers of *ob/ob* mice displayed a slight decrease in insulin-stimulated Akt phosphorylation. This is consistent with previous findings in these animals, where it was shown that the livers of *ob/ob* mice exhibit a 29% and 72% decrease in IRS-1 and IRS-2 expression, respectively (119). In addition *ob/ob* livers showed a change in expression of the alternatively spliced isoforms of the regulatory subunits for PI3K. However it should be noted that these studies were carried out in eight-ten week-old *ob/ob* mice. In contrast current studies were carried out in four-week-old *ob/ob* mice, an age when *ob/ob* mice were determined to have normal glucose tolerance. It would be important to assess whether these changes in IRS expression are a genetic consequence of the loss of leptin expression in *ob/ob* mice or if they occur due to secondary effects associated with the onset of obesity and glucose intolerance in *ob/ob* mice.

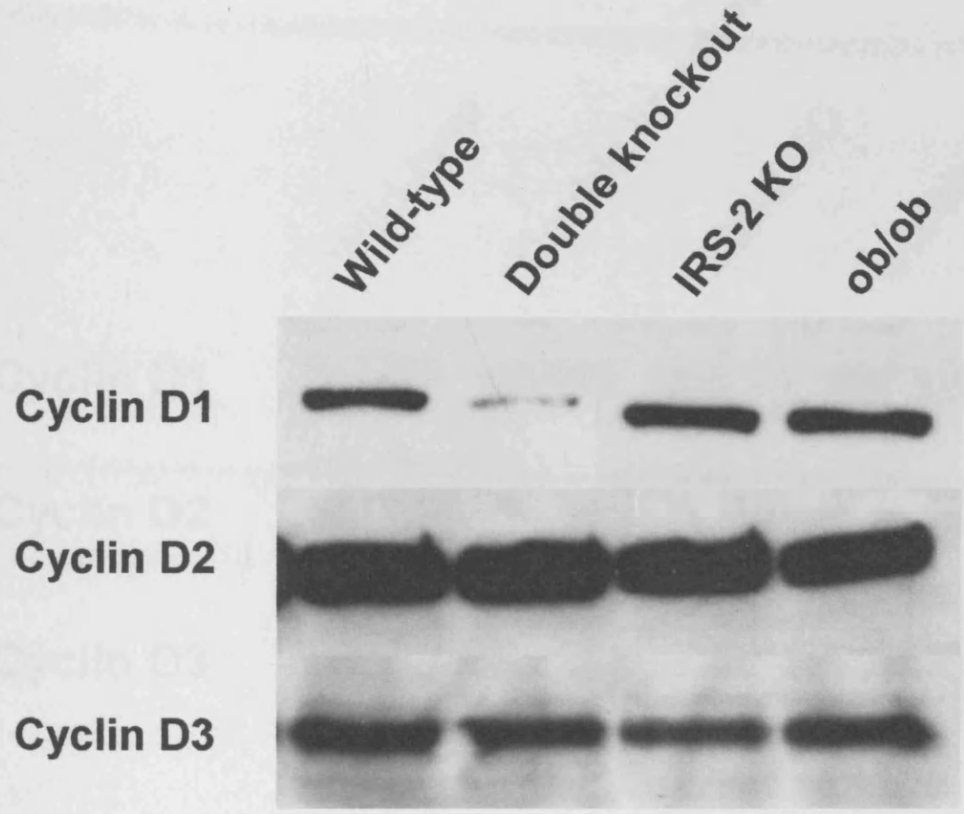

Figure 6.8 Insulin signalling analysis of livers of wild-type, Irs-2$^{-/-}$, ob/ob and double-knockout mice.

Expression of Cyclins D1, D2 and D3 was assessed in the livers of wild-type, double knockout, Irs-2$^{-/-}$and ob/ob mice at 4 weeks of age. Results are representative of three experiments.

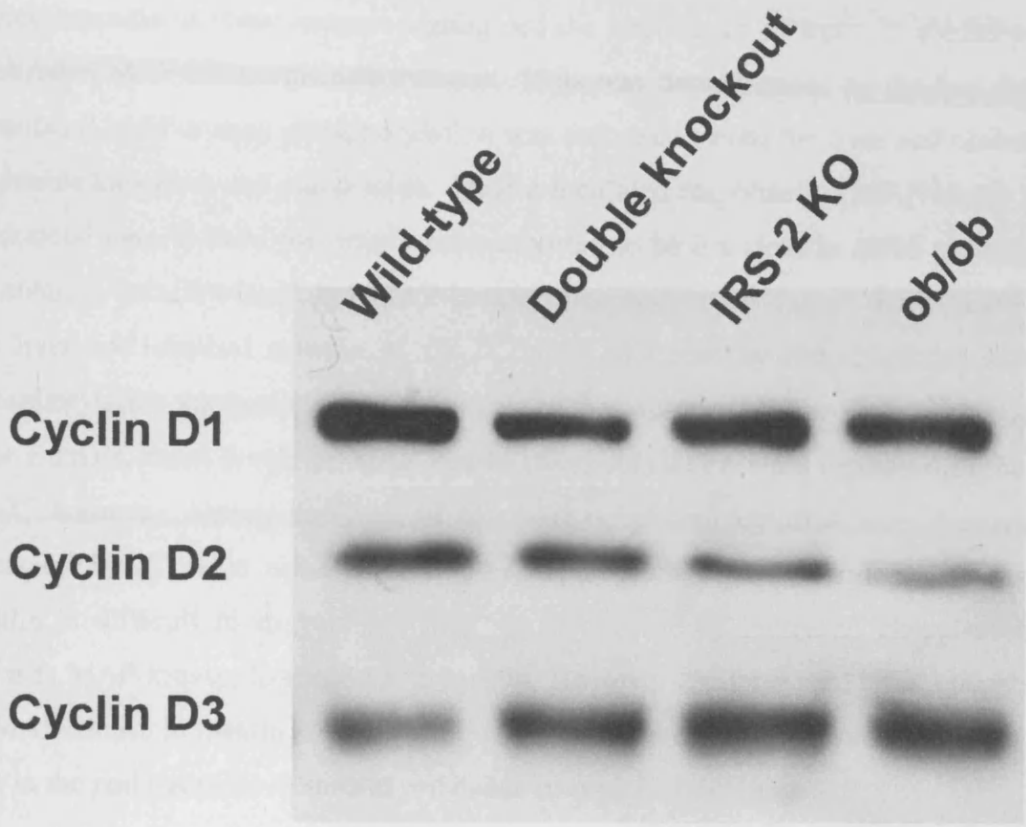

Figure 6.9 Insulin signalling analysis of skeletal muscle of wild-type, Irs-2$^{-/-}$, ob/ob and double-knockout mice.

Expression of Cyclins D1, D2 and D3 was assessed in the skeletal muscle of wild-type, double knockout, Irs-2$^{-/-}$and ob/ob mice at 4 weeks of age. Results are representative of three experiments.

In contrast assessment of the same downstream mediators of IRS/PI3K signalling in skeletal muscle revealed normal responses to insulin for all genotypes.

Interestingly analysis of the mitogenic limb of insulin signalling in the liver and skeletal muscle of these animals highlighted the importance of leptin in mediating insulin-stimulated MAP-kinase phosphorylation. This was demonstrated by the fact that insulin-stimulated MAP-kinase phosphorylation was reduced in both the liver and skeletal muscle of double knockout and *ob/ob* mice. Insulin-mediated responses on MAP-kinase signalling in skeletal muscle have previously been reported to be impaired in *ob/ob* mice (171, 172). In contrast insulin-stimulated MAP-kinase phosphorylation varied dramatically between the liver and skeletal muscle of *Irs-2*$^{-/-}$ mice. Whereas insulin-stimulated MAP-kinase phosphorylation appeared to be comparable to that observed in the skeletal muscle of wild-type animals, basal levels of MAP-kinase phosphorylation were increased in the livers of *Irs-2*$^{-/-}$ animals. Moreover levels of MAP-kinase phosphorylation were decreased in the livers of *Irs-2*$^{-/-}$ mice upon insulin-stimulation. Such dephosphorylation in response to insulin is difficult to explain but may result because of increased phosphatase activity towards MAP-kinase, in response to insulin. However the increased basal phosphorylation of MAP-kinase in insulin target tissues would indicate that MAP-kinase may play a pivotal role in the pathogenesis of insulin resistance in type 2 diabetes.

As p70^{s6k} controls cell size, growth and proliferation some focus was given to the cell cycle machinery. Similar to *Irs-2*$^{-/-}$ mice, both *p70*$^{s6k-/-}$ and *Cdk-4*$^{-/-}$ mice also display glucose intolerance and a reduced β-cell mass. The D-type cyclins are the regulatory partners of Cdk-4 and are required to mediate the initiation of cell cycle progression. Hence the expression of D-type cyclins was assessed in the liver and skeletal muscle of wild-type, double knockout, *Irs-2*$^{-/-}$ and *ob/ob* mice. Overall expression of the D-type cyclins was comparable in both liver and skeletal muscle for all genotypes. However there appeared to be a dramatic decrease in cyclin D1 levels in the livers of double knockout mice. This finding could be indicative of defects to the cell cycle machinery in the hepatocytes of double knockout mice. Assessment hepatocyte morphology in liver sections stained with haemotoxylin and eosin would provide insight into the effectiveness of cell division. It would be interesting to determine whether the lower cyclin D1 levels were a result of decreased expression or increased degradation. Indeed GSK-3α/β has been proposed to

phosphorylate cyclin D1 on Thr-286 (173), an event which prepares cyclin-D1 for 26S proteosome degradation. Interestingly, insulin-stimulated GSK-3 α/β phosphorylation was impaired in the livers of double knockout mice. As insulin-stimulation is proposed to inhibit GSK-3 α/β activity it is possible that insulin resistance in the livers of double knockout mice manifests an increased GSK-3 α/β activity. This increased GSK-3 α/β activity results in an increased phosphorylation of cyclin D1 on Thr-286 and subsequent 26S proteosome-mediated degradation.

In summary PI3K and MAP-kinase couple insulin signalling to metabolic and mitogenic events, respectively. It is evident that the liver is a major site of insulin resistance in these diabetic murine models, with impairment to both the PI3K and MAP-kinase limbs of the insulin signalling cascade. However, although IRS/PI3K-mediated signalling appear to be normal in the skeletal muscle of these four genotypes, double knockout and *ob/ob* mice exhibit impaired insulin-stimulated MAP-kinase phosphorylation. This impairment to insulin-stimulated MAP-kinase phosphorylation seen both in the liver and skeletal muscle of leptin-deficient mice, suggests that MAP-kinase may act as a point of convergence for insulin and leptin signalling.

Further assessment of insulin and leptin signalling action in these peripheral tissues and others may provide greater insights into the differences in peripheral insulin resistance observed in these animals. Indeed similar signalling analysis of peripheral tissues obtained from; *Irs-2*$^{-/-}$*db*$^{-/-}$ double knockout, *db/db*, *Irs-2*$^{-/-}$*db*$^{+/-}$ and *Irs-2*$^{-/-}$*ob*$^{+/-}$ mice would hopefully further our understanding of how leptin deficiency leads to impaired insulin-stimulated MAP-kinase phosphorylation. However, these initial findings demonstrate the complex overlap of insulin and leptin action in the periphery.

CHAPTER 7

Generation and metabolic analysis of β-HypIRS2+STAT3KO mice.

The striking growth impairment and dramatic diabetes seen in both *Irs-2*$^{-/-}$*ob*$^{-/-}$ and *Irs-2*$^{-/-}$*db*$^{-/-}$ double knockout mice, highlights the importance of *Irs-2* signalling in the β-cell compensatory response. The complex interplay between leptin and insulin sensitivity, is also highlighted by the other genotypes resulting from these intercrosses. For example, the presence of a single allele of the leptin gene upon an *Irs-2*$^{-/-}$ background was sufficient in preventing the early-onset diabetes seen in double knockout mice. This was achieved by preservation of β-cell function in these animals. This effect was also noted in the *Irs-2*$^{+/-}$*db*$^{+/-}$ intercross, where the expression of a single allele of the leptin long-form receptor upon an *Irs-2*$^{-/-}$ background, also rescued the dramatic phenotype displayed by *Irs-2*$^{-/-}$*db*$^{-/-}$ double knockout mice. These findings suggest that either directly in the β-cell or indirectly via altering insulin sensitivity restoration of leptin function permitted an appropriate β-cell compensatory response.

The marked growth retardation and ketoacidosis displayed by four-week-old double knockout mice was rescued by daily administration of insulin. Indeed insulin treatment of double knockout mice over a period of forty days, rescued catabolism and permited an anabolic state that encouraged fat deposition. Similarly, *Irs-2*$^{+/-}$*ob*$^{-/-}$ mice also exhibit an obese phenotype, suggesting that restoration of just a single allele of *Irs-2*, is sufficient for mounting a β-cell compensatory response to peripheral insulin resistance. It is therefore likely that deletion of *Irs-2* gene function is largely responsible for the metabolic phenotype seen in double knockout mice. However it is also evident that the early-onset diabetes observed in double knockout mice is not solely attributable to the loss of *Irs-2* gene function. As described, *Irs-2*$^{-/-}$ mice do not develop a diabetic phenotype until approximately eight weeks of age (83). Hence loss of leptin gene function or leptin long-form receptor gene function, in addition to *Irs-2* gene function, must have an additive effect with regards to insulin sensitivity. It is possible that

deficiency of leptin or leptin long-form receptor in these mice leads to an increased resistance to the actions of insulin.

The metabolic phenotype of *Irs-2*$^{-/-}$*ob*$^{-/-}$ and *Irs-2*$^{-/-}$*db*$^{-/-}$ double knockout mice is complex and it is difficult to fully dissect the specific contribution of signalling and pathophysiology to the phenotype. However it is evident that the restoration of a single allele of leptin or its long-form receptor, results in improved glucose tolerance and insulin sensitivity. The impairment to energy homeostasis described in β-HypIRS2KO (88, 89) and β-HypSTAT3KO (81, 82) mice demonstrates a critical role for both intrinsic IRS-2 and STAT-3 signalling pathways in the β-cell and hypothalamus. Hence β-HypIRS2KO mice were inter-crossed with β-HypSTAT3KO mice to produce β-HypIRS2+STAT3KO mice. These mice lack *Irs-2* and *stat-3* expression in the β-cell and hypothalamus. This tissue-specific approach would hopefully address the roles of insulin and leptin signalling pathways in relation to islet and hypothalamic function and provide some clues as to whether these intrinsic pathways converge to effect whole-body energy homeostasis. By deleting both these genes in two of the major sites (β-cell and hypothalamus) where leptin and IRS-2 are thought to act in energy homeostasis, we envisaged that we would recapitulate the double knockout phenotype.

7.1 Generation of β-HypIRS2+STAT3KO mice

Both β-HypIRS2KO and β-HypSTAT3KO mice had previously been generated within the laboratory, by intercrossing IRS2lox and STAT3lox mice with mice expressing Cre-recombinase under the control of the rat insulin II promoter (RIP-Cre mice). Initially mice heterozygous (with regards to floxed alleles) and positive for the RIP-cre transgene (ie.both β-HypIRS2lox$^{+/-}$ and β-HypSTAT3lox$^{+/-}$ mice) were intercrossed. These matings yielded compound heterozygotes that were positive for the RIP-cre transgene (ie.RIP-cre^{+ve}β-HypIRS2lox$^{+/-}$STAT3lox$^{+/-}$mice). These mice were then inter-crossed to generate wild-type, β-HypIRS2KO, β-HypSTAT3KO and β-HypIRS2+STAT3KO mice. PCR genotyping carried out at three weeks of age revealed that β-HypIRS2+STAT3KO mice were viable.

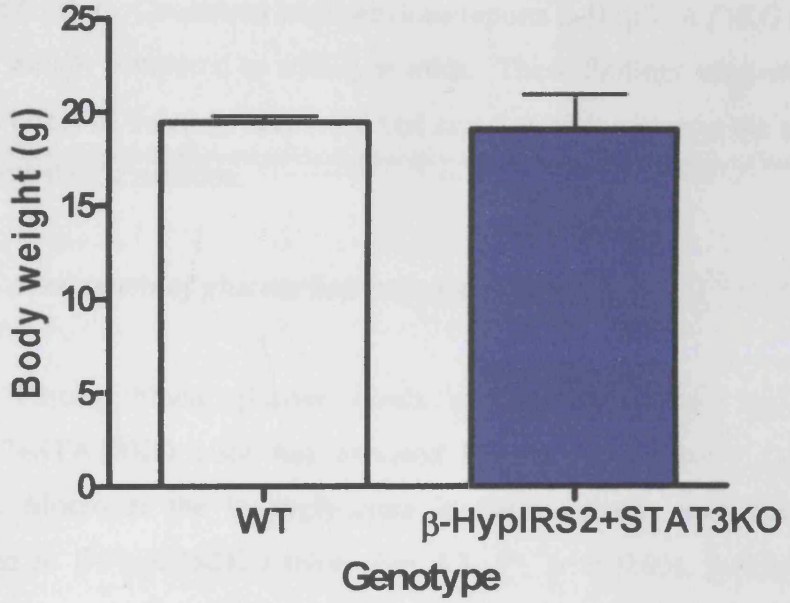

Figure 7.1 Analysis of body weights of wild-type and β-HypIRS2+STAT3KO mice at four weeks of age.

Results are representative as mean weights ± s.e.m of 5 animals per genotype.

7.2 *Analysis of β-HypIRS2+STAT3KO mice body weight*

Body weights measured at four weeks of age indicated that β-HypIRS2+STAT3KO mice were comparable in weight to wild-types (Fig 7.1). In contrast, body weight data obtained at eight weeks of age, showed β-HypIRS2+STAT3KO mice now weighed significantly more than wild-type controls (Fig 7.2, $p < 0.0001$). A significant increase in body weight relative to wild-type controls was also evident in the β-HypIRS2KO mice (Fig 7.2, $p < 0.05$). However, this increase was less dramatic than observed in the β-HypIRS2+STAT3KO mice. Indeed β-HypIRS2+STAT3KO mice were significantly heavier than β-HypIRS2KO mice (Fig 7.2, $****p < 0.0001$). Consistent with previous reports β-HypSTAT3KO mice were increased in body weight compared to wild-type mice. These findings suggested that there was an additive effect of deleting both *Irs-2* and *stat-3* gene function at the same time, in β-cells and hypothalamic neurons.

7.3 *Assessment of glucose homeostasis in β-HypIRS2+STAT3KO mice*

Fasting blood glucose levels at eight weeks of age indicated that β-HypIRS2+STAT3KO mice had elevated fasting blood glucose relative to wild-type controls. Moreover the hyperglycemia in these animals was significantly increased compared to β-HypIRS2KO mice (Fig 7.3, **, $p < 0.01$). β-HypIRS2KO mice also exhibited elevated fasting blood glucose levels relative to controls (Fig 7.3, $*p < 0.05$) but β-HypSTAT3KO mice displayed normal fasting blood glucose levels. The hyperglycaemia observed in β-HypIRS2+STAT3KO mice suggested the presence of glucose intolerance and possibly diabetes.

Glucose tolerance testing carried out on β-HypIRS2+STAT3KO mice at eight weeks of age, confirmed them to be glucose intolerant (Fig 7.4). Analysis of area under the curve (AUC) showed β-HypIRS2+STAT3KO mice to have a highly significant increase in AUC relative to wild-type controls (Fig 7.5, $p < 0.001$). Interestingly both β-HypIRS2KO and β-HypSTAT3KO mice appeared to be relatively glucose tolerant (Fig 7.4) and although demonstrating a trend towards being glucose intolerant relative to control mice, this was not significant (Fig 7.5).

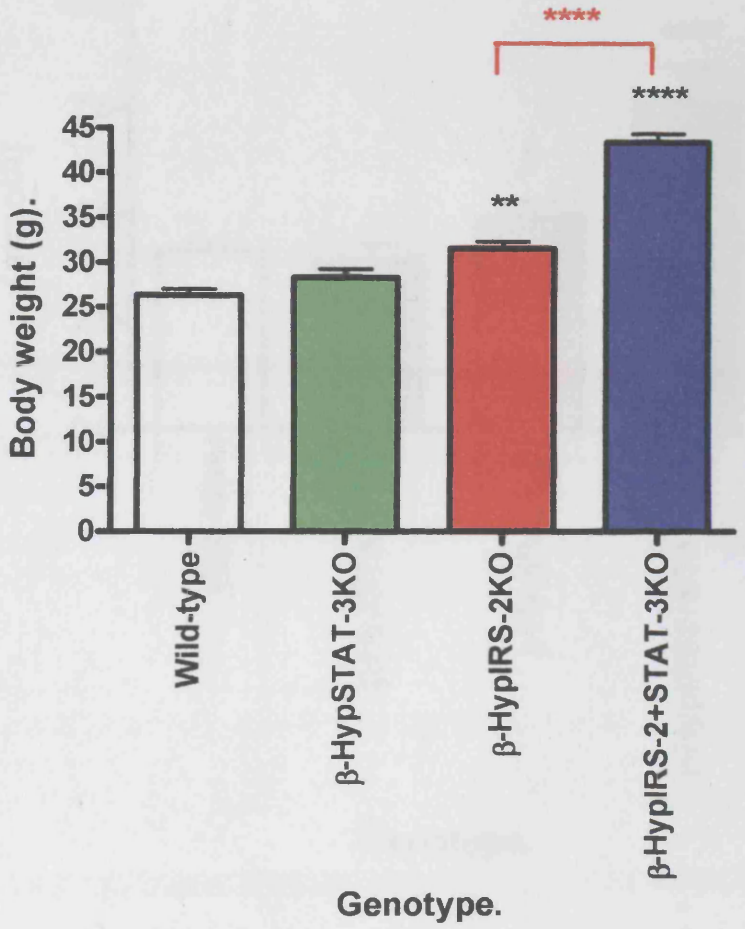

Figure 7.2 Analysis of body weights of wild-type, β-HypSTAT3KO, β-HypIRS2KO and β-HypIRS2+STAT3KO mice at eight weeks of age.

*Results are representative as mean weights ± s.e.m of 5 animals per genotype. Statistical analysis was carried out by means of t-tests comparing all genotypes to their wild-type controls; *, $p < 0.05$, **, $p < 0.01$, ***, $p < 0.001$, ****, $p < 0.0001$ and β-HypIRS2KO mice vs β-HypIRS2+STAT3KO mice, ****, $p < 0.0001$.*

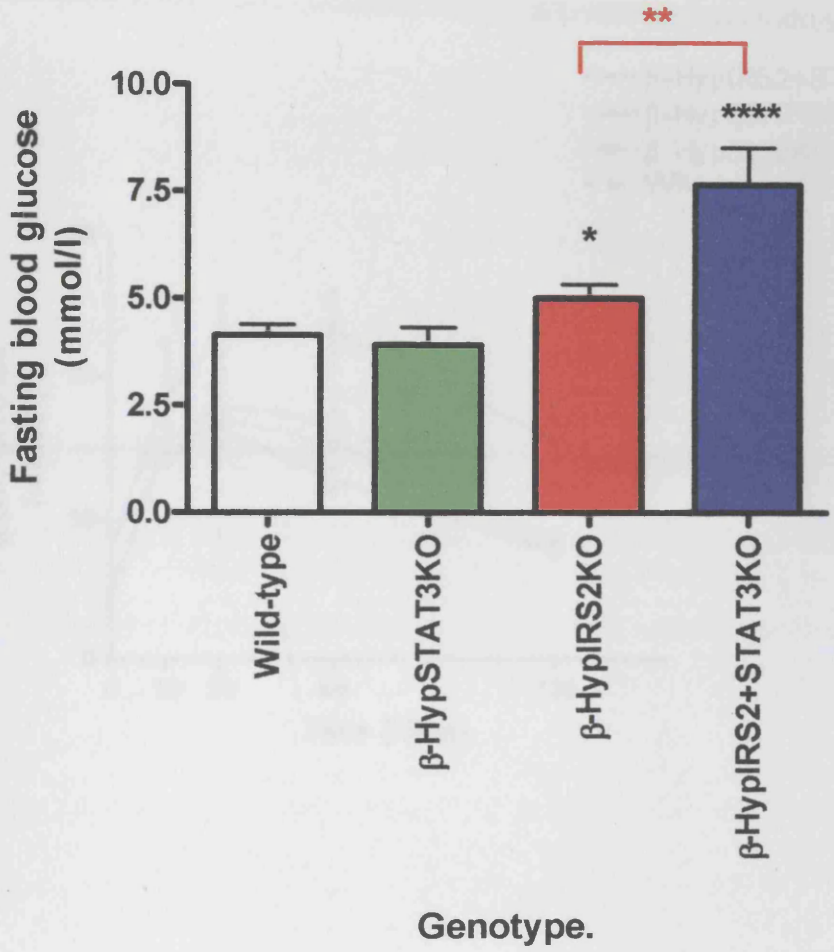

Figure 7.3 Fasting blood glucose of wild-type, β-HypSTAT3KO, β-HypIRS2KO and β-HypIRS2+STAT3KO mice at eight weeks of age.

Results are expressed as mean fasting blood glucose ± s.e.m and are representative of at least 7 animals per genotype, except for β-HypIRS2+STAT3KO mice n=4.

**p < 0.05 and ****p < 0.0001 for genotypes vs wild-type mice and β-HypIRS2KO mice vs β-HypIRS2+STAT3KO mice, **, p < 0.01.*

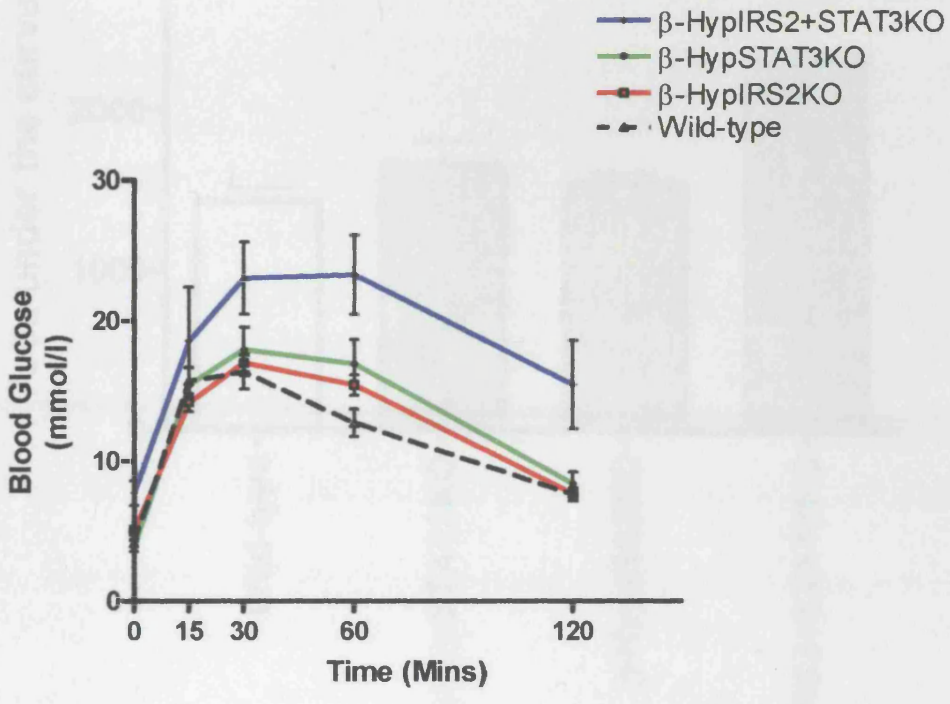

Figure 7.4 Glucose tolerance tests of wild-type, β-HypSTAT3KO, β-HypIRS2KO and β-HypIRS2+STAT3KO mice at eight weeks of age.

Results are expressed as mean blood glucose ± s.e.m and are representative of at least 7 animals per genotype, except for β-HypIRS2+STAT3KO mice n=4.

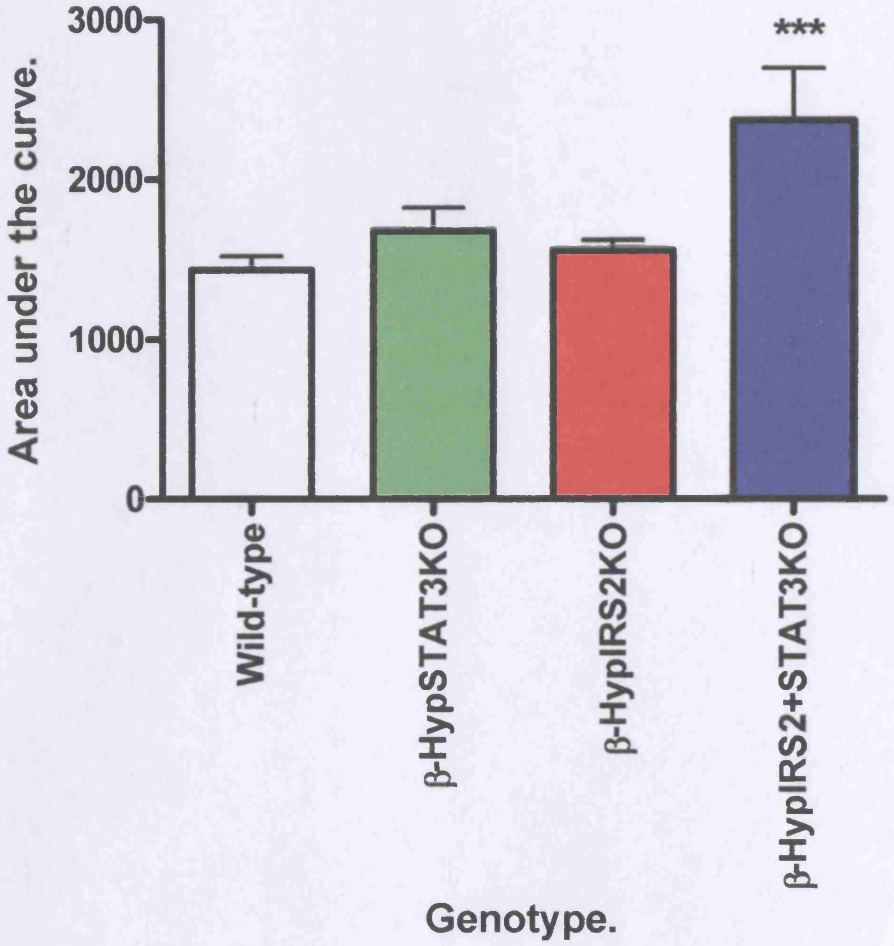

Figure 7.5 Statistical anaylsis of glucose tolerance tests carried out at eight weeks of age on wild-type, β-HypSTAT3KO, β-HypIRS2KO and β-HypIRS2+STAT3KO mice. *Results are expressed as mean area under the curve ± s.e.m and are representative of at least 7 animals per genotype, except for β-HypIRS2+STAT3KO mice n=4. t-tests were performed comparing all genotypes to their wild-type controls; ***, $p < 0.001$.*

This finding supports the idea that combined deletion of *Irs-2* and *stat-3* gene function in the β-cell and hypothalamus, leads to an additive effect upon glucose homeostasis.

To address the glucose intolerance displayed by β-HypIRS2+STAT3KO mice, pancreatic β-cell function was assessed. Initially fasting insulin and leptin levels were determined at eight weeks of age. Relative islet density and relative islet area were then determined by morphometric analysis of pancreatic sections immunostained for insulin.

7.4 Determination of fasting serum insulin and leptin levels in wild-type, β-HypSTAT3KO, β-HypIRS2KO and β-HypIRS2+STAT3KO mice

Since β-HypIRS2+STAT3KO mice exhibit both an increase in body weight and glucose intolerance relative to β-HypSTAT3KO and β-HypIRS2KO mice, pancreatic islet function was assessed.

Initially fasting insulin levels were assessed for wild-type, β-HypSTAT3KO, β-HypIRS2KO and β-HypIRS2+STAT3KO mice at eight weeks of age. Both β-HypSTAT3KO and β-HypIRS2KO mice had elevated fasting insulin levels compared to wild-type mice, being significant in β-HypSTAT3KO mice (Fig 7.6, $*p < 0.05$). However β-HypIRS2+STAT3KO mice also exhibited significantly elevated fasting insulin levels compared to wild-type mice (Fig 7.6, $**p < 0.01$). Moreover the hyperinsulinaemia displayed by β-HypIRS2+STAT3KO mice was significantly elevated relative to the hyperinsulinaemia in β-HypIRS2KO mice (Fig 7.6, $*p < 0.05$).

Although not quantified it was noticed that β-HypSTAT3KO, β-HypIRS2KO and β-HypIRS2+STAT3KO mice all exhibited an increased adiposity. Indeed assessment of fasting leptin levels showed that β-HypSTAT3KO, β-HypIRS2KO and β-HypIRS2+STAT3KO mice all displayed relative hyperleptinemia compared to wild-type controls at eight weeks of age (Fig 7.7). However, this was only shown to be significant for β-HypIRS2+STAT3KO mice (Fig 7.7, $*p < 0.05$). Elevated fasting leptin levels would be indicative of increase body fat mass.

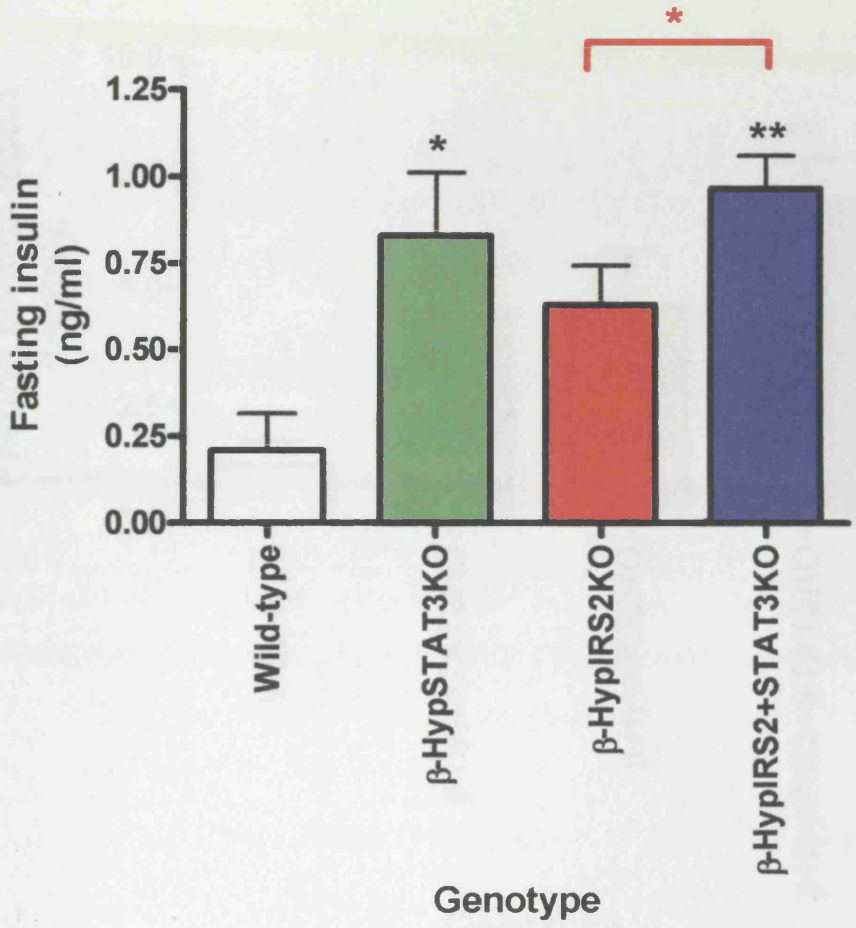

Figure 7.6 Fasting serum insulin levels of wild-type, β-HypSTAT3KO, β-HypIRS2KO and β-HypIRS2+STAT3KO mice at eight weeks of age.

Cardiac puncture was performed on anaesthetized, 15 hr fasted mice. Bloods were clarified by centrifugation (13,000rpm for 20 mins at 4°C) and the resulting serum was quantified for insulin concentration by a commercially available rat ultra-sensitive insulin ELISA assay, using a mouse standard for calibration. All assays were assayed in duplicate and results are presented as average serum insulin ± s.e.m, being representative of at least 4 animals per genotype. *, $p < 0.05$, **, $p < 0.01$, *and* *, $p < 0.05$, *for β-HypIRS2KO mice vs β-HypIRS2+STAT3KO mice.*

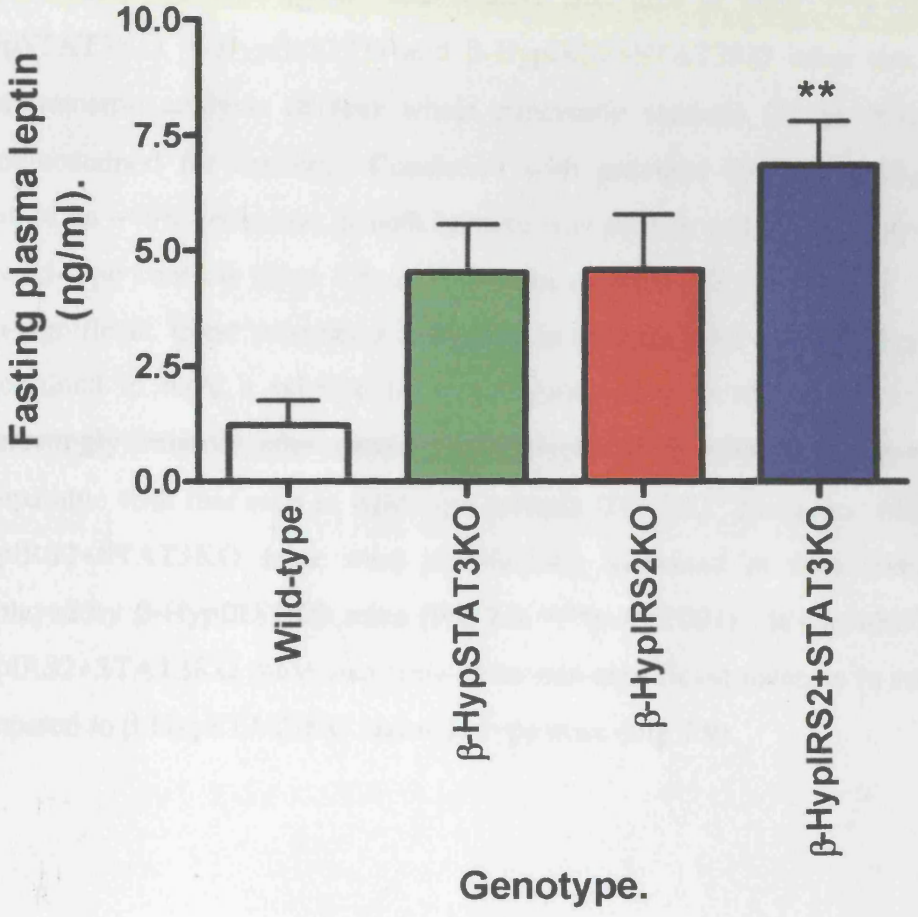

Figure 7.7 Fasting serum leptin levels of wild-type, β-HypSTAT3KO, β-HypIRS2KO and β-HypIRS2+STAT3KO mice at eight weeks of age.

Cardiac puncture was performed on anaesthetized, 15 hr fasted mice. Bloods were clarified by centrifugation (13,000rpm for 20 mins at 4°C) and the resulting serum was quantified for leptin concentration, by a commercially available mouse leptin ELISA assay (CrystalChem Inc.) All assays were assayed in duplicate and results are presented as average serum insulin ± s.e.m, being representative of at least 7 animals per genotype. **, $p < 0.05$ for β-HypIRS2KO and β-HypSTAT3KO mice vs wild-type.**, $p < 0.01$ for β-HypIRS2+STAT3KO vs wild-type mice.*

7.5 *Quantification of relative islet density and relative islet area in wild-type, β-HypSTAT3KO, β-HypIRS2KO and β-HypIRS2+STAT3KO mice*

Relative islet density and relative islet area of eight-week-old; wild-type, β-HypSTAT3KO, β-HypIRS2KO and β-HypIRS2+STAT3KO mice was determined by morphometric analysis of four whole pancreatic sections (5μm), from four animals, immunostained for insulin. Consistent with previous findings β-HypIRS2KO mice showed an ~40% reduction in both relative islet density and relative islet area compared to wild-type controls (Figs 7.8 and 7.9). In contrast β-HypSTAT3KO mice showed a non-significant trend towards a reduction in relative islet density (Fig 7.8) but were determined to have a relative islet area comparable to wild-type controls (Fig 7.9). Interestingly relative islet density in β-HypIRS2+STAT3KO mice appeared to be comparable with that seen in wild-type animals (Fig 7.8). Moreover islets present in β-HypIRS2+STAT3KO mice were significantly increased in area compared to those displayed by β-HypIRS2KO mice (Fig 7.9, $***p < 0.001$). It was also evident that β-HypIRS2+STAT3KO mice also showed an non-significant increase in relative islet area compared to β-HypSTAT3KO and wild-type mice (Fig 7.9).

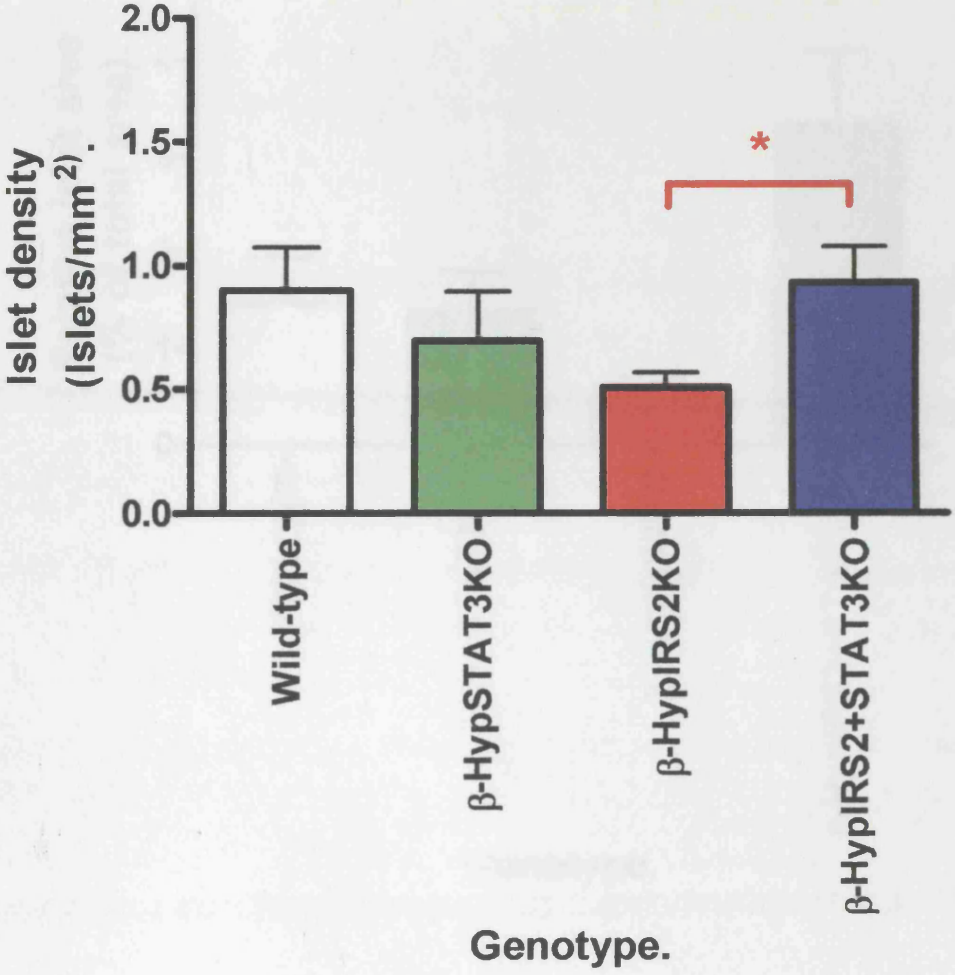

Figure 7.8 Quantification of relative islet density in wild-type, β-HypSTAT3KO, β-HypIRS2KO and β-HypIRS2+STAT3KO mice at eight weeks of age.

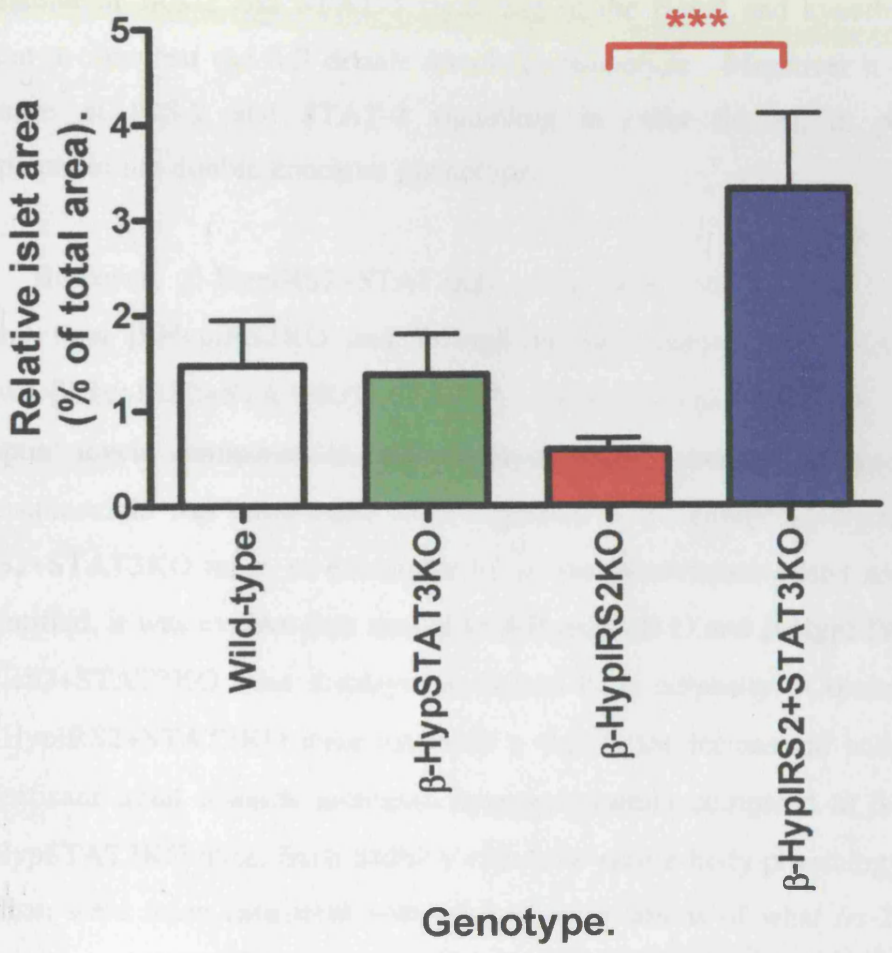

Figure 7.9 Quantification of relative islet area in wild-type, β-HypSTAT3KO, β-HypIRS2KO and β-HypIRS2+STAT3KO mice at eight weeks of age.

7.6 *Summary and discussion*

In contrast to the growth retardation and diabetes observed in both *Irs-2*$^{-/-}$*ob*$^{-/-}$ and *Irs-2*$^{-/-}$*db*$^{-/-}$ double knockout mice, β-HypIRS-2+STAT-3KO mice exhibited a significant increase in body weight and were not diagnosed diabetic. This demonstrates that deletion of IRS-2 and STAT-3 signalling in the β-cell and hypothalamus is not sufficient to manifest the full double knockout phenotype. Moreover it highlights the importance of IRS-2 and STAT-3 signalling in other tissues, in preventing the development of the double knockout phenotype.

However, β-HypIRS2+STAT3KO mice were significantly more glucose intolerant than β-HypIRS2KO and β-HypSTAT3KO mice, at eight weeks of age. Moreover β-HypIRS2+STAT3KO mice also tended to display elevated fasting insulin and leptin levels compared to both β-HypIRS2KO and β-HypSTAT3KO mice. Hyperinsulinaemia was attributable to an improved β-cell compensatory response in β-HypIRS2+STAT3KO mice, as evidenced by an increased relative islet area. Although not quantified, it was evident that similar to β-HypIRS2KO and β-HypSTAT3KO mice, β-HypIRS2+STAT3KO mice displayed increased body adiposity. Consistent with this idea β-HypIRS2+STAT3KO mice exhibited a significant increase in body weight and non-significant trend towards increased hyperleptinaemia compared to β-HypIRS2KO and β-HypSTAT3KO mice. Such additive effects on whole-body physiology and glucose metabolism were more consistent with original expectations of what *Irs-2*$^{-/-}$*ob*$^{-/-}$ double knockout mice might exhibit.

Although β-HypIRS2+STAT3KO mice did not display the same phenotype described for global double knockout animals, there were some common features between these animals. In particular was their ability to increase β-cell mass in response to insulin resistance. As discussed in chapter five, four-week-old *Irs-2*$^{-/-}$*ob*$^{-/-}$ double knockout mice displayed an improved preservation of β-cell mass and function in response to insulin resistance, compared to age-matched *Irs-2*$^{-/-}$ mice. Indeed it is also reported that both *ob/ob* and *db/db* mice exhibit β-cell hyperplasia, suggesting leptin deficiency promotes an increased β-cell response even in the absence of IRS-2 function.

Consistent with this idea β-HypIRS2+STAT3KO mice had a significantly increased relative islet density and area compared to β-HypIRS2KO mice. Interestingly the relative islet area of β-HypIRS2+STAT3KO mice was also increased compared to that seen in β-HypSTAT3KO mice, indicating that such tissue-specific deletion of IRS-2 and STAT-3 resulted in an additive effect with regards to islet function.

The fact that deletion of IRS-2 and STAT-3 in the β-cell and hypothalamus did not recapitulate the global double knockout phenotype, suggests that dysregulation of IRS-2 and leptin action in other tissues is critical for the manifestation of their severe diabetic phenotype. In view of the results obtained in chapter six, insulin resistance in the liver is likely to play a key role in the manifestation of the double knockout phenotype. However it will be essential to determine whether insulin resistance arises in the liver through direct effects or via the indirect actions of other insulin target tissues (ie. adipose and muscle tissues).

In summary, global deletion of IRS-2 in combination with either leptin or its functional receptor in mice resulted in growth retardation and early-onset diabetes. Additive effects were also observed with regards to body weight, insulin resistance and glucose homeostasis in β-HypIRS2+STAT3KO mice. These observations provide further genetic evidence that IRS-2 and STAT-3 signalling intrinsic to the β-cell and hypothalamus are important for mediating the effects of insulin and leptin in these target tissues. Moreover the additive effects of their deletion suggest that IRS-2 and STAT-3 mediate these effects by acting in separate signalling pathways, as opposed to converging upon a linear pathway.

CHAPTER 8

Discussion

Insulin and leptin have complex and convergent physiological roles in the regulation of whole body energy homeostasis (19). Leptin is thought to predominantly work in the central nervous system to regulate adiposity through the control of food intake and energy expenditure. Insulin is primarily considered to act in insulin-sensitive peripheral tissues such as skeletal muscle, adipose tissue and liver, regulating glucose and lipid metabolism. Both hormones have also been implicated in regulating additional physiological processes. For example, insulin also serves as an adiposity signal acting upon the same CNS mechanisms as leptin (16). In addition both leptin and insulin have been implicated in regulating β-cell function. Leptin has also been shown to modulate insulin secretion reducing its release (90, 91). Insulin signalling mechanisms have been shown to regulate insulin production and secretion and regulate β-cell development and growth (85, 92).

Recent evidence has also suggested that insulin and leptin utilise common signal transduction processes to mediate their physiological effects. For example, in mice with targeted disruption of *Irs2*, leptin-stimulated STAT-3 phosphorylation is impaired (84). Similarly, both insulin and leptin have been shown to activate PI3K in a number of cellular systems and it has been suggested that leptin-induced anorexia requires PI3K activation in hypothalamic neurons (132).

The work described in this thesis was undertaken to further understand the interaction between leptin and insulin signalling mechanisms and their contribution to energy homeostasis using a genetic approach. In particular, it was hoped that this would help address the role of IRS-2, as a potential convergence point for insulin and leptin signalling.

Initially mice lacking *Irs-2*, a key insulin signalling intermediate were intercrossed with *ob/ob* mice lacking leptin and also with *db/db* mice, which lack the functional leptin long-form receptor. The various genetic offspring resulting from these two intercrosses were then phenotyped with respect to growth, glucose homeostasis, β-cell function and preliminary insights were gained into insulin signalling events in their peripheral metabolic tissues.

As *Irs-2*$^{-/-}$, *ob/ob* and *db/db* mice are hyperphagic, leading to obesity and eventually the development of insulin resistance and type 2 diabetes, it was hypothesised that the combined deletion of these genes in mice was likely to produce an exaggerated adiposity phenotype prior to the development of diabetes. In contrast both *Irs-2*$^{-/-}$*ob*$^{-/-}$ and *Irs-2*$^{-/-}$*db*$^{-/-}$ double knockout mice were markedly growth retarded and exhibited significantly reduced fat mass. Moreover, assessment of glucose homeostasis in double knockout animals showed that they were severely diabetic as indicated by glucose intolerance as early as four weeks of age. These mice also exhibited fasting hyperinsulinaemia at four weeks of age, demonstrating their insulin resistance.

Interestingly despite having similar fasting blood glucose levels to *Irs-2*$^{-/-}$*ob*$^{-/-}$ mice at four weeks of age, *Irs-2*$^{-/-}$*db*$^{-/-}$ mice exhibited only mild glucose intolerance. Although the original *db*$^{+/-}$ mice were derived from a slightly different genetic background, it was evident that glucose homeostasis in wild-type, *Irs-2*$^{-/-}$ and *db/db* mice derived from the *Irs-2*$^{+/-}$*db*$^{+/-}$ intercross, was consistent with previous reports on these animals (21, 92). Hence the observation that *Irs-2*$^{-/-}$*db*$^{-/-}$ have improved glucose homeostasis at four weeks of age implies that subtle differences exist between these double knockout mice, as a result of the loss of either *ob/ob* or *db/db* gene function. This idea finds further support from the observation that *Irs-2*$^{+/-}$*ob*$^{-/-}$ mice weighed significantly more than *Irs-2*$^{+/-}$*db*$^{-/-}$ mice at eight weeks of age.

Despite exhibiting similar phenotypes, *ob/ob* and *db/db* mice are not exactly identical. As *db/db* mice are deleted for the expression of the leptin long-form receptor, they are highly leptin resistant, resulting in an increase in circulating leptin levels. Whilst the leptin long-form receptor has been shown to be the major mediator of leptin action, the shorter isoforms may also facilitate some of leptin's effects (56-58). If the leptin

short-isoform receptors do mediate some leptin signalling in the hyperleptinemic *db/db* mice, then these mice would exhibit some degree of leptin sensitivity. In contrast, leptin signalling is completely obliterated in *ob/ob* mice, as these mice do not express leptin. Previous reports have demonstrated that adult mice heterozygous for either the *ob* or *db* gene function have equivalent fat mass and percentage body fat. Interestingly mice heterozygous for both the *ob* or *db* genes ($ob^{+/-}db^{+/-}$), demonstrate further increases in fat mass and percentage body fat (157). Therefore it is reasonable to assume that differences exist between mice deleted for either leptin or leptin receptor function upon an *Irs-2* null background.

In contrast to double knockouts, $Irs\text{-}2^{-/-}ob^{+/-}$ and $Irs\text{-}2^{-/-}db^{+/-}$ mice displayed normal growth and glucose homeostasis at four weeks of age. This indicates that a single allele of leptin or leptin long-form receptor expression was sufficient to rescue mice from the severe metabolic phenotype seen in double knockout mice. These findings emphasize the importance of leptin sensitivity and in particular how leptin action is essential for the maintenance of glucose homeostasis. The observation that eight-week-old $Irs\text{-}2^{-/-}ob^{+/-}$ female mice were more glucose intolerant than $Irs\text{-}2^{-/-}$ female mice but less so than female double knockout mice, further illustrates the importance of leptin sensitivity in regulating peripheral glucose metabolism.

In view of the marked glucose intolerance displayed by double knockout mice their pancreatic islet function was assessed, to gain insights into the peripheral insulin sensitivity of these animals. Fasting insulin levels determined at four weeks of age showed $Irs\text{-}2^{-/-}ob^{-/-}$ mice to be significantly hyperinsulinaemic relative to wild-type mice, indicating the presence of insulin resistance. However by eight weeks of age these double knockout mice were relatively hypoinsulinaemic, suggesting β-cell failure.

Quantification of relative islet density and area at four and eight weeks of age was consistent with this pattern of fasting insulin levels. At four weeks of age double knockout mice displayed a relative islet density and area comparable to that seen in wild-type animals. However by eight weeks of age despite exhibiting a slight increase in relative islet density, the relative islet area of double knockout mice was reduced compared to that seen in wild-type mice, this suggested that this relative islet

compensation is short-lived and β-cell failure soon follows. Although not proven to be significant the trend for double knockout mice to display an increased relative islet density and area at four weeks of age compared to *Irs-2*$^{-/-}$ mice, would indicate the loss of leptin function in combination with *Irs-2* deletion, permits an initial β-cell compensatory response in double knockout mice. Indeed *ob/ob* mice display β-cell hyperplasia in the presence of peripheral insulin resistance well beyond eight weeks of age.

Interestingly *Irs-2*$^{-/-}$*db*$^{-/-}$ double knockout mice had fasting insulin levels comparable to wild-type controls even at eight weeks of age. This was consistent with the milder impairment to glucose homeostasis seen in these mice compared to age-matched *Irs-2*$^{-/-}$*ob*$^{-/-}$ double knockout mice. The improved fasting insulin levels noted in *Irs-2*$^{-/-}$*db*$^{-/-}$ mice, suggests that they are able to preserve some β-cell response to insulin resistance. The possibility that the shorter isoforms of the leptin receptor are capable of mediating some of leptin's actions in *db/db* mice, finds further support from this finding.

Consistent with their improved glucose homeostasis, *Irs-2*$^{-/-}$*ob*$^{+/-}$ mice displayed fasting insulin levels comparable to *Irs-2*$^{-/-}$ mice at eight weeks of age. Furthermore, despite showing a percentage decrease in relative islet area at four weeks of age compared to wild-type mice, a greater percentage decrease was observed for *Irs-2*$^{-/-}$ mice. This would further suggest that relative leptin deficiency can promote a greater β-cell response. Interestingly *Irs-2*$^{-/-}$*ob*$^{+/-}$ mice had a reduced relative islet area compared to double knockout mice at eight weeks of age. However, immunostaining with insulin reveal that those islets present contained more insulin. This would account for the increased fasting insulin levels seen in *Irs-2*$^{-/-}$*ob*$^{+/-}$ mice compared to double knockout mice at this age.

Dysregulation of the adipo-insular axis is thought to be a major contributor to the onset of type 2 diabetes, in obese subjects (113). Interestingly the lack of adipose tissue (lipodystrophy) can also lead to severe insulin resistance and the development of type 2 diabetes (14, 106). It follows that adipokines, such as leptin, act as regulators of insulin sensitivity. To assess the role of leptin in these various genotypes, fasting plasma leptin levels were determined at eight weeks of age. The lack of leptin expression was confirmed in mice homozygous delete for the leptin gene (*ob/ob*, *Irs-2*$^{+/-}$*ob*$^{-/-}$ and *Irs-2*$^{-/-}$

ob$^{-/-}$ mice – data not shown). Elevated fasting leptin levels were only reported in female *Irs-2*$^{-/-}$ mice resulting from the *Irs-2*$^{+/-}$*ob*$^{+/-}$ intercross. In contrast male *Irs-2*$^{-/-}$ mice showed a non significant trend towards having reduced fasting leptin levels. It is known that female *Irs-2*$^{-/-}$ mice exhibit increased adiposity compared to male *Irs-2*$^{-/-}$ mice (84), and this is exaggerated by the increased catabolic nature of male *Irs-2*$^{-/-}$ mice, which leads to a depletion of fat stores. Hence despite the presence of leptin resistance, reduced fat mass in eight-week-old male *Irs-2*$^{-/-}$ mice may lead to lower circulating leptin levels compared to females.

In *Irs-2*$^{+/-}$*db*$^{-/-}$ and *db/db* mice the complete loss of leptin receptor function resulted in leptin resistance, as indicated by significant hyperleptinemia at eight weeks of age. In contrast fasting leptin levels in *Irs-2*$^{-/-}$*db*$^{-/-}$ double knockout mice were comparable with that observed in wild-type animals. This was presumably due to the lack of white adipose tissue in these double knockout mice.

Taken together these observations highlight the importance of both insulin and leptin action in maintenance of the β-cell response to insulin resistance. Moreover, they provide evidence that leptin deficiency promotes an increased β-cell response even in the absence of IRS-2 function. These findings perhaps indicate that leptin has the ability to negatively regulate β-cell mass, acting either in the periphery or intrinsically to the β-cell. It is also possible that defects in the central actions of leptin result in the negative regulation of β-cell mass in response to insulin resistance.

The marked growth retardation and ketoacidosis displayed by four-week-old double knockout mice was rescued by daily administration of insulin. Insulin treatment of double knockout mice rescued catabolism and permited an anabolic state that encouraged fat deposition. Similarly, *Irs-2*$^{+/-}$*ob*$^{-/-}$ mice also exhibit an obese phenotype, suggesting that restoration of just a single allele of *Irs-2*, is sufficient for mounting a β-cell compensatory response to insulin resistance. However the systemic loss of gene function in the double knockout mice makes it difficult to assess the contribution of their loss in various cell types, to the development of insulin resistance.

Analysis of insulin signalling pathways in the liver and skeletal muscle of wild-type, double knockout, *Irs-2*$^{-/-}$ and *ob/ob* mice indicated that the liver is a major site of insulin resistance in these diabetic murine models. However, although IRS/PI3K-mediated signalling appear to be normal in the skeletal muscle of these four genotypes, double knockout and *ob/ob* mice exhibit impaired insulin-stimulated MAP-kinase phosphorylation. Insulin-mediated responses on MAP-kinase signalling in skeletal muscle have previously been reported to be impaired in *ob/ob* mice (171, 172). This impairment to insulin-stimulated MAP-kinase phosphorylation seen both in the liver and skeletal muscle of leptin-deficient mice, suggests that MAP-kinase may act as a point of convergence for insulin and leptin signalling. Indeed the finding that basal MAP-kinase phosphorylation was increased in the livers of *Irs-2*$^{-/-}$mice, would also indicate that MAP-kinase plays an important role in the pathogenesis of insulin resistance in type 2 diabetes. Further assessment of insulin and leptin signalling action in the periphery of these genotypes and others, may provide greater insights into the differences in peripheral insulin resistance, observed in these animals.

These genetic studies have therefore provided new insights into the role of leptin in the regulation of insulin sensitivity. The molecular basis for leptin's insulin sensitising effect is not clear but two basic mechanisms have been suggested to operate (8). Firstly, the effects of leptin may mainly occur via the CNS with the central effects being transmitted to the periphery through neural or neuroendocrine mechanisms including the hypothalamo-pituitary adrenal axis and the autonomic nervous system (134). The other mechanism that has been suggested to operate involves the direct effects of leptin upon peripheral insulin sensitive tissues such as liver, muscle and fat. Neuronal-specific deletion of the leptin receptor largely recapitulates the phenotype of the *ob/ob* mice suggesting that most of the effects of leptin are initiated in the CNS (174). More recently it has been proposed that leptin action is critical for the development of hypothalamic projection pathways, involved in the control of food intake and energy homeostasis (175, 176). Leptin has also been shown to acutely regulate the responsiveness of these projection pathways (177). Whilst the above observations suggest that deletion of *Irs-2* is perhaps the major factor in the metabolic phenotype exhibited by double knockout mice, it is also evident that the early-onset diabetes observed in double knockout mice is not solely attributable to the loss of *Irs-2* gene function. As described above, *Irs-2*$^{-/-}$ mice do not develop a diabetic phenotype until

approximately eight weeks of age (83), whereas double knockout mice have a marked phenotype at 3-4 weeks of age. Hence the finding that leptin and IRS-2 action is critical for the development as well as the function of neuronal networks involved in the regulation of energy homeostasis, may in part account for the more severe metabolic phenotype exhibited by double knockout mice. Indeed, shortly following the physiological assessment of *Irs-2*$^{-/-}$*ob*$^{-/-}$ double knockout mice, Schubert et al reported that disruption of the *Irs2* gene reduced neuronal proliferation during development by 50% (145). Such findings highlight the importance of IRS-2 signalling in the development of the CNS and further suggest that a component of the phenotype observed in double knockout mice may result from developmental defects.

The impairment of energy homeostasis regulation described in β-HypIRS2KO (88, 89) and β-HypSTAT3KO mice (81, 82) demonstrates a critical role for both intrinsic IRS-2 and STAT-3 signalling pathways in β-cell and hypothalamic function. Hence to address the roles of these insulin and leptin signalling intermediates in relation to islet and hypothalamic function, β-HypIRS2KO mice were inter-crossed with β-HypSTAT3KO mice to produce β-HypIRS2+STAT3KO mice. The study of these mice would hopefully increase our understanding of whether these intrinsic pathways converge to effect whole-body energy homeostasis. Such a tissue-specific approach would hopefully provide some insight into the contribution of developmental defects in the CNS to the systemic double knockout metabolic phenotype.

In contrast to systemic double knockout mice, β-HypIRS2+STAT3KO mice were not growth retarded, exhibiting a significant increase in body weight. Similarly they did not develop early-onset diabetes. This demonstrates that deletion of *Irs-2* and *stat-3* in the β-cell and hypothalamus is not sufficient to manifest the systemic double knockout phenotype. Moreover it highlights the importance of IRS-2 and leptin signalling in other tissues, in preventing the development of the double knockout phenotype.

However, it was evident β-HypIRS2+STAT3KO mice weighed significantly more than β-HypIRS2KO and β-HypSTAT3KO mice, at eight weeks of age. Moreover, consistent with an increased impairment to glucose homeostasis, β-HypIRS2+STAT3KO mice also tended to display elevated fasting insulin and leptin levels compared to both β-

HypIRS2KO and β-HypSTAT3KO mice. This hyperinsulinemia was attributable to an improved β-cell compensatory response in the β-HypIRS2+STAT3KO mice, as evidenced by an increased relative islet area.

Although β-HypIRS2+STAT3KO mice did not display the same phenotype described for global double knockout animals, there were some common features between these animals. In particular was their ability to increase β-cell mass in response to insulin resistance. As discussed in chapter five, four-week-old *Irs-2*$^{-/-}$*ob*$^{-/-}$ double knockout mice displayed an improved preservation of β-cell mass and function in response to insulin resistance, compared to age-matched *Irs-2*$^{-/-}$ mice. Indeed it is also reported that both *ob/ob* and *db/db* mice exhibit β-cell hyperplasia. These findings suggest that leptin deficiency promotes an increased β-cell response even in the absence of IRS-2 function. Consistent with this idea β-HypIRS2+STAT3KO mice had a significantly increased relative islet density and area compared to β-HypIRS2KO mice. Interestingly, the relative islet area of β-HypIRS2+STAT3KO mice was also increased compared to that seen in β-HypSTAT3KO mice, indicating that the combined tissue-specific deletion of IRS-2 and STAT-3 resulted in an additive effect with regards to islet function.

Considering either systemic or tissue-specific approaches, it is evident that insults to leptin signalling in combination with *Irs-2* deletion results in additive effects upon growth, adiposity, glucose homeostasis and islet function. These additive effects would indicate that IRS-2 and STAT-3 mediate these effects by acting in separate signalling pathways, as opposed to converging upon a linear pathway (Fig 8.1). However cross-talk between these pathways is likely to be critical for the maintenance of insulin and leptin sensitivity in target tissues.

The generation of β-HypIRS2+STAT3KO mice provides further evidence that IRS-2 and STAT-3 signalling, intrinsic to the β-cell and hypothalamus are important for mediating the effects of insulin and leptin upon energy homeostasis. However, previous murine studies have demonstrated that defective signalling in one tissue can affect actions of insulin and other hormones in the next. An example is the muscle and liver insulin resistance exhibited by mice with selective deletion of GLUT-4 in adipose tissue (178).

The liver is known to play a central role in the control of glucose homeostasis and is subject to complex regulation by insulin and other hormones (118, 179). The liver-specific deletion of the insulin receptor in mice showed that insulin receptor signalling is critical for regulating glucose homeostasis, facilitating insulin clearance, and maintaining normal hepatic function (118). In contrast, conditional deletion of hepatic leptin long-form receptor function did not lead to a discernable phenotype in terms of energy balance (174), suggesting that leptin signalling is redundant in the liver.

However considering the signalling data presented in chapter six, it was evident that the liver was a major site of insulin resistance. Moreover, leptin deficiency led to a major impairment of insulin-stimulated MAP-kinase phosphorylation in liver. The presence of hepatic insulin resistance in these animals might be explained by indirect effects, owing to leptin dysfunction in other metabolic tissues, like muscle and adipose tissue. Indeed similar defects in insulin-stimulated MAP-kinase phosphorylation were observed in skeletal muscle of *ob/ob* mice (see chapter 6). Such defects could lead to an altered transcriptional program in the skeletal muscle of *ob/ob* mice. Alterations in transcription could promote the secretion of metabolic precursors that have insulin desensitizing effects in neighbouring tissues like the liver. Interestingly the deletion of STAT-3 in the liver of mice, suggests an important role for STAT-3 signalling in the regulation of hepatic gluconeogenic genes (64).

The accumulation of free fatty acids (FFAs) in non-adipose tissue like the pancreatic β-cell, muscle and liver, often precedes the onset of hyperglycaemia and insulin resistance (180). An emerging body of evidence suggests that AMP-activated protein kinase (AMPK) may play a critical role in the pathogenesis of β-cell glucolipotoxicity and type 2 diabetes (181). Interest in AMPK has heightened since the demonstration that leptin can stimulate its activity acting either in the periphery or centrally (34). It has also been implicated as mediating leptin's effects in the CNS to regulate food intake (182, 183). Moreover, it is known that AMPK can regulate the expression of a number of transcription factors, including peroxisome proliferative-activated receptor α (PPARα), the uncoupling proteins UCP2 and UCP3 and the Sterol-regulatory-element-binding protein-1c (SREBP-1c). Alterations in the expression of

these transcription factors in mice, has been shown to manifest various metabolic phenotypes (106, 184-186).

The SREBPs transcription factors are of particular interest as they have been shown to suppress IRS-2-mediated insulin signalling in the liver (14, 120). Interestingly microarray analysis has indicated that the livers of *Irs-2*$^{-/-}$ mice exhibit increased SREBP-1 gene expression (121). In addition systemic deletion of SREBP-1 in *ob/ob* mice ameliorated their fatty livers but had no effect upon obesity and insulin resistance, highlighting their importance in the regulation of lipogenesis. This is further evidenced by the lipodystrophy exhibited by mice expressing a constitutively active form of SREBP-1c (103). Furthermore, leptin treatment reverses the insulin resistance and fatty livers displayed by these lipodystrophic mice, indicating that SREBP-1c may be a critical mediator of insulin and leptin action (106).

In summary the genetic studies described in this thesis have provided some useful insight into the complex interplay that exists between insulin and leptin action, in the regulation of energy homeostasis. In particular they have shown that;

1). Global deletion of IRS-2 in combination with either leptin production (*ob/ob*) or function (*db/db*) in mice, results in the development of growth retardation and severe diabetes at an earlier age than *Irs-2*$^{-/-}$ mice. Such additive effects and the finding that a single allele of leptin or leptin receptor gene function was sufficient to prevent this severe metabolic phenotype, highlight the importance of leptin function in the maintenance of insulin sensitivity.

2). Assessment of pancreatic β-cell function indicated that double knockout animals had an increased β-cell area compared to *Irs-2*$^{-/-}$ at four weeks of age. As both *ob/ob* and *db/db* mice display β-cell hyperplasia, it is proposed that leptin may have an inhibitory effect upon β-cell mass.

3). Generation of β-HypIRS2+STAT3KO mice demonstrated the importance of both IRS-2 and STAT-3 signalling pathways in β-cell and hypothalamic function. Furthermore these mice exhibited additive effects with regards to body weight and impairment of glucose homeostasis, compared to β-HypIRS2KO and β-HypSTAT3KO mice. This would indicate that IRS-2 and STAT-3 do not act within a linear pathway to mediate the effects of insulin and leptin on energy homeostasis. Instead it is proposed that these proteins mediate these effects in parallel pathways, potentially interacting with similar cytoplasmic enzymes or by initiating overlapping transcriptional programs (Fig 8.1).

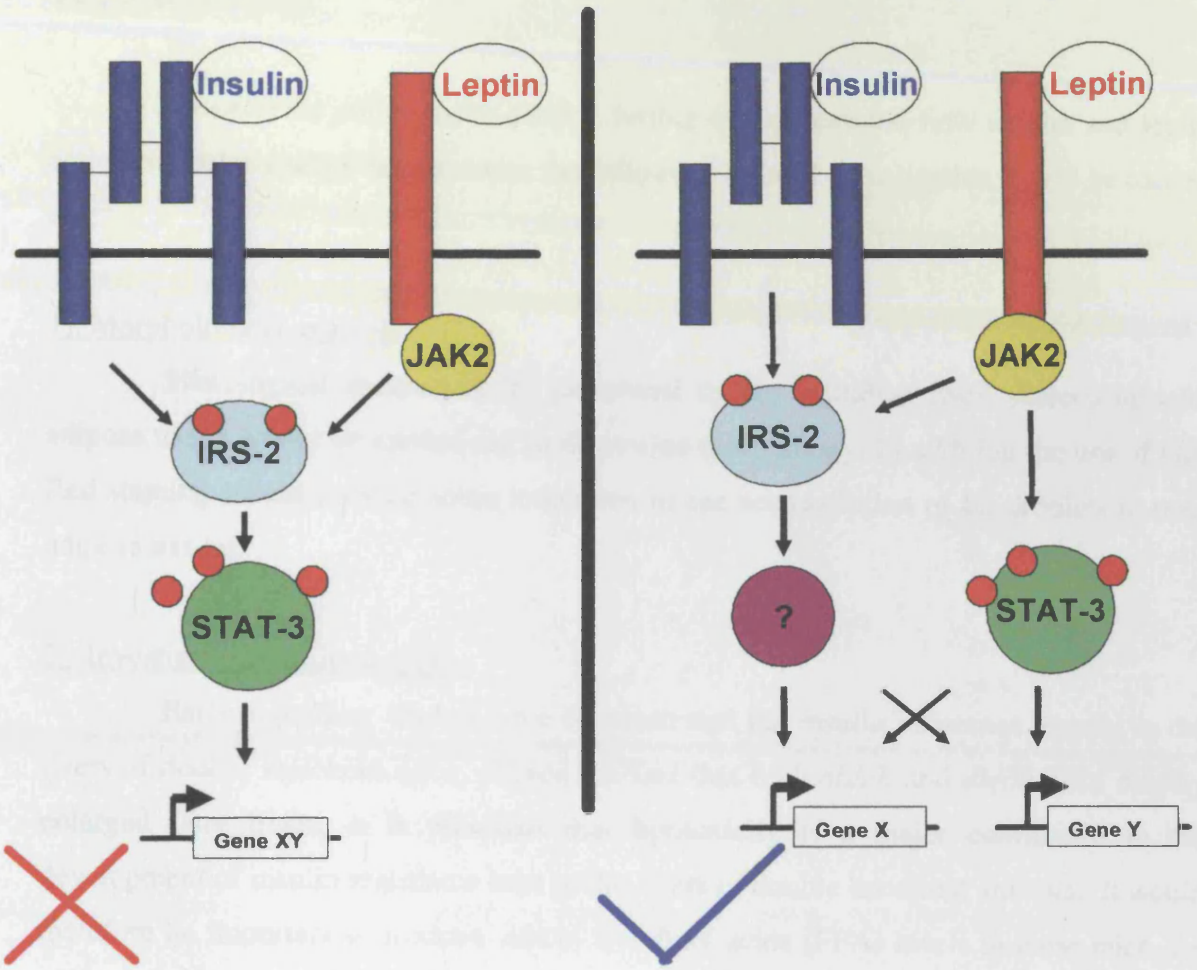

Figure 8.1 Schematic of how IRS-2 and STAT-3 potentially mediate the effects of insulin and leptin upon gene transcription

In view of the observations from both systemic and tissue-specific gene knockout studies, it is unlikely that IRS-2 acts upstream of STAT-3 to mediate the effects of insulin and leptin upon energy homeostasis. Instead, IRS-2 may regulate the activation of other proteins that interact with STAT-3 directly or activate a transcriptional program that has implication for STAT-3 activity. mediating the effects of insulin and leptin upon energy homeostasis

FUTURE WORK:

In order to utilise these models further and understand how insulin and leptin action regulates energy homeostasis, the following lines of investigation would be carried out;

1). Morphological analysis:

Histological analysis of the peripheral tissues including liver, skeletal muscle, adipose tissue would be carried out to determine morphology. In addition the use of Oil-Red staining would provide some indication of the accumulation of fat droplets in non-adipose tissues.

2). Investigation of Lipotoxicity:

Early signalling studies have demonstrated the insulin resistance present in the livers of double knockout mice. Given the fact that both *ob/ob* and *db/db* mice display enlarged fatty livers, it is plausible that lipotoxicity is a major contributor to the development of insulin resistance seen in the livers of double knockout animals. It would therefore be important to measure serum free fatty acids (FFA) levels in these mice. As discussed previously, the volumes of blood serum required for these assays were not obtainable from double knockout animals. However assessment of FFA levels in other genotypes resulting from the global intercrosses may provide some insight into relative gene dosage effects upon FFA metabolism.

3). Analysis of peripheral signal transduction:

Further analysis of insulin signalling pathways would be carried out in the offspring resulting from both global intercrosses. This would provide further insight into the differences in peripheral insulin resistance seen in the various insulin target tissues of these mice. It may also provide insight into the improved glucose homeostasis seen in *Irs-2*$^{-/-}$*db*$^{-/-}$ double knockout mice compared to *Irs-2*$^{-/-}$*ob*$^{-/-}$. It would also be interesting to analyse these signalling mechanisms in the tissue-specific knockouts, to address how peripheral insulin resistance is affected by deleting IRS-2 and STAT-3 specifically in the β-cell and hypothalamus.

4). Assessment of gene expression in hepatic and adipose tissue:

Quantification of mRNA species would be carried out by use of semiquantitative real-time PCR (TaqMan). In particular it would be interesting to measure the levels of expression of proteins involved in the regulation of fatty acid metabolism in the livers of these animals.

5). Studies in isolated islets:

In view of the dramatic impairment to islet function reported in β-HypIRS2KO and β-HypSTAT3KO mice and the fact that β-HypIRS2+STAT3KO mice had an increased relative islet area compared to these mice at eight weeks of age, it would be important to carry out islet function assays on these animals. For example isolated islets could be stimulated with glucose to assess glucose-stimulated insulin release. Interestingly, it has been shown that β-HypSTAT3KO mice exhibit a major loss of acute 1st phase insulin release (82). Indeed quantification of mRNA levels in isolated islets from β-HypSTAT3KO mice, showed VEGF-1, GLUT-2 and SUR-1 expression to be significantly lower compared to control islets (82). Assessment of these RNA species in β-HypIRS2+STAT3KO mice may prove useful insight into the relative contribution of IRS-2 and STAT-3 to their expression.

6). Role of AMP-Activated Protein Kinase (AMPK):

AMPK is an important mediator of leptin's effects upon energy homeostasis and appetite control, highlighting it as a potential convergence point for insulin and leptin action (117, 182, 183). It would therefore be interesting to assess the activity of AMPK in the various peripheral tissues in these genotypes.

7). Overcoming developmental defects:

Since the undertaking of this project, developmental defects have been reported in the CNS of *ob/ob*, *db/db* and *Irs-2* null mice (145, 175-177). Axonal labelling of ARC axons with the anterograde tracer DiI revealed that ARC projection pathways are severely reduced in *ob/ob* and *db/db* mice (Fig 8.2) and that leptin deficiency (*ob/ob*) or leptin resistance (*db/db*) causes a significant delay in the formation of projections from the ARC to each major target nucleus (176). Indeed that all three of these mouse mutants exhibit reduced brain weight and morphological defects, supports this notion (84, 145,

187-191). Hence, the combination of such defects as would be presented in the systemic double knockout mice, presumably contributes significantly to the observed dramatic phenotype of growth retardation and marked type 2 diabetes. Histological assessment of hypothalamus obtained from wild-type, *ob/ob*, *Irs-2*$^{-/-}$ and double knockout animals by *in situ* hybridisation or Immunocytochemistry, would provide some insight into any morphological defects present in the double knockout mice.

Further investigation of the roles of IRS-2 and STAT-3 could be achieved by more sophisticated conditional deletion. In particular the development transgenic murine models capable of mediating post-natal, deletion of genes, has already been reported (192, 193). In addition more restricted deletion of either IRS-2 and STAT-3 in POMC and AgRP neurons may not be associated with developmental abnormalities. Applying such transgenic systems to both the IRS2lox and STAT-3lox mice would facilitate the deletion of these genes following the normal development of the CNS. This would provide a more defined understanding of the relative contributions of these genes to the central actions of both insulin and leptin.

APPENDIX I.

ABBREVIATIONS

AgRP	Agouti-related protein
AMPK	AMP-activated protein kinase
AMP	Adenosine monophosphate
ARC	Arcuate nucleus
ATP	Adenosine triphosphate
CART	Cocaine-amphetamine-regulated transcript
CDK4	Cyclin-dependent kinase 4
CDK6	Cyclin-dependent kinase 6
CNS	Central nervous system
db	Diabetes gene
DMH	Dorsomedial hypothalamus
DMV	Dorso-motor nucleus of the vagus
DTT	Dithiothreitol
ELISA	Enzyme-linked immunoabsorbance assay
FA	Fatty acid
FFAs	Free Fatty Acids
FIRKO mice	Fat insulin receptor knockout mice
GLUT-4	glucose transporter protein-4
Grb2	Growth factor receptor-bound protein-2
GSK-3	Glycogen synthase kinase-3
GST	Glutathione
Hyp	Hypothalamus
I.U.	International units
Igf-1	Insulin growth factor-1
Igf-1r	Insulin growth factor-1 receptor
IR	Insulin receptor
IRS-1	Insulin receptor substrate-1
IRS-2	Insulin receptor substrate-2
IRS-3	Insulin receptor substrate-3
IRS-4	Insulin receptor substrate-4

JAK2	Janus-kinase 2
K+	Potassium+
KO	Knockout
LHA	Lateral hypothalamus
LIRKO mice	Liver insulin receptor knockout mice
MAPK	Mitogen-activated protein kinase
MIRKO mice	Muscle insulin receptor knockout mice
NPY	Neuropeptide Y
NTS	Nucleus of the solitary tract
ob	Obese gene
ObRb	Leptin long-form receptor
p70s6k	p70 ribosomal s6 protein kinase
PCR	Polymerase chain reaction
PDK-1	Phosphoinositide-dependent kinase-1
PH-domain	Pleckstrin-homology domain
PI 3-K	Phosphoinositol 3-kinase
PIP3	Phosphatidylinositol 3,4,5-tris-phosphate
PKB	Protein kinase B
POMC	Proopiomelanocortin
PVN	Paraventricular nucleus
Rb	Retinoblastoma protein
RIP	Rat insulin II promoter
Ser	Serine
SH2-domain	Src-homology 2 domain
SOCS	Suppressor of cytokine signalling
SOS	Son of sevenless
SREBP-1c	Sterol regulatory element binding protein
STAT-3	Signal transducer and activators of transcription 3
TAG	Triacylglycerides
Thr	Threonine
T2DM	Type 2 diabetes
Tyr	Tyrosine
VMH	Ventromedial hypothalamus
WAT	White adipose tissue
WT	Wild-type

APPENDIX II.

Genotyping primers for global deletions.

Irs-2 genotyping

Irs-2 upper	ctt ggc tac cat gtt gtt att gtc
Irs-2 lower	agc tct gga ggt tta ctt tcc tag
Irs-2 neo	gct acc cgt gat att gct gaa gag

ob genotyping

APC-Fow	ccg gag taa gca gag aca caa gc
APC-Rev	cca ata cct cgc tct ctc tcc a
OB-Fow	ttg gac ttc att cct ggg ctt c
OB-WT	cag cag atg gag gag gtc tcg
OB-MUT	cag cag atg gag gag gtc tca

db genotyping

db-F	atg acc act aca gat gaa ccc agt cta
db-R	cat tca aac cat agt tta ggt ttg tct

Genotyping primers for tissue-specific deletions.

RIP-Cre genotyping

CRE 1084	gcg gtc tgg cag taa aaa cta tc
CRE 1085	gtg aaa cag cat tgc tgt cac tt
IL2F	cta ggc cac aga att gaa aga tct
IL2R	gta ggt gga aat tct agc atc atc c

STAT3lox genotyping

APRF-11 UP	cac caa cac atg cta ttt gta gg
APRF-11 DOWN	cct gtc tct gac agg cca tc
APRF-14 DOWN	gca gca gaa tac tct aca gct c

IRS2lox genotyping

LoxPF	act tga agg aag cca cag tcg
LoxPR	agt cca ctt tcc tga caa gc

APPENDIX III.

SUPPLIERS

SUPPLIER	ADDRESS
AB-gene	Epsom, Surrey KT19 9AP, UK
Amersham Pharmacia	Little Chalfont, Buckinghamshire, UK
Anachem	Luton, Bedfordshire LU2 0EB, UK.
Bayer Diagnostics	Bury St. Edmunds, UK
BD Biosciences:Pharmingen	San Diego, CA 92121, USA
BDH	Poole, Dorset, UK
Becton Dickinson	NJ, 07417, USA
CAMLAB	Cambridge, CB4 5WE, UK
Fisher Scientific UK	Loughborough, Leicestershire, UK
Guilbert	Andover, UK
ICN Pharmaceuticals	Thame, Oxfordshire, UK
Immuno-diagnostic systems Ltd	Tyne and Wear, NE35 9PD, UK.
Insight Direct Ltd	Sheffield, S9 2BU England
Invitrogen	Paisley, PA4 9RF, UK
Jencons	Bedfordshire, LU7 4UA, UK
Merck Biosciences	Lutterworth, Leicestershire, UK
New England Biolabs (UK) Ltd	Hitchin, Hertfordshire, UK
Promega	Southampton, UK
Qiagen	Crawley, West Sussex, UK
Roche Diagnostics	East Sussex, BN7 1LG, UK
Santa Cruz	Santa Cruz, California 95060, U.S.A.
Scientific Lab Supplies	Nottingham NG11 7EP, UK
Sigma-aldrich company Ltd	Poole, Dorset, UK
Stratagene Ltd	La Jolla, CA, USA
ThermoLife Sciences	Basingstoke, Hampshire, RG21 6YH

SUPPLIER	ADDRESS
VWR International	East Sussex BN7 1LG, United Kingdom
Eppendorf	Hamburg, Germany
Gibco BRL (LifeTechnologies Ltd)	Paisley, UK
CrystalChem Inc	suite A, Downers grove, IL 60515 USA
Millipore	Watford, UK
National Diagnostics	Aylesbury, Buckinghamshire, UK
GraphPad Software Inc	San Diego, USA
Helena Biosciences	Sunderland, Tyne and Wear, UK
Sartorius Instrument Ltd	Gottingen, Germany
Upstate Ltd	Milton Keynes, UK

REFERENCES

1. **Kopelman PG** 2000 Obesity as a medical problem. Nature 404:635-43
2. **Peeters A, Barendregt JJ, Willekens F, Mackenbach JP, Al Mamun A, Bonneux L** 2003 Obesity in adulthood and its consequences for life expectancy: a life-table analysis. Ann Intern Med 138:24-32
3. **Pinhas-Hamiel O, Dolan LM, Daniels SR, Standiford D, Khoury PR, Zeitler P** 1996 Increased incidence of non-insulin-dependent diabetes mellitus among adolescents. J Pediatr 128:608-15
4. **Bundred P, Kitchiner D, Buchan I** 2001 Prevalence of overweight and obese children between 1989 and 1998: population based series of cross sectional studies. Bmj 322:326-8
5. **DeFronzo RA** 2004 Pathogenesis of type 2 diabetes mellitus. Med Clin North Am 88:787-835, ix
6. **Bonner-Weir S** 2001 beta-cell turnover: its assessment and implications. Diabetes 50 Suppl 1:S20-4
7. **Butler AA, Cone RD** 2001 Knockout models resulting in the development of obesity. Trends Genet 17:S50-4
8. **Kahn BB, Flier JS** 2000 Obesity and insulin resistance. J Clin Invest 106:473-81
9. **Kahn BB** 1998 Type 2 diabetes: when insulin secretion fails to compensate for insulin resistance. Cell 92:593-6
10. **Beck-Nielsen H, Vaag A, Poulsen P, Gaster M** 2003 Metabolic and genetic influence on glucose metabolism in type 2 diabetic subjects--experiences from relatives and twin studies. Best Pract Res Clin Endocrinol Metab 17:445-67
11. **Friedman J** 2002 Fat in all the wrong places. Nature 415:268-9
12. **Unger RH** 2004 The hyperleptinemia of obesity-regulator of caloric surpluses. Cell 117:145-6
13. **Zraika S, Dunlop M, Proietto J, Andrikopoulos S** 2002 Effects of free fatty acids on insulin secretion in obesity. Obes Rev 3:103-12
14. **Shimomura I, Matsuda M, Hammer RE, Bashmakov Y, Brown MS, Goldstein JL** 2000 Decreased IRS-2 and increased SREBP-1c lead to mixed

insulin resistance and sensitivity in livers of lipodystrophic and ob/ob mice. Mol Cell 6:77-86

15. **Obici S, Feng Z, Karkanias G, Baskin DG, Rossetti L** 2002 Decreasing hypothalamic insulin receptors causes hyperphagia and insulin resistance in rats. Nat Neurosci 5:566-72

16. **Porte D, Jr., Baskin DG, Schwartz MW** 2002 Leptin and insulin action in the central nervous system. Nutr Rev 60:S20-9; discussion S68-84, 85-7

17. **Kennedy GCT** 1953. he role of depot fat in the hypothalamic control of food intake in the rat. Proc. R. Soc. Lond. B 140,:579-592

18. **Hetherington AWaRSW** 1983 Nutrition Classics. The Anatomical Record, Volume 78, 1940: Hypothalamic lesions and adiposity in the rat. Nutr Rev 41:124-7

19. **Schwartz MW, Woods SC, Porte D, Jr., Seeley RJ, Baskin DG** 2000 Central nervous system control of food intake. Nature 404:661-71

20. **Woods SC, Lotter EC, McKay LD, Porte D, Jr.** 1979 Chronic intracerebroventricular infusion of insulin reduces food intake and body weight of baboons. Nature 282:503-5

21. **Zhang Y, Proenca R, Maffei M, Barone M, Leopold L, Friedman JM** 1994 Positional cloning of the mouse obese gene and its human homologue. Nature 372:425-32

22. **Frederich RC, Hamann A, Anderson S, Lollmann B, Lowell BB, Flier JS** 1995 Leptin levels reflect body lipid content in mice: evidence for diet-induced resistance to leptin action. Nat Med 1:1311-4

23. **Ahima RS, Prabakaran D, Mantzoros C, et al.** 1996 Role of leptin in the neuroendocrine response to fasting. Nature 382:250-2

24. **Farooqi IS, Jebb SA, Langmack G, et al.** 1999 Effects of recombinant leptin therapy in a child with congenital leptin deficiency. N Engl J Med 341:879-84

25. **Barash IA, Cheung CC, Weigle DS, et al.** 1996 Leptin is a metabolic signal to the reproductive system. Endocrinology 137:3144-7

26. **Kaji H, Tai S, Okimura Y, et al.** 1998 Cloning and characterization of the 5'-flanking region of the human growth hormone secretagogue receptor gene. J Biol Chem 273:33885-8

27. **Mizuno TM, Makimura H, Silverstein J, Roberts JL, Lopingco T, Mobbs CV** 1999 Fasting regulates hypothalamic neuropeptide Y, agouti-related peptide, and proopiomelanocortin in diabetic mice independent of changes in leptin or insulin. Endocrinology 140:4551-7

28. **Mizuno TM, Mobbs CV** 1999 Hypothalamic agouti-related protein messenger ribonucleic acid is inhibited by leptin and stimulated by fasting. Endocrinology 140:814-7

29. **Cowley MA, Smart JL, Rubinstein M, et al.** 2001 Leptin activates anorexigenic POMC neurons through a neural network in the arcuate nucleus. Nature 411:480-4

30. **Unger JW, Betz M** 1998 Insulin receptors and signal transduction proteins in the hypothalamo-hypophyseal system: a review on morphological findings and functional implications. Histol Histopathol 13:1215-24

31. **Bruning JC, Gautam D, Burks DJ, et al.** 2000 Role of brain insulin receptor in control of body weight and reproduction. Science 289:2122-5

32. **Air EL, Benoit SC, Clegg DJ, Seeley RJ, Woods SC** 2002 Insulin and leptin combine additively to reduce food intake and body weight in rats. Endocrinology 143:2449-52

33. **Liu L, Karkanias GB, Morales JC, et al.** 1998 Intracerebroventricular leptin regulates hepatic but not peripheral glucose fluxes. J Biol Chem 273:31160-7

34. **Minokoshi Y, Kim YB, Peroni OD, et al.** 2002 Leptin stimulates fatty-acid oxidation by activating AMP-activated protein kinase. Nature 415:339-43

35. **Hardie DG** 2004 The AMP-activated protein kinase pathway - new players upstream and downstream. J Cell Sci 117:5479-87

36. **Myers MG, Jr., White MF** 1996 Insulin signal transduction and the IRS proteins. Annu Rev Pharmacol Toxicol 36:615-58

37. **Holman GD, Kasuga M** 1997 From receptor to transporter: insulin signalling to glucose transport. Diabetologia 40:991-1003

38. **Withers DJ** 2001 Insulin receptor substrate proteins and neuroendocrine function. Biochem Soc Trans 29:525-9

39. **Araki E, Lipes MA, Patti ME, et al.** 1994 Alternative pathway of insulin signalling in mice with targeted disruption of the IRS-1 gene. Nature 372:186-90

40. **Terauchi Y, Tsuji Y, Satoh S, et al.** 1999 Increased insulin sensitivity and hypoglycaemia in mice lacking the p85 alpha subunit of phosphoinositide 3-kinase. Nat Genet 21:230-5

41. **Vanhaesebroeck B, Alessi DR** 2000 The PI3K-PDK1 connection: more than just a road to PKB. Biochem J 346 Pt 3:561-76

42. **Casamayor A, Morrice NA, Alessi DR** 1999 Phosphorylation of Ser-241 is essential for the activity of 3-phosphoinositide-dependent protein kinase-1: identification of five sites of phosphorylation in vivo. Biochem J 342 (Pt 2):287-92

43. **Lawlor MA, Mora A, Ashby PR, et al.** 2002 Essential role of PDK1 in regulating cell size and development in mice. Embo J 21:3728-38

44. **Kohn AD, Summers SA, Birnbaum MJ, Roth RA** 1996 Expression of a constitutively active Akt Ser/Thr kinase in 3T3-L1 adipocytes stimulates glucose uptake and glucose transporter 4 translocation. J Biol Chem 271:31372-8

45. **Datta SR, Brunet A, Greenberg ME** 1999 Cellular survival: a play in three Akts. Genes Dev 13:2905-27

46. **Shepherd PR, Withers DJ, Siddle K** 1998 Phosphoinositide 3-kinase: the key switch mechanism in insulin signalling. Biochem J 333 (Pt 3):471-90

47. **Welsh GI, Foulstone EJ, Young SW, Tavare JM, Proud CG** 1994 Wortmannin inhibits the effects of insulin and serum on the activities of glycogen synthase kinase-3 and mitogen-activated protein kinase. Biochem J 303 (Pt 1):15-20

48. **Cross DA, Alessi DR, Vandenheede JR, McDowell HE, Hundal HS, Cohen P** 1994 The inhibition of glycogen synthase kinase-3 by insulin or insulin-like growth factor 1 in the rat skeletal muscle cell line L6 is blocked by wortmannin, but not by rapamycin: evidence that wortmannin blocks activation of the mitogen-activated protein kinase pathway in L6 cells between Ras and Raf. Biochem J 303 (Pt 1):21-6

49. **Hurel SJ, Rochford JJ, Borthwick AC, et al.** 1996 Insulin action in cultured human myoblasts: contribution of different signalling pathways to regulation of glycogen synthesis. Biochem J 320 (Pt 3):871-7

50. **Berwick DC, Dell GC, Welsh GI, et al.** 2004 Protein kinase B phosphorylation of PIKfyve regulates the trafficking of GLUT4 vesicles. J Cell Sci 117:5985-93

51. **Garami A, Zwartkruis FJ, Nobukuni T, et al.** 2003 Insulin activation of Rheb, a mediator of mTOR/S6K/4E-BP signaling, is inhibited by TSC1 and 2. Mol Cell 11:1457-66

52. **Toker A** 2000 Protein kinases as mediators of phosphoinositide 3-kinase signaling. Mol Pharmacol 57:652-8

53. **Dufner A, Thomas G** 1999 Ribosomal S6 kinase signaling and the control of translation. Exp Cell Res 253:100-9

54. **Tartaglia LA, Dembski M, Weng X, et al.** 1995 Identification and expression cloning of a leptin receptor, OB-R. Cell 83:1263-71

55. **Ghilardi N, Ziegler S, Wiestner A, Stoffel R, Heim MH, Skoda RC** 1996 Defective STAT signaling by the leptin receptor in diabetic mice. Proc Natl Acad Sci U S A 93:6231-5

56. **Fukuda H, Iritani N, Sugimoto T, Ikeda H** 1999 Transcriptional regulation of fatty acid synthase gene by insulin/glucose, polyunsaturated fatty acid and leptin in hepatocytes and adipocytes in normal and genetically obese rats. Eur J Biochem 260:505-11

57. **Bjorbaek C, Uotani S, da Silva B, Flier JS** 1997 Divergent signaling capacities of the long and short isoforms of the leptin receptor. J Biol Chem 272:32686-95

58. **Murakami T, Yamashita T, Iida M, Kuwajima M, Shima K** 1997 A short form of leptin receptor performs signal transduction. Biochem Biophys Res Commun 231:26-9

59. **Banks AS, Davis SM, Bates SH, Myers MG, Jr.** 2000 Activation of downstream signals by the long form of the leptin receptor. J Biol Chem 275:14563-72

60. **White DW, Kuropatwinski KK, Devos R, Baumann H, Tartaglia LA** 1997 Leptin receptor (OB-R) signaling. Cytoplasmic domain mutational analysis and evidence for receptor homo-oligomerization. J Biol Chem 272:4065-71

61. **Tartaglia LA** 1997 The leptin receptor. J Biol Chem 272:6093-6

62. **Baumann H, Morella KK, White DW, et al.** 1996 The full-length leptin receptor has signaling capabilities of interleukin 6-type cytokine receptors. Proc Natl Acad Sci U S A 93:8374-8

63. **Bates SH, Stearns WH, Dundon TA, et al.** 2003 STAT3 signalling is required for leptin regulation of energy balance but not reproduction. Nature 421:856-9

64. **Inoue H, Ogawa W, Ozaki M, et al.** 2004 Role of STAT-3 in regulation of hepatic gluconeogenic genes and carbohydrate metabolism in vivo. Nat Med 10:168-74

65. **Huang L, Wang Z, Li C** 2001 Modulation of circulating leptin levels by its soluble receptor. J Biol Chem 276:6343-9

66. **Brabant G, Horn R, von zur Muhlen A, et al.** 2000 Free and protein bound leptin are distinct and independently controlled factors in energy regulation. Diabetologia 43:438-42

67. **Fei H, Okano HJ, Li C, et al.** 1997 Anatomic localization of alternatively spliced leptin receptors (Ob-R) in mouse brain and other tissues. Proc Natl Acad Sci U S A 94:7001-5

68. **Morton NM, Emilsson V, Liu YL, Cawthorne MA** 1998 Leptin action in intestinal cells. J Biol Chem 273:26194-201

69. **Siegrist-Kaiser CA, Pauli V, Juge-Aubry CE, et al.** 1997 Direct effects of leptin on brown and white adipose tissue. J Clin Invest 100:2858-64

70. **Leclercq-Meyer V, Considine RV, Sener A, Malaisse WJ** 1996 Do leptin receptors play a functional role in the endocrine pancreas? Biochem Biophys Res Commun 229:794-8

71. **Sweeney G** 2002 Leptin signalling. Cell Signal 14:655-63

72. **Kellerer M, Koch M, Metzinger E, Mushack J, Capp E, Haring HU** 1997 Leptin activates PI-3 kinase in C2C12 myotubes via janus kinase-2 (JAK-2) and insulin receptor substrate-2 (IRS-2) dependent pathways. Diabetologia 40:1358-62

73. **Cohen B, Novick D, Rubinstein M** 1996 Modulation of insulin activities by leptin. Science 274:1185-8

74. **Harvey J, McKay NG, Walker KS, Van der Kaay J, Downes CP, Ashford ML** 2000 Essential role of phosphoinositide 3-kinase in leptin-induced K(ATP) channel activation in the rat CRI-G1 insulinoma cell line. J Biol Chem 275:4660-9

75. **Szanto I, Kahn CR** 2000 Selective interaction between leptin and insulin signaling pathways in a hepatic cell line. Proc Natl Acad Sci U S A 97:2355-60

76. **Nandi A, Kitamura Y, Kahn CR, Accili D** 2004 Mouse models of insulin resistance. Physiol Rev 84:623-47

77. **Coleman DL** 1978 Obese and diabetes: two mutant genes causing diabetes-obesity syndromes in mice. Diabetologia 14:141-8

78. **Friedman JM, Leibel RL** 1992 Tackling a weighty problem. Cell 69:217-20

79. **Chen H, Charlat O, Tartaglia LA, et al.** 1996 Evidence that the diabetes gene encodes the leptin receptor: identification of a mutation in the leptin receptor gene in db/db mice. Cell 84:491-5

80. **Balthasar N, Coppari R, McMinn J, et al.** 2004 Leptin receptor signaling in POMC neurons is required for normal body weight homeostasis. Neuron 42:983-91

81. **Cui Y, Huang L, Elefteriou F, et al.** 2004 Essential role of STAT3 in body weight and glucose homeostasis. Mol Cell Biol 24:258-69

82. **Gorogawa S, Fujitani Y, Kaneto H, et al.** 2004 Insulin secretory defects and impaired islet architecture in pancreatic beta-cell-specific STAT3 knockout mice. Biochem Biophys Res Commun 319:1159-70

83. **Withers DJ, Gutierrez JS, Towery H, et al.** 1998 Disruption of IRS-2 causes type 2 diabetes in mice. Nature 391:900-4

84. **Burks DJ, de Mora JF, Schubert M, et al.** 2000 IRS-2 pathways integrate female reproduction and energy homeostasis. Nature 407:377-82

85. **Kulkarni RN, Bruning JC, Winnay JN, Postic C, Magnuson MA, Kahn CR** 1999 Tissue-specific knockout of the insulin receptor in pancreatic beta cells creates an insulin secretory defect similar to that in type 2 diabetes. Cell 96:329-39

86. **Postic C, Shiota M, Niswender KD, et al.** 1999 Dual roles for glucokinase in glucose homeostasis as determined by liver and pancreatic beta cell-specific gene knock-outs using Cre recombinase. J Biol Chem 274:305-15

87. **Choudhury** 2005 Essential role of IRS2 in the beta cell and hypothalamus for glucose and energy homeostasis. Journal of Clinical Investigation

88. **Kubota N, Terauchi Y, Tobe K, et al.** 2004 Insulin receptor substrate 2 plays a crucial role in beta cells and the hypothalamus. J Clin Invest 114:917-27

89. **Lin X, Taguchi A, Park S, et al.** 2004 Dysregulation of insulin receptor substrate 2 in beta cells and brain causes obesity and diabetes. J Clin Invest 114:908-16

90. **Pallett AL, Morton NM, Cawthorne MA, Emilsson V** 1997 Leptin inhibits insulin secretion and reduces insulin mRNA levels in rat isolated pancreatic islets. Biochem Biophys Res Commun 238:267-70

91. **Islam MS, Morton NM, Hansson A, Emilsson V** 1997 Rat insulinoma-derived pancreatic beta-cells express a functional leptin receptor that mediates a proliferative response. Biochem Biophys Res Commun 238:851-5

92. **Withers DJ, Burks DJ, Towery HH, Altamuro SL, Flint CL, White MF** 1999 Irs-2 coordinates Igf-1 receptor-mediated beta-cell development and peripheral insulin signalling. Nat Genet 23:32-40

93. **Shimabukuro M, Koyama K, Chen G, et al.** 1997 Direct antidiabetic effect of leptin through triglyceride depletion of tissues. Proc Natl Acad Sci U S A 94:4637-41

94. **Unger RH, Zhou YT, Orci L** 1999 Regulation of fatty acid homeostasis in cells: novel role of leptin. Proc Natl Acad Sci U S A 96:2327-32

95. **Muoio DM, Dohm GL, Fiedorek FT, Jr., Tapscott EB, Coleman RA, Dohn GL** 1997 Leptin directly alters lipid partitioning in skeletal muscle. Diabetes 46:1360-3

96. **Muoio DM, Dohm GL, Tapscott EB, Coleman RA** 1999 Leptin opposes insulin's effects on fatty acid partitioning in muscles isolated from obese ob/ob mice. Am J Physiol 276:E913-21

97. **Ferrannini E, Galvan AQ, Gastaldelli A, et al.** 1999 Insulin: new roles for an ancient hormone. Eur J Clin Invest 29:842-52

98. **Cline GW, Petersen KF, Krssak M, et al.** 1999 Impaired glucose transport as a cause of decreased insulin-stimulated muscle glycogen synthesis in type 2 diabetes. N Engl J Med 341:240-6

99. **Bruning JC, Michael MD, Winnay JN, et al.** 1998 A muscle-specific insulin receptor knockout exhibits features of the metabolic syndrome of NIDDM without altering glucose tolerance. Mol Cell 2:559-69

100. **Shefi-Friedman L, Wertheimer E, Shen S, Bak A, Accili D, Sampson SR** 2001 Increased IGFR activity and glucose transport in cultured skeletal muscle from insulin receptor null mice. Am J Physiol Endocrinol Metab 281:E16-24

101. **Wojtaszewski JF, Higaki Y, Hirshman MF, et al.** 1999 Exercise modulates postreceptor insulin signaling and glucose transport in muscle-specific insulin receptor knockout mice. J Clin Invest 104:1257-64

102. **Ahima RS, Flier JS** 2000 Adipose tissue as an endocrine organ. Trends Endocrinol Metab 11:327-32

103. **Shimomura I, Hammer RE, Richardson JA, et al.** 1998 Insulin resistance and diabetes mellitus in transgenic mice expressing nuclear SREBP-1c in adipose tissue: model for congenital generalized lipodystrophy. Genes Dev 12:3182-94

104. **Moitra J, Mason MM, Olive M, et al.** 1998 Life without white fat: a transgenic mouse. Genes Dev 12:3168-81

105. **Brown MS, Goldstein JL** 1997 The SREBP pathway: regulation of cholesterol metabolism by proteolysis of a membrane-bound transcription factor. Cell 89:331-40

106. **Shimomura I, Hammer RE, Ikemoto S, Brown MS, Goldstein JL** 1999 Leptin reverses insulin resistance and diabetes mellitus in mice with congenital lipodystrophy. Nature 401:73-6

107. **Hu E, Liang P, Spiegelman BM** 1996 AdipoQ is a novel adipose-specific gene dysregulated in obesity. J Biol Chem 271:10697-703

108. **Arita Y, Kihara S, Ouchi N, et al.** 1999 Paradoxical decrease of an adipose-specific protein, adiponectin, in obesity. Biochem Biophys Res Commun 257:79-83

109. **Yamauchi T, Kamon J, Waki H, et al.** 2001 The fat-derived hormone adiponectin reverses insulin resistance associated with both lipoatrophy and obesity. Nat Med 7:941-6

110. **Marin P, Andersson B, Ottosson M, et al.** 1992 The morphology and metabolism of intraabdominal adipose tissue in men. Metabolism 41:1242-8

111. **Golay A, Defronzo RA, Thorin D, Jequier E, Felber JP** 1988 Glucose disposal in obese non-diabetic and diabetic type II patients. A study by indirect calorimetry and euglycemic insulin clamp. Diabete Metab 14:443-51

112. **Rosen ED, Spiegelman BM** 2000 Peroxisome proliferator-activated receptor gamma ligands and atherosclerosis: ending the heartache. J Clin Invest 106:629-31

113. **Seufert J** 2004 Leptin effects on pancreatic beta-cell gene expression and function. Diabetes 53 Suppl 1:S152-8

114. **Bluher M, Michael MD, Peroni OD, et al.** 2002 Adipose tissue selective insulin receptor knockout protects against obesity and obesity-related glucose intolerance. Dev Cell 3:25-38

115. **Laustsen PG, Michael MD, Crute BE, et al.** 2002 Lipoatrophic diabetes in Irs1(-/-)/Irs3(-/-) double knockout mice. Genes Dev 16:3213-22

116. **Valverde AM, Burks DJ, Fabregat I, et al.** 2003 Molecular mechanisms of insulin resistance in IRS-2-deficient hepatocytes. Diabetes 52:2239-48

117. **Halse R, Fryer LG, McCormack JG, Carling D, Yeaman SJ** 2003 Regulation of glycogen synthase by glucose and glycogen: a possible role for AMP-activated protein kinase. Diabetes 52:9-15

118. **Michael MD, Kulkarni RN, Postic C, et al.** 2000 Loss of insulin signaling in hepatocytes leads to severe insulin resistance and progressive hepatic dysfunction. Mol Cell 6:87-97

119. **Kerouz NJ, Horsch D, Pons S, Kahn CR** 1997 Differential regulation of insulin receptor substrates-1 and -2 (IRS-1 and IRS-2) and phosphatidylinositol 3-kinase isoforms in liver and muscle of the obese diabetic (ob/ob) mouse. J Clin Invest 100:3164-72

120. **Ide T, Shimano H, Yahagi N, et al.** 2004 SREBPs suppress IRS-2-mediated insulin signalling in the liver. Nat Cell Biol 6:351-7

121. **Tobe K, Suzuki R, Aoyama M, et al.** 2001 Increased expression of the sterol regulatory element-binding protein-1 gene in insulin receptor substrate-2(-/-) mouse liver. J Biol Chem 276:38337-40

122. **Farooqi IS, Keogh JM, Kamath S, et al.** 2001 Partial leptin deficiency and human adiposity. Nature 414:34-5

123. **Farooqi IS, Matarese G, Lord GM, et al.** 2002 Beneficial effects of leptin on obesity, T cell hyporesponsiveness, and neuroendocrine/metabolic dysfunction of human congenital leptin deficiency. J Clin Invest 110:1093-103

124. **Sindelar DK, Havel PJ, Seeley RJ, Wilkinson CW, Woods SC, Schwartz MW** 1999 Low plasma leptin levels contribute to diabetic hyperphagia in rats. Diabetes 48:1275-80

125. **Emilsson V, Liu YL, Cawthorne MA, Morton NM, Davenport M** 1997 Expression of the functional leptin receptor mRNA in pancreatic islets and direct inhibitory action of leptin on insulin secretion. Diabetes 46:313-6

126. **Rosenbaum M, Murphy EM, Heymsfield SB, Matthews DE, Leibel RL** 2002 Low dose leptin administration reverses effects of sustained weight-reduction on energy expenditure and circulating concentrations of thyroid hormones. J Clin Endocrinol Metab 87:2391-4

127. **Kulkarni RN, Wang ZL, Wang RM, et al.** 1997 Leptin rapidly suppresses insulin release from insulinoma cells, rat and human islets and, in vivo, in mice. J Clin Invest 100:2729-36

128. **Smith SJ, Cases S, Jensen DR, et al.** 2000 Obesity resistance and multiple mechanisms of triglyceride synthesis in mice lacking Dgat. Nat Genet 25:87-90

129. **Chen HC, Smith SJ, Ladha Z, et al.** 2002 Increased insulin and leptin sensitivity in mice lacking acyl CoA:diacylglycerol acyltransferase 1. J Clin Invest 109:1049-55

130. **Zhao AZ, Shinohara MM, Huang D, et al.** 2000 Leptin induces insulin-like signaling that antagonizes cAMP elevation by glucagon in hepatocytes. J Biol Chem 275:11348-54

131. **Spanswick D, Smith MA, Mirshamsi S, Routh VH, Ashford ML** 2000 Insulin activates ATP-sensitive K+ channels in hypothalamic neurons of lean, but not obese rats. Nat Neurosci 3:757-8

132. **Niswender KD, Morton GJ, Stearns WH, Rhodes CJ, Myers MG, Jr., Schwartz MW** 2001 Intracellular signalling. Key enzyme in leptin-induced anorexia. Nature 413:794-5

133. **Yamauchi T, Kamon J, Minokoshi Y, et al.** 2002 Adiponectin stimulates glucose utilization and fatty-acid oxidation by activating AMP-activated protein kinase. Nat Med 8:1288-95

134. **Bjorbaek C, Kahn BB** 2004 Leptin signaling in the central nervous system and the periphery. Recent Prog Horm Res 59:305-31

135. **Bjorbaek C, Elmquist JK, Frantz JD, Shoelson SE, Flier JS** 1998 Identification of SOCS-3 as a potential mediator of central leptin resistance. Mol Cell 1:619-25

136. **Yasukawa H, Misawa H, Sakamoto H, et al.** 1999 The JAK-binding protein JAB inhibits Janus tyrosine kinase activity through binding in the activation loop. Embo J 18:1309-20

137. **Eyckerman S, Broekaert D, Verhee A, Vandekerckhove J, Tavernier J** 2000 Identification of the Y985 and Y1077 motifs as SOCS3 recruitment sites in the murine leptin receptor. FEBS Lett 486:33-7

138. **Mori H, Hanada R, Hanada T, et al.** 2004 Socs3 deficiency in the brain elevates leptin sensitivity and confers resistance to diet-induced obesity. Nat Med 10:739-43

139. **Shi H, Tzameli I, Bjorbaek C, Flier JS** 2004 Suppressor of cytokine signaling 3 is a physiological regulator of adipocyte insulin signaling. J Biol Chem 279:34733-40

140. **Rahmouni K, Haynes WG, Morgan DA, Mark AL** 2003 Intracellular mechanisms involved in leptin regulation of sympathetic outflow. Hypertension 41:763-7

141. **Myers MG, Jr.** 2004 Leptin receptor signaling and the regulation of mammalian physiology. Recent Prog Horm Res 59:287-304

142. **Bradford MM** 1976 A rapid and sensitive method for the quantitation of microgram quantities of protein utilizing the principle of protein-dye binding. Anal Biochem 72:248-54

143. **Halaas JL, Gajiwala KS, Maffei M, et al.** 1995 Weight-reducing effects of the plasma protein encoded by the obese gene. Science 269:543-6

144. **Hamrick MW** 2004 Leptin, bone mass, and the thrifty phenotype. J Bone Miner Res 19:1607-11

145. **Schubert M, Brazil DP, Burks DJ, et al.** 2003 Insulin receptor substrate-2 deficiency impairs brain growth and promotes tau phosphorylation. J Neurosci 23:7084-92

146. **Miki H, Yamauchi T, Suzuki R, et al.** 2001 Essential role of insulin receptor substrate 1 (IRS-1) and IRS-2 in adipocyte differentiation. Mol Cell Biol 21:2521-32

147. **Warmington SA, Tolan R, McBennett S** 2000 Functional and histological characteristics of skeletal muscle and the effects of leptin in the genetically obese (ob/ob) mouse. Int J Obes Relat Metab Disord 24:1040-50

148. **Evert M, Sun J, Pichler S, Slavova N, Schneider-Stock R, Dombrowski F** 2004 Insulin receptor, insulin receptor substrate-1, Raf-1, and Mek-1 during hormonal hepatocarcinogenesis by intrahepatic pancreatic islet transplantation in diabetic rats. Cancer Res 64:8093-100

149. **Friedman JM, Halaas JL** 1998 Leptin and the regulation of body weight in mammals. Nature 395:763-70

150. **Yahagi N, Shimano H, Hasty AH, et al.** 2002 Absence of sterol regulatory element-binding protein-1 (SREBP-1) ameliorates fatty livers but not obesity or insulin resistance in Lep(ob)/Lep(ob) mice. J Biol Chem 277:19353-7

151. **Lord G** 2002 Role of leptin in immunology. Nutr Rev 60:S35-8; discussion S68-84, 85-7

152. **Lord GM, Matarese G, Howard JK, Baker RJ, Bloom SR, Lechler RI** 1998 Leptin modulates the T-cell immune response and reverses starvation-induced immunosuppression. Nature 394:897-901

153. **Howard JK, Lord GM, Matarese G, et al.** 1999 Leptin protects mice from starvation-induced lymphoid atrophy and increases thymic cellularity in ob/ob mice. J Clin Invest 104:1051-9

154. **Meade CJ, Sheena J, Mertin J** 1979 Effects of the obese (ob/ob) genotype on spleen cell immune function. Int Arch Allergy Appl Immunol 58:121-7

155. **Chandra RK, Au B** 1980 Spleen hemolytic plaque-forming cell response and generation of cytotoxic cells in genetically obese (C57Bl/6J ob/ob) mice. Int Arch Allergy Appl Immunol 62:94-8

156. **Wurster AL, Withers DJ, Uchida T, White MF, Grusby MJ** 2002 Stat6 and IRS-2 cooperate in interleukin 4 (IL-4)-induced proliferation and differentiation but are dispensable for IL-4-dependent rescue from apoptosis. Mol Cell Biol 22:117-26

157. **Chung WK, Belfi K, Chua M, et al.** 1998 Heterozygosity for Lep(ob) or Lep(rdb) affects body composition and leptin homeostasis in adult mice. Am J Physiol 274:R985-90

158. **Unger RH, Zhou YT** 2001 Lipotoxicity of beta-cells in obesity and in other causes of fatty acid spillover. Diabetes 50 Suppl 1:S118-21

159. **Garofalo RS, Orena SJ, Rafidi K, et al.** 2003 Severe diabetes, age-dependent loss of adipose tissue, and mild growth deficiency in mice lacking Akt2/PKB beta. J Clin Invest 112:197-208

160. **George S, Rochford JJ, Wolfrum C, et al.** 2004 A family with severe insulin resistance and diabetes due to a mutation in AKT2. Science 304:1325-8

161. **Pende M, Kozma SC, Jaquet M, et al.** 2000 Hypoinsulinaemia, glucose intolerance and diminished beta-cell size in S6K1-deficient mice. Nature 408:994-7

162. **Um SH, Frigerio F, Watanabe M, et al.** 2004 Absence of S6K1 protects against age- and diet-induced obesity while enhancing insulin sensitivity. Nature 431:200-5

163. **Sherr CJ** 1996 Cancer cell cycles. Science 274:1672-7

164. **Kamb A, Gruis NA, Weaver-Feldhaus J, et al.** 1994 A cell cycle regulator potentially involved in genesis of many tumor types. Science 264:436-40

165. **Serrano M, Hannon GJ, Beach D** 1993 A new regulatory motif in cell-cycle control causing specific inhibition of cyclin D/CDK4. Nature 366:704-7

166. **Morgan DO** 1997 Cyclin-dependent kinases: engines, clocks, and microprocessors. Annu Rev Cell Dev Biol 13:261-91

167. **Mulligan G, Jacks T** 1998 The retinoblastoma gene family: cousins with overlapping interests. Trends Genet 14:223-9

168. **Dyson N** 1998 The regulation of E2F by pRB-family proteins. Genes Dev 12:2245-62

169. **Rane SG, Dubus P, Mettus RV, et al.** 1999 Loss of Cdk4 expression causes insulin-deficient diabetes and Cdk4 activation results in beta-islet cell hyperplasia. Nat Genet 22:44-52

170. **Shima H, Pende M, Chen Y, Fumagalli S, Thomas G, Kozma SC** 1998 Disruption of the p70(s6k)/p85(s6k) gene reveals a small mouse phenotype and a new functional S6 kinase. Embo J 17:6649-59

171. **Leng Y, Steiler TL, Zierath JR** 2004 Effects of insulin, contraction, and phorbol esters on mitogen-activated protein kinase signaling in skeletal muscle from lean and ob/ob mice. Diabetes 53:1436-44

172. **Osman A, Otero J, Brizolara A, et al.** 2004 Effect of rosiglitazone on restenosis after coronary stenting in patients with type 2 diabetes. Am Heart J 147:e23

173. **Diehl JA, Cheng M, Roussel MF, Sherr CJ** 1998 Glycogen synthase kinase-3beta regulates cyclin D1 proteolysis and subcellular localization. Genes Dev 12:3499-511

174. **Cohen P, Zhao C, Cai X, et al.** 2001 Selective deletion of leptin receptor in neurons leads to obesity. J Clin Invest 108:1113-21

175. **Bouret SG, Simerly RB** 2004 Minireview: Leptin and development of hypothalamic feeding circuits. Endocrinology 145:2621-6

176. **Bouret SG, Draper SJ, Simerly RB** 2004 Trophic action of leptin on hypothalamic neurons that regulate feeding. Science 304:108-10

177. **Pinto S, Roseberry AG, Liu H, et al.** 2004 Rapid rewiring of arcuate nucleus feeding circuits by leptin. Science 304:110-5

178. **Abel ED, Peroni O, Kim JK, et al.** 2001 Adipose-selective targeting of the GLUT4 gene impairs insulin action in muscle and liver. Nature 409:729-33

179. **Previs SF, Withers DJ, Ren JM, White MF, Shulman GI** 2000 Contrasting effects of IRS-1 versus IRS-2 gene disruption on carbohydrate and lipid metabolism in vivo. J Biol Chem 275:38990-4

180. **Lee Y, Hirose H, Ohneda M, Johnson JH, McGarry JD, Unger RH** 1994 Beta-cell lipotoxicity in the pathogenesis of non-insulin-dependent diabetes mellitus of obese rats: impairment in adipocyte-beta-cell relationships. Proc Natl Acad Sci U S A 91:10878-82

181. **Ruderman N, Prentki M** 2004 AMP kinase and malonyl-CoA: targets for therapy of the metabolic syndrome. Nat Rev Drug Discov 3:340-51

182. **Minokoshi Y, Alquier T, Furukawa N, et al.** 2004 AMP-kinase regulates food intake by responding to hormonal and nutrient signals in the hypothalamus. Nature 428:569-74

183. **Andersson U, Filipsson K, Abbott CR, et al.** 2004 AMP-activated protein kinase plays a role in the control of food intake. J Biol Chem 279:12005-8

184. **Spiegelman BM, Flier JS** 2001 Obesity and the regulation of energy balance. Cell 104:531-43

185. **Rhee J, Inoue Y, Yoon JC, et al.** 2003 Regulation of hepatic fasting response by PPARgamma coactivator-1alpha (PGC-1): requirement for hepatocyte nuclear factor 4alpha in gluconeogenesis. Proc Natl Acad Sci U S A 100:4012-7

186. **Norris AW, Chen L, Fisher SJ, et al.** 2003 Muscle-specific PPARgamma-deficient mice develop increased adiposity and insulin resistance but respond to thiazolidinediones. J Clin Invest 112:608-18

187. **Steppan CM, Swick AG** 1999 A role for leptin in brain development. Biochem Biophys Res Commun 256:600-2

188. **Sena A, Sarlieve LL, Rebel G** 1985 Brain myelin of genetically obese mice. J Neurol Sci 68:233-43

189. **Garris DR** 1989 Morphometric analysis of obesity (ob/ob)- and diabetes (db/db)-associated hypothalamic neuronal degeneration in C57BL/KsJ mice. Brain Res 501:162-70

190. **Bereiter DA, Jeanrenaud B** 1979 Altered neuroanatomical organization in the central nervous system of the genetically obese (ob/ob) mouse. Brain Res 165:249-60

191. **Bereiter DA, Jeanrenaud B** 1980 Altered dendritic orientation of hypothalamic neurons from genetically obese (ob/ob) mice. Brain Res 202:201-6

192. **Mallucci GR, Ratte S, Asante EA, et al.** 2002 Post-natal knockout of prion protein alters hippocampal CA1 properties, but does not result in neurodegeneration. Embo J 21:202-10

193. **Schuler M, Dierich A, Chambon P, Metzger D** 2004 Efficient temporally controlled targeted somatic mutagenesis in hepatocytes of the mouse. Genesis 39:167-72